

**Impacts of Mesenchymal KITL/SCF in
Pancreatic Tissue Homeostasis
and
Pancreatic Ductal Adenocarcinoma**

By

Maria Kathrina C. Oñate

A DISSERTATION

Presented to the Department of Cell, Developmental, & Cancer Biology
Oregon Health & Science University
School of Medicine

in partial fulfillment of
the requirements for the degree of

Doctor of Philosophy

February 2025

School of Medicine
Oregon Health & Science University

CERTIFICATE OF APPROVAL

This is to certify that the PhD dissertation of
Maria Kathrina C. Oñate
has been approved

Mara H. Sherman, Advisor

Anupriya Agarwal, Member

Sudarshan Anand, Member

Amanda McCullough, Chair

Rosalie C. Sears, Member

Table of Contents

i. List of Figures	i
ii. Abbreviations	iii
iii. Acknowledgements	v
Abstract.....	1
Chapter I. Introduction	3
A. Pancreatic Ductal Adenocarcinoma	3
I. Pancreas and Its Associated Diseases	3
II. Early Detection Methods of PDAC	6
III. Past to Present PDAC Therapies.....	7
B. PDAC Development and Desmoplasia	9
I. Development.....	9
II. Desmoplasia and its Impact on Tumorigenesis	11
C. Cancer-Associated Fibroblasts	13
I. Fibroblasts and CAFs: Back to Basics	14
II. CAF Subtypes	17
III. CAF Lineages.....	20
D. Stellate Cells: A “fibroblast” and beyond.....	24
I. Pancreatic Stellate Cells	25
E. KITL/SCF and c-KIT signaling pathway	27
I. KITL/SCF	28
II. C-KIT	30
III. Signaling Cascade.....	31
IV. Roles in Tissue Development and Homeostasis	33
V. Roles in Cancer.....	33
F. Rationale and Hypothesis.....	34
Chapter II. Impacts of Mesenchymal KITL in Pancreatic Tissue Homeostasis and Pancreatic Ductal Adenocarcinoma	36
A. Abstract	36
B. Introduction.....	37
C. Contributions.....	40
D. Materials and Methods	42
E. Results	64

F. Discussion	105
Chapter III. Conclusions, Limitations, and Future Directions	108
A. Temporal and Spatial Organization of Pancreatic Stellate Cells.....	108
B. Strengths and Limitations of Single cell Technologies.....	109
C. RNA as a measurement of KITL expression.....	111
D. Complementary <i>in vitro</i> methods assessing murine KITL expression	113
E. Alternative Sources of pancreatic KITL.....	114
F. Implications of gradual loss of mesenchymal KITL in PDAC	115
G. Genetic, Epigenetic, and Proteomic Factors controlling mesenchymal KITL expression	116
H. Fibroblast lineage contribution and function in the presence of early mesenchymal KITL loss.....	117
I. Mesenchymal KITL and the Immune Compartment.....	118
J. Mesenchymal KITL maintains tissue architecture.....	119
K. “All Models are Wrong...”: Mouse Models.....	120
L. Potential KITL/c-KIT tumor-promoting capacity in PDAC.....	121
M. Dysfunctional Mechanisms from mesenchymal KITL loss as Evidence for Liver Metastasis and Disease	122
N. Anti-stromal/fibrotic Cancer Treatments as Treatments for other Fibroinflammatory Diseases	123
O. Concluding Remarks	124
References	126

i. List of Figures

Figure 1.1. Key anatomical features of the human pancreas.....	3
Figure 1.2. Pancreatic Diseases.....	5
Figure 1.3. Timeline of USA FDA Approvals for Metastatic Pancreatic Cancer Treatment.....	8
Figure 1.4. Genetic and environmental perturbations of PDAC tumorigenesis.....	10
Figure 1.5. Early PDAC event of oncogenic KRAS mutation coincides and produces a desmoplastic reaction.....	12
Figure 1.6. Cells in wound healing.....	15
Figure 1.7. Heterogeneous functions of PDAC CAFs.....	16
Figure 1.8. PDAC cancer-associated fibroblast subtypes.....	18
Figure 1.9. Breast cancer CAF subtypes.....	19
Figure 1.10. Contributions of Gli1+ and Hoxb6+ fibroblasts in healthy murine pancreas and murine PDAC.....	22
Figure 1.11. Fibroblast lineages in healthy murine pancreas and their contributions to the murine PDAC CAF population.....	23
Figure 1.12. Stellate cell functions.....	24
Figure 1.13. Hematopoietic stem cells require KITL/SCF from the perisinusoidal niche in the developing liver.....	26
Figure 1.14. Structure of membrane-bound and soluble KITL/SCF.....	29
Figure 1.15. Structure of c-KIT receptor.....	30
Figure 1.16. c-KIT signaling cascade and phosphorylation sites.....	32
Figure 2.1. Pancreatic stellate cells contribute to the stromal microenvironment throughout tumorigenesis.....	64-68
Figure 2.2. Mesenchymal KITL loss within PSCs accompanies pancreatic tumorigenesis.....	69-70, 74-75, 78-81, 83-85
Supplementary Figure 2.S1. scRNA-seq reveals gene expression programs in PSCs and PSC-derived CAFs.....	71-73
Supplementary Figure 2.S2. <i>Kitl</i> is expressed by healthy pancreatic mesenchyme and reduced upon activation to a CAF phenotype.....	76-78, 82-83
Supplementary Figure 2.S3. Stromal KITL promotes regulation of pancreas tissue architecture.....	86-87, 90-91
Figure 2.3. KITL regulates PSC state and pancreas tissue homeostasis.....	89-90, 92-95, 98-100

Supplementary Figure 2.S4. Stromal KITL promotes pancreas tissue homeostasis.....	92, 94, 96-97
Figure 2.4. Mesenchymal KITL restrains pancreatic tumor growth.....	101-105
Figure 2.5. Mesenchymal KITL regulates healthy tissue homeostasis and normal tissue function.....	107
Figure 3. Secondary clustering analysis of scRNA-seq reveals distinct populations of pancreatic stellate cells from healthy and PDAC murine pancreata.....	110-111

ii. Abbreviations

5FU	5-fluorouracil
α SMA	Alpha smooth muscle actin
ADM	Acinar-to-ductal metaplasia
apCAF	Antigen-presenting cancer-associated fibroblast
APS	Adapter protein with Pleckstrin homology and Src homology 2 domains
BRCA	Breast cancer type susceptibility protein
C-KIT	C-KIT receptor
CAF	Cancer-associated fibroblast
CBL	Casitas B-lineage Lymphoma
CD	Cluster of differentiation
COL	Collagen
CT	Computed tomography
CTLA-4	Cytotoxic T-lymphocyte associated protein 4
CXCL	C-X-C motif chemokine ligand
dCAFs	Developmental cancer-associated fibroblasts
DEG	Differentially expressed gene
ECM	Extracellular matrix
ED	Endoscopic ultrasound
FAP	Fibroblast activation protein
FABP	Fatty acid binding protein
FANCC	Fanconi anemia, complementation group C
FBLN	Fibulin
FGF	Fibroblast growth factor
FlpO	Murine-specific FLP Recombinase (derived from <i>S. cerevisiae</i> flippase)
FFPE	Formalin-fixed paraffin-embedded
FSF	FRT-stop-FRT cassette
FSP	Fibroblast-specific protein
GDF	Growth differentiation factor
GEMM	Genetically engineered mouse model
GFP	Green fluorescent protein
GRB	Growth factor receptor-bound protein
HCC	Hepatocellular carcinoma
Hh	Hedgehog (can also be labeled as Shh)
HIF	Hypoxia-induced factors
HSC	Hepatic stellate cell
iCAF	Inflammatory cancer-associated fibroblast
ICB/ICI	Immune checkpoint blockade/inhibitors
IFN	Interferon
Ig	Immunoglobulin
IL	Interleukin
IPMN	Intraductal papillary mucinous neoplasm
ISH	<i>In situ</i> hybridization
JAK	Janus kinase
KITL/KITLG/Kitl	Kit ligand (see SCF)
KPC	<i>Kras</i> ^{+/<i>LSL-G12D</i>} ; <i>Trp53</i> ^{+/<i>LSL-R172H</i>} ; <i>Pdx1-Cre</i> (an established and common GEMM in PDAC)
KRAS	Kirsten rat sarcoma virus

LEPR	Leptin receptor
LNK	Lymphocyte adapter protein (also known as SH2B3)
Lox	Lysyl oxidase
Lum	Lumican
MAPK	Mitogen-activated protein kinase
mCAF	Matrix cancer-associated fibroblast
MDSC	Myeloid-derived suppressor cell
MMR-D	Mismatch repair deficient
MMTV-PyMT	FVB/N-Tg(MMTV-PyVT)634Mul/J (an established GEMM for breast cancer)
mPDAC	Murine PDAC
myCAF	Myofibroblast cancer-associated fibroblast
MRI	Magnetic Resonance Imaging
OS	Overall survival
PanIN	Pancreatic intraepithelial neoplasm
PDA/PDAC	Pancreatic (ductal) adenocarcinoma
PDGFR	Platelet-derived growth factor receptor
Pdx1	Pancreatic and duodenal homeobox 1
PD-1	Programmed cell death protein 1
PD-L1	Programmed cell death-ligand 1
PECAM-1/PECAM1	Platelet endothelial cell adhesion molecule 1 (see CD31)
PI3K	Phosphoinositide 3-kinase
PLC-gamma	Phospholipase C gamma
POU3F2	POU domain, class 3, transcription factor 2
PP	Pancreatic polypeptide
PSC	Pancreatic stellate cell
PRSS1	Cationic trypsinogen (also known as Trypsin-1, TRP1)
RNA-seq	RNA-sequencing
RTK	Receptor tyrosine kinase
TAGLN	Transgelin
TAM	Tumor-associated macrophage
TFIID	Transcription factor II D
TGF- β	Transforming growth factor beta
TME	Tumor microenvironment
TNF α	Tumor necrosis factor alpha
SCF	Stem cell factor (see KITL)
SCRG1	Stimulator of chondrogenesis 1
scRNA-seq	Single-cell RNA-sequencing
SHP	Src homology region 2 domain-containing phosphatase
SMAD	Suppressor of mother against decapentaplegic
SP1	Specificity protein 1
STAT	Signal transducer and activator of transcription
vCAFs	Vascular cancer-associated fibroblasts
VIM	Vimentin
ZBTB	Zinc finger and BTB Domain

iii. Acknowledgements

Ah, now to my favorite part of this dissertation. Don't get me wrong—I thoroughly enjoyed writing my dissertation, although I must admit that if I continued my unhealthy writing schedule any further, I would become a husk of a human being. Nevertheless, I must be lucky because I have been blessed throughout my entire PhD experience. It's so cliché, but I truly mean it when I write that I raised by a loving village, and I succeeded only because I stood on the shoulders of giants.

First and foremost, to my mentor, Dr. Mara Sherman: Mara, thank you for always creating an environment that is safe, thoughtful, and caring above all else. I have always admired your intellectual insight that appeared eerily clairvoyant (how?!) and the eloquence with which you articulate scientific findings and phenomena. I always wished that by being your mentee your awesome prowess would rub off on me, even if it were a sprinkling. But more importantly, your dedication to creating a space that holds tight to the values of kindness and respect—especially during these dark times—is what truly makes you a wonderful boss and person.

I cannot forget my lab mates and colleagues from both the Pacific and Atlantic coasts, my day-to-day buddies who made painful and frustrating days more bearable: Annachiara (Anny), Ari, Erin, Frank, Hannah, Holly, Jaime, Luis, Mark, Sneha, Vivien (Viv), Zainab. You guys make lab so fun and funny. Also, y'all are so brilliant, your individual and collective shine makes my eyes hurt. Thank you all for imparting all your knowledge as a bumbled my way through graduate school. A 10-minute standing ovation to Chet and Sohinee for figuratively carrying me to the proverbial finish line (in addition to what I said above); if I had even 10% of each of your expertise and intellect, I would be a better scientist by 200%.

To my 2018 cohort and friends in Portland, OR: I miss you all so much. To my new MSK friends and acquaintances in New York, NY: thank you for making me feel like I belong, as if I've been here the whole time.

To my long-time friends: thank you all for reminding me of my power. Thank you all for letting me vent. Thank you all for putting things in a new perspective. Thank you for reminding me that there is more to life. Thank you for understanding why I sacrifice my time and effort to this endeavor. Thank you for always including me, even when I at times could not join.

To Homma, my "grad wife": Thank you so much for being my first friend, colleague, and teammate in this wild unknown. I'm sorry I'm so far away, I miss you. Thank you for support always. I hope you know that I'm always cheering you on, even if I am far away.

To my parents: it is from the depths of my heart that I write—thank you. Thank you for your ever-flowing support, love, and encouragement. It has been a challenging few years, to say the least. Alam na alam ko na mahal nyo ako. Hindi ko makakalimutan ang hirap na naranasan nyo noong lumipat tayo sa USA. Ngayon, tinatapos ng iyong anak ang kanyang PhD. I love you both very much and I hope I have made you two proud.

To my partner, Jason: thank you for being there by my side the entire time (and space), holding my hand. Thank you for being the best teammate in life. '92 Dream Team.

Last but not least, to myself: I thank myself for not giving up. I did not apply to graduate school lightly as I heard from many before me of its internal and external trials. Time and time again I stumbled in the darkness, and drank heavy from the well called "imposter syndrome". I kept drinking from that well because, deep down, I probably felt it would make me better, even though it felt like poison. Despite my loud negative thinking, I acted otherwise. I reached out to friends, family, loved ones; I did my best to take care of myself;

I aimed as high as I could hoping to surpass my own expectations; I reminded myself of my goals and dreams, even when those appeared so far away. Somewhere deep inside me was someone who believed in herself, even if her voice was soft. I'm so glad I listened to her—she was right. I can do this, I just needed to ask for help.

Abstract

Steady improvements to the five-year survival rate for patients with pancreatic ductal adenocarcinoma (PDAC) have largely been due to improvements in patient care as opposed to effective treatments across all disease stages. Limited treatment efficacy in PDAC is due in part to its signature immunosuppressive desmoplasia. In the past 20 years, cancer-associated fibroblasts (CAFs) have gained attention for their therapeutic potential as they have been shown to be the main contributors to PDAC's fibrotic nature. However, recent studies on CAF ablation exposed deleterious consequences in pre-clinical models, confusing the field as to whether CAFs are altogether pro-tumorigenic (Özdemir et al., 2014; Rhim et al., 2014). This prompted a new era towards elucidating the functional roles of CAFs. Current literature has typically categorized much of CAF functions as tumor permissive; however, quiescent fibroblasts in healthy organs—which give rise to CAFs in a cancer context—are activated in wound repair and tissue homeostasis. Current literature supports the notion that fibroblasts transition from tumor-restraining to tumor-promoting as tumorigenesis progresses, however the tumor-restraining mechanisms of fibroblasts in the pancreas are unknown.

In this dissertation, we show how kit ligand (KITL, also known as stem cell factor) derived from normal pancreatic mesenchyme has implications in tissue homeostasis and tumor-suppressive features. Through single-cell transcriptomics and analysis of tissue architecture, we show that mesenchymal cells in healthy pancreas and PDAC are found in distinct spatial subpopulations positioned to interact with diverse cell types; from this, we observed the loss of KITL as mesenchymal cells transition to CAFs in tumorigenesis. *In vivo* genetic manipulation in mouse models, allowed us to assess the impacts of mesenchymal KITL in the pancreas. Loss of mesenchymal KITL led to an increase of

leukocytes in normal pancreas, and an increase in ductal marker expression upon caerulein-induced acute pancreatitis, as evidence for acinar-to-ductal metaplasia (ADM). Murine tumor models also showed that KITL loss caused faster tumor growth and shortened survival compared to control models. Collectively, these data suggest that stromal KITL has tumor-suppressive functions by maintaining tissue equilibrium.

Chapter I. Introduction

A. Pancreatic Ductal Adenocarcinoma

I. Pancreas and Its Associated Diseases

Tucked beneath the stomach, the pancreas is surrounded by other related gastrointestinal organs (liver, gall bladder, and small intestine) and vascularized by the celiac and superior mesenteric arteries. Its structure consists of the “head” (which touches the duodenum of the small intestine); the uncinate process, the “neck” or “body” found in the center of the pancreas, and the thin end aptly named the “tail”. This organ continuously grows in the human body until age 30, which plateaus then declines in volume as humans age (Saisho et al., 2007).

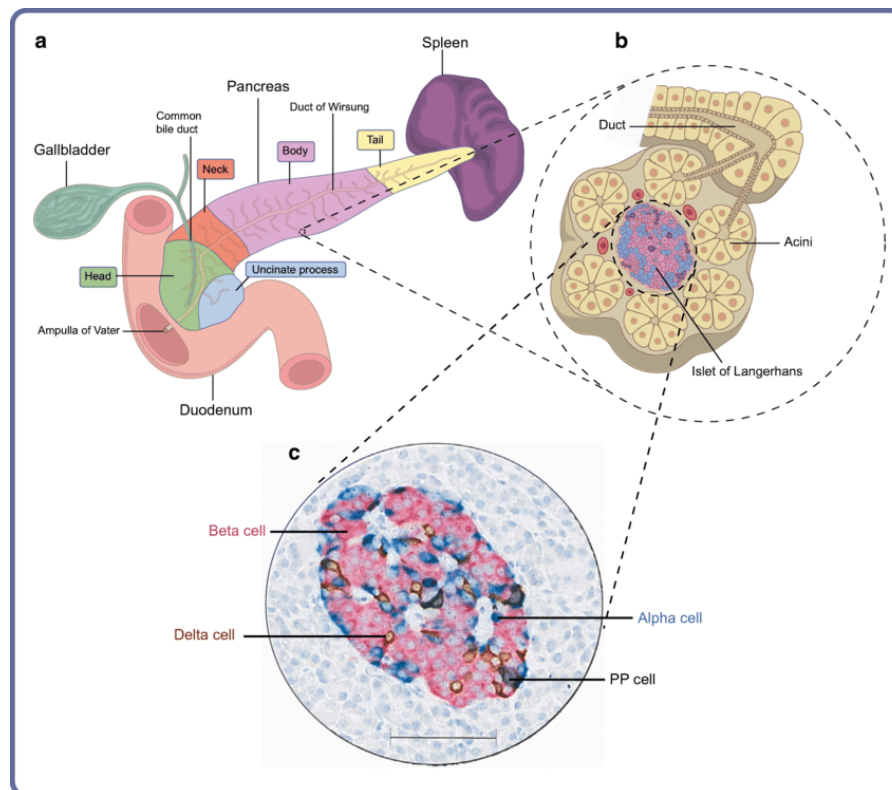


Figure 1.1. Key anatomical features of the human pancreas. A, Anatomy of the pancreas with some of its surrounding organs, gallbladder and spleen. **B,** Cellular organization of exocrine and endocrine cells in the pancreas. **C,** Section of human pancreas showing an islet with four endocrine cell types: alpha, beta, delta, and PP cells. Scale bar, 100 μm . Reprinted from *Diabetologia*, Organisation of the human pancreas in health and in diabetes, Atkinson et al., 2020, with permission from Springer Nature.

The pancreas connects to the duodenum through the pancreatic duct (also named Duct of Wirsung), wherein digestive enzymes—lipase, protease, and amylase—produced by exocrine cells (i.e. acinar cells) flow to further catabolize food. Among other vital functions, the pancreas is also involved in regulating blood sugar levels via its endocrine cells called islet cells, which are clustered together and sporadically found throughout the organ. These islet cells consist of alpha, beta, delta, pancreatic polypeptide (PP), and epsilon cells that produce hormones such as glucagon, insulin, somatostatin, pancreatic polypeptide, and ghrelin, respectively (Atkinson et al., 2020; Campbell & Newgard, 2021). (Interestingly, "sweetbread" is the etymological meaning for the word "pancreas," yet its literal Greek translation is "all whole flesh," potentially describing this organ's odd texture.)

Like all organs, the pancreas is not immune to damages that can lead to diseases. Type 1 and 2 diabetes, hyper- and hypoglycemia are commonly known diseases associated with pancreas dysfunction, all of which are highly prevalent in the United States; as of 2020, 11.6% of the total U.S. population have diabetes (Andes et al., 2020). Pancreatitis, or inflammation of the pancreas, may be acute or chronic. It is commonly caused by alcohol consumption and gallstones (excess cholesterol from a high-fat diet can significantly contribute to gallstone formation); however, one may have increased risk due to family history (e.g. hereditary pancreatitis). Further complicating matters, these diseases have overlapping symptoms with a more lethal condition—cancer. Pancreatic cancer can be subdivided into two groups distinguished by their cell-of-origin: pancreatic neuroendocrine tumors (PNET) and exocrine tumors, with the latter including pancreatic ductal adenocarcinoma.

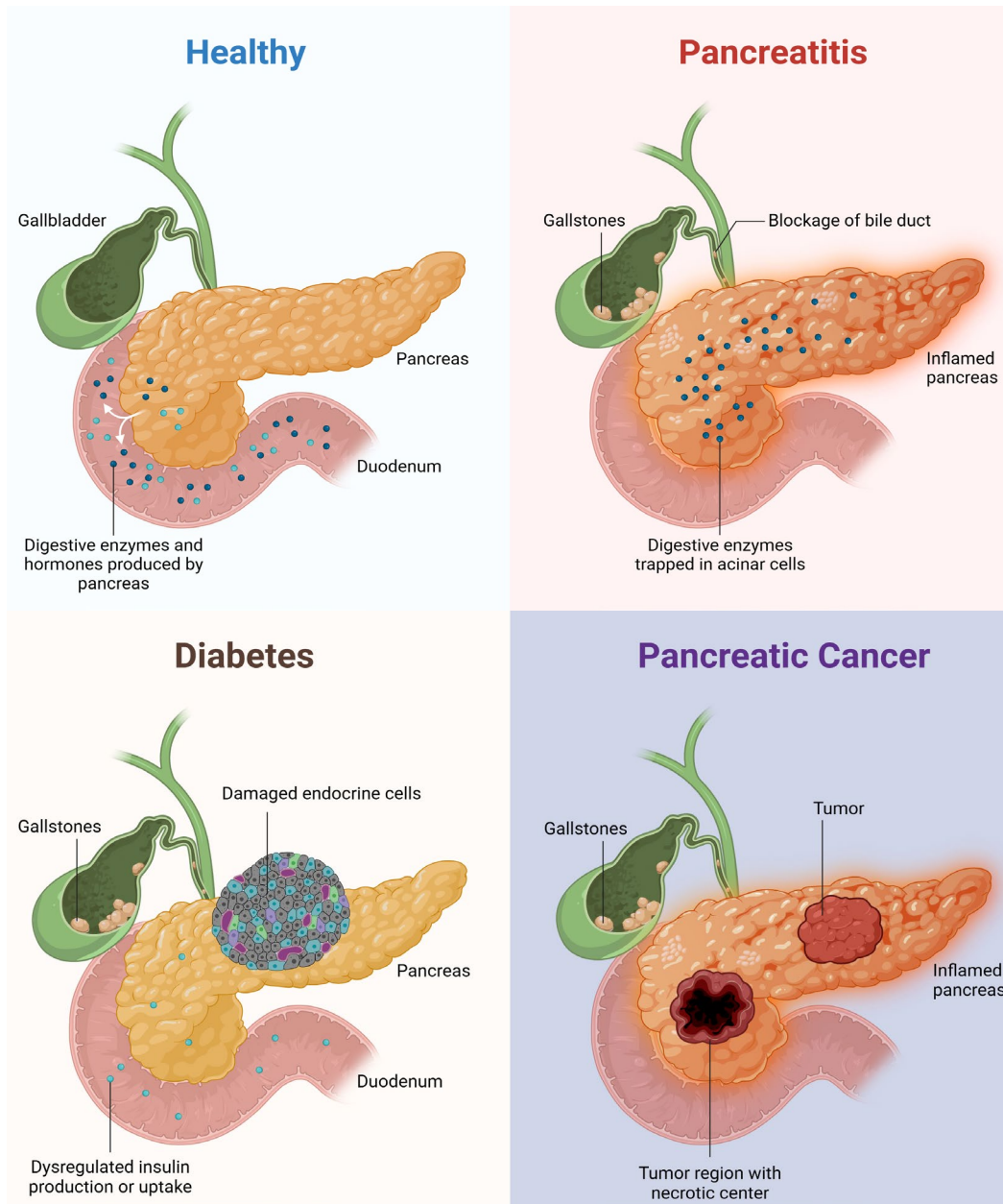


Figure 1.2. Pancreatic Diseases. Healthy pancreatic functions include release of digestive enzymes and hormones produced by exocrine and endocrine cells, respectively (top left). Loss of healthy tissue homeostasis in the pancreas results in damaged tissue and inflammation that can lead to pancreatitis, diabetes, and pancreatic cancer. Created with Biorender.

Pancreatic ductal adenocarcinoma (also known as pancreatic adenocarcinoma, shortened as PDA or PDAC), an aggressive pancreatic exocrine tumor driven by oncogenic *KRAS* mutations, is the third leading cause of cancer deaths in the United States as of 2024 (*Common Cancer Sites - Cancer Stat Facts*, n.d.). Its 5 year-survival

rate has increased from 10% in 2020 to 12.8% in 2024 due to improved efforts in patient care and developments in combination neoadjuvant and adjuvant systemic chemotherapies, with FOLFIRINOX (5-fluorouracil (5-FU), leucovorin, irinotecan, and oxaliplatin), gemcitabine, and nab-paclitaxel (Conroy et al., 2011; Hoff et al., 2013; Klatter et al., 2023; Springfield et al., 2023). Pancreaticoduodenectomy (or Whipple surgery), first successfully performed in 1935, is still the best way to improve overall survival (OS); with Whipple surgery, patients can increase their 5-year survival rate between 20 to 25% (Syed Nabeel Zafar, 2024). However, this option is available to only 15 to 20% of patient cases as this requires the disease to be at a localized stage (primary site only), whereas at least 80% of patients have been diagnosed with regional to distant stages PDAC (*Cancer of the Pancreas - Cancer Stat Facts*, n.d.).

II. Early Detection Methods of PDAC

Patients are typically caught at later stages due to limited methodologies in early detection.

These methodologies are specifically imaging modalities (e.g. abdominal ultrasound, magnetic resonance imaging (MRI), computed tomography (CT), and endoscopic ultrasound (EUS)) that vary in each of their diagnostic accuracy and precision, impacted by tumor size and image quality (Wu et al., 2022). Expensive systems, such as CT and MRI scans, are more sensitive than the accessible standard abdominal ultrasound, reducing the chances of a patient being earlier identified. As of the 2010s, there has been significant expansion and progress in novel screening methods including liquid biopsies and the implementation of artificial intelligence to improve imaging modality sensitivity. Most of the success in early detection, however, comes from improved studies in understanding genetic and lifestyle risk factors. Hereditary pancreatitis, germline mutations associated with other diseases such as breast and ovarian cancer (e.g. *BRCA1*,

BRCA2, FANCC, PRSS1) (Earl et al., 2020; Grant et al., 2015) and new onset diabetes are highly associated or correlated with increased risk of PDAC (Pannala et al., 2009). Patients with these genetic factors are recommended for early enhanced screening, around 10 years younger than the general population (e.g. patients with BRCA mutations are recommended to be screened with MRI and mammography around age 30 rather than in their 40s) (*BRCA Gene Changes*, 2024). Lifestyle risk factors including smoking, high fat diet, excessive alcohol consumption, and diabetes are all highly associated or correlated with increased risk of PDAC. Parallel to early detection, cancer treatments have also improved.

III. Past to Present PDAC Therapies

Prior to chemotherapy, PDAC patients were either treated via surgery or radiotherapy. Early exploration into adjuvant therapies for patients with resectable PDAC began in the 1980s, when the Gastrointestinal Tumor Study group published in 1985 that patients who were treated with fluorouracil (5FU) survived for an additional nine months in contrast to patients who did not receive 5FU-based chemoradiotherapy (Gaskill et al., 2021). Unfortunately, later studies could not replicate these findings. However, studies have successfully shown and replicated that PDAC patients with resectable tumors survived for longer than their control counterparts when provided with systemic chemotherapy, whether with gemcitabine or FOLFIRINOX. It is now recommended standard clinical practice, based off the American Society of Clinical Oncology (ASCO) Guidelines, to provide patients with potentially curable PDAC six months of adjuvant treatment if they have not received perioperative therapy (Khorana et al., 2019).

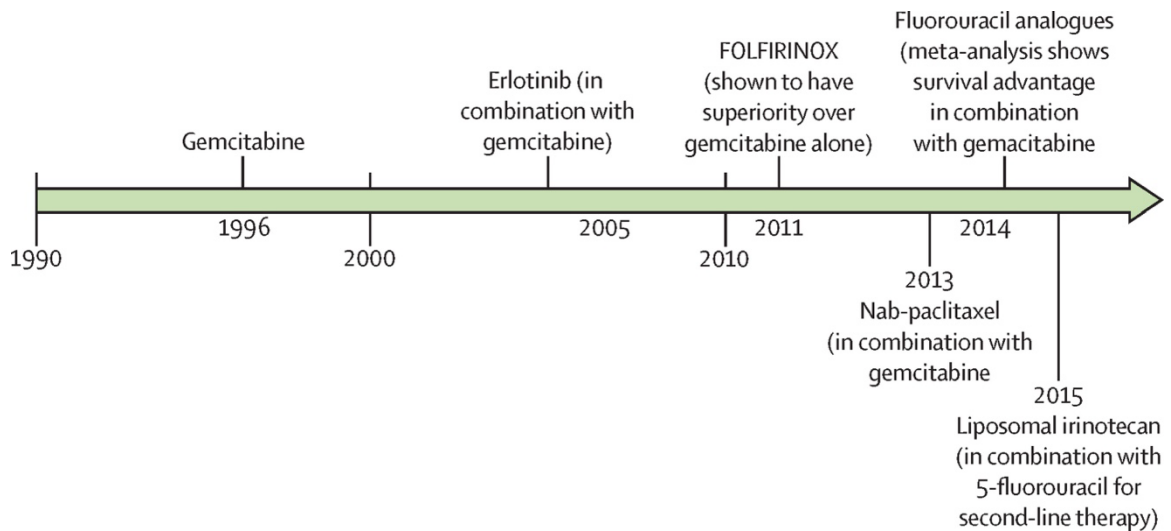


Figure 1.3. Timeline of USA FDA Approvals for Metastatic Pancreatic Cancer Treatment. FOLFIRINOX and fluorouracil analogues combined with gemcitabine treatment are included due to their common use, despite without specific FDA approval of combinatory treatments. Reprinted from *The Lancet Oncology*, Current and emerging therapies for patients with advanced pancreatic ductal adenocarcinoma: a bright future, Christenson, Jaffee, and Azad, 2020, with permission from Elsevier.

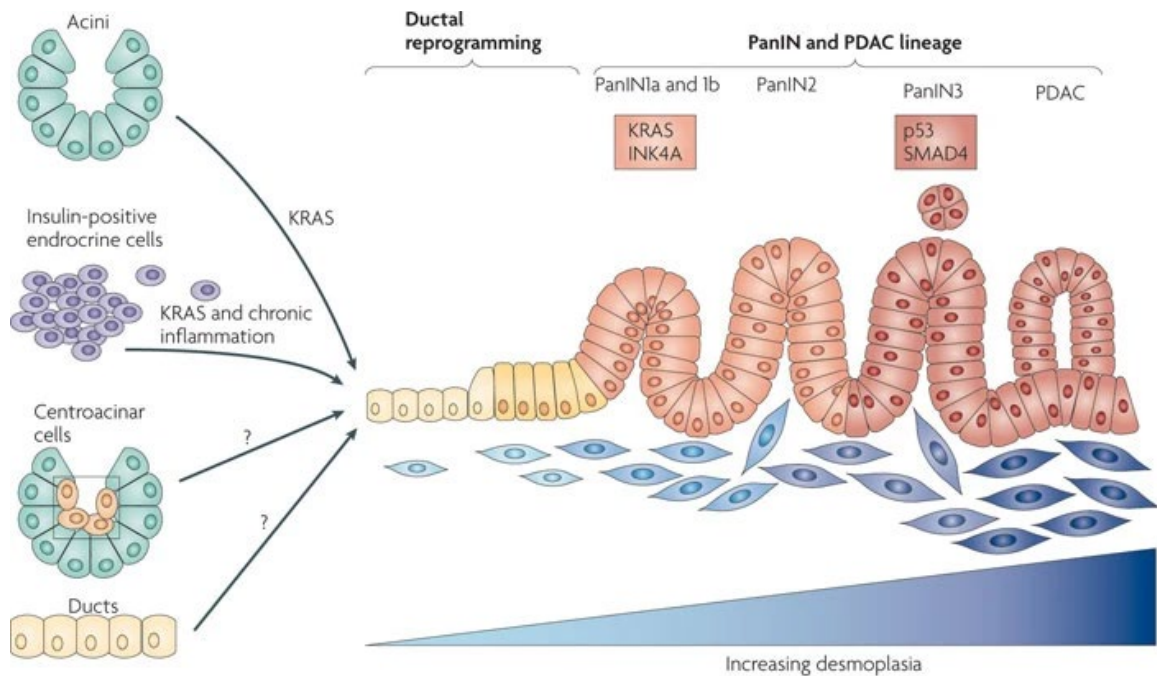
The success of anti-CTLA4 antibody ipilimumab as the first approved immune checkpoint blockade (ICB) treatment for multiple cancers—such as colorectal cancer, esophageal cancer, hepatocellular carcinoma, melanoma, non-small cell lung carcinoma, renal cell carcinoma, and mesothelioma—in 2021 led to cautious optimism for ICB therapies as a potential PDAC treatment (Korman et al., 2022). Frustrating for all, PDAC’s genetic landscape and tumor microenvironment (TME) produces a naturally immune-suppressive environment and is thus resistant to most ICB therapies. Currently, only PDAC patients with unique and sporadic mismatch repair-deficient (MMR-D) genomic subtypes show promising results when treated with ICB therapies (Ebia et al., 2023; Z. I. Hu et al., 2018; O’Connor et al., 2024). Around the early 2020s, pre-clinical and clinical studies in PDAC patients have shown that novel monotherapy of KRAS-mutant inhibitors led to anticancer activity, and in mice, combination of KRAS inhibition with ICBs showed greater efficacy in

tumor reduction and tumor elimination (Mahadevan, LeBleu, et al., 2023; Mahadevan, McAndrews, et al., 2023; Strickler et al., 2023). Notwithstanding the great enthusiasm over the initial success of these KRAS-mutant inhibitors, discussions regarding intrinsic drug resistance loom as patient response to current inhibitors were mixed (Zhang et al., 2022). Additionally, it is possible that KRAS inhibitor-based treatments may, understandably, require adjustments according to tissue- or tumor-of-origin (Zeissig et al., 2023). Because of this—and considering that *KRAS* mutations are insufficient to trigger low-grade neoplasms to PDAC—it is gravely important to understand the intricacies of this disease that lead to its immunosuppressive environment to find successful combinatory treatments.

B. PDAC Development and Desmoplasia

I. Development

Unlike other solid tumors such as colorectal and uterine cancer, PDAC is characterized by a select few genomic drivers that design PDAC's stepwise morphological dedifferentiation and progression (Kinnersley et al., 2024). Up to 95% of patients have a *KRAS* mutation (Iacobuzio-Donahue et al., 2012) and is often considered as PDAC'S first genetic event as *KRAS* mutations have been found in both low-grade pancreatic intraepithelial neoplasms (PanIN) and intraductal papillary mucinous neoplasms (IPMN) (Collet et al., 2020; Morris et al., 2010). Both precursor lesions, which can develop from acinar or ductal cells, require combinatory mutations of *TP53*, *SMAD4*, and/or *CDKN2A* to worsen as high-grade cancerous lesions. *TP53* mutations, for example, can be found between 50 to 75% in all PDAC patients (Scarpa et al., 1993). This stepwise tumorigenic progression creates an immune-evasive TME due to direct and indirect effects of PDAC's signature oncogenic mutations.



Nature Reviews | Cancer

Figure 1.4. Genetic and environmental perturbations of PDAC tumorigenesis. Exocrine or endocrine cell-Kras mutations combined with loss of tumor-suppressor gene functions activate epithelial and mesenchymal alterations in support of tumorigenesis. Reprinted from Nature Reviews Cancer, KRAS, Hedgehog, Wnt, and the twisted developmental biology of pancreatic ductal adenocarcinoma, Morris IV et al., 2010, with permission from Springer Nature.

KRAS^{G12D}-mutated human and murine PDAC (hPDAC and mPDAC, respectively) cells have been shown to produce granulocyte-macrophage colony-stimulating factor (GM-CSF), which leads to the accumulation of Gr-1+CD11b+ myeloid-derived suppressor cells (MDSCs) that suppress CD8+ T cells (Bayne et al., 2012; Pylayeva-Gupta et al., 2012). The deletion of *CDKN2A* coincides with a co-deletion of type I interferon (IFN) cluster, as both these regions are found in chromosome 9p21.3, resulting in immune evasion (Barriga et al., 2022). Indirectly, the continuous evolution of these neoplasms (particularly PanINs) over time conjures chronic inflammation, inducing a tumor-specific fibro-inflammatory reaction described as desmoplasia.

II. Desmoplasia and its Impact on Tumorigenesis

Diagnostically disregarded until around the 1980s, desmoplasia and its individual components are now nominated as potential drug targets for PDAC therapies. Desmoplasia is the growth of fibrous connective tissue that consists of dense extracellular matrix (ECM), immune cells, and activated fibroblasts aptly named as cancer-associated fibroblasts (CAFs). Within the ECM is an abundance of collagens, integrins, proteoglycans, and glycoproteins that appear to have both tumor-promoting and tumor-suppressing functions. In both human and murine PanIN and PDAC ECM, there is a robust increase in type I, III, and IV collagens; hyaluronic acid; glycoproteins fibrillin-1 (FBN-1), fibronectin (FN1), fibroninogens (FGA, FGB, and FGG), periostin (POSTN), and others (Linder et al., 2001; Öhlund et al., 2013; Tian et al., 2019). Patients with higher extracellular matrix components of hyaluronic acid and type I collagen were correlated with lower median overall survival in comparison to patients with lower expression of stated ECM components (Whatcott et al., 2015). The aberrant abundance of these high molecular weight ECM components creates a physical barrier with high interstitial pressure, resulting in vascular dysfunction, limiting the flow of oxygen, nutrients, and therapies at the intended carcinogenic site (DelGiorno et al., 2020; DuFort et al., 2016; Provenzano et al., 2012). PDAC cells adapt to this hypoxic and nutrient-depleted milieu through metabolic changes, producing highly adaptable, aggressive, and resilient cancer cells that further drives PDAC's therapeutic resistance and metastatic potential. For example, in hypoxic conditions, PDAC cells activate a family of transcription factors known as hypoxia-inducible factors (HIFs) that can induce glycolytic gene expression (via HIF-1 α), and promote invasion and metastasis via the RhoC-ROCK pathway (via HIF-3 α) (C.-J. Hu et al., 2003; X. Zhou et al., 2018). Additionally, both human PDAC and murine PDAC show desmoplastic reactions coinciding with accelerated growth in liver metastases,

strengthening the argument for desmoplasia's importance in PDAC progression (Zhong et al., 2017).

It is now understood and appreciated that desmoplasia stimulates and sustains PDAC's chemoresistance and aggressiveness as much as its own cancer cells. Yet, much of the initial work studying PDAC and its evolution focused more on its cell-of-origin, ignoring its fibrotic component (Jamieson, 1975; Pour et al., 1977). Despite decades of effort, the field could neither improve patient responses to chemotherapy nor understand determinants of tumor growth, leading to the larger question whether PDAC's cancer cell-extrinsic desmoplastic reaction is important, if not vital, to disease progression and therapy resistance.

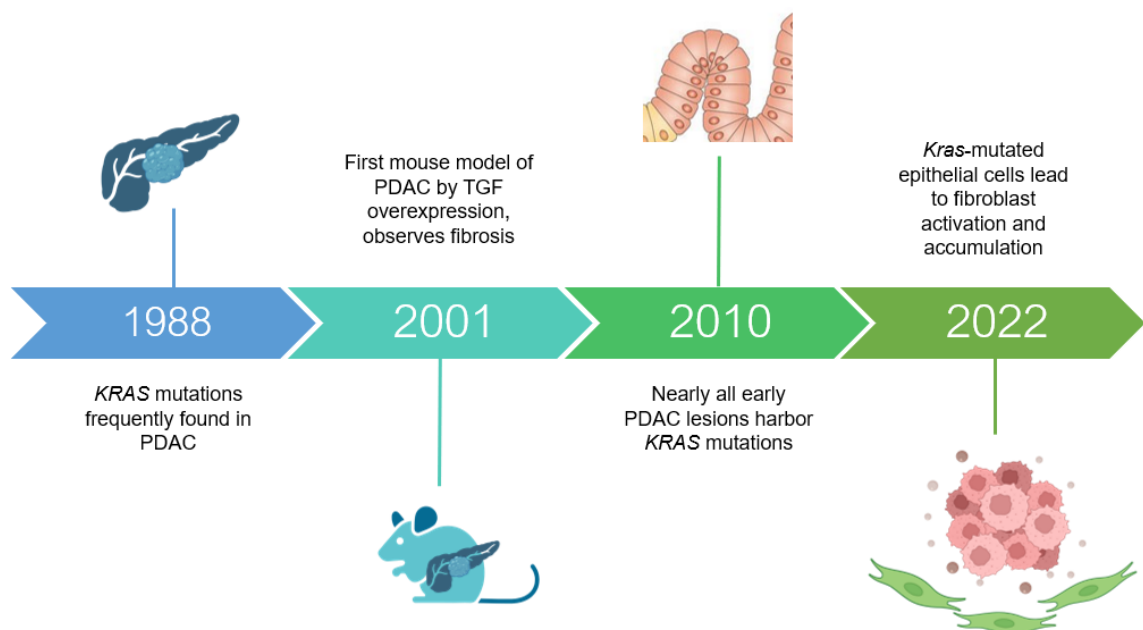


Figure 1.5. Early PDAC event of oncogenic *KRAS* mutation coincides and produces a desmoplastic reaction. Collective evidence in over 30 years show that oncogenic *KRAS* mutations in pancreatic epithelial cells are an early event in PDAC tumorigenesis, and alters the tumor microenvironment towards a fibro-inflammatory response that supports in tumor-promotion. Created with Biorender and PowerPoint.

The first question was whether desmoplasia preceded or succeeded tumorigenesis. Findings that *KRAS* mutations were a frequent and early event in PDAC tumorigenesis (Kanda et al., 2012; Smit et al., 1988) coincided with observations of fibrosis and overexpression of growth factor ligands and receptors, such as fibroblast growth factors (FGF) and transforming growth factor beta (TGF- β) (Greten et al., 2001; Korc, 1998). Within the three-stage theory of tumorigenesis (Pitot, 1993), this proposed that desmoplastic development occurred in the “promotion” stage, wherein cellular crosstalk through ligand-receptor interactions mediate gene expression changes towards a more cancerous environment. Recent evidence has also shown in mouse models that extrinsic signaling by oncogenic *Kras* in epithelial cells leads to fibroblast activation and immune-suppressive myeloid cell recruitment, all before acinar-to-ductal metaplasia (ADM) formation, therefore causally linking *Kras* mutations and features of desmoplasia (Velez-Delgado et al., 2022). This collection of studies also opened the possibility that other cells within either the parenchyma or stroma supported the creation of desmoplasia, organically leading to the next question: which cells are the major contributors to the formation of desmoplasia?

C. Cancer-Associated Fibroblasts

Myofibroblasts, fibroblasts with markers and contractile nature of smooth muscles, are the keystone to wound healing and—when activated by cancer-cell derived ligands such as TGF- β —a major contributor to desmoplasia (Dimanche-Boitrel et al., 1994; Moore et al., 1989; Racine-Samson et al., 1997; Simon-Assmann et al., 1988). The same cells were also observed to precipitate desmoplastic reaction in PDAC, and the field specifically pointed to pancreatic stellate cells (PSCs, described in a later section) as the source of myofibroblasts; this initial finding was built on the basis that hepatic stellate cells (HSCs)—

a morphological and functional proxy to PSCs—were activated into myofibroblasts in hepatocellular carcinomas (HCCs) (Ooi et al., 1997; Schmitt-Gräff et al., 1991; Yen et al., 2002). To distinguish from myofibroblasts activated in wound healing circumstances or other inflammatory diseases, “cancer-associated fibroblasts” (CAFs) appeared in the literature around the early to mid-2000s to categorize myofibroblasts modified in a cancer cell-dependent manner (Micke & Tman, 2004; Rosenthal et al., 2004). Considering that cancer-associated fibroblasts are the major contributors and regulators of ECM components, CAFs clearly play a leading role in developing this desmoplastic environment. Yet for such a leading player in PDAC tumorigenesis, the multitude of nuanced functions CAFs hold leaves the field perplexed about this dynamic cell type and its potential as a therapeutic target.

I. Fibroblasts and CAFs: Back to Basics

Fibroblasts are mesenchymal cells that can originate from the mesoderm, neural crest, and bone marrow (Ogawa et al., 2006; Plikus et al., 2021); found throughout the body, these cells have a variety of functions that are dictated according to temporal and spatial residence. During development, these mesenchymal cells have conserved roles supporting homeostasis (Attali et al., 2007; Ting et al., 2005) that are preserved in adulthood to regulate tissue architecture. For example, the activation of Hedgehog (Hh) signaling pathway in *LeprB*⁺ dermal papilla fibroblasts triggers growing hair follicles (Liu et al., 2022). Fibroblastic reticular cells (FRCs) also support the immune system by providing extracellular matrix pathways in lymph nodes—as if directing traffic—creating more efficient interactions between leukocytes and antigens (Fletcher et al., 2011). In addition to these roles in healthy, non-perturbed tissues (and referred to earlier), fibroblast activation occurs to support all four phases of wound healing: hemostasis, inflammation,

proliferation, and remodeling (Gharbia et al., 2023; Schultz et al., 2011) These phases require adjustments in the ECM for proper repair.

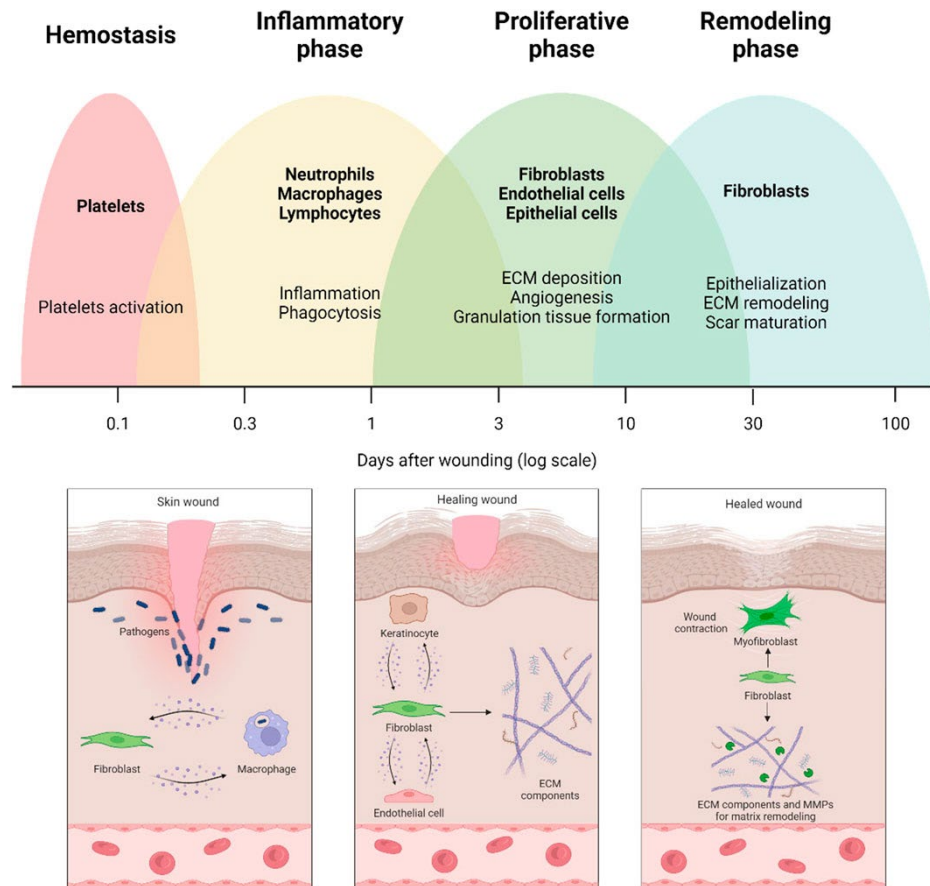


Figure 1.6. Cells in wound healing. Fibroblasts, among other cells in the wound healing process, directly and indirectly support through all four phases of wound repair. Reprinted from *Frontiers in Bioengineering and Biotechnology*, Role of fibroblasts in wound healing and tissue remodeling on Earth and in space, Cialdai, Risaliti, and Monici, 2022. Permission not required by copyright.

But in a cancer-context, CAFs are chronically activated in a dysregulated wound healing process to support tumorigenesis (Auciello et al., 2019; Dumont et al., 2013; Olivares et al., 2017). Due to their shared lineages, there is a large overlap of biomarkers between acutely activated fibroblasts for wound repair and cancer-associated fibroblasts, including fibroblast activation protein (FAP), alpha smooth muscle actin (α SMA), vimentin (VIM), and fibroblast-specific protein 1 (FSP1) (C. Han et al., 2020; Yang et al., 2023).

Naturally, many within the PDAC field proposed to ablate cancer-associated fibroblasts altogether, either through inhibition of the Hh pathway or targeted ablation of α SMA-expressing fibroblasts, hypothesizing a diminished desmoplastic reaction would improve PDAC outcomes by reducing the abundance of tumor-promoting factors CAFs produce, such as matrix components and growth factors. Unfortunately, these hypotheses were proven false with pre-clinical methods, wherein CAF ablation led to poorly differentiated tumors and shorter survival compared to control mice with PDAC, adding further confusion and complication to their functionality in the TME (Özdemir et al., 2014; Rhim et al., 2014).

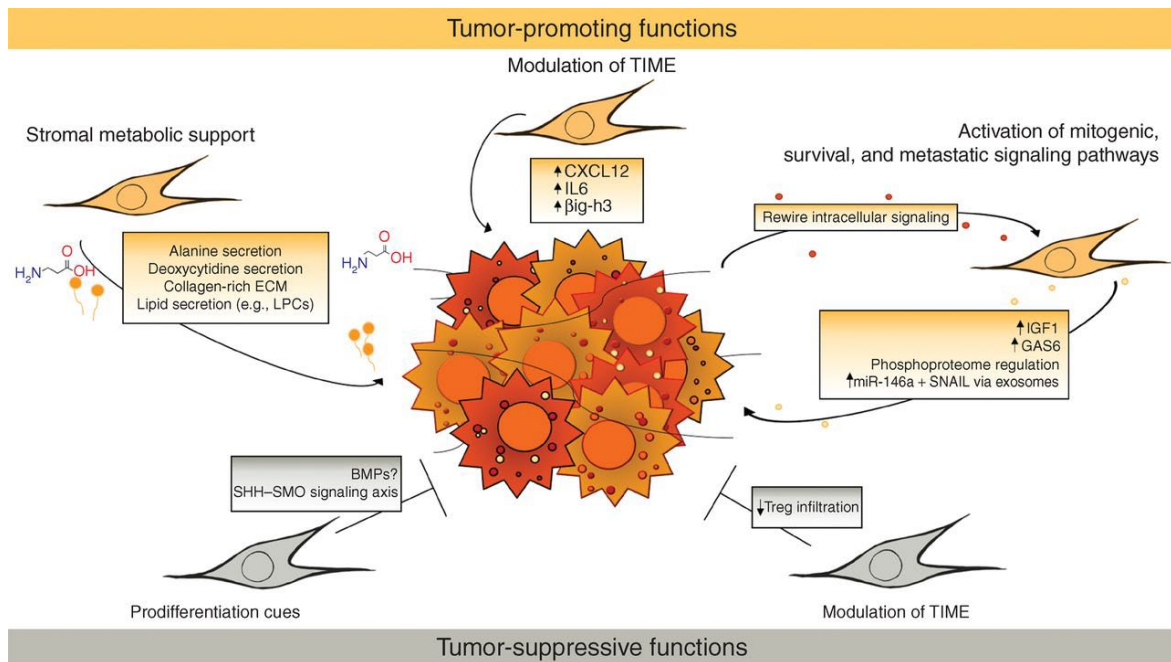


Figure 1.7. Heterogeneous functions of PDAC CAFs. Tumor-promoting functions of CAFs include metabolomic support, modulation of the tumor immune microenvironment (TIME), and activation of mitogenic, survival and metastatic signaling pathways. Tumor-suppressing functions of CAFs include pro-differentiation cues and reduction of regulatory T cells. Reprinted from Cancer Discovery, Fibroblast Heterogeneity in the Pancreatic Tumor Microenvironment, Helms, Onate, and Sherman, 2020. Permission not required by copyright.

Additionally, in stark contrast to initial findings that the Hh pathway promotes tumorigenesis and desmoplasia (Bailey et al., 2008; Thayer et al., 2003), Hedgehog

inhibitor clinical trials were largely unsuccessful (Catenacci et al., 2012; De Jesus-Acosta et al., 2020; Ko et al., 2016). In retrospect, these hypotheses were perhaps overly optimistic (or somewhat naive) as ablation of whole populations with biological functions in tissue homeostasis and wound repair might suggest that these CAFs have the potential for anti-tumorigenic functions. But at the time, CAFs were largely viewed as a monolith with the sole purpose of cancer growth. These unexpected findings illuminated the greater complexity of this cell population, warranting further investigation.

II. CAF Subtypes

In order to reconcile these seemingly incongruent findings, the scientific community collectively launched multiple studies across different cancers affected by cancer-associated fibroblasts supported by the advancement of single-cell technologies, particularly single-cell RNA sequencing (scRNA-seq). Researchers were limited by the lack of specific and all-encompassing CAF markers to capture all known and unknown CAF populations; thus cells-of-interests were negatively selected against a combination of epithelial cell adhesion molecule (EpCAM), CD45, CD31, or nerve/glia antigen 2 (NG2) in respective genetically-engineered mouse models (GEMMs) of breast cancer (MMTV-PyMT mice) and PDAC (KPC mice) (Bartoschek et al.; Elyada et al.).

Work from Elyada et al. observed what appeared to be three different CAF functional subtypes—myofibroblastic CAFs (myCAF), inflammatory CAFs (iCAF), and a novel functional subtype the authors named as antigen-presenting CAFs (apCAF). Corroborated by the same group's earlier findings (Öhlund et al., 2017), myCAF have higher gene expressions of *ACTA2* (gene for α SMA) and *TAGLN* (gene for transgelin), with differentially expressed genes directed towards smooth muscle contraction (as expected) and extracellular matrix organization, akin to myofibroblasts found in wound

healing. iCAFs, on the other hand, were distinguished with higher gene expressions of cytokine *IL6* and other inflammatory chemokines such as *CXCL1*, *CXCL2*, and *CXCL12*.

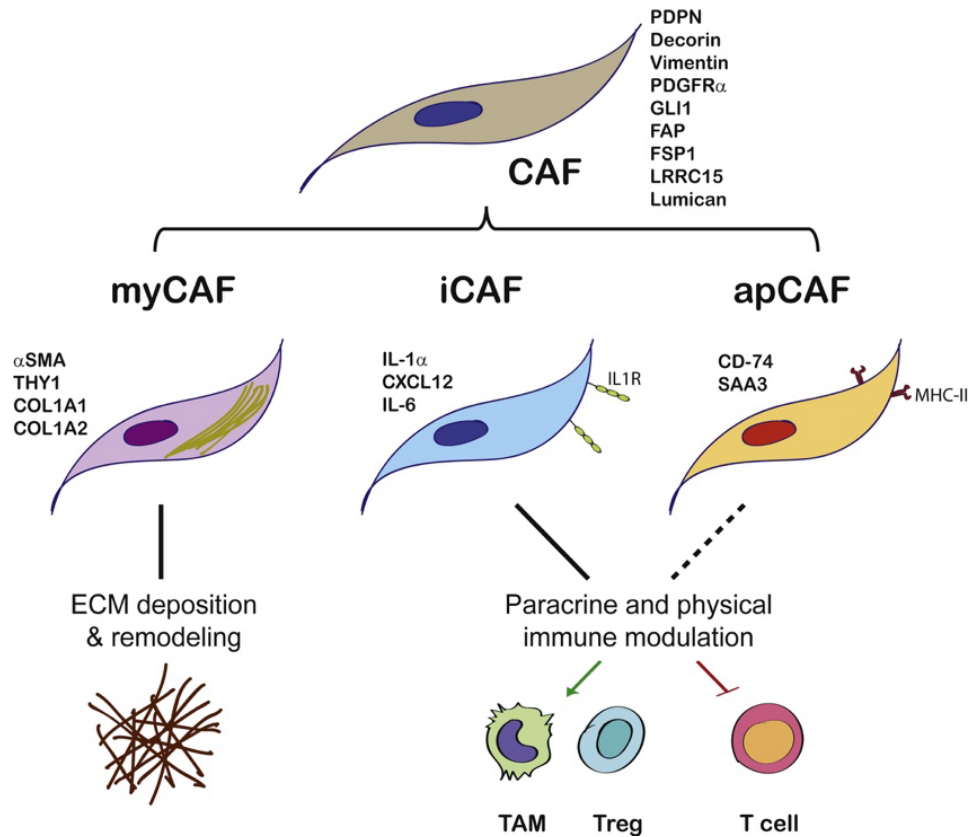


Figure 1.8. PDAC cancer-associated fibroblast subtypes. Elyada et al. categorize three different CAF subtypes based on function in murine and human PDAC: myCAFs (myofibroblastic CAFs); iCAFs (inflammatory CAFs); and apCAFs (antigen-presenting CAFs). Reprinted from Cancer Cell, Activated fibroblasts in cancer: Perspectives and challenges, Caligiuri and Tuveson, 2023. Permission not required by copyright.

Expectedly, the iCAF population was found to have upregulated gene expressions in inflammatory pathways including IL6/JAK/STAT3 and IFN- γ response. Lastly, apCAFs were distinctly clustered due to their unique expression of MHC class II family-related genes, which are found in “professional antigen-presenting cells”: dendritic cells, macrophages, and B cells (Kambayashi & Laufer, 2014). These three functional subtypes of murine PDAC CAFs were also found in human PDAC tissues.

In breast cancer, Bartoschek and colleagues also observed at least three distinct subtypes of cancer-associated fibroblasts that appear to cluster according to spatial residence and cell lineage: vascular CAFs (vCAFs), matrix CAFs (mCAFs), and developmental CAFs (dCAFs). vCAFs were labeled as such for their increased gene expressions associated with vascular regulators (e.g. *Espas1* and *Nr2f2*). This cluster also expressed genes associated with endothelial cells (e.g. *PECAM1* and *CD34*) and localized in perivascular regions, but were distinct from endothelial cells, using vCAF markers Nidogen-1 and Desmin.

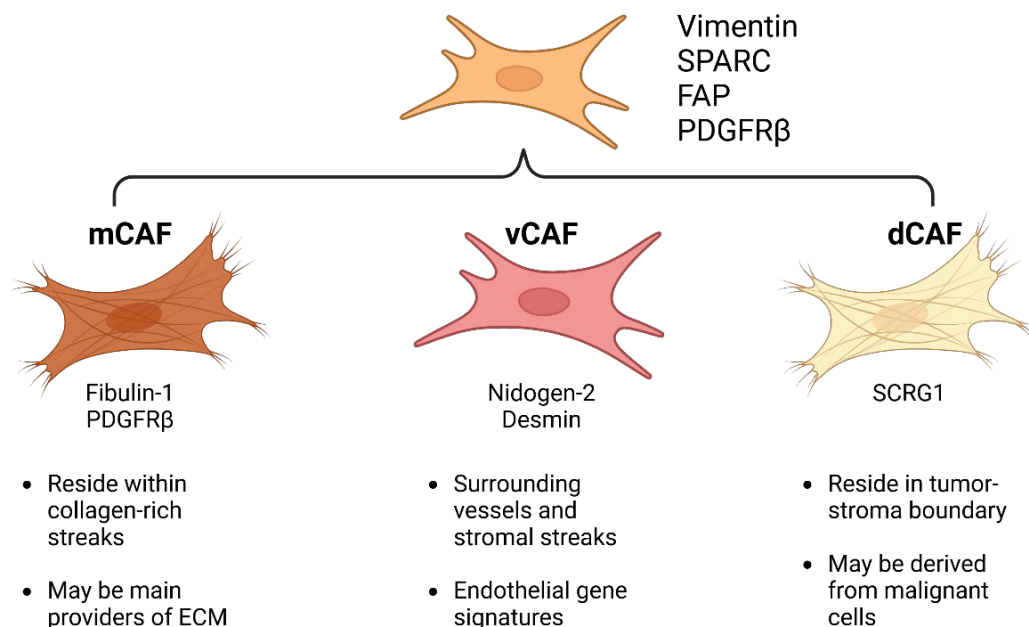


Figure 1.9. Breast cancer CAF subtypes. Bartoschek et al. categorize at least three different CAF subtypes based on biomarkers and function in murine and human breast cancer: mCAFs (matrix CAFs vCAFs (vascular CAFs); and dCAFs (developmental CAFs). Created with Biorender.

The authors also observed greater abundance of vCAFs at the tumor core of MMTV-PyMT mice in contrast to the tumor periphery as the cancer progressed. mCAFs are discrete from vCAFs as they express ECM-associated genes including *Lum*, *Col14a1*, *Fbln1*, and *Lox*. Additionally, the authors showed that 89% of fibroblasts from healthy murine

mammary glands expressed mCAF markers (Fibulin-1 and PDGFR α), and are markedly reduced as murine breast cancer develops, implicating an inverse relationship between mCAFs and vCAFs. Lastly, developmental CAFs expressed ECM-associated genes distinct from mCAF ECM-associated genes and possessed gene expressions geared towards the epithelial compartment.

While the mCAF subtype found in Bartoschek and colleagues' work appears analogous to the myCAF subtype found in Öhlund's and Elyada's works, intriguingly mCAFs in breast cancer also expressed chemokine *CXCL14*, indicating that this CAF subtype could impact immune response—a function that Öhlund's and Elyada's findings more assign to the inflammatory CAFs. Other works related to CAFs in different cancers resulted in similar findings to Öhlund's and Elyada's myCAF/iCAF categorization (Forsthuber et al., 2024), but due to Bartoschek et al., it is plausible that these CAF functional subtypes are dynamic (possibly transient) rather than fixed, and are dependent upon tissue, spatial, temporal, and ancestral cues.

III. CAF Lineages

Simultaneously, others in the field sought to investigate cancer-associated fibroblast lineages as a potential means to explain the heterogeneity previously observed. In PDAC, CAFs were originally thought to derive from only pancreatic stellate cells (PSCs), but the past decade has challenged this belief. Previous work from Sherman and colleagues focused on fatty acid binding protein 4 (*Fabp4*) as a novel marker for pancreatic stellate cells (Sherman et al., 2014). This seminal discovery led to the establishment of *Fabp4-Cre;Rosa^{mTmG}* GEMM, which lineage trace PSCs with green fluorescent protein (GFP); from this, researchers observed that, using podoplanin (PDPN) or platelet-derived growth

factor receptor alpha (PDGFR α) as pan-CAF markers, only a minority of PDAC CAFs were derived from PSCs, and corroborated in human PDC, much to the field's surprise (Helms et al., 2022). Helms's study also included the specific ablation of PSC-derived CAFs in orthotopic models of murine PDAC to understand its impact in tumorigenesis and observed reduced tissue stiffness due to decreased abundance of ECM components such as tenascin C. This suggested that different CAF lineages may have specific roles within the tumor microenvironment that cannot necessarily be fulfilled by CAFs of other origins. The authors did note a difference in PSC-derived CAF frequencies between p53-mutated murine PDAC (i.e. R172H) versus p53-null murine PDAC; hence, CAF cell-of-origin alone is insufficient to explain CAF heterogeneity.

Coinciding studies from Marina Pasca di Magliano's group also analyzed pancreatic CAFs with sophisticated dual-recombinase GEMMs, focusing on Gli1 and Hoxb6 as fibroblast markers (Garcia et al., 2020). The authors selected these markers as they were earlier established to express in subpopulations of normal fibroblast in the pancreas (Larsen et al., 2015; Mathew et al., 2014). Garcia and colleagues showed that 1) Gli1+ and Hoxb6+ fibroblasts reside in different, seemingly non-overlapping regions of the pancreas; and 2) not all resident fibroblasts in the pancreas activate in PDAC, as Gli1+ fibroblasts expanded and transitioned to CAFs in mPDAC whereas Hoxb6+ fibroblasts did not. In a *KPF;Gli1^{CreER};RYFP* GEMM, wherein mice have *Kras^{G12D}* and *p53* null mutations, Gli1+ fibroblasts contributed to an average of 70% of PDAC cancer-associated fibroblasts (using α SMA to distinguish CAFs).

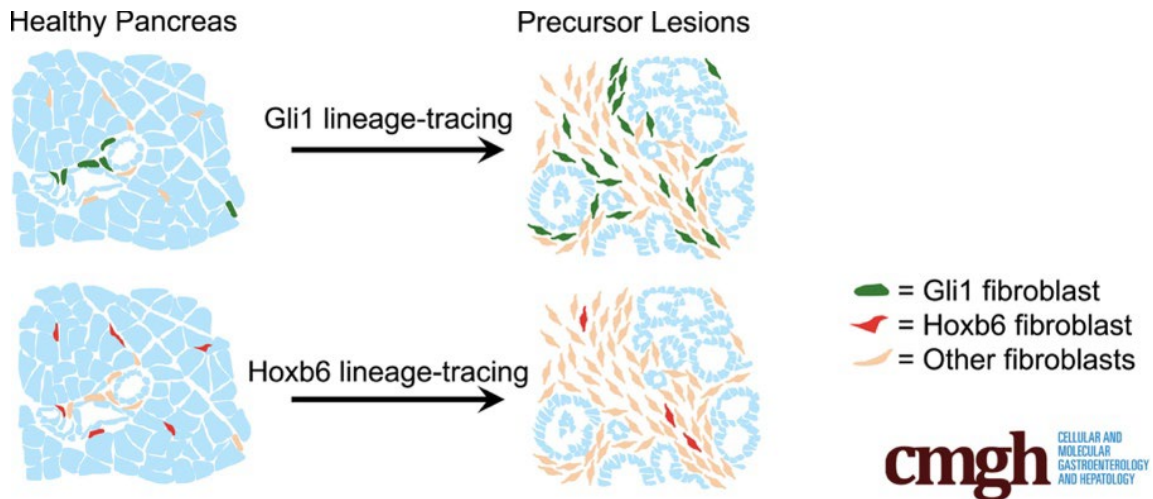


Figure 1.10. Contributions of Gli1+ and Hoxb6+ fibroblasts in healthy murine pancreas and murine PDAC. Lineage-tracing of Gli1+ and Hoxb6+ fibroblasts from murine healthy pancreas to PDAC tumorigenesis showed different spatial and numerical contributions in normal mesenchyme and cancer-associated mesenchyme. Reprinted from Cellular and Molecular Gastroenterology and Hepatology, Differential Contributions of Pancreatic Fibroblast Subsets to the Pancreatic Cancer Stroma, Garcia et al., 2020. Permission not required by copyright.

These Gli1+ cells also happen to reside near the vasculature and ductal cells. On the other hand, Hoxb6+ fibroblasts were dispersed throughout the pancreas. Additionally, in a murine PanIN model (i.e. pancreatitis-induced KF GEMM), only 2% of platelet-derived growth factor beta (PDGFR β +) positive activated fibroblasts were Hoxb6+, while 14% of PDGFR β + were double-positive for Gli1+. Lastly, not all Gli1+ fibroblasts in early pancreatic lesions were α SMA+, nor were all α SMA+ cells double positive for Gli1+, indicating other resident fibroblasts—including Gli1+ fibroblasts—give rise to myCAFs at the earlier stages of tumorigenesis. Extensive work from Helms and Garcia ultimately showed that 1) PSCs were only one of the fibroblast lineages that contribute to PDAC CAFs; 2) different CAF lineages may have overlapping functions with one another with respect to their spatial organization within the pancreas and proximity to cancer cells (hence some can appear myCAF, iCAF, or apCAF); and, 3) unique CAF functions may be partially derived from their lineage.

Although not fully discussed, both works indicated that CAF heterogeneity can also be explained by varied concentrations of signaling gradients (Steele et al., 2021) or by tumor genotype (Vennin et al., 2019). Rather than viewing CAF functional subtypes and CAF lineages as mutually exclusive phenomena, both perspectives can elucidate the heterogeneity the field has observed over the past two decades. For the purposes of this dissertation, the focus will be given to pancreatic stellate cells and their prospective specific functions within the PDAC milieu.

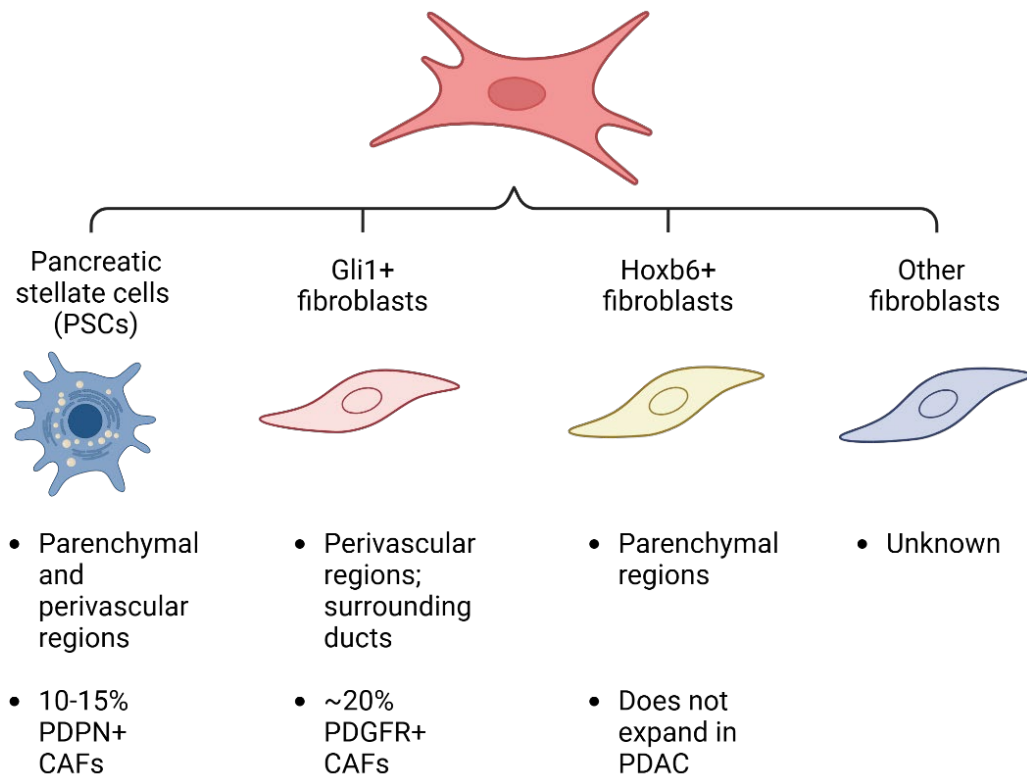


Figure 1.11. Fibroblast lineages in healthy murine pancreas and their contributions to the murine PDAC CAF population. Pancreatic stellate cells (PSCs), Gli1+ fibroblasts, and Hoxb6+ fibroblasts, potentially with other resident fibroblasts, coexist within the parenchymal and perivascular regions of murine pancreas. In PDAC, these fibroblasts have varying numerical contributions to the CAF population. Created with Biorender.

D. Stellate Cells: A “fibroblast” and beyond

Stellate cells in the liver and pancreas are aptly named for their star-like appearance. First discovered in the liver by Carl von Kupffer in 1876 (Geerts, 2001; Kupffer, 1876), these cells store lipid droplets that were confirmed a century later to be vitamin A in the form of retinyl esters (Blomhoff et al., 1985; Wake, 1971). This unique feature not found in other fibroblasts-like or mesenchymal cells enabled scientists to study these cells *in vitro* by isolating hepatic stellate cells (HSCs) from rat, mouse, and human through density gradient centrifugation (Chen et al., 1989; Friedman et al., 1992; Margreet Leeuw et al., 1984). In an *in vitro* setting, HSCs from all three species lost their lipid droplets and, over time in culture, acquired a myofibroblastic phenotype, producing collagen IV, laminin, other ECM proteins, and matrix metalloproteinases (MMPs) (Geerts et al., 1989; Sherman, 2018), hinting at their function in extracellular matrix production, maintenance, and liver fibrosis.

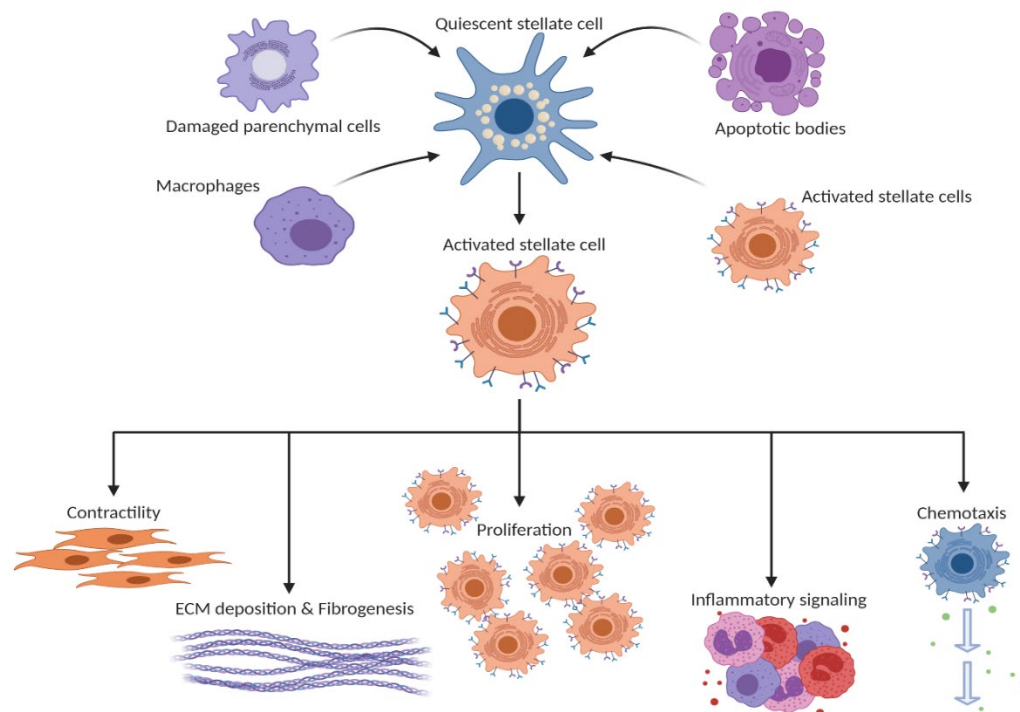


Figure 1.12. Stellate cell functions. Pancreatic and hepatic stellate cells (PSCs and HSCs), in the context of wound healing and cancer, release their lipid droplets and produce a fibro-inflammatory response akin to other fibroblasts, including ECM deposition and inflammatory signaling. Created with Biorender.

As a result, scientists hypothesized that stellate cells may also explain pancreatic fibrosis, leading to the discovery of pancreatic stellate cells (PSCs) (Apte et al., 1998). Whilst stellate cells do express FAP like other fibroblasts (X. M. Wang et al., 2005), hinting functional similarities to one another, as of 2024 there appears to be no other vitamin A-storing stellate cell in other organs, which suggests unique ancestral origins and functions in comparison to other fibroblasts.

I. Pancreatic Stellate Cells

Pancreatic stellate cells are quiescent tissue-resident mesenchymal cells consisting of about 4% of the normal pancreas and appear to be distributed throughout the organ (Jaster, 2004). Based on pancreatitis and PDAC studies, PSCs can be activated from their normal quiescent state through TGF β /SMAD, mitogen-activated protein kinase (MAPK), phosphoinositide 3-kinase (PI3K), and Hh signaling pathways (Masamune & Shimosegawa, 2009). Within the TGF β /SMAD signaling pathway, Galectin-1 and Hic-5 have been found to support the activation of PSCs (L. Gao et al., 2020; Tang et al., 2018). Other growth factors and cytokines including PDGFs, tumor necrosis factor-alpha (TNF α), and interleukins 1 and 6 (IL-1 and IL-6, respectively) also awaken PSCs to manifest its fibrotic nature (Apte et al., 1999; Mews et al., 2002; Schneider et al., 2001). Specific functions of PSCs have been illuminated through studies in fibrosis, in both pancreatitis and cancer. *In vivo* pancreatitis models have shown acinar cell-derived TGF β activates PSCs to produce type I collagen, and confirmed in human tissue (Haber et al., 1999). Highlighting their wound healing capacity, activated PSCs have also been shown to contribute to pancreatic regeneration after acute pancreatitis (Zimmermann et al., 2002). In cancer, PSC tumor-promoting roles include PSC-mediated alanine secretion to support cancer cell-metabolism and PSC-derived extracellular vesicles (EVs) with components

upregulating proliferation and migration (Sarkar et al., 2023; Sousa et al., 2016). PSCs and HSCs both exhibit myofibroblastic features when activated, but to truly address if PSCs and HSCs functioned alike, Buchholz and colleagues analyzed primary human HSCs, PSCs, and skin fibroblasts through RNA oligonucleotide micro-arrays (Buchholz et al., 2005). Human HSCs and PSCs had only 29 differentially expressed genes (DEGs), while skin fibroblasts had 88 and 73 DEGs between HSCs and PSCs, respectively. There were also 36 differentially expressed genes that were found in both HSCs and PSCs that were not expressed in skin fibroblasts, e.g. collagen 3 α 1 (COL3A1), collagen 4 α 1 (COL4A1), and netrin 4 (NTN4). In contrast, forkhead box F1 (FOXF1) and IKAROS family zinc finger 5 (IKZF5) were overexpressed only in HSCs, while HIF1A was overexpressed in PSCs. Even lecithin retinol acyltransferase (LRAT), the most robust lineage tracing model for hepatic stellate cells, is strangely not expressed in PSCs (Mederacke et al., 2013; Sherman et al., 2014).

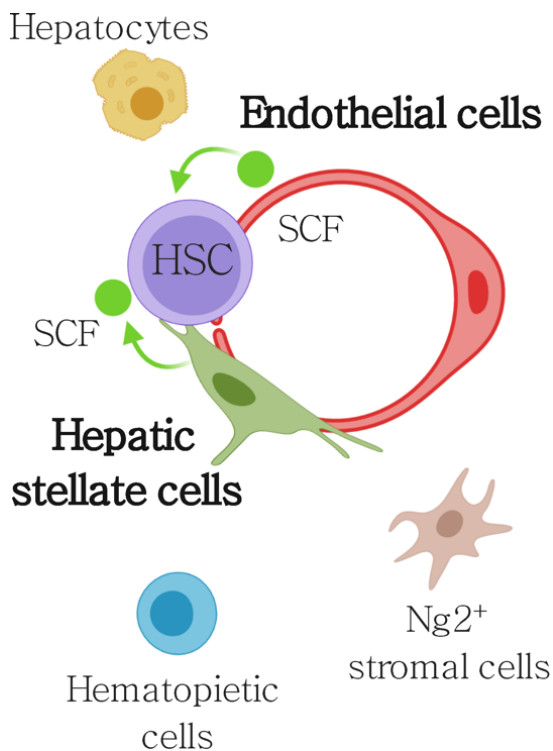


Figure 1.13. Hematopoietic stem cells require KITL/SCF from the perisinusoidal niche in the developing liver.

Hepatic stellate cells and endothelial cells in the perisinusoidal space are necessary to maintain hematopoietic stem cells the developing mouse. Reprinted from Journal of Experimental Medicine, Hepatic stellate and endothelial cells maintain hematopoietic stem cells in the developing liver, Lee et al., 2020, with permission from Rockefeller University Press.

A unique function of HSCs not shared by PSCs is their ability to maintain hematopoietic stem cells in the developing liver (Lee et al., 2020). The bone marrow perivascular niche maintains hematopoietic

stem cells in adults, which include endothelial cells, perivascular stromal cells, and leptin receptor positive (LEPR+) mesenchymal cells through the expression of either CXCL12 or kit ligand (KITL), also known as stem cell factor (SCF) (Comazzetto et al., 2019; Ding et al., 2012; Ding & Morrison, 2013; Greenbaum et al., 2013).

But *in utero*, the liver is the primary organ responsible for hematopoietic stem cell expansion and maturity (Mikkola & Orkin, 2006). However, it was unclear as to which cells supported this particular function. Lee and colleagues were able to parse through genetically modified mouse models and flow cytometry that, similar in the bone marrow niche, immature hematopoietic stem cells require KITL/SCF. More importantly, hepatic stellate cells and endothelial cells within the perisinusoidal space are the main providers of KITL/SCF, and hematopoietic stem cells require KITL/SCF from both sources. Considering the tantalizing amount of literature highlighting the similarities and differences between these sibling cells, it is a fascinating time to hypothesize what seemingly discrete roles each cell plays in their respective organs-of-residence that may be applied to the other cell, in a different context. Pancreatic stellate cells do not have any association with hematopoietic stem cell maintenance, but it is understandable to suspect that PSCs express KITL/SCF—at least transiently—for the purposes of pancreatic development and homeostasis.

E. KITL/SCF and c-KIT signaling pathway

c-KIT was discovered through its retrovirus. *v-kit*, found in the Hardy-Zuckerman 4 feline sarcoma virus, has structural features reflective of receptor tyrosine kinases (RTKs), which hinted at its cellular origin (Besmer et al., 1986). A year later it was discovered to share sequences with human proto-oncogene *c-KIT*, officially symbolized as *KIT* (Yarden et al.,

1987). Its murine ortholog was discovered whilst studying mutations affecting embryonic development and hematopoiesis, which coincided with additional unexpected phenotypes such as a white coat color and sterility (Geissler et al., 1988). Soon after, scientists discovered kit ligand (KITL), also known as stem cell factor (SCF), when it was shown that mice that harbored c-KIT mutations expressed the same or similar phenotypic alterations in mice that harbored mutations found in the *Sf* locus (Copeland et al., 1990; Williams et al., 1990; Zsebo et al., 1990).

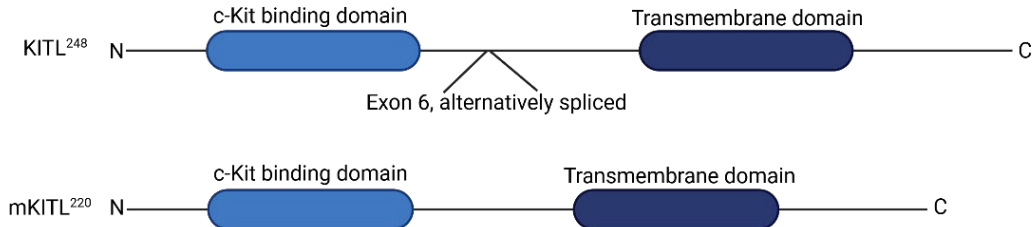
I. KITL/SCF

Typically expressed in fibroblasts and endothelial cells, Kit ligand/stem cell factor has a total of nine exons (conserved among rat, mouse, and human species) that can be alternatively spliced at its sixth exon; an unspliced *KITL* mRNA maintains a proteolytic cleavage site that produces a soluble isoform, while an alternatively spliced mRNA produces a membrane-bound isoform (Lennartsson & Rönstrand, 2012; Martin et al., 1990). Both isoforms activate the c-KIT signaling pathway to varying degrees of signal strength. For example, *in vitro* studies have shown that both soluble and membrane-bound KITL/SCF support hematopoietic expansion; however, the membrane-bound KITL/SCF from a murine stromal cell line continued to maintain hematopoietic progenitor cells significantly longer than soluble KITL/SCF (Toksoz et al., 1992).

KITL/SCF expression, similar to all other genes, is regulated by a series of combinatorial mechanisms that include *cis*-acting factors (i.e. mechanisms that affect genes within the same locus, such as promoters, enhancers, silencers, and epigenetic marks) and *trans*-acting factors (i.e. mechanisms that affect genes throughout the entire genome, such as transcription factors, histone acetyltransferases, and histone deacetylases). Both factors,

which are affected by cell-intrinsic and cell-extrinsic mechanisms, can express or repress gene expression depending upon the factors that come into play.

Creation of membrane-bound KITL



Creation of Soluble KITL

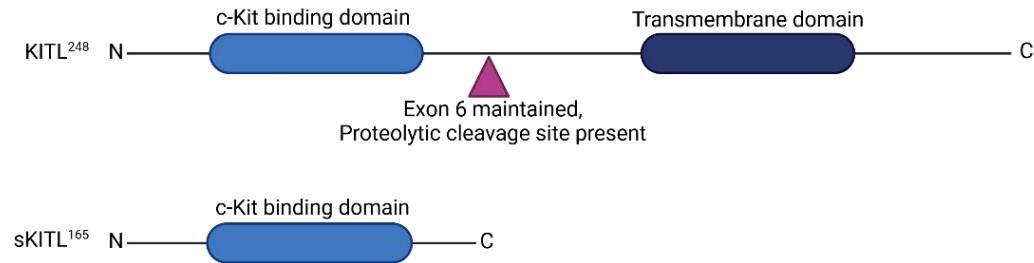


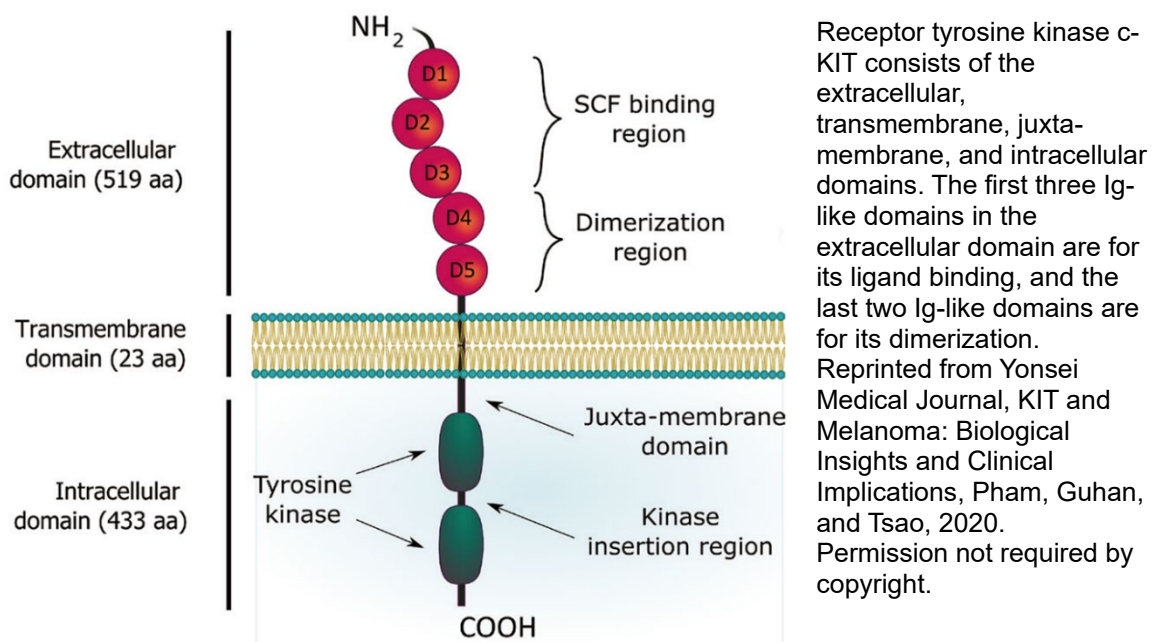
Figure 1.14. Structure of membrane-bound and soluble KITL/SCF. Kit ligand (or stem cell factor) can exist either in membrane-bound form or in soluble isoform, depending on its mRNA splice variant. Membrane-bound *KITL* mRNA is alternatively sliced in exon 6, whereas soluble *KITL* mRNA is not. Adapted from Lennartsson and Rönstrand, 2012. Created with Biorender.

Upstream of the *KITL/SCF* transcription initiation site are *cis*-acting transcription factor binding motifs: 1) a TATA box consensus sequence; and 2) three overlapping GGCGGG motifs; these two motifs are binding sites for transcription factors Transcription Factor II D (shortened as TFIID, a general transcription factor) and SP1, respectively ¹³². Although a TATA box is not necessary to initiate transcription, this sequencing motif allows greater stabilization of TFIID to land at the intended genomic site to further support the RNA Polymerase II preinitiation complex, suggesting the importance of *KITL/SCF* expression. SP1, while also a ubiquitously expressed transcription factor, is associated with tissue-

specific changes in hematopoiesis (Gilmour et al., 2014), further linking KITL/SCF in hematopoietic development. It has also been shown that HIF-1 α and transcription factor POU3F2 can also upregulate its expression (Z.-B. Han et al., 2008; Kobi et al., 2010); and, in normoxia, KITL/SCF can induce HIF-1 α in hematopoietic cells (Pedersen et al., 2008), suggesting a potential positive feedback loop between KITL/SCF and HIF-1 α .

II. C-KIT

Figure 1.15. Structure of c-KIT receptor.



C-KIT belongs to the type III receptor tyrosine kinase family, also known as the PDGF family, and consists of four domains: extracellular, transmembrane, juxtamembrane, and intracellular. Its extracellular domain comprises five immunoglobulin-like (Ig-like) domains, with domains 4 and 5 supporting its dimerization process when in contact with KITL/SCF. The two subdomains found at the intracellular level, tyrosine kinase domain 1 and 2, are separated by a kinase insert sequence. Like its ligand, this RTK has alternative splicing regions, producing at least four known isoforms in humans and two known isoforms in mice, but the impacts of these isoforms are still debated. The mechanisms of

c-KIT gene expression are nuanced as its promoter regions include one Myb binding motif that appears to be essential for c-KIT expression, and another that represses expression (Vandenbark et al., 1996). Additionally, interaction between cyclin-dependent kinase p21 and transcriptional repressor Zbtb18 have been shown to co-suppress c-KIT expression in hematopoietic stem cells (N. Wang et al., 2024).

III. Signaling Cascade

The c-KIT signaling cascade requires two c-KIT monomers, using its Ig-like domains 1 through 3, to tightly bind to a KITL/SCF homodimer (Reber et al., 2006). c-KIT Ig-like subdomains 4 and 5 come together from each monomer to stabilize this structure, improving intracellular domain protein interactions where the tyrosine kinase regions reside, allowing for efficient activation and transphosphorylation (Philo et al., 1996). There are currently eight known tyrosine phosphorylation sites (Feng et al., 2015). Initiating site Y568 can bind to the Src family kinases, CBL, SHP2, LNK, and APS; and initiating site Y570 binds to SHP1. Sites Y703 (binding partner of GRB2), Y721 (binds to PI3K subunits p85 and p110), and Y730 (binds to PLC-gamma) are located in the kinase insert sequence. Sites Y823 and Y900, which also interact with the Src family kinases, are found in the last tyrosine kinase domain near its carboxyterminal tail. All phosphorylation sites activate downstream signaling pathways: Y703 further activates the MAPK signaling pathway; Y721 and Y900 activates the PI3K pathway; and Y730 activates the PLC-gamma and JAK-STAT pathways.

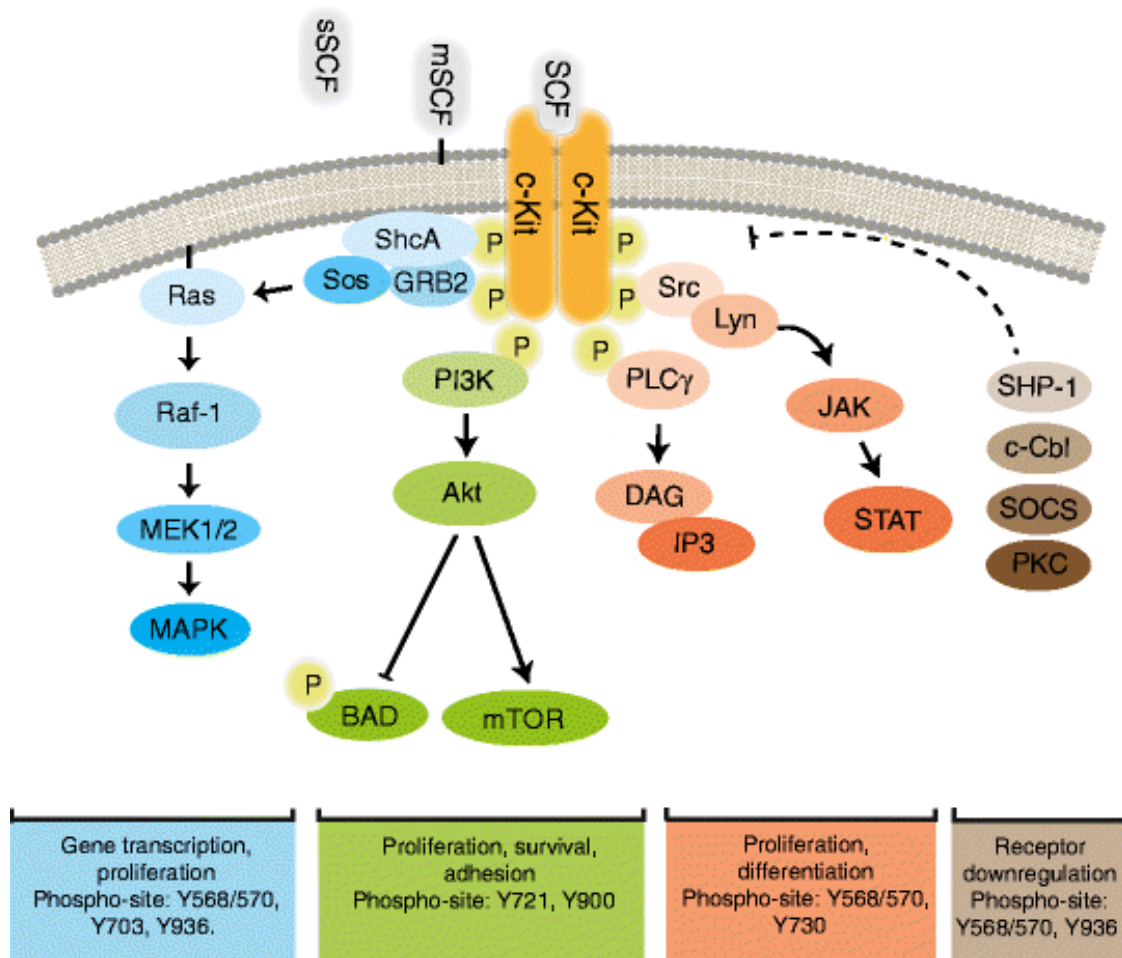


Figure 1.16. c-KIT signaling cascade and phosphorylation sites. Dimerization of c-KIT after binding to KITL/SCF activates downstream signaling pathways associated with cellular processes such as gene transcription (MAPK pathway), proliferation (MAPK, PI3K, PLC γ , JAK-STAT), survival (PI3K), adhesion (PI3K), and differentiation (PLC γ and JAK-STAT). c-KIT signaling is downregulated by the SHP-1 pathway. Reprinted from *Diabetologica, A survival Kit for pancreatic beta cells: stem cell factor and c-KIT receptor tyrosine kinase*, Feng et al., 2015, with permission from Springer Nature.

Initiating sites Y568 and Y570 have dual roles by both interacting with all the above pathways associated with proliferation, differentiation, apoptosis inhibition, and survival, as well as its own receptor downregulation (Wollberg et al., 2003). The last c-KIT phosphorylation site Y936, found in its carboxyterminal trail, has also been associated with receptor downregulation (Masson et al., 2006).

IV. Roles in Tissue Development and Homeostasis

The c-KIT signal transduction pathway has been implicated in hematopoiesis, angiogenesis, pigmentation, reproduction, and regeneration. This transduction pathway has been reported to support in capillary tube formation of human umbilical vein endothelial cells specifically through the PI3K/AKT and ERK1/2 pathways (Matsui et al., 2004). In liver regeneration, c-KIT-mediated signal transduction triggers hepatocyte and bile epithelial cell production (Matsusaka et al., 1999). c-KIT⁺ hepatocytes increased in number after partial hepatectomy, that coincided with an increase of binuclear hepatocytes as part of the liver's regeneration process (Yushkov et al., 2011). More importantly, there is growing evidence for its role in pancreatic tissue maturation. In human fetal pancreatic development, c-KIT⁺ cells also expressed cytokeratin 19 (a ductal marker), and appeared to reside in ductal regions and islet clusters, while its ligand was expressed throughout the entire organ (Li et al., 2006), upon analysis of isolated human islet-epithelial clusters. Additionally, the authors observed that *in vitro* the KITL/c-KIT axis increases islet-epithelial cluster proliferation and differentiation, by the enhancement of Pdx-1 gene and protein expression, and by activation of the Akt-phosphorylation pathway. Other *in vitro* studies have also highlighted this pathway's capacity to promote beta cell differentiation and regeneration (Gong et al., 2012; Rachdi et al., 2001).

V. Roles in Cancer

The c-KIT signaling pathway is known mostly for its oncogenic properties. Cancers impacted by c-KIT include gastrointestinal stromal tumors (GIST), melanoma, small cell lung carcinoma, testicular carcinoma, acute and chronic myeloid leukemia (AML/CML), chronic, and mastocytosis. These cancers either have overexpression of c-KIT receptor or constitutively activating mutations of c-KIT, eliminating the use of its ligand. However, GIST still produce soluble KITL/SCF, which may select for weaker activating c-KIT

mutations in exon 11 (Théou-Anton et al., 2006). Imatinib was the first tyrosine kinase inhibitor used for CML treatment, aimed to target BCR-ABL fusion protein and PDGF receptors. Since c-KIT is part of the PDGF kinase family, it was hypothesized that imatinib may also be effective for GIST patients (Demetri et al., 2002; Heinrich et al., 2000). Imatinib successfully inhibited wild-type c-KIT and some exon 11 mutations, but other mutations were resistant (Frost et al., 2002).

F. Rationale and Hypothesis

There are limited effective treatments for pancreatic ductal adenocarcinoma due to its immunosuppressive fibrotic nature, as well as limited opportunities for early intervention. Therapeutic potential may lie in cancer-associated fibroblasts, which are the main effectors of pancreatic desmoplasia, with both pro- and anti-tumorigenic functions. However, successful development of therapies requires understanding of precise mechanisms that underlie the varying functions of CAFs. Pancreatic stellate cell-derived CAFs, although a minor contributor to the total PDAC CAF population in both murine and human PDAC, show non-redundant functions in comparison to alternatively derived tissue resident CAFs, suggesting mesenchymal lineage can also impact CAF functions.

Hepatic stellate cells are the only other stellate cells existing outside of the pancreas. Its lipid-storing properties and shared myofibroblastic phenotype in fibrosis implies shared ancestral origins, with further implications regarding other functions. In the liver, hepatic stellate cell-derived Kit ligand (also known as stem cell factor) plays a significant role in the expansion and maintenance of hematopoietic stem cells during development. The KITL/c-KIT signaling pathway is also important in the organization of pancreatic development, wherein neuroendocrine cells in the pancreas require c-KIT signaling

transduction for beta cells differentiation. However, it is unclear whether pancreatic stellate cells express KITL and for what purpose.

We hypothesize that pancreatic stellate cells in healthy pancreas express KITL and its expression supports the maintenance of healthy tissue homeostasis through paracrine interactions with ductal and endothelial cells. Additionally, we hypothesize that activation of pancreatic stellate cells during tumorigenesis leads to KITL loss. Therefore, ablation of PSC-derived KITL may lead to more aggressive tumor growth. We will investigate PSC functions by comparing PSCs in healthy and tumor pancreata at tissue and single cell resolution.

Chapter II.

Impacts of Mesenchymal KITL in Pancreatic Tissue Homeostasis and Pancreatic Ductal Adenocarcinoma

A. Abstract

Components of normal tissue architecture serve as barriers to tumor progression. Inflammatory and wound-healing programs are requisite features of solid tumorigenesis, wherein alterations to immune and non-immune stromal elements enable loss of homeostasis during tumor onset. The precise mechanisms by which normal stromal cell states limit tissue plasticity and tumorigenesis, and which are lost during tumor progression, remain largely unknown. Here we show that healthy pancreatic mesenchyme expresses the paracrine signaling molecule kit ligand (shortened as KITL, also known as stem cell factor), and identify loss of mesenchymal KITL during tumorigenesis as tumor-promoting. Genetic inhibition of mesenchymal KITL in the contexts of health, injury, and cancer together indicate a role for KITL signaling in maintenance of pancreas tissue architecture, such that loss of the stromal KITL pool increased tumor growth and reduced survival of tumor-bearing mice. Together, these findings implicate loss of mesenchymal KITL as a mechanism for establishing a tumor-permissive microenvironment.

This chapter is adapted from a manuscript published in bioRxiv (2024) and published in *Cancer Discovery* (2025) as a Brief Report titled, “Stromal KITL/SCF maintains pancreas tissue homeostasis and restrains tumor progression.”

M. Kathrina Oñate, Chet Oon, Sohinee Bhattacharyya, Vivien Low, Canping Chen, Xiaofan Zhao, Frank Arnold, Ziqiao Yan, Sneha Pramod, Yan Hang, Yu-Jui Ho, Scott W. Lowe, Seung K. Kim, Zheng Xia, Mara H. Sherman. doi: <https://doi.org/10.1158/2159-8290.CD-24-1079>.

B. Introduction

While much of cancer research has been directed toward illuminating genetic, epigenetic, cellular, and tissue-level mechanisms of tumor progression (Guedj et al., 2012; Jakobsen et al., 2024; Salas-Escabillas et al., 2024; Schwitalla et al., 2013; Shiozawa et al., 2011; P. Wang et al., 2017), there is an increasing appreciation for the mechanisms of tissue homeostasis as a means of tumor restraint. Mechanisms maintaining tissue homeostasis and limiting tumorigenesis include epithelial-epithelial interactions, such as regenerative or competitive epithelial functions (Brown et al., 2017; Gallini et al., 2023; Pineda et al., 2019); epithelial-immune interactions, wherein innate (Blaisdell et al., 2015; Cui Zhou et al., 2022) or adaptive (DuPage et al., 2011; Goto et al., 2024) immune cells clear mutated cells or early pre-invasive lesions; and, epithelial-mesenchymal interactions, with evidence that mesenchymal elements like normal tissue fibroblasts can restrain growth of transformed epithelial cells (Brügger et al., 2020; Cukierman, 2021; Kaukonen et al., 2016). These epithelial cell-extrinsic processes through juxtacrine or paracrine signaling collaborate with epithelial cell-intrinsic tumor suppressor gene products to synergize a combination of genetic, cellular, and tissue-level checks and balances on cancer development. Literature in the past two decades has paid particular attention in understanding both the epithelial cell-intrinsic mechanisms of tumor suppression and the anti-tumor functions of the innate and adaptive immune systems. However, mechanisms on the tumor restraining potential of the normal mesenchyme largely have not been identified.

Fibro-inflammatory reactions induced by the tissue mesenchyme alter tissues towards a tumor-permissive state (Mueller & Fusenig, 2004; Quail & Joyce, 2013). Local or systemic cues, including paracrine signaling from transformed epithelial cells or diverse sources of tissue damage, cause alterations to resident mesenchymal cells—such as the transition

from quiescent fibroblasts to activated myofibroblasts—and changes to or accumulation of immune cells. This wound healing reaction can promote plasticity in the epithelial compartment and overcome intrinsic barriers to tumor formation and growth (Gupta et al., 2019). Though normal primary fibroblasts can suppress hyperplastic growth of mammary epithelial cells *in vivo*, tumor outgrowth is supported by activated, myofibroblastic stroma (M. Hu et al., 2008; Kuperwasser et al., 2004). The causality between inflammation and cancer has been appreciated for some time (Tlsty & Coussens, 2006), and recent studies of patient tissues have begun to identify specific mechanisms by which inflammatory insults promote cancer development. For example, environmental pollutants result in an accumulation of IL-1 β producing macrophages in the lung, and this inflammatory signaling drives plasticity in the lung epithelium to promote tumorigenesis (Hill et al., 2023). Further study of the specific signals engaged by healthy or inflamed tissue components to restrain or promote tumorigenesis, respectively, may point to new avenues for early cancer intervention.

The recent discovery that normal, adult human pancreas tissue harbors up to hundreds of *KRAS* mutant pre-invasive lesions impels the field to understand intracellular and intercellular mechanisms restraining neoplastic progression in the pancreas (Braxton et al., 2024; Carpenter et al., 2023). To assess a role for mesenchymal cell state alterations in the transition from a homeostatic to tumor-permissive tissue context, we performed transcriptional profiling of healthy and cancer-associated pancreatic mesenchyme using an established fate mapping mouse model (Helms et al., 2022). These experiments focused on pancreatic stellate cells (PSCs), tissue-resident mesenchymal cells that serve as cells of origin for a sub-population of PDAC CAFs.

We found that this mesenchymal lineage in normal human and murine pancreas tissue expresses KITL—this lineage has lipid storage capacity and co-expresses the leptin receptor (LEPR), with parallels to LEPR-positive mesenchyme previously implicated in tissue homeostasis in the bone marrow (Ding et al., 2012) and brown adipose tissue (Haberman et al., 2024). Mesenchymal KITL expression is lost during tumor evolution and acquisition of a cancer associated fibroblast (CAF) stromal phenotype, with functional significance for tissue state and tumorigenic potential.

C. Contributions

Figure 1:

A, B, C, and E were designed, performed, and quantified M.K. Oñate

D and F were performed by S. Bhattacharyya

Figure 2:

A, B, C, and D were performed and analyzed by C. Chen (*in silico*), M.K. Oñate (*in vivo*), and X. Zhao (*in silico*)

E was performed by C. Oon; analyzed by C. Oon and F. Arnold; quantified by C. Oon

F was performed and analyzed by C. Oon and S. Pramod

G, H, and I were performed, analyzed, and quantified by S. Bhattacharyya

J, K, and L performed by S. Bhattacharyya; analyzed and quantified by M.K. Oñate

M was performed by W. Kang (MSKCC Molecular Cytology); designed and quantified by M.K. Oñate

N and O were performed by M.K. Oñate

Figure 3:

A, B, and C were performed and analyzed by C. Oon, with support from Azenta Life Sciences

D and E were performed, analyzed, and quantified by Y. Han and Z. Yan

F, G, H, J, K and L were performed and quantified by S. Bhattacharyya

I was performed by S. Bhattacharya and M.K. Oñate

Figure 4 was performed, analyzed, and quantified by M.K. Oñate

Supplementary Figure 1:

A and E were performed and analyzed by C. Chen (*in silico*), M.K. Oñate (*in vivo*), and X. Zhao (*in silico*)

B, C, and F were performed by S. Bhattacharyya

D was performed and analyzed by Y. Ho

Supplementary Figure 2:

A was performed and analyzed by C. Chen, M.K. Oñate (*in vivo*), and X. Zhao

B, C, and D were performed by C. Oon; analyzed by C. Oon and F. Arnold; quantified by C. Oon

E was performed by S. Bhattacharyya; analyzed and quantified by M.K. Oñate

F was performed by W. Kang (MSKCC Molecular Cytology); designed and quantified by M.K. Oñate

Supplementary Figure 3:

A was performed, analyzed, and quantified by C. Oon; analyzed by F. Arnold; created by M. Sherman (figure)

B was performed, analyzed, and quantified by C. Oon

C and D were performed and analyzed by C. Oon, with support from Azenta Life Sciences

Supplementary Figure 4:

A, B, and C were performed, analyzed, and quantified by Y. Han and Z. Yan

D and E were performed, analyzed, and quantified by M.K. Oñate

F was performed, analyzed, and quantified by C. Oon

D. Materials and Methods

Human tissue samples

All experiments with human patient-derived material were performed with approval of the Oregon Health & Science University and Memorial Sloan Kettering Cancer Center Institutional Review Boards. Sections from formalin-fixed, paraffin-embedded human PDAC patient tissue samples harboring benign adjacent pancreas tissue were donated to the Oregon Pancreas Tissue Registry program with informed written patient consent in accordance with full approval by the OHSU Institutional Review Board, or were obtained with informed consent of biospecimen collection with full approval by the MSKCC Institutional Review Board. Prospective collection of benign human pancreas tissue was performed with full approval by the MSKCC Institutional Review Board.

Animals

All experiments involving mice were reviewed and overseen by the Institutional Animal Care and Use Committees at OHSU and MSKCC in accordance with National Institutes of Health guidelines for the humane treatment of animals. Male and female mice were used for all experiments, with ages specified in the experimental sections to follow. Littermate controls were used whenever possible. Animals included in pancreatitis and PDAC experiments were assessed daily based on score sheets with criteria including body condition scoring and physical examination to ensure humane treatment. Orthotopic tumors were grown to a maximum diameter of 1.0 cm based on institutional guidelines. Maximal burden was not exceeded with any animal. The following mice were used in this study, all purchased from the Jackson Laboratory: C57BL/6J (000664), *Rosa26^{mTmG}* (007676), *Fabp4-Cre* (005069), *Kit^{fllox}* (shortened as *Kit^{fl}*, 017861), *Trp53^{fl}* (017767), *Kras^{FSF-G12D}* (023590). The *Pdx1-FlpO* mouse strain was kindly provided by Dr. Michael Ostrowski (Medical University of South Carolina).

Pancreatitis Induction

Acute pancreatitis was induced in male and female mice at 8 weeks of age by intraperitoneal injection of caerulein (80 µg/kg, Sigma-Aldrich C9026) 8 times per day with one (1) hour between injections for two (2) consecutive days, consistent with prior studies (Collins et al., 2012). Mice were then euthanized two (2) days after the final caerulein injection and pancreata were collected.

Orthotopic Transplantation of PDAC cells

The 6419c5, FC1199, and FC1245 cell lines were derived from autochthonous PDAC in the *Kras*^{LSL-G12D/+};*Trp53*^{LSL-R172H/+};*Pdx1-Cre* genetically engineered mouse model of pure C57BL/6J background, and were kindly provided by Dr. Ben Stanger (6419c5, University of Pennsylvania) and Dr. David Tuveson (FC1199 and FC1245, Cold Spring Harbor Laboratory). Male or female mice at 8-10 weeks of age were anesthetized and orthotopically implanted with 5 x 10⁴ (6419c5) or 5 x 10³ (FC1199, FC1245) PDAC cells in a 50% Matrigel solution into the body of the pancreas. Tumor progression was monitored longitudinally by high-resolution ultrasound using the Vevo 2100 imaging system. Mice were euthanized and tumors collected either when the first mouse of the experiment reached humane endpoint, or at different time points when each individual mouse in the experiment reached humane endpoint.

Single-cell RNA-seq

Cell isolation

To isolate healthy PSCs, pancreata were harvested from *Rosa26*^{mTmG/+};*Fabp4-Cre* mice at 6-9 weeks of age, trimmed to remove any associated adipose tissue, minced with scissors, digested with 0.02% Pronase (Sigma-Aldrich), 0.05% Collagenase P (Sigma-Aldrich), and 0.1% DNase I (Sigma-Aldrich) in Gey's balanced salt solution (GBSS; Sigma-Aldrich) at

37°C for 10 minutes. Pancreata were further mechanically dissociated via serological pipette before returning to chemical dissociation at 37°C for five (5) minutes. The resulting cell suspension was filtered through a 100 µm cell strainer nylon mesh. Cells were washed with GBSS, pelleted, and subject to red blood cell lysis via ACK lysis buffer (Thermo Fisher Scientific) for three (3) minutes at room temperature. Then, cells were washed in cold FACS buffer (PBS containing 2% FBS), pelleted, and resuspended in FACS buffer. Cells were kept on ice as a single-cell suspension, then GFP-positive cells were isolated by FACS using a BD FACSAria III or BD FACSymphony S6.

To isolate CAFs, 8-week-old *Rosa26^{mTmG/+};Fabp4-Cre* mice were orthotopically implanted with FC1245 PDAC cells as described above. At 21 days post-implantation, pancreata were harvested, and any apparent normal pancreas tissue was trimmed away from the PDAC specimen. Tumors were briefly minced, placed in digestion media (DMEM with 1 mg/mL Collagenase IV, 0.1% soybean trypsin inhibitor, 50 U/mL DNase, and 0.125 mg/mL Dispase), and incubated at 37°C for one (1) hour. Whole tissue digests were centrifuged at 450 × g for five (5) minutes, then resuspended in 10 mL pre-warmed 0.25% Trypsin and incubated at 37°C for 10 minutes. Cold DMEM (10 mL) was added to the suspension, which was then passed through a 100 µm cell strainer. Cells were centrifuged as above, washed with DMEM containing 10% FBS and centrifuged again, then centrifuged as above and resuspended in 1 mL ACK red cell lysis buffer. Cells were incubated at room temperature for three (3) minutes, then 9 mL FACS buffer added and cells centrifuged as above. Pelleted cells were counted and resuspended at 1 × 10⁷ cells/mL in FACS buffer, CD16/CD32 Fc block (BD 553141) added 1:20 and incubated at room temperature for two (2) minutes, then biotinylated PDPN antibody (BioLegend 127404) was added 1:200. Cell suspensions were incubated on ice for 30 minutes. Cold FACS buffer was added, cells

centrifuged at 300× g for five (5) min at 4°C, and cell pellets were resuspended in 500 µL cold FACS buffer containing 1:1000 APC-streptavidin (BD500 554067) and incubated for 30 minutes on ice protected from light. Cold FACS buffer (2 mL) was added, cells were pelleted as above and resuspended in cold FACS buffer containing SYTOX Blue Dead Cell Stain (Invitrogen S34857). Cells were incubated for 30 min on ice, washed with FACS buffer, pelleted, and resuspended in cold FACS buffer. GFP-positive, PDPN-positive cells were isolated by FACS using a BD FACSAria III or BD FACSymphony S6.

Sequencing and analysis

The isolated pancreatic mesenchymal cells were immediately used for single-cell RNA-seq library preparation. Single cell capture and cDNA library generation were performed using the 10x Genomics Chromium Next GEM single-cell 3' library construction dual index kit v3.1 (1000215) according to the manufacturer's instructions. Libraries were pooled prior to sequencing based on estimated cell number in each library per flow cytometry cell counts. Sequencing was performed on the Illumina NovaSeq 6000 platform at the OHSU Massively Parallel Sequencing Shared Resource, sequencing 20,000 read pairs/cell. Sequenced reads were aligned to the mm10 mouse reference genome, and the unique molecule identifier (UMIs) for each gene in each cell were counted using the Cell Ranger (10x Genomics). Then, resulting gene expression matrices were imported into R (version 4.0.3) and analyzed the data using the Seurat (Hao et al., 2021) pipeline (version 4.0.1). Genes had to be expressed in at least three cells to be considered for downstream analyses. Cells were filtered to retain those that contained at least 1,000 minimum unique genes expressed, no more than 5,000 unique genes, more than 200 total UMIs, and less than 10% of counts mapped to the mitochondrial genome. Batch correction was performed to integrate the samples from different conditions using the reciprocal PCA (RPCA) integration workflow within Seurat (Stuart et al., 2019). The first 30 principal

components were selected for downstream analysis, based on the elbow point on the plot of standard deviations of principal components. UMAP was generated using the RunUMAP function with the same first 30 principal components used in clustering analysis.

Pseudotime trajectory analysis was performed to elucidate the differentiation pathways of normal pancreatic and cancerous cells using Monocle 3 (v.1.3.7) (Cao et al., 2019). To achieve this, single-cell RNA-seq datasets were integrated using Harmony (v.0.1.1) (Korsunsky et al., 2019) to correct for batch effects, enabling a unified visualization of cellular heterogeneity across samples. Subsequent trajectory inference with Monocle 3 was conducted using default parameters to order cells in pseudotime, thus highlighting the dynamic progression of cellular states. To visualize gene expression patterns along the trajectories, the 'plot_cell_trajectory' function was utilized, specifically focusing on the expression of *Kitl* in the harmony-adjusted dimensional space.

Mouse mesenchymal cell isolation

Primary mPSCs were isolated from wild-type C57BL/6J (000664) mice from The Jackson Laboratory at 8-9 weeks of age. Our isolation protocol is adapted from previously described methods (Apte et al., 1998; Zhao et al., 2016) with some minor modifications. Healthy pancreatic tissues from eight (8) male mice were pooled, trimmed, and digested in Hank's balanced salt solution (HBSS; Sigma Aldrich, H8264) containing 0.5 mM of magnesium chloride hexahydrate ($MgCl_2 \times 6H_2O$; Sigma Aldrich, M9272), 10 mM HEPES (Cytiva, SH30237.01), 0.13% Collagenase P (Roche, 11213873001), 0.1% Pronase (Sigma Aldrich, 10165921001), and 0.001% DNase (Roche, 04716728001) for seven (7) minutes in shaking water bath (120 cycles/min) at 37°C. Remaining connective and

adipose tissues were removed before the second incubation at 37°C in a shaking water bath (80 cycles/min) for an additional seven (7) minutes. Digested tissues were then filtered through a 250 µm nylon mesh (Thermo Fisher Scientific, 87791) and centrifuged at 450 × g for 10 minutes at 4°C. Cell pellet was washed in Gey's balanced salt solution (GBSS) containing 120 mM salt (NaCl; Sigma Aldrich, S3014) and 0.3% BSA (Fisher Scientific, BP9703100) before repeating the same centrifugation step above. Upon removing the wash buffer, cells were resuspended in GBSS + NaCl containing 0.3% BSA, to which equal volume of 28.7% solution of Nycodenz (ProteoGenix, 1002424) in GBSS - NaCl were added and mixed well. The cell suspension in Nycodenz is then gently layered beneath GBSS containing 120 mM NaCl and 0.3% BSA using a long needle and subjected to centrifugation at 1400 × g for 20 minutes at 4°C. Primary quiescent PSCs were carefully harvested from the interface using sterile pipette and washed with GBSS + NaCl containing 0.3% BSA. Cells were pelleted and plated into multiple wells of a 6-well dish in Iscove's modified Dulbecco's medium (IMDM; Cytiva, SH30228.02) containing 10% FBS (VWR, 97068-085) and 1% Antibiotics-Antimycotic (Thermo Fisher Scientific, 15240-062). Cell culture was maintained in a humidified atmosphere at 37°C with 5% CO₂ and subjected to verification using qPCR and immunostaining upon treatment with 20 ng/mL recombinant TGF-β1 (R&D Systems 7666-MD-005) over the course of 7 days.

To isolate PDGFRα⁺ mesenchymal cells from healthy mouse pancreas, five (5) normal pancreata from wild-type male C57BL/6J mice were pooled and subjected to primary mouse pancreatic stellate cell isolation as described above. The FACS protocol is provided in the "Flow cytometry" section below.

Human mesenchymal cell isolation

Normal benign pancreas tissue was obtained from patients undergoing surgical resection for pancreatic disease. Tissue samples were collected in ice-mold MACS Tissue Storage Solution (Miltenyi Biotech, 130-100-008) and processed immediately. PSCs were isolated by density centrifugation as described previously (Vonlaufena et al., 2010). The resected tissue was trimmed of adipose tissue, transferred to 20 mL of digestion solution containing Collagenase P, Pronase, and DNase in GBSS as described above for mouse PSC isolation, and incubated at 37°C for seven (7) minutes in a shaking water bath. After the initial incubation, the partially digested tissue was transferred to a dish, finely minced with scissors, and subject to an addition 7-minute incubation. The digested tissue was then transferred to a 50 mL Falcon tube, thoroughly pipetted, and filtered through a nylon mesh to obtain a single cell suspension. The cell suspension was centrifuged at 450 × g for 10 minutes at 4°C and the resulting pellet was washed in GBSS + NaCl containing 0.3% bovine serum albumin (BSA). The wash and centrifugation steps were repeated as described. The pellet was resuspended in 9.5 mL of GBSS + NaCl containing 0.3% BSA, and 8 mL of a 28.7% Nycodenz solution in GBSS – NaCl was added and mixed thoroughly. A gradient was prepared by layering 6 mL of GBSS + NaCl with 0.3% BSA over the Nycodenz-cell suspension in a round bottom polycarbonate centrifuge tube. The sample was centrifuged at 1400 × g for 20 minutes at 4°C. PSCs separated into a distinct fuzzy band just above the interface between the BSA solution and the Nycodenz layer. This band was carefully harvested using a pipette without disturbing the gradient layers. The harvested cells were washed in GBSS + NaCl with 0.3% BSA, centrifuged at 450 × g for 10 minutes.

To isolate additional pancreatic mesenchyme, the cells below the interface band from the gradients described above were harvested, resuspended in GBSS + NaCl with 0.3% BSA, and centrifuged at $450 \times g$ for 10 minutes. Cells were resuspended in 1 mL of IMDM culture medium and blocked for 15 minutes with human FcR blocking reagent (Miltenyi Biotech, 130-059-901, 1:200 dilution). Post-blocking, the cells were washed with 1 mL of GBSS 595 + NaCl with 0.3% BSA and centrifuged again at $450 \times g$ for 10 minutes. The cell pellet was resuspended in 120 μ L of IMDM culture medium (Cytiva, SH30228.01), and 20 μ L each of anti-human CD45 (Miltenyi Biotech, 130-118-780), CD326/EpCAM (Miltenyi Biotech, 130-061-101), Cytokeratin (Miltenyi Biotech, 130-123-094), and CD31 (Miltenyi Biotech, 130-091-935) MicroBeads were added. The suspension was incubated for 30 minutes at 4°C . Following incubation, the cells were washed with one (1) mL of GBSS + NaCl with 0.3% BSA and centrifuged at $450 \times g$ for 10 minutes. The pellet was resuspended in 1 mL of IMDM culture medium. A magnetic column was prepared using a MACS separator (Miltenyi Biotech, 130-042-202) and washed with two (2) mL of IMDM culture medium. The labeled cell suspension was applied to the column and allowed to flow through completely. The CD45-negative, cytokeratin-negative, CD31-negative, and CD326-negative flow-through was collected and centrifuged at $300 \times g$ for 10 minutes. Gene expression analysis was performed on freshly isolated cells, with a sampling of each fraction plated on coverslips and imaged to validate stellate cell and fibroblast morphology. To culture-activate primary human pancreatic mesenchymal cells, the cells were seeded onto collagen-coated coverslips (Corning, 354089) immediately after isolation. Serum-free conditioned media was collected from MIA PaCa-2 human PDAC cells, concentrated using a Vivaspin 3 kDa concentration unit (Cytiva, 28-9323-58), and mixed 1:1 with fresh complete IMDM containing 20% FBS and 2% glutamine, and added to the plated cells. Media was replenished every two (2) days for a total of 14 days.

Stable *Kitl* knock down and overexpression in pancreatic stellate cells

Kitl knock down (*shKitl*) and overexpression (*Kitl* OE) mPSC-1 cell lines were generated using Mission Lentiviral shRNA (Millipore Sigma, Clone ID: TRCN0000067872) and *Kitl* open reading frame lentivirus (Genecopoeia, EX-Mm03868-Lv158) respectively. Vector PLKO.1 Neo (*shCtrl*; Addgene, 13425) and *Egfp* open reading frame (*Egfp* OE; Genecopoeia, EX-EGFP-Lv158) were included as controls. Immortalized mPSC-1 cells were transduced with specified lentiviral particles for 48 hours prior to selection with 1 mg/mL Geneticin (Fisher Scientific, 10131035) for 4 days. KITL protein and transcript expression were then quantified using qPCR and ELISA to assess silencing and overexpression efficiency. Stable cells were maintained in a humidified atmosphere at 37°C with 5% CO₂ and routinely passed in DMEM (Thermo Fisher Scientific, 11965118) containing 10% FBS (VWR, 97068-085) 1 mM sodium pyruvate (Thermo Fisher Scientific, 11360070), and 1% Antibiotics-Antimycotic (Thermo Fisher Scientific, 15240-062).

RNA-sequencing of *shKitl* and *Kitl* OE pancreatic stellate cells

Total RNA was isolated using RNeasy Microkit (Qiagen, 74004) per manufacturer's instructions and quantified using NanoDrop microvolume spectrophotometer before submission for bulk RNA sequencing. RNA library preparation, sequencing, and analysis were conducted at Azenta Life Sciences (South Plainfield, NJ, USA) as follows. Total RNA samples were quantified using Qubit 2.0 Fluorometer (Life Technologies, Carlsbad, CA, USA) and RNA integrity was checked using Agilent TapeStation 4200 (Agilent Technologies, Palo Alto, CA, USA). ERCC RNA Spike-In Mix (Cat: #4456740) from ThermoFisher Scientific, was added to normalized total RNA prior to library preparation following manufacturer's protocol. Total RNA underwent polyA selection and RNA sequencing libraries preparation using the NEBNext Ultra II RNA Library Prep Kit for Illumina using manufacturer's instructions (NEB, Ipswich, MA, USA). Briefly, mRNAs were

initially enriched with Oligod(T) beads. Enriched mRNAs were fragmented for 15 minutes at 94°C. First strand and second strand cDNA were subsequently synthesized. cDNA fragments were end repaired and adenylated at 3'ends, and universal adapters were ligated to cDNA fragments, followed by index addition and library enrichment by PCR with limited cycles. The sequencing library was validated on the Agilent TapeStation (Agilent Technologies, Palo Alto, CA, USA), and quantified by using Qubit 2.0 Fluorometer (Invitrogen, Carlsbad, CA) as well as by quantitative PCR (KAPA Biosystems, Wilmington, MA, USA). The sequencing libraries were multiplexed and clustered onto a flowcell on the Illumina NovaSeq instrument according to manufacturer's instructions. The samples were sequenced using a 2x150bp Paired End (PE) configuration at an average of 30 million reads per sample. Image analysis and base calling were conducted by the NovaSeq Control Software (NCS). Raw sequence data (.bcl files) generated from Illumina NovaSeq was converted into fastq files and de-multiplexed using Illumina bcl2fastq 2.20 software. One mismatch was allowed for index sequence identification.

After investigating the quality of the raw data, sequence reads were trimmed to remove possible adapter sequences and nucleotides with poor quality. The trimmed reads were mapped to the reference genome GRCm38.91 (mm10) available on ENSEMBL using the STAR aligner v.2.5.2b. The STAR aligner is a splice aligner that detects splice junctions and incorporates them to help align the entire read sequences. BAM files were generated as a result of this step. Unique gene hit counts were calculated by using feature Counts from the Subread package v.1.5.2. Only unique reads that fell within exon regions were counted. The gene hit counts table was used for downstream differential expression analysis. Using DESeq2, a comparison of gene expression between the groups of samples was performed. The Wald test was used to generate p-values and Log2 fold

changes. Genes with adjusted p-values < 0.05 and absolute log₂ fold changes > 1 were called as differentially expressed genes for each comparison. Volcano plot visualization of significant DEGs were performed in Galaxy (Galaxy C., Nucleic Acids Res, 2022) using the ggplot2 R package. Significant gene labels from top gene ontologies categories were included.

Functional enrichment analysis was performed using EnrichR (Chen et al., Bioinformatics, 2013) on the statistically significant set of genes by implementing Fisher exact test (GeneSCF v1.1-p2). Significance of tests was assessed using adjusted p-values defined by enrichR. Enrichment bar plots were generated using srPlot (Tang et al., PLoS One, 2023) to include Top 10 upregulated and downregulated gene ontology (GO) categories. A similar approach was used for conserved functional analysis, with significance determined by p values < 0.05 , as defined by EnrichR. To screen for the conserved GO categories, we compared the upregulated GO terms in *shKitl* with the downregulated GO terms in *Kitl* OE, and conversely, the downregulated GO terms in *shKitl* with the upregulated GO terms in *Kitl* OE.

Immunohistochemistry, immunofluorescence, and lipid staining

Mouse and human tissue sample staining

Standard protocols were performed for IHC. Briefly, tissue samples were fixed overnight in 10% neutral-buffered formalin (Sigma-Aldrich, HT501128-4L) and submitted to MSKCC Laboratory of Comparative Pathology or Molecular Cytology Core Facility for paraffin embedding, sectioning and H&E sectioning. Sectioned tissues were deparaffinized using CitriSolv (Fisher Scientific, 22-143-975) and rehydrated in ethanol series (Decon labs, 2701) before undergoing antigen retrieval using citrate or tris-based antigen unmasking

solution (Vector laboratories, H3300, H3301). The slides were then blocked with 8% BSA (Fisher Bioreagents, BP9703100) for 1 hour at room temperature and incubated in primary antibodies at 4°C overnight. Primary antibodies for α SMA (Cell Signaling Technology, 19245S), PDPN (eBio 8.1.1 Invitrogen, 14538182), GFP (Thermo Fisher, A10262; Abcam, ab1218; Rockland Immunochemicals, 600-101-215), pan-cytokeratin (Thermo Fisher Scientific, MA5-13156), CD31 (R&D AF3628 or Abcam ab7388), biotinylated anti c-KIT (R&D BAF1356), Vimentin (Cell Signaling Technology 5741 D21H3 XP), CD45 (R&D Systems, AF114), CD68 (R&D Systems, MAB101141), NG2 (EMD Millipore, MAB5384), CD105 (R&D Systems, MAB1320) or pancreatic amylase (Thermo Scientific PA5-25330) were diluted at 1:200-1:400 in 8% BSA in PBS. The next day, slides were washed with PBS (Biotum, 22020) and incubated in α -chicken Alexa Fluor 488 (Thermo Fisher Scientific, A32931), α -rabbit Alexa Fluor 647 (Fisher Scientific, A21245), α -Syrian hamster Alexa Fluor 647 (Abcam, ab180117), or α -mouse Alexa Fluor 555 (Fisher Scientific, A21424) secondary antibodies 697 at 1:200-1:400 dilution for 1 hour at room temperature. Tissue slides were washed with PBS and mounted with Vectashield mounting media containing DAPI (Vector laboratories, H-1200-10).

For phospho-c-KIT staining, fresh-frozen, OCT-embedded tissue sections were washed with TBST (Santa Cruz Biotechnology, sc-362311) to dissolve OCT. Samples were then permeabilized with 1% FBS (Thermo Scientific, A4766801) in PBS-T, 0.1% Triton X-100 (Sigma-Aldrich, X100-500ML). The slides were blocked with 5% FBS in PBS for 30 minutes at room temperature, then incubated in primary antibodies for two (2) hours at room temperature, before incubating further at 4°C overnight. Primary antibodies for human p-c-KIT (Y703) (Thermo Scientific, 710762) and human Vimentin (Thermo Scientific, PA1-16759) were diluted at 1:50 and 1:100, respectively, in 1% FBS in PBS.

Primary antibody for mouse p-c-KIT (G Biosciences, ITA0925) was diluted at 1:50 in 1% FBS in PBS. The next day, slides were washed with 1% FBS in PBS-T, 0.1% Triton X-100 and incubated in α -chicken Alexa Fluor 488 (Invitrogen, A78948), α -rabbit Alexa Fluor 594 (Invitrogen, A21207), or α -rat Alexa Fluor 488 (Invitrogen, A21208) secondary antibodies at 1:100-1:200 dilution for two (2) hours at room temperature. Tissue slides were further stained with DAPI (Thermo Fisher Scientific, 62248) at 1:1000 dilution for 30 minutes at room temperature, washed with PBS, and mounted with Vectashield Vibrance mounting media (Vector Laboratories, H-1700-2).

All images were acquired on a Carl Zeiss LSM880 laser-scanning confocal inverted microscope using 20x, 40x, or 63x objective. Whole slide scans were completed by MSKCC Molecular Cytology Core Facility. Image analysis was performed using QuPath quantitative pathology and FIJI/ImageJ open-source software. Where applicable, co-localization analysis was performed using the JaCoP plugin in ImageJ.

Cell staining and imaging

Cells seeded in chamber slides were fixed in 4% paraformaldehyde for 15 minutes and permeabilized with 0.1% Triton X-100 for 10 minutes before undergoing blocking in 5% BSA for one (1) hour at room temperature. Sample slides were then probed with α SMA primary antibodies (ThermoFisher, MA5-11547) overnight at 4°C followed by standard Alexa Fluor 647-conjugated secondary antibody (Fisher Scientific, A21235) incubation for an hour at room temperature. Upon repeating standard washing steps, slides were mounted for imaging using Vectashield mounting media containing DAPI (Vector laboratories, H-1200-10). For lipid staining, cells seeded in chamber slides were stained with Nile Red (MCE, HY-D0718) at 1 μ M final working concentration for 10 minutes and

counterstained with DAPI (Thermo Fisher Scientific, 62248). Nile Red signals were detected at excitation/emission wavelengths 559 nm/635 nm.

Two-plex fluorescence *in situ* hybridization

Transcript expression on tissues, except where RNAscope was indicated, was performed using the Thermo Fisher Scientific ViewRNA ISH Tissue Assay kit (two plex) for use on mouse and human tissue samples. Briefly, samples were first permeabilized with controlled protease digestion, followed by incubation with proprietary probe-containing solution, according to the manufacturer's instructions. During incubation, samples had to remain fully submerged. After hybridization with the probe, samples were washed, followed by sequential hybridization with the preamplifier and amplifier DNA. In accordance with the manufacturer's instructions, hybridizations were performed with the preamplifier, amplifier and fluorophore. Mounting medium with DAPI (Vectashield Hardset mounting media with DAPI) was used to mount samples.

RNAscope combined with immunohistochemistry

Paraffin-embedded tissue sections were cut at five (5) μm and kept at 4°C. Samples were loaded into Leica Bond RX, baked for 30 minutes at 60°C, dewaxed with Bond Dewax Solution (Leica, AR9222), and pretreated with EDTA-based epitope retrieval ER2 solution (Leica, AR9640) for 15 minutes at 95°C. The probe mKitL (Advanced Cell Diagnostics, ready to use, no dilution, 423408) was hybridized for two (2) hours at 42°C. Mouse PPIB (ACD, Cat# 313918) and dapB (ACD, Cat# 312038) probes were used as positive and negative controls, respectively. The hybridized probes were detected using RNAscope 2.5 LS Reagent Kit – Brown (ACD, Cat# 322100) according to manufacturer's instructions with some modifications (DAB application was omitted and replaced with Fluorescent CF594/Tyramide (Biotium,92174) for 20 minutes at room temperature.

After the run was finished, slides were washed in PBS and incubated in five (5) µg/mL 4',6-diamidino-2-phenylindole (DAPI) (Sigma Aldrich) in PBS for five (5) min, rinsed in PBS, and mounted in Mowiol 4–88 (Calbiochem). Slides were kept overnight at -20°C before imaging.

After the slides were scanned, coverslips were removed and slides were loaded into Leica Bond RX for double immunofluorescence staining. Samples were pretreated with EDTA-based epitope retrieval ER2 solution (Leica, AR9640) for 20 minutes at 100°C. The double antibody staining and detection were conducted sequentially. The primary antibodies against GFP (2 µg/mL, chicken, abcam, ab13970) and CD31 (CD31/A647 (0.08, rb, abcam, ab182981) were incubated for one (1) hour at room temperature. For rabbit antibodies, Leica Bond Polymer anti-rabbit HRP (included in Polymer Refine 765 Detection Kit (Leica, DS9800) was used; for the chicken antibody, a rabbit anti-chicken (Jackson ImmunoResearch303-006-003) secondary antibody was used as a linker for eight (8) minutes before the application of the Leica Bond Polymer anti-rabbit HRP for eight (8) min at room temperature. The Leica Bond Polymer anti-rabbit HRP secondary antibody was applied followed by Alexa Fluor tyramide signal amplification reagents (Life Technologies, B40953 and B40958) were used for immunofluorescence detection. After the run was finished, slides were washed in PBS and mounted in Mowiol 4–88 (Calbiochem). Slides were kept overnight at -20°C before imaging.

CODEX

Antibody panel development, CODEX staining and imaging

To construct an antibody panel visualizing pancreatic architecture in FFPE mouse samples using CODEX (Goltsev et al., 2018), conventional IHC staining was performed to screen for antibodies binding canonical markers of pancreatic epithelial cells (E-cadherin, Novus

Biologicals #NBP2-33006 clone 1A4(asm-1); Amylase, Cell Signaling Technology #3796 clone D55H10], endothelial cells (CD31, Cell Signaling Technology #14472 clone 4A2), stromal cells (Vimentin, Cell Signaling Technology #70257 clone D3F8Q; α SMA, Cell Signaling Technology #77699 clone D8V9E), leukocytes (CD45, Cell Signaling Technology #46173 clone D21H3) and lineage reporter (GFP, Rockland Immunochemicals #600-101-215 polyclonal). Identified antibody clones were then conjugated with oligonucleotide barcodes using Antibody Conjugation Kit (Akoya Biosciences). Prior to CODEX imaging, each conjugated antibody was validated following manufacturer instructions and tissue staining patterning was confirmed with published literature.

CODEX staining and imaging was performed as described in user manual (<https://www.akoyabio.com/wp-content/uploads/2021/01/CODEX-User-Manual.pdf>). In brief, five (5) μ m FFPE pancreas sections were mounted onto 22 mm x 22 mm glass coverslips (Electron Microscopy Sciences) coated in 0.1% poly-L-lysine (Sigma) and stained with using CODEX Staining Kit (Akoya Biosciences). A cocktail of above-conjugated antibodies was incubated with tissue overnight at 4°C. The next day, fluorescent oligonucleotide-conjugated reporters were combined with Nuclear Stain and CODEX Assay Reagent (Akoya Biosciences) in sealed light-protected 96-well plates (Akoya Biosciences). Automated fluidics exchange and image acquisition were performed using the Akoya CODEX instrument integrated with a BZ-X810 epifluorescence microscope (Keyence) and CODEX Instrument Manager (CIM) v1.30 software (Akoya Biosciences). The exposure times were as follows: E-cadherin, barcode BX006, 600 ms; Amylase, barcode BX031, 250 ms; Vimentin, barcode BX025, 300 ms; α SMA, barcode BX052, 250 ms; CD31, barcode BX002, 350 ms; CD45, barcode 799 BX007, 400 ms; GFP, barcode BX041, 250 ms. All images were acquired using a CFI plan Apo I 20 \times /0.75

objective (Nikon). “High resolution” mode was specified in Keyence software to reach a final resolution of 377.44 nm/pixel.

Processing of CODEX images and analysis

Image stitching, drift compensation, deconvolution, z-plane selection, and background subtraction were performed using the CODEX processor v1.7 (Akoya Biosciences) per manufacture instruction (<https://help.codex.bio/codex/processor/technical-notes>). Individual channel images were then imported into ImageJ v1.53t for analyses as described below. Total pancreatic areas were annotated by sum of Amylase+ and Ecadherin+ region. Immune cells were defined by DAPI and CD45 double positivity while vasculature area was annotated by CD31+ region. Vimentin and α SMA signal were used to mark total and activated fibroblast cells, respectively. GFP positivity was used to track PSC lineage-derived cells.

Flow cytometry

To analyze c-KIT expression, normal pancreas tissues were harvested from wild-type C57BL/6J mice aged 6-9 weeks and digested as described above. Following ACK lysis, cells were incubated with CD16/CD32 antibody (BD Biosciences, 553141) to block Fc receptors for two (2) minutes at room temperature. Cells were then stained with the following for 30 minutes on ice: SYTOX Blue Dead Cell Stain (Invitrogen S34857); biotinylated m-SCF R/c-KIT antibody (R&D Systems BAF1356). Cells were then washed with cold FACS buffer, pelleted, then stained with PE/Cy7 Streptavidin (Biolegend, 405206), anti-mouse CD31 APC (Invitrogen 17-0311-82), anti-mouse EpCAM (CD326) FITC (Invitrogen 11-5791-82) for 30 minutes on ice, before cells were washed with FACS buffer, pelleted, then resuspended in cold FACS buffer for flow cytometry.

To analyze epithelial cells, immune cells, and c-KIT, pancreata from C57Bl/6J mice aged 6-9 weeks old were harvested and digested as described above. After ACK lysis, cells were incubated with CD16/CD32 antibody (BD Biosciences 553141) for two (2) minutes at room temperature. Cells were then stained with SYTOX Blue and a biotinylated c-KIT antibody on ice for 30 minutes on ice, were washed with cold FACS buffer, pelleted, then stained with PE/Cy7 Streptavidin (Biolegend 405206), anti-mouse CD45 PE-Cyanine 5 (Invitrogen 15-0451-82), anti-mouse EpCAM (CD326) FITC (Invitrogen 11-5791-82) for 30 minutes on ice. Cells were washed with FACS buffer, pelleted, then resuspended in cold FACS buffer for flow cytometry.

To isolate PDGFR α + mesenchymal cells from healthy mouse pancreas, five (5) normal pancreata from wild-type C57BL/6J were pooled and subjected to primary mouse pancreatic stellate cell isolation as described above. The isolated cells were first stained with Zombie NIR dye (Fisher Scientific, 50-604-714) for five (5) minutes at room temperature to exclude dead cells. Next, cells were blocked with CD16/CD32 (BD Biosciences, 553141) for 10 minutes at 4°C to prevent non-specific antibody binding, then incubated with anti-mouse PDGFR α PE (BioLegend, 135905) at a 1:100 dilution for 20 minutes at 4°C. Upon staining, the cells were washed with FACS buffer containing HBSS (Thermo Fisher Scientific, 14175095) and 0.5% BSA (Fisher Bioreagents, BP9703100), sorted using a BD Biosciences Symphony S6 cell sorter and then processed for RNA isolation.

Gene expression analysis by qPCR

Total RNA was isolated using RNeasy Microkit (Qiagen, 74004) per manufacturer's instructions and quantified using NanoDrop microvolume spectrophotometer. 500 ng to 1

µg of RNA was reverse transcribed using iScript reverse transcriptase supermix (Bio-Rad, 1708841) to produce cDNA. Real-time PCR was performed using Power SYBR Green PCR master mix (Thermo Fisher Scientific, 4367659). Gene specific primer pairs were designed using the NCBI Nucleotide database or acquired from Millipore Sigma. Gene expression is normalized to reference gene *Rplp0*. Primer pair sequences were as follows:

Rplp0 Forward 5'-GTGCTGATGGGCAAGAAC-3',

Reverse 5'-AGGTCCTCCTTGGTGAAC-3';

mKitl Forward 5'-TTATGTTACCCCCTGTTGCAG-3',

Reverse 5'- CTGCCCTTGTAAGACTTGACTG-3';

mKit Forward 5'-GAGACGTGACTCCTGCCATC-3',

Reverse 5'-TCATTCCTGATGTCTCTGGC-3';

mActa2 Forward 5'-AGCCATCTTTCATTGGGATGGA-3',

Reverse 5'-CATGGTGGTACCCCCTGACA-3';

mPdpr Forward 5'-AGATAAGAAAGATGGCTTGC-3',

Reverse 5'-AACAACAATGAAGATCCCTC-3';

mPdgfra Forward 5'-GCAGTTGCCTTACGACTCCAGA-3',

Reverse 5'-GGTTTGAGCATCTTCACAGCCAC-3';

mPcdhga12 Forward 5'-ACAATGCCCTGAAGTAGCC-3',

Reverse 5'- TCCAGTGCGAGGTGAGTTTC-3';

mCdh26 Forward 5'-CCTCGTCGTTGTTGTGGAGA-3',

Reverse 5'- CTCTGAGGGTGAAAGGCTGG-3';

mItga1 Forward 5'-GGCAGTGGCAAGACCATAAGGA-3',

Reverse 5'-CATCTCTCCGTGGATAGACTGG-3';

mIrf5 Forward 5'-CCTACAGAACCACTCTTGCCTG-3',

Reverse 5'- CCTTGTGGGTTGCTGATGGTGA-3';

mLrrc15 Forward 5'-TTCAGCCACCTGAACCAGTTGC-3',

Reverse 5'- GTCCTGTAGAGCATTGGTGTGG-3';

hFABP4 Forward 5'- ACGAGAGGATGATAAACTGGTGG -3',

Reverse 5'- GCGAACTTCAGTCCAGGTCAA-3';

hPDGFRA Forward 5'- GACTTTCGCCAAAGTGGAGGAG -3',

Reverse 5'-AGCCACCGTGAGTTCAGAACGC -3';

hCOL1A1 Forward 5'-CATGGAGACTGGTGAGACCT-3',

Reverse 5'- GCCATACTCGAACTGGAATC 867 -3';

hKITLG Forward 5'-CTGGAGACTCCAGCCTACACTG-3',

Reverse 5'- CTGCCCTTGTAAGACTTGGCTG -3'.

ELISA quantikine assay

Immortalized parental and *shKitl* mPSC-1 cells were seeded into 6 well dish at 3×10^5 confluency in growth media containing DMEM (Thermo Fisher Scientific, 11965126), 10% VWR Seradigm FBS (VWR, 97068-085), 1 mM Sodium Pyruvate (Thermo Fisher Scientific, 11360070), and 1% Antibiotics-Antimycotic (Thermo Fisher Scientific, 15240-062). Primary PSCs were seeded in a 6-well dish at 1×10^4 confluency in Iscove's modified Dulbecco's medium (IMDM; Cytiva, SH30228.02) containing 10% FBS (VWR,

97068-085) and 1% Antibiotics-Antimycotic (Thermo Fisher Scientific, 15240-062). Conditioned media were collected at indicated time points and concentrated using Vivaspin Turbo 20 3K MWCO concentrator (Cytiva, 28932358) in accordance with manufacturer's protocol. Concentrated supernatants were quantified using Pierce BCA Protein Assay Kit (Thermo Fisher Scientific, 23225) and mouse KITL protein quantification was performed using Mouse SCF Quantikine ELISA Kit (R&D Systems, MCK00) according to manufacturer's protocol.

Cell proliferation assay

Human and mouse PDAC, macrophage and endothelial cells were seeded into 96-well white walled plates at a density of 5×10^3 cells per well. All cells were maintained in DMEM (Thermo Fisher Scientific, 11965126) containing 10% FBS (VWR, 97068-085) except for human endothelial cells, which were cultured in endothelial cell media (Cell applications, 213-500). The following day, cells were washed with PBS (Cytiva SH30028.FS) and treated with recombinant KITL/SCF at final concentration of 100ng/mL: human SCF (R&D Systems, 255-SC-010) or mouse KITL/SCF (R&D Systems, 455-MC-010). Plates were replenished with recombinant KITL/SCF daily and collected for read every 24 hours for three (3) continuous days. Proliferation assay was performed using CellTiter-Glo Luminescent Cell Viability Assay reagent (Promega, G7572) per manufacturer's protocol and read using a GloMax plate reader.

Statistical analysis

No statistical methods were used to predetermine sample sizes. The experiments were not randomized. For animal studies, a minimal number of mice was selected based on preliminary studies, with an effort to achieve a minimum of $n = 3$, mostly $n = 5-10$ mice per treatment group for each experiment. Age-matched mice were selected for experiments.

For histological staining quantification, analyses were performed in a blinded fashion. For batch-processed images, image analyses were done in an unbiased manner using image analysis software. Some western blots and RT-qPCR assays were performed by a researcher blind to the experimental hypothesis. Animals were excluded if an animal needed to be removed from an experiment early for reasons seemingly unrelated to tumor burden. All experiments were performed and reliably reproduced at least two independent times. GraphPad Prism 10 was used to generate graphs and for statistical analyses. Statistical significance was calculated for two unmatched groups by unpaired t-test with Welch's correction or Mann-Whitney test. One- or two-way ANOVAs were used for more than two groups as specified, followed by Tukey's multiple comparisons tests; experiments that did not fulfill normal distribution requirements were calculated with Brown-Forsythe and Welch one- or two-way ANOVA. Datasets are presented as mean \pm S.E.M. *P* values under 0.05 were considered significant.

E. Results

To assess stromal evolution during stepwise tumorigenesis, we applied a previously established fate mapping approach (Helms et al., 2022) to analyze the contributions of PSCs to the stroma of normal pancreas tissue, pancreatic intraepithelial neoplasia (PanINs), and invasive PDAC. To this end, we generated a dual recombinase genetically engineered mouse model of the genotype $Kras^{FSF-G12D/+}; Trp53^{FRT/+}; Pdx1-FlpO; Rosa26^{mTmG/+}; Fabp4-Cre$ (Figure 2.1A) and assessed the presence of GFP+ stroma, indicating a lipid-storing origin.

A

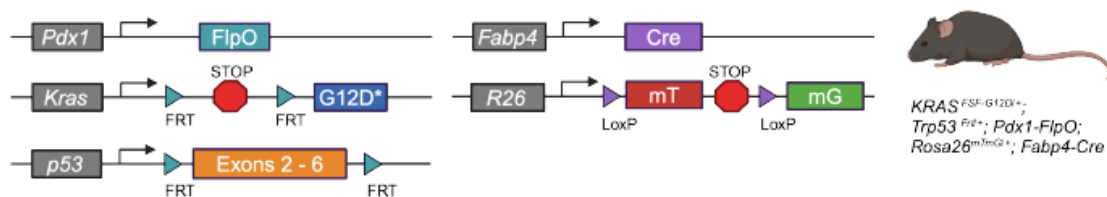


Figure 2.1. Pancreatic stellate cells contribute to the stromal microenvironment throughout tumorigenesis. A, Genetic schema of $Kras^{FSF-G12D/+}; Trp53^{FRT/+}; Pdx1-FlpO; Rosa26^{mTmG/+}; Fabp4-Cre$ murine model.

While GFP+ PSCs were found in normal pancreas tissue as expected, very few were positive for PDPN, a cell surface marker upregulated upon fibroblast activation in PDAC. We found GFP+PDPN+ and GFP+ α SMA+ cells associated with low grade PanIN lesions as well as invasive cancer in this model (Figures 2.1B & 2.1C), with a significant increase in PSC-derived fibroblastic cells in the context of PDAC compared to pre-invasive lesions. In normal pancreas tissue and in tumors, PSCs or PSC-derived CAFs had a spatial distribution similar to the reported tissue distribution of stellate cells in the liver, the other tissue in the body where these mesenchymal cells reside.

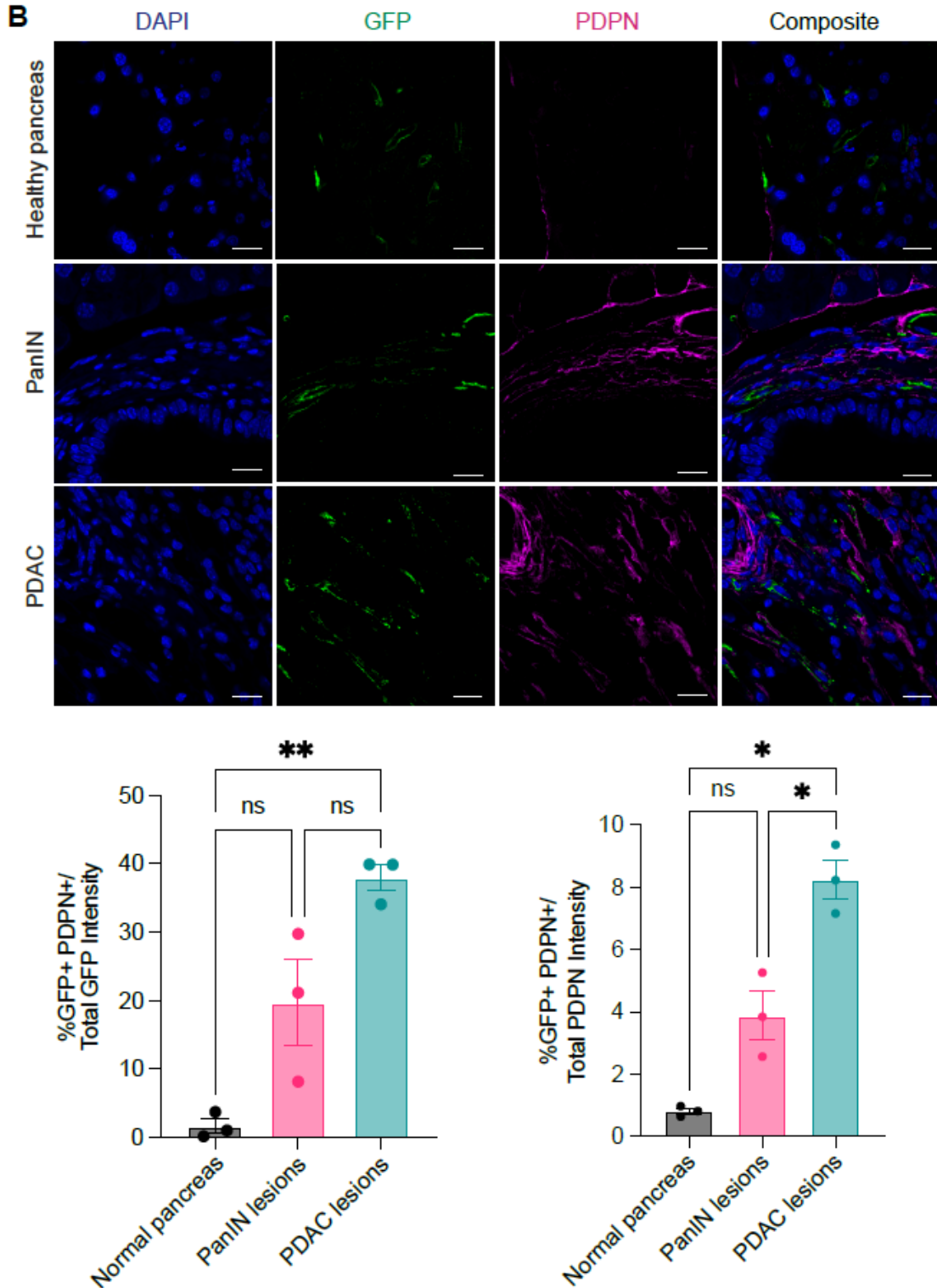


Figure 2.1. Pancreatic stellate cells contribute to the stromal microenvironment throughout tumorigenesis. B, Representative images (above) and quantification (below, n = 3) of IHC staining for GFP (green) and Podoplanin (PDPN, magenta) among normal pancreas, PanIN lesions, and PDAC lesions. Scale bar, 10 μ m. Data are represented as mean \pm SEM. Brown Forsythe and Welch One-way ANOVA test was used. ns = not significant, *P \leq 0.05, **P \leq 0.01, ***P \leq 0.001, ****P \leq 0.0001.

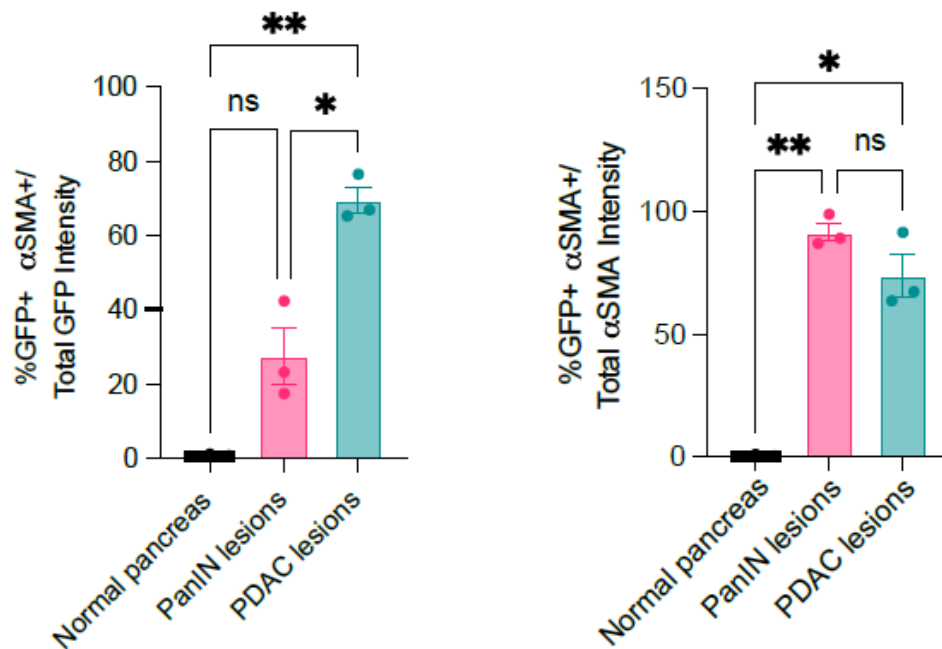
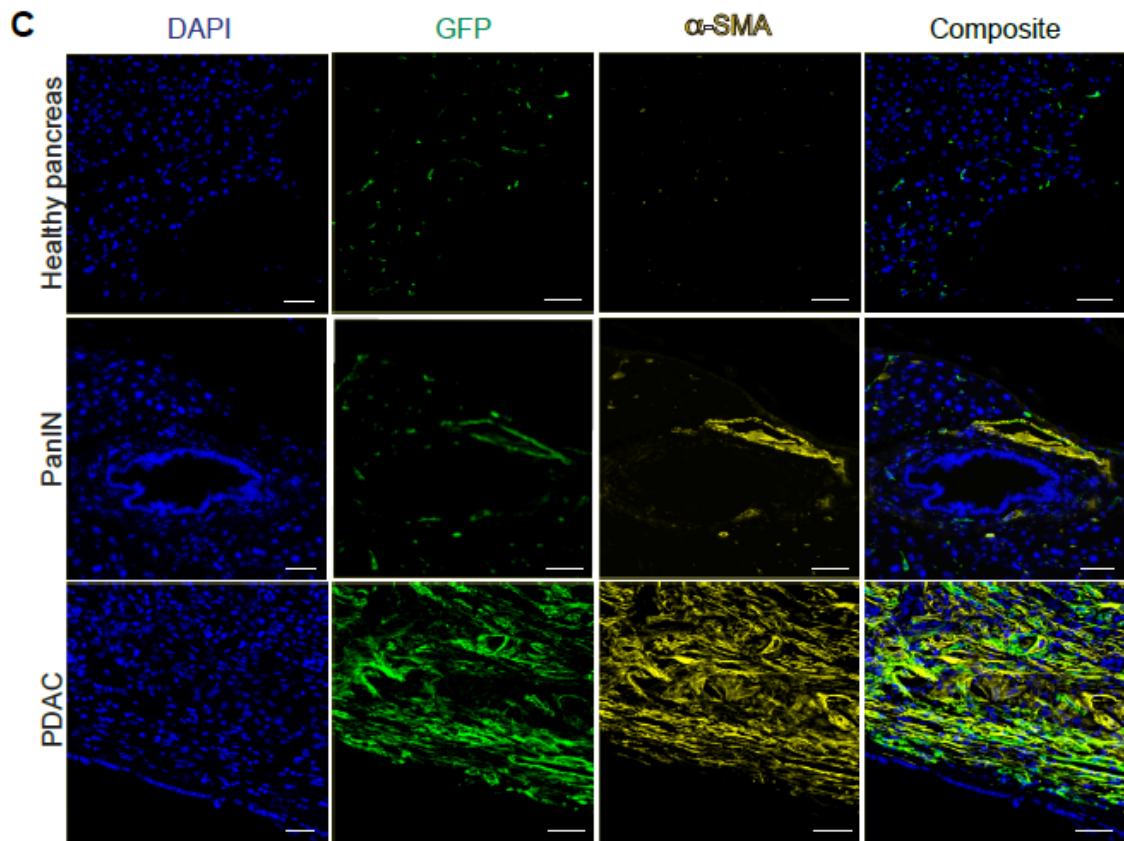


Figure 2.1. Pancreatic stellate cells contribute to the stromal microenvironment throughout tumorigenesis. C, Representative images (above) and quantification (below, n = 3) of IHC staining for GFP (green) and a-SMA (yellow) on normal pancreas, PanIN lesions, and PDAC lesions. Scale bar, 20 μ m. Data are represented as mean \pm SEM. Brown Forsythe and Welch One-way ANOVA test was used. ns = not significant, *P \leq 0.05, **P \leq 0.01, ***P \leq 0.001, ****P \leq 0.0001.

Hepatic stellate cells (HSCs) are found in perivascular regions in close proximity to endothelial cells, and adjacent to neighboring parenchymal cells (Mederacke et al., 2013). We found PSCs in normal pancreas tissue similarly to localize in perivascular regions, and in the tissue parenchyma spatially poised for cell-cell communication with epithelial cells (Figure 2.1D). This spatial distribution was conserved upon differentiation to a CAF phenotype, as GFP⁺ CAFs were found both immediately adjacent to and distant from endothelial cells in the genetically engineered PDAC model (Figure 2.1E).

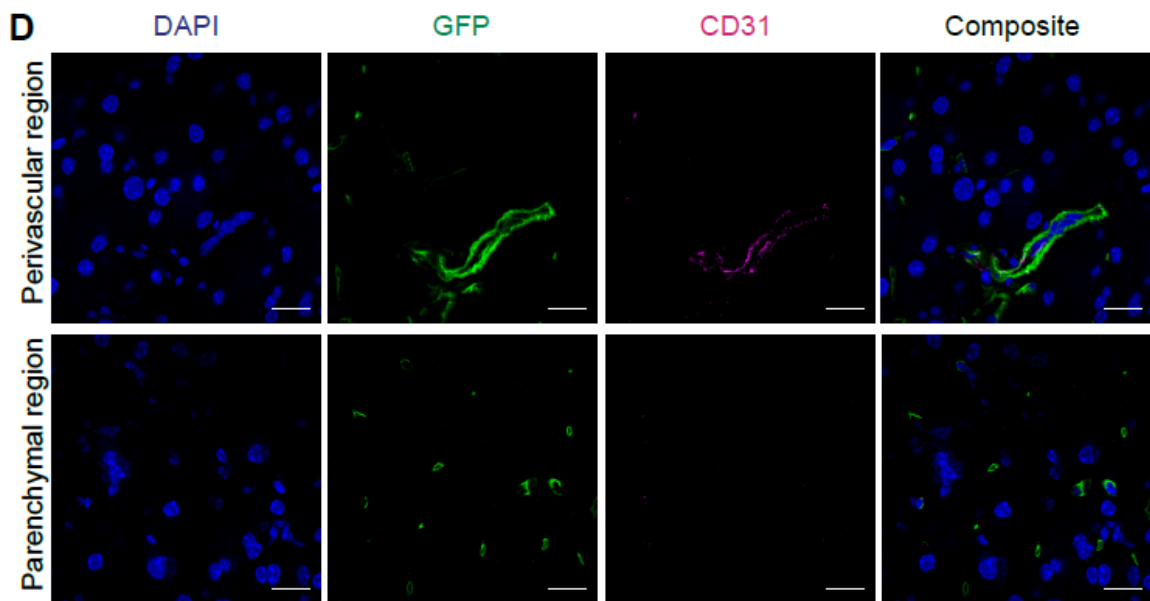


Figure 2.1. Pancreatic stellate cells contribute to the stromal microenvironment throughout tumorigenesis. D, Representative images of IHC staining for GFP (green) and CD31 (magenta) within mouse normal pancreas (n = 5). Scale bar, 10 μ m.

Similar results were observed in an orthotopic model wherein PDAC cells derived from the *Kras*^{LSL-G12D/+}; *Trp53*^{LSL-R172H/+}; *Pdx1-Cre* (KPC) autochthonous model were implanted into syngeneic *Rosa26*^{mTmG/+}; *Fabp4-Cre* hosts (Figure 2.1F). These observations indicate that PSCs contribute to the stromal microenvironment throughout pancreatic tumorigenesis and are spatially distributed to engage in direct cell-cell contact with both endothelial cells and epithelial cells in healthy and cancerous pancreas tissue.

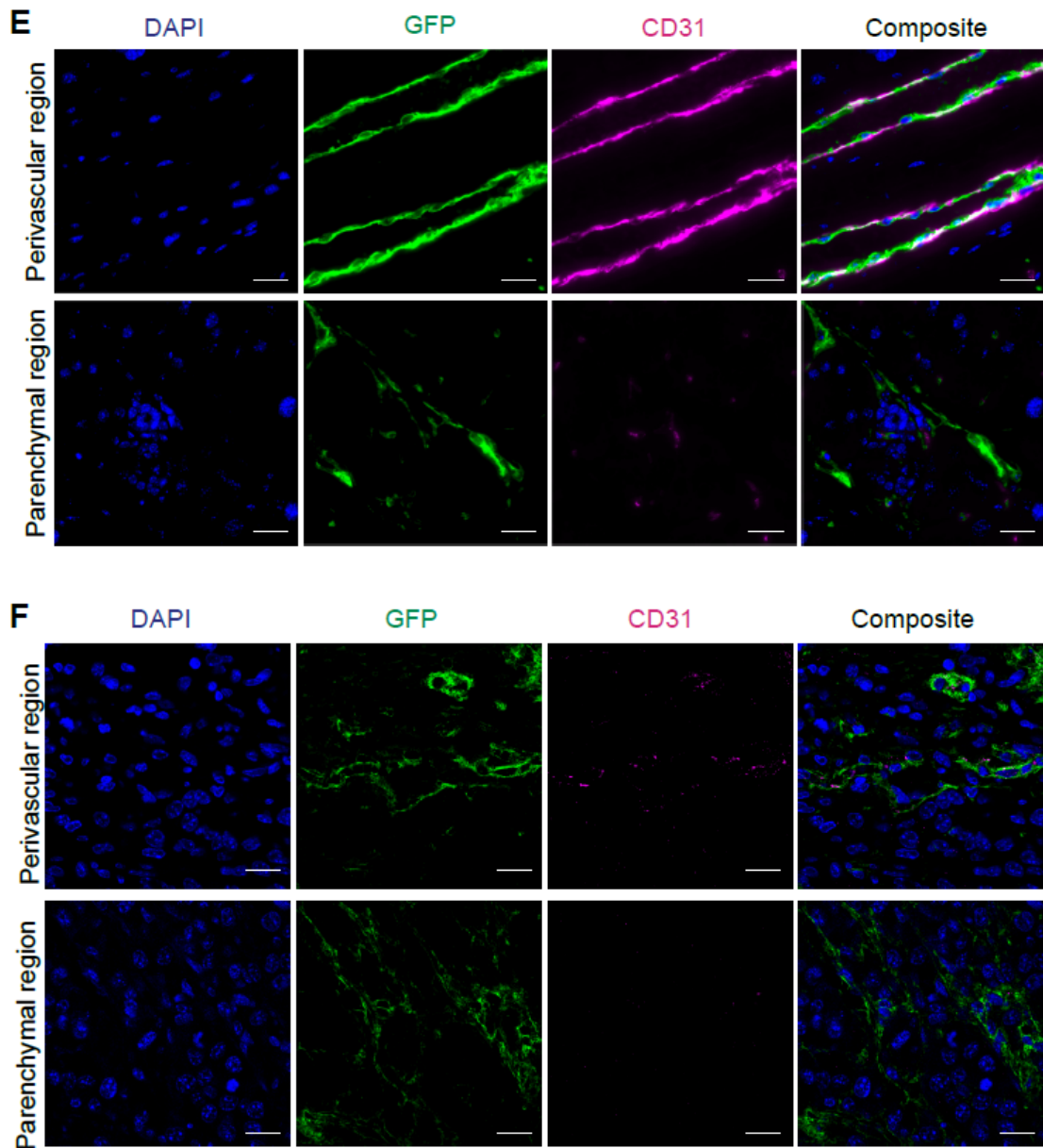
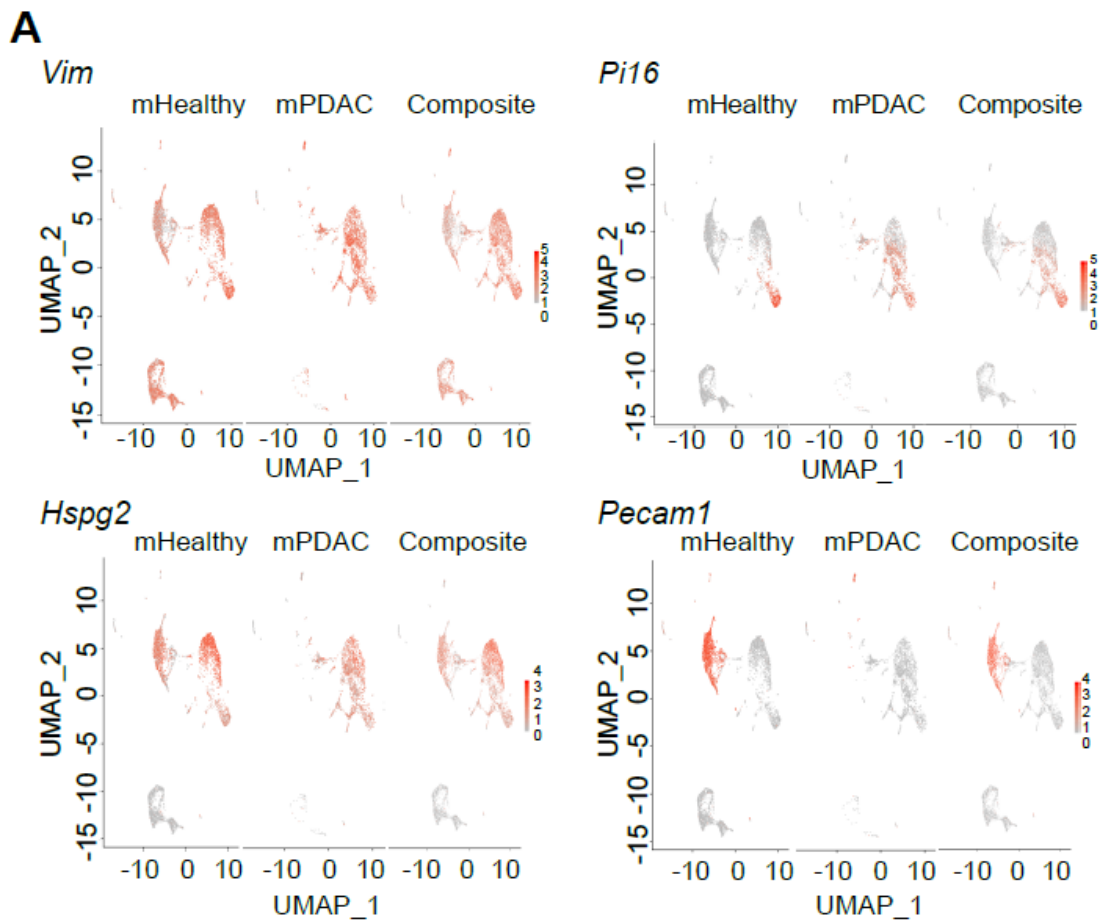


Figure 2.1. Pancreatic stellate cells contribute to the stromal microenvironment throughout tumorigenesis. **E**, Representative images of IHC staining for GFP (green) and CD31 (magenta) within GEMM pancreata (n = 3). Scale bar, 20 μ m. **F**, Representative images of IHC staining for GFP (green) and CD31 (magenta) within pancreata of KPC-derived orthotopically implanted PDAC in *Rosa26^{mTmG/+};Fabp4-Cre* mice (n = 3). Scale bar, 10 μ m.

We next assessed alterations in expression of cell surface ligands or receptors in this mesenchymal lineage during pancreatic tumorigenesis. We reasoned that paracrine signaling factors important for normal tissue architecture may be lost from the mesenchyme during the transition from normal tissue homeostasis to cancer. To identify

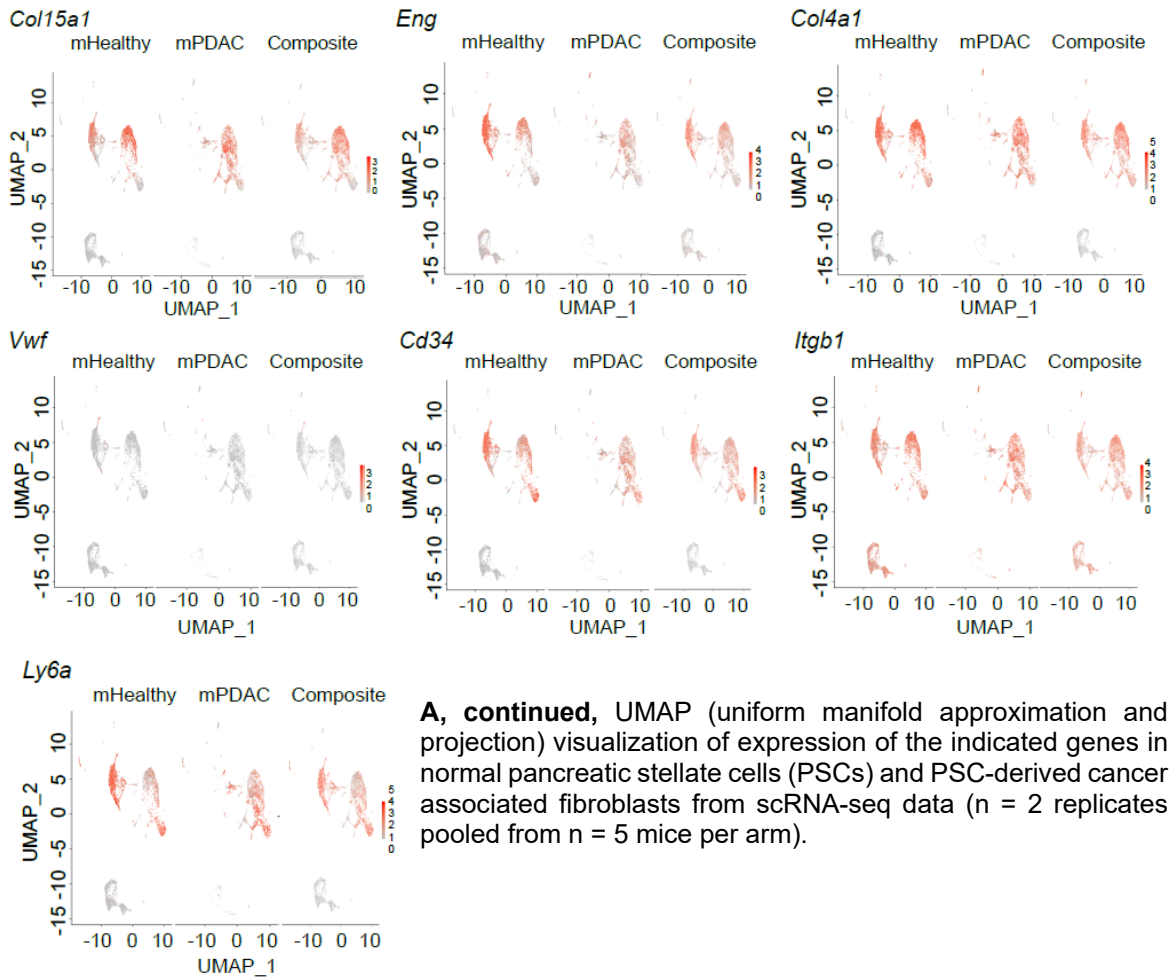
candidate paracrine factors associated with normal mesenchymal function whose loss may be tumor-permissive, we analyzed the transcriptional profiles of PSCs and PSC-derived CAFs. To this end, we sorted GFP+ PSCs and GFP+PDPN+ CAFs from healthy pancreas tissue and PDAC, respectively, and performed single-cell RNA-seq (scRNA-seq) to assess gene expression differences in this cellular compartment within and across tissue states. As expected, these cells in normal pancreas and PDAC were pervasively positive for mesenchymal markers *Vim* and *Eng* and almost all positive for pan-tissue fibroblast markers *Pi16* or *Col15a1* and universal fibroblast markers *Col4a1* and *Hspg2* (Buechler et al., 2021) (Figure 2.2A).

Figure 2.2. Mesenchymal KITL loss within PSCs accompanies pancreatic tumorigenesis.



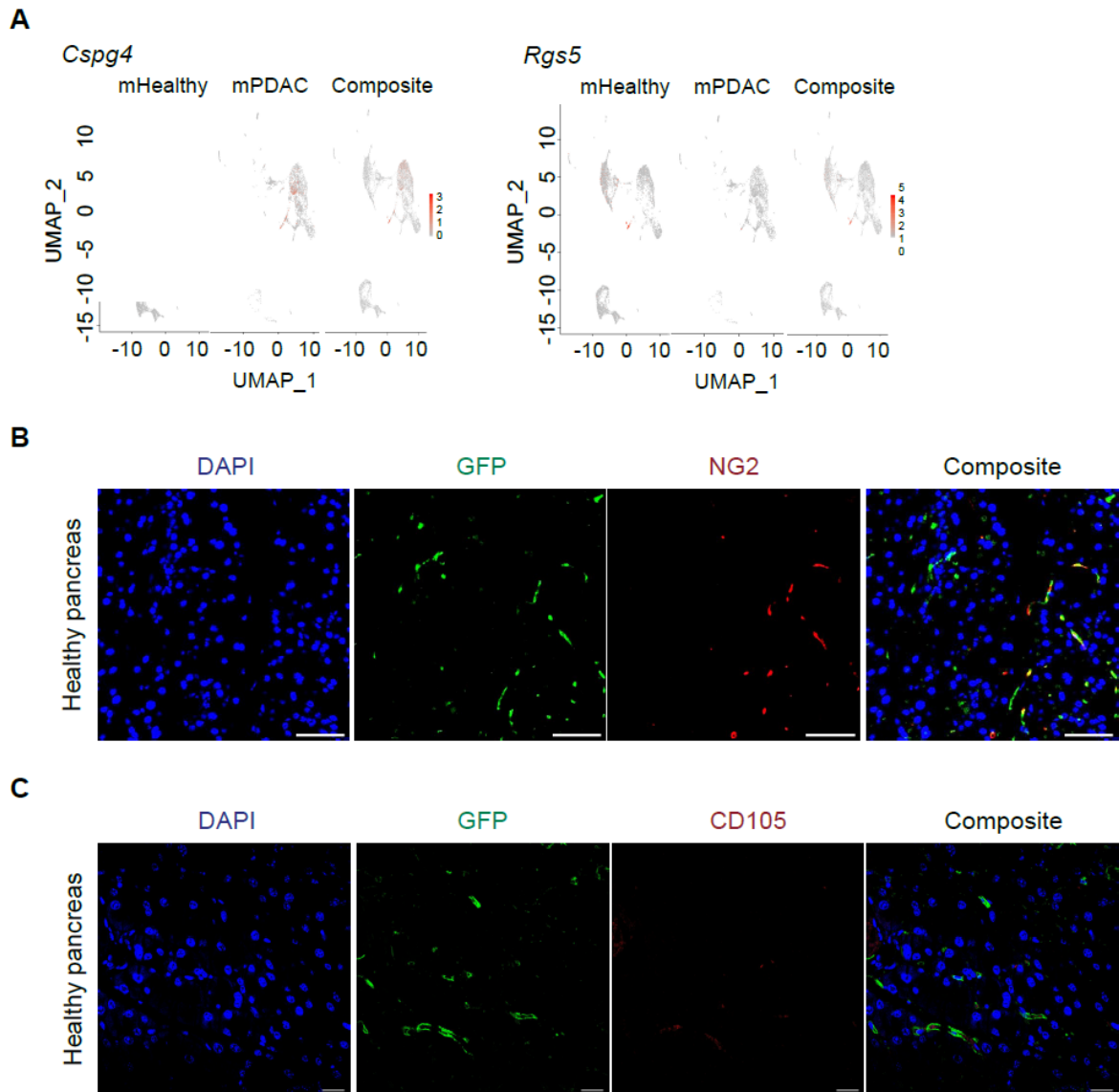
A, UMAP (uniform manifold approximation and projection) visualization of expression of the indicated genes in normal pancreatic stellate cells (PSCs) and PSC-derived cancer associated fibroblasts from scRNA-seq data (n = 2 replicates pooled from n = 5 mice per arm).

Figure 2.2. Mesenchymal KITL loss within PSCs accompanies pancreatic tumorigenesis.



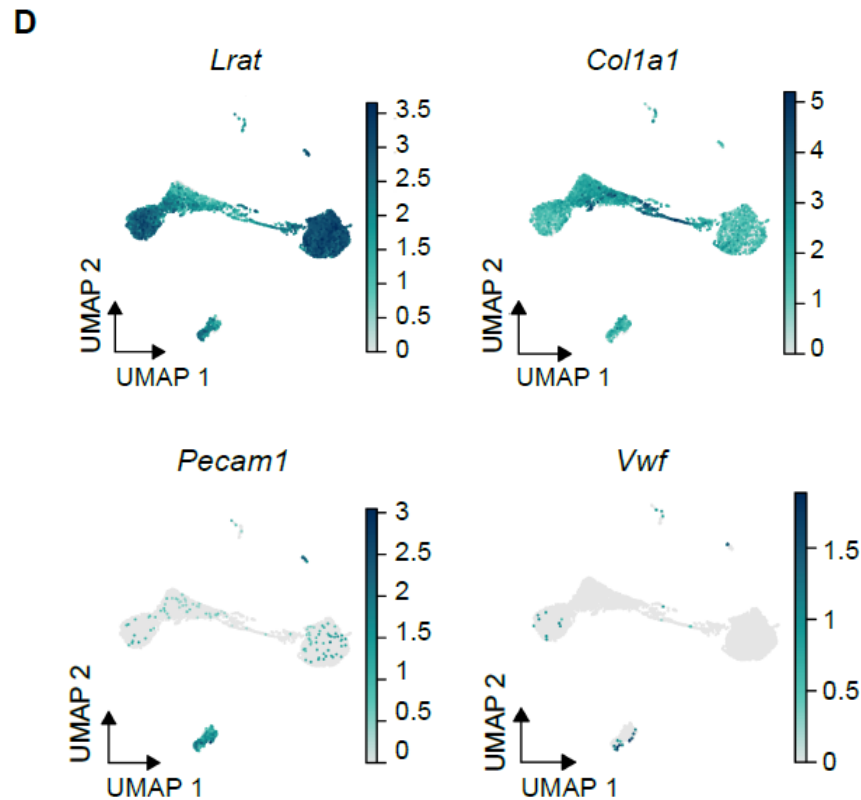
Though not all cells expressed one of these two universal fibroblast markers, we note that PSCs are not strictly fibroblasts albeit fibroblast-like. While PSCs and PSC derived CAFs are partially perivascular as described above, these cells lacked expression of classical pericyte markers such as *Cspg4* (encoding NG2) and *Rgs5* (Supplementary Figures 2.S1A & 2.S1B) and, despite detectable transcript, expressed low to absent CD105 (encoded by *Eng*) at the protein level (Supplementary Figure 2.S1C). CD105 expression at the protein level was rather low and sparse with the models and reagents used here. We also noted expression of established markers of perivascular reticular cells (Cheng et

al., 2019; Prados et al., 2021), specialized fibroblastic cells of lymphoid tissues, including *Cd34*, *Cd29/Itgb1*, and *Ly6a* (Figure 2.2A).



Supplementary Figure 2.S1. scRNA-seq reveals gene expression programs in PSCs and PSC-derived CAFs. **A**, UMAP (uniform manifold approximation and projection) visualization of *Cspg4* and *Rgs5* gene expression in scRNA-seq dataset of pancreatic stellate cells (PSCs) and PSC-derived cancer associated fibroblasts (CAFs) isolated from healthy pancreas and orthotopic tumors, respectively. **B**, Representative images of IHC staining for GFP (green) and NG2 (red) in healthy murine pancreas from *Rosa26^{mTmG/+};Fabp4-Cre* mice. Scale bar, 10 μ m. **C**, Representative images of IHC staining for GFP (green) and CD105 (red) in healthy murine pancreas. Scale bar, 10 μ m.

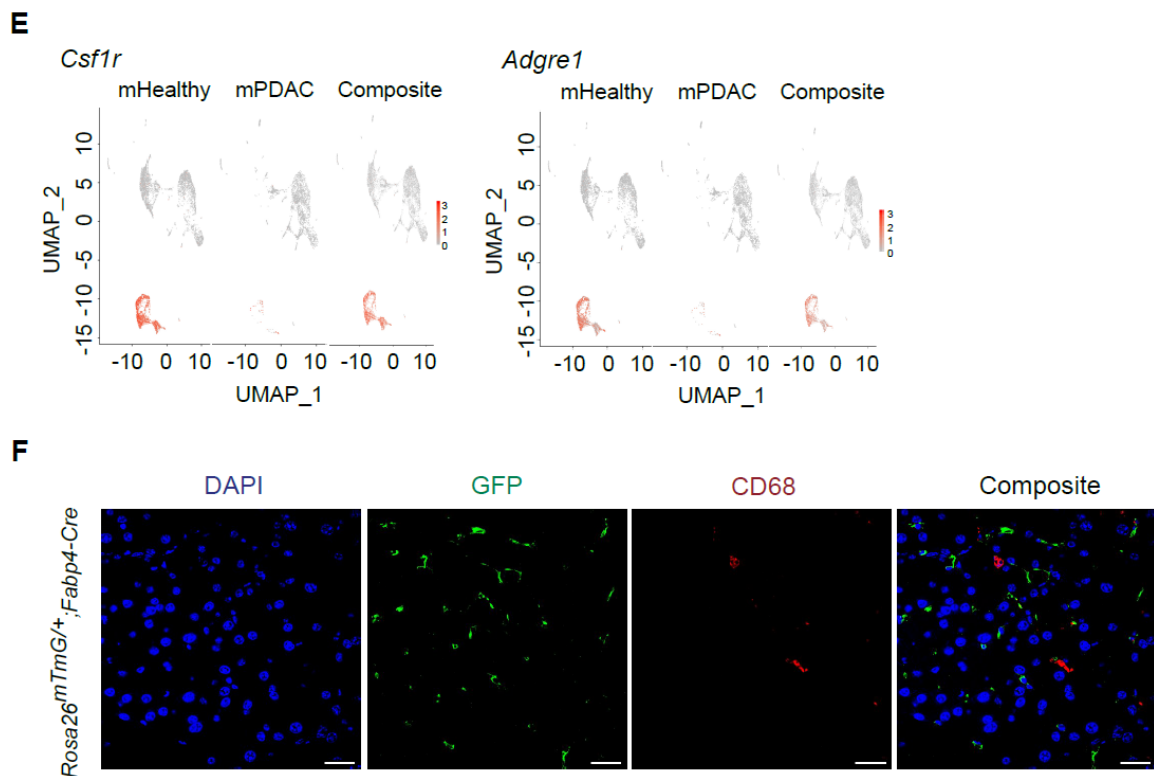
A sub-population of these cells in normal tissue also expressed adhesion molecules associated with endothelial cell identity, including *Pecam1*, which was also observed sporadically among HSCs in normal liver upon analysis of a previously published scRNA-seq dataset (Figure 2.2.A, Supplementary Figure 2.S1.D).



Supplementary Figure 2.S1. scRNA-seq reveals gene expression programs in PSCs and PSC-derived CAFs. D, UMAP visualization of *Lrat*, *Col1a1*, *Pecam1* and *Vwf* gene expression from a previously published scRNA-seq dataset hepatic stellate cells fate-mapped using *Lrat-Cre* and enriched by density centrifugation.

However, these cells did not express other endothelial markers such as *Vwf* (Figure 2.2A, Supplementary Figure 2.S1D) and seem to express far lower levels of both CD31 and CD105 (encoded by *Pecam1* and *Eng*, respectively) than *bona fide* endothelial cells given the limited overlap of these markers with GFP at the protein level by immunohistochemistry (Figure 2.1C, Supplementary Figure 2.S1C). That said, these results may indicate a shared precursor for stellate cells and endothelial cells late in

development. Interestingly, the sub-population in normal pancreas tissue lacking universal fibroblast markers expressed *Vim*, *Eng*, and genes generally associated with a macrophage identity, such as *Csf1r* and *Adgre1* (encoding F4/80) (Supplementary Figure 2.S1E). However, when we stained for GFP and macrophages in pancreas tissues we detected no overlap (Supplementary Figure 2.S1F), suggesting that this sub-population of cells in normal pancreas tissue may be fibrocyte-like or otherwise express some macrophage-associated genes without assuming a macrophage identity.



Supplementary Figure 2.S1. scRNA-seq reveals gene expression programs in PSCs and PSC-derived CAFs. **E**, UMAP visualization of *Csf1r* and *Adgre1* gene expression in pancreatic stellate cells (PSCs) and PSC-derived cancer associated fibroblasts scRNA-seq dataset (n = 2 replicates pooled from n = 5 mice per arm). **F**, Representative images of IHC staining for GFP (green) and CD68 (red) in normal pancreas tissue from *Rosa26^{mTmG}/+;Fabp4-Cre* mice (n = 3 mice). Scale bar, 50 μ m.

In the context of cancer, PSCs gained expression of immune modulatory cytokines such as *Il6* and *Il33* as expected for CAFs (Donahue et al., 2024) and pervasively expressed

extracellular matrix (ECM) components such as *Col1a1* and *Col1a2* (Figure 2.2B). These results validate activation of PSCs to a CAF phenotype in PDAC.

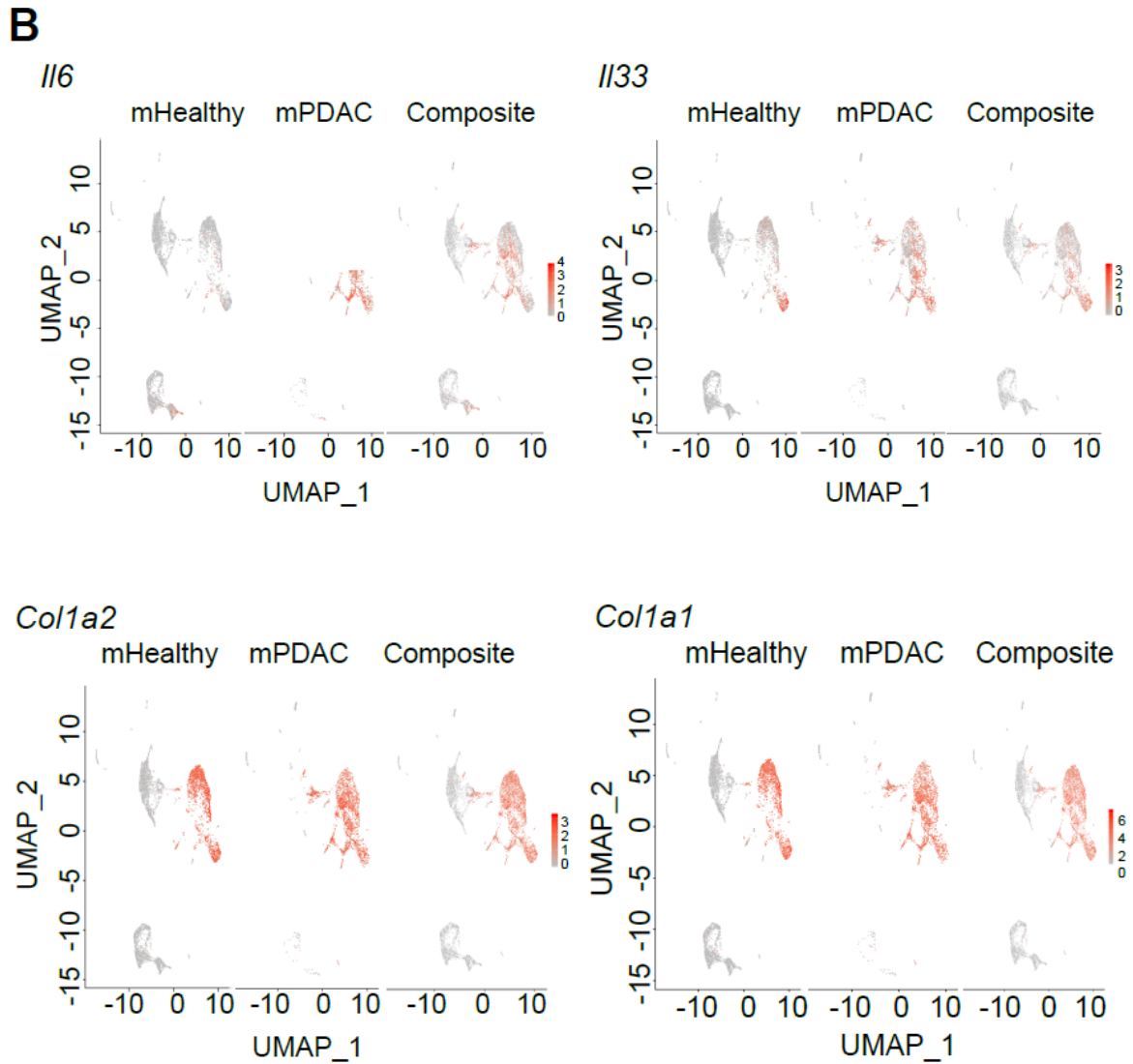
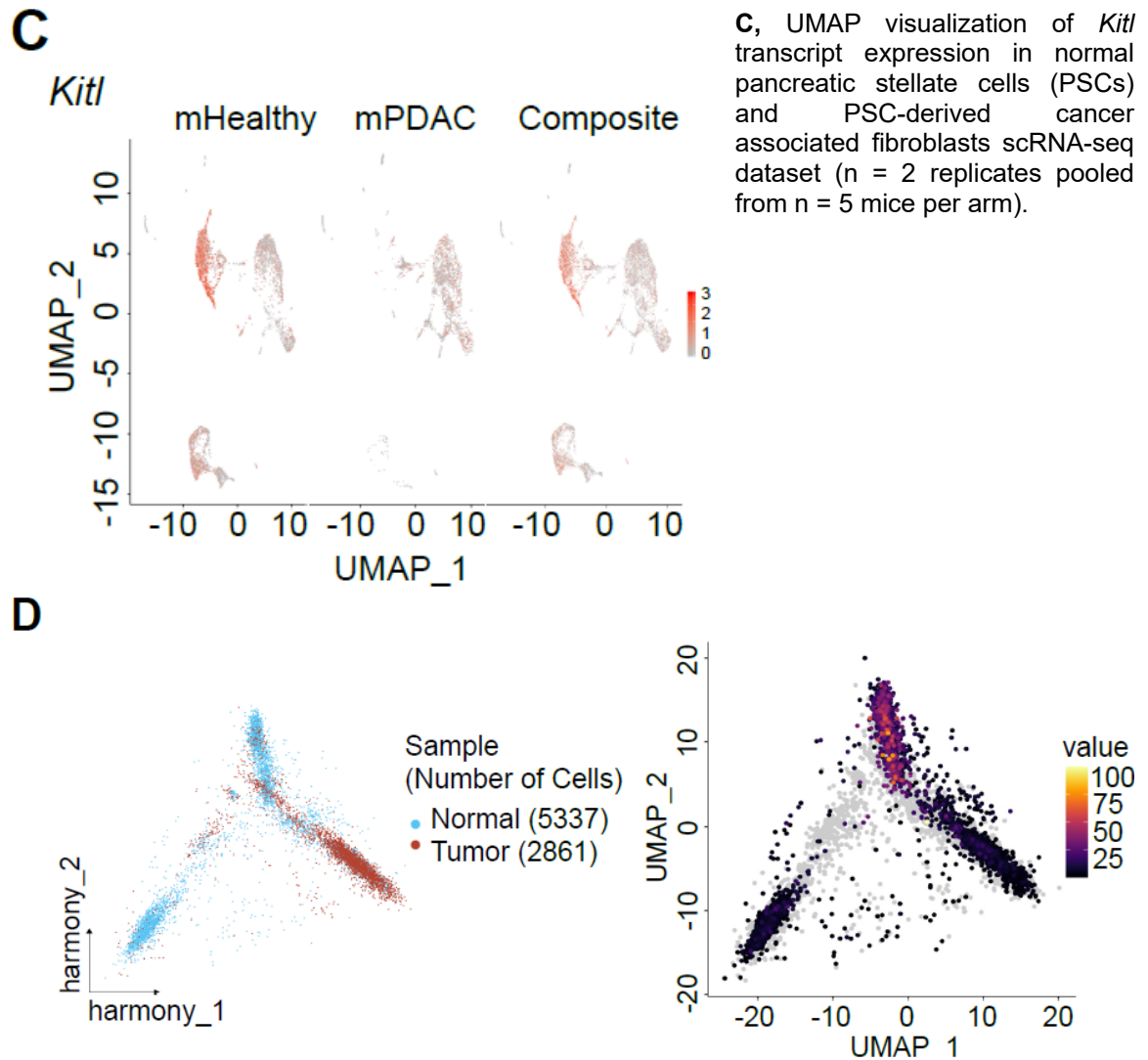


Figure 2.2. Mesenchymal KITL loss within PSCs accompanies pancreatic tumorigenesis. B, UMAP visualization of *Il6*, *Il33*, *Col1a1*, and *Col1a2* gene expression from normal pancreatic stellate cells (PSCs) and PSC-derived cancer associated fibroblasts scRNA-seq dataset (n = 2 replicates pooled from n = 5 mice per arm).

We next focused on paracrine signaling factors expressed in healthy pancreatic mesenchyme and lost in PDAC which may represent barriers to tumor progression. We noted expression of *Kitl* (also known as stem cell factor or SCF) in normal pancreas tissue

but lost in CAFs (Figure 2.2C), supported by pseudo-time analysis (Figure 2.2D). *KITL* expression has not previously been reported in normal pancreas tissue, and was of interest to us in light of the significance of *KITL*-positive mesenchyme in the perivascular niche of the bone marrow, where stromal *KITL* is crucial for normal tissue structure and function (Ding et al., 2012).

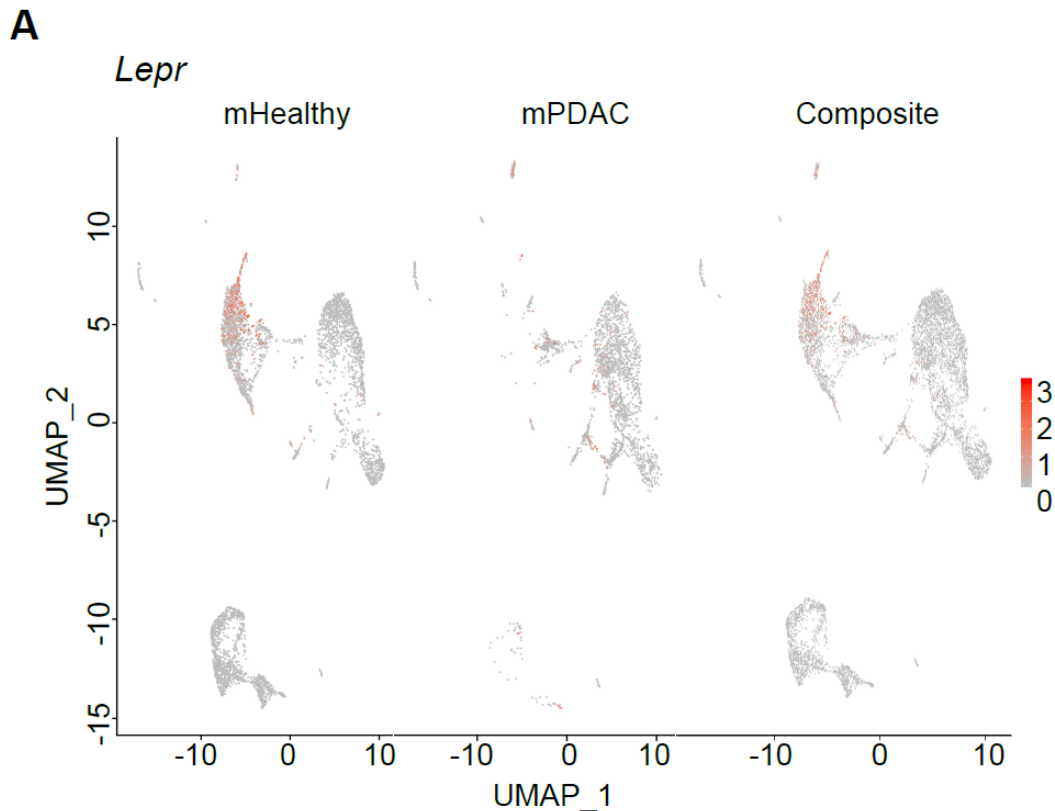
Figure 2.2. Mesenchymal *KITL* loss within PSCs accompanies pancreatic tumorigenesis.



D, Left: UMAP illustrating the cellular landscape of normal pancreatic (blue) and PDAC (red) mesenchymal cells, comprising 5,337 normal and 2,861 tumor cells. Harmony was used to integrate the datasets and correct for batch effects.

Right, Monocle 3 trajectory analysis was used to depict expression of the *Kitl* gene along the inferred pseudotime trajectory. Cells are colored based on *Kitl* expression levels, with values ranging from low (black) to high (yellow), revealing the temporal expression patterns of *Kitl* (n = 2 replicates pooled from n = 5 mice per arm).

Further, HSCs in the developing liver are critical sources of KITL to support the hematopoietic stem cell niche (Lee et al., 2020), providing precedent for functionally significant KITL production by stellate cells. KITL-positive mesenchyme in the bone marrow express leptin receptor (LEPR), and we detected low levels of *Lepr* expression among normal PSCs by scRNA-seq (Supplementary Figure 2.S2A).

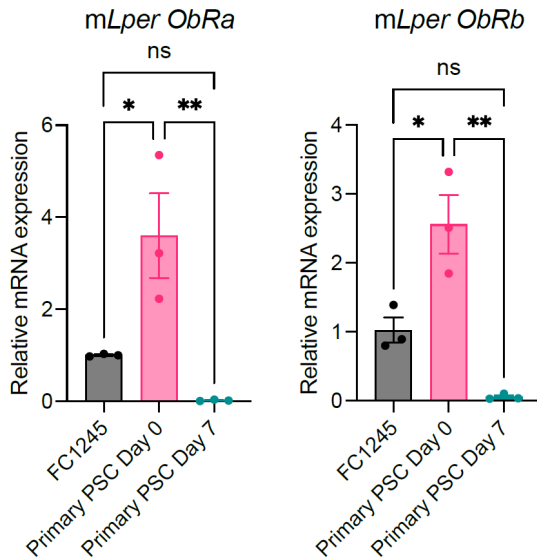


Supplementary Figure 2.S2. *Kitl* is expressed by healthy pancreatic mesenchyme and reduced upon activation to a CAF phenotype. **A**, UMAP visualization of *Lepr* gene expression in normal pancreatic stellate cells (PSCs) and PSC-derived cancer associated fibroblasts scRNA-seq dataset (n = 2 replicates pooled from n = 5 mice per arm).

We validated these findings by isolating primary PSCs from healthy pancreas tissue and activating them to a CAF phenotype in culture: These cells expressed *Kitl* and *Lepr* in their normal tissue state but progressively lost expression of both factors upon activation to a CAF-like state upon exposure to a stiff growth substrate with or without recombinant TGF- β (Figure 2.2E, Supplementary Figures 2.S2B-D).

Supplementary Figure 2.S2. *Kitl* is expressed by healthy pancreatic mesenchyme and reduced upon activation to a CAF phenotype.

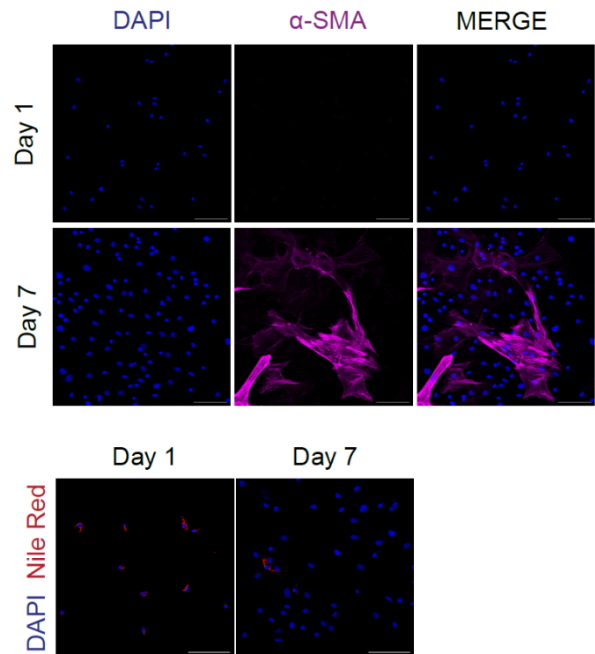
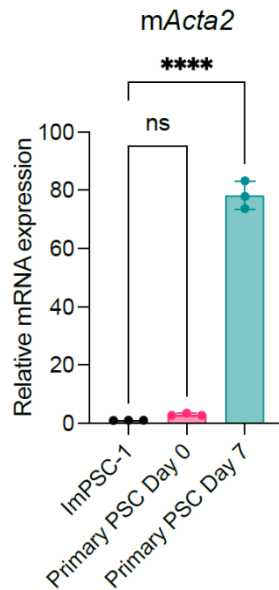
B



B, qRT-PCR of *Lepr ObRa* and *Lepr ObRb* isoforms in primary pancreatic stellate cells harvested at indicated time point. FC1245 PDAC cell line was included as a reference point. Data represents biological triplicates plotted as mean ± SEM. Significance was determined by ordinary one-way ANOVA; ns = not significant, *P ≤ 0.05, **P ≤ 0.01.

C, Left: qRT-PCR analysis of *Acta2* in quiescent (Day 0) and activated (Day 7) primary pancreatic stellate cells (PSCs) with immortalized ImpSC-1 included as reference point. Data represents biological triplicate plotted as mean ± SEM. Significance was determined by ordinary one-way ANOVA; ns = not significant, ****P ≤ 0.0001.

C



Right: Representative immunofluorescence images for α-SMA and Nile Red staining in primary pancreatic stellate cells fixed at indicated time point (n= 3 biological replicates). Scale Bar: 100 μm.

Supplementary Figure 2.S2. *Kitl* is expressed by healthy pancreatic mesenchyme and reduced upon activation to a CAF phenotype. D, qRT-PCR of *Kitl*, *Acta2* and *Pdpr* in primary mouse pancreatic stellate cells (mPSCs) treated with recombinant KITL at the indicated time point. Immortalized mPSC-1 cell line was included as a reference point. Data represents technical triplicates plotted as mean \pm SD. Significance was determined by ordinary one-way ANOVA; * $P \leq 0.05$, ** $P \leq 0.01$, *** $P \leq 0.001$, **** $P \leq 0.0001$.

D

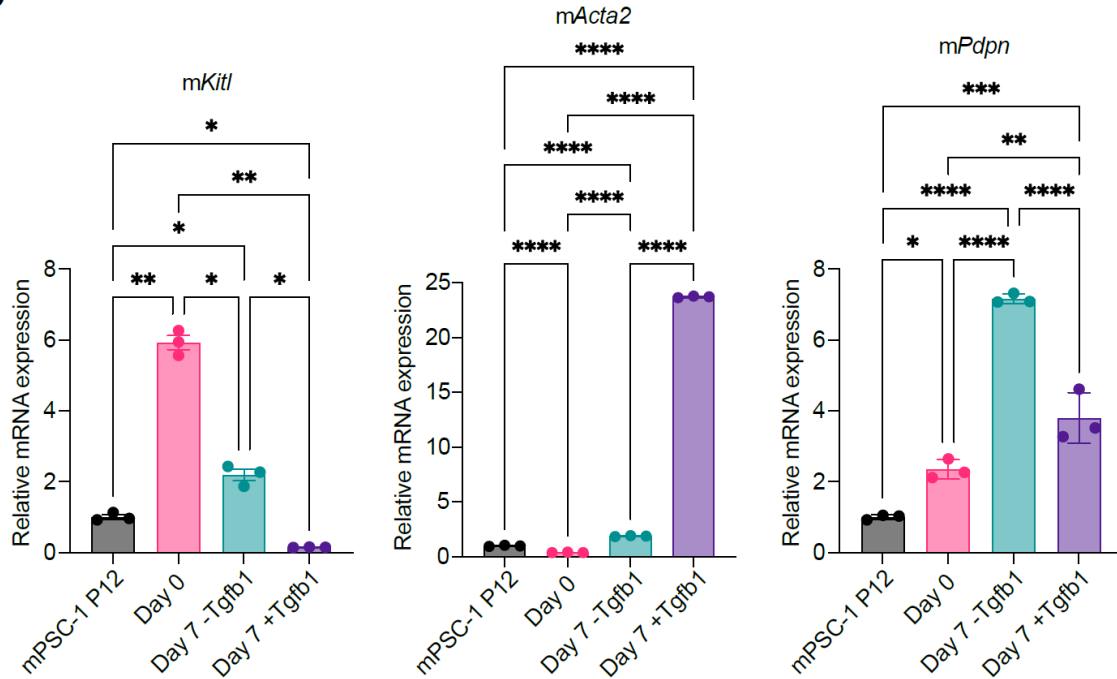
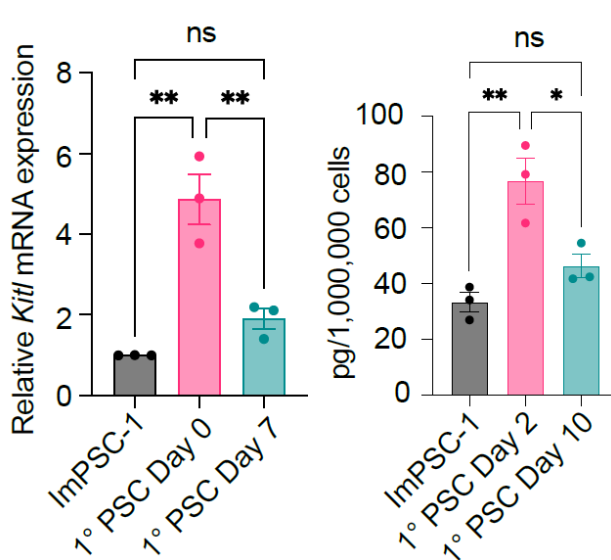


Figure 2.2. Mesenchymal KITL loss within PSCs accompanies pancreatic tumorigenesis.

E



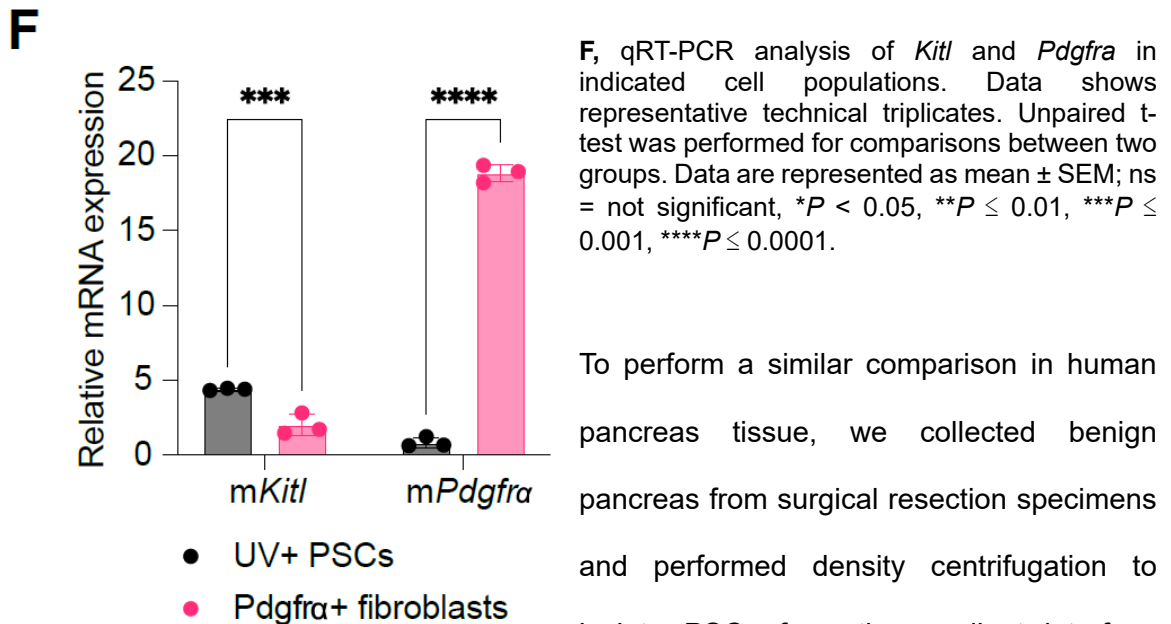
E, Left: qRT-PCR analysis of *Kitl* in quiescent (Day 0) and culture-activated (Day 7, on plastic) primary pancreatic stellate cells (PSCs). Data represents biological triplicate.

Right: Quantikine ELISA KITL measurement of supernatant collected from primary PSCs in pre-activated (Day 2) and activated state (Day 10) after 48 hours incubation with media change on Day 8 to harvest for Day 10 sample. Immortalized ImpSC-1 included as reference point. Data represents biological triplicate.

For comparisons more than two groups, significance was determined by ordinary one-way ANOVA. Data are represented as mean \pm SEM; ns = not significant, * $P < 0.05$, ** $P \leq 0.01$, *** $P \leq 0.001$, **** $P \leq 0.0001$.

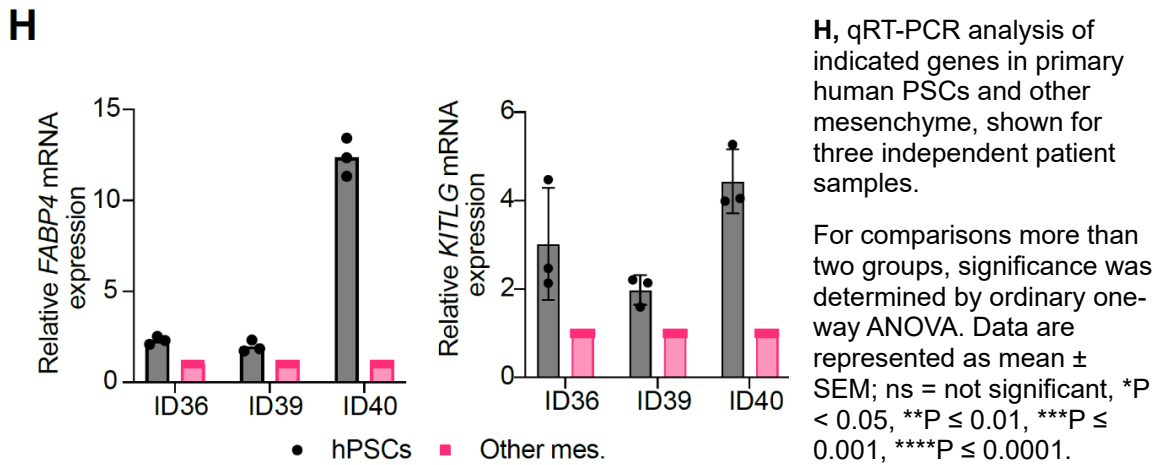
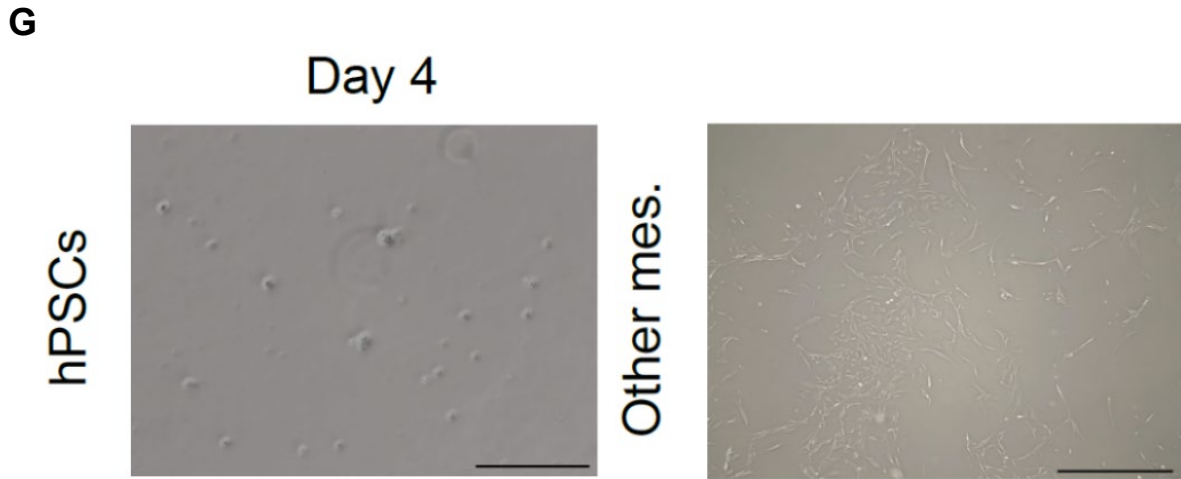
We next validated expression of *Kitl* in intact murine pancreas tissue. To further understand *Kitl* expression patterns in the pancreatic mesenchyme, we used standard density centrifugation to isolate PSCs from the gradient interface (Apte et al., 1998) and also isolated PDGFR α + pancreatic fibroblasts from the lower layers of the gradient (Garcia et al., 2020). We found significantly higher *Kitl* expression in PSCs than in conventional tissue fibroblasts (Figure 2.2F), which may contribute to the substantial contribution of these PDGFR α -expressing fibroblasts to early pancreatic neoplasia.

Figure 2.2. Mesenchymal KITL loss within PSCs accompanies pancreatic tumorigenesis.



(Vonlaufena et al., 2010), then performed negative selection for EpCAM, CD45, and CD31 on remaining cells to collect mesenchymal cells from the lower layers of the gradient. We analyzed gene expression across these freshly isolated fractions, plating a small sampling on coverslips to image and validate, and found that human PSCs expressed higher levels of *KITLG* than non-PSC components of the pancreatic mesenchyme, though we note that degree of difference varied among patients (Figures 2.2G & 2.2H).

Figure 2.2. Mesenchymal KITL loss within PSCs accompanies pancreatic tumorigenesis.
G, Representative brightfield images of primary human PSCs and other mesenchyme. Scale bar, 50 μ m.



To further validate our findings from mice, we cultured human PSCs from these benign resection specimens and activated them to a CAF-like phenotype by exposure to a stiff growth substrate with or without PDAC cell conditioned media. Human PSC activation featured a significant reduction in *KITLG* expression (Figure 2.2I), further supporting the notion that normal pancreatic mesenchyme expresses *Kit/KITLG* but this factor is lost as these cells transition to a CAF state in the tumor microenvironment.

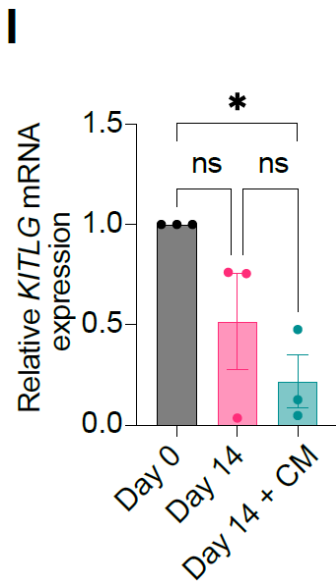


Figure 2.2. Mesenchymal KITL loss within PSCs accompanies pancreatic tumorigenesis. I, qRT-PCR analysis of *KITLG* in quiescent (Day 0) and conditioned media activated (Day 14) primary human PSCs. Data represents biological triplicate. For comparisons more than two groups, significance was determined by ordinary one-way ANOVA. Data are represented as mean ± SEM; ns = not significant, *P < 0.05, **P ≤ 0.01, ***P ≤ 0.001, ****P ≤ 0.0001.

We next assessed patterns of *Kitl* expression in intact pancreas tissues. By RNA *in situ* hybridization (ISH, due to lack of specific antibodies, using branched cDNA hybridization), we detected *Kitl* expression in mesenchymal

cells of normal pancreas tissue which share markers with PSCs, while *Kitl* expression was lost among CAFs in PDAC (Figure 2.2J). We also combined RNA ISH for *Kitl* (here using RNAscope, compatible with protein co-staining) with immunohistochemistry (IHC) for GFP on pancreas tissue from *Rosa26^{mTmG/+};Fabp4-Cre* mice and confirmed *Kitl* expression in fate-mapped PSCs (Figure 2.2J).

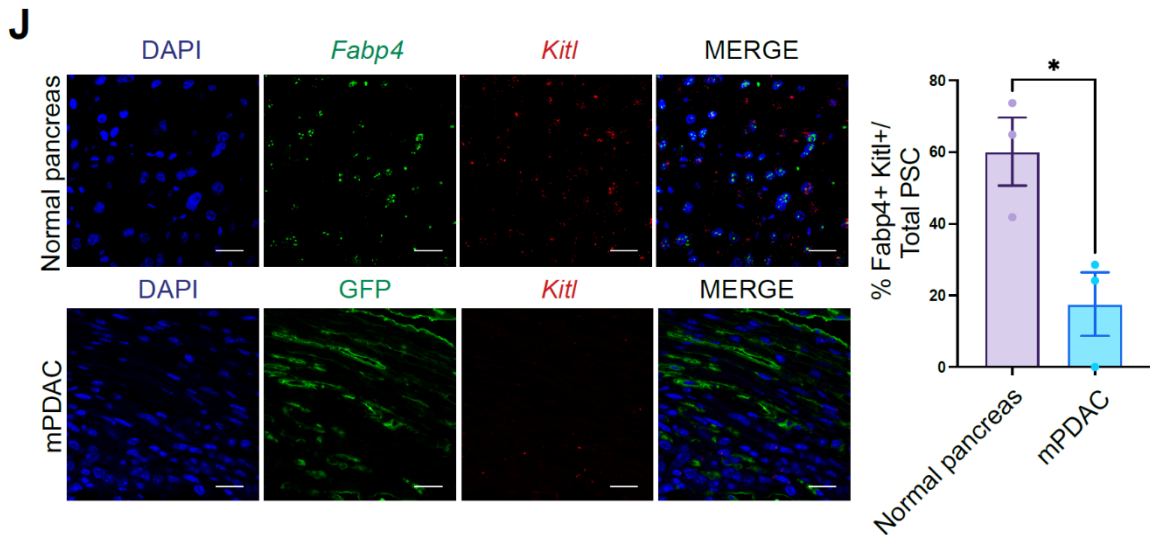
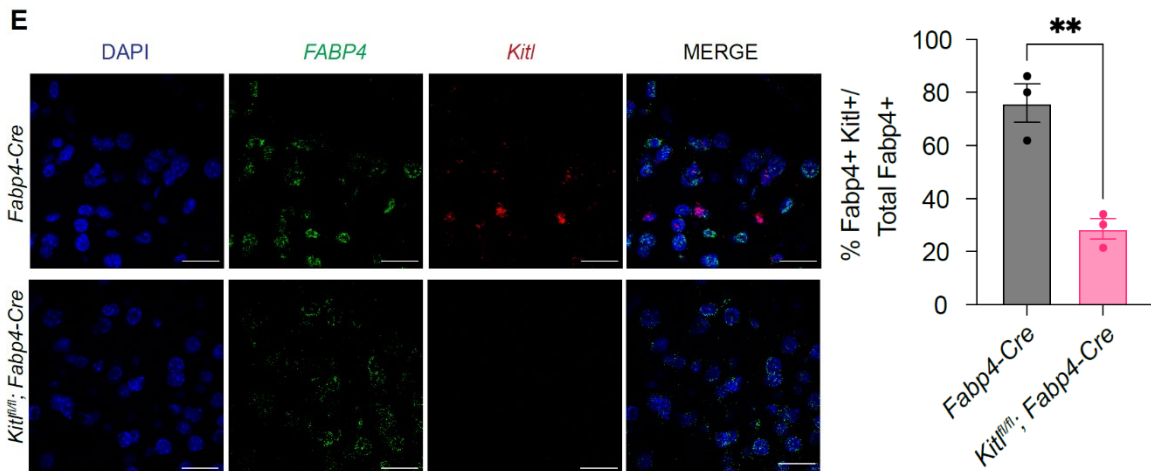


Figure 2.2. Mesenchymal KITL loss within PSCs accompanies pancreatic tumorigenesis. J, Representative image (top left) of RNA FISH staining for *Fabp4* (green) and *Kitl* (red) in murine normal pancreas (n = 3). Scale bar, 10 μm. **Bottom left**, representative RNAscope staining of GFP (green) protein and *Kitl* (red) mRNA in PDAC from the GEMM depicted in 2.1A (n = 3). Scale bar, 10 μm. **Right**, quantification for *Fabp4*+ cells (*Fabp4*+ or GFP+) and *Kitl* between murine normal pancreas and mPDAC. Unpaired test was performed for comparisons between two groups. Data are represented as mean ± SEM; ns = not significant, *P < 0.05, **P ≤ 0.01, ***P ≤ 0.001, ****P ≤ 0.0001.

Specificity of our *Kitl* probe was confirmed by reduction in mesenchymal *Kitl* signal in pancreas tissues from *Kitl^{fl/fl};Fabp4-Cre* mice (Supplementary Figure 2.S2E). We extended these analyses to human pancreas tissue, and performed RNA ISH for *KITLG* (shortened as *KITL*) and mesenchymal marker *VIM*. While benign human pancreas harbored *KITL*-positive mesenchyme, CAFs within human PDAC showed reduced *KITL* expression, consistent with observations in mice (Figure 2.2K), though we note that *KITL/VIM* frequency was highly variable in benign adjacent regions and this difference did not reach statistical significance. Human pancreas tissue showed minimal expression of *KITL* in CD45-positive leukocytes (Supplementary Figure 2.S2F).



Supplementary Figure 2.S2. *Kitl* is expressed by healthy pancreatic mesenchyme and reduced upon activation to a CAF phenotype. E, Representative images of RNA FISH staining for *Fabp4* (green) and *Kitl* (red) mRNA in murine normal pancreas between *Fabp4-Cre* control and *Kitl^{fl/fl};Fabp4-Cre* mice (n = 3), quantified below. Scale bar, 10 μ m. Unpaired test was performed for comparisons between two groups. Data are represented as mean \pm SEM; ns = not significant, *P < 0.05, **P \leq 0.01, ***P \leq 0.001, ****P \leq 0.0001.

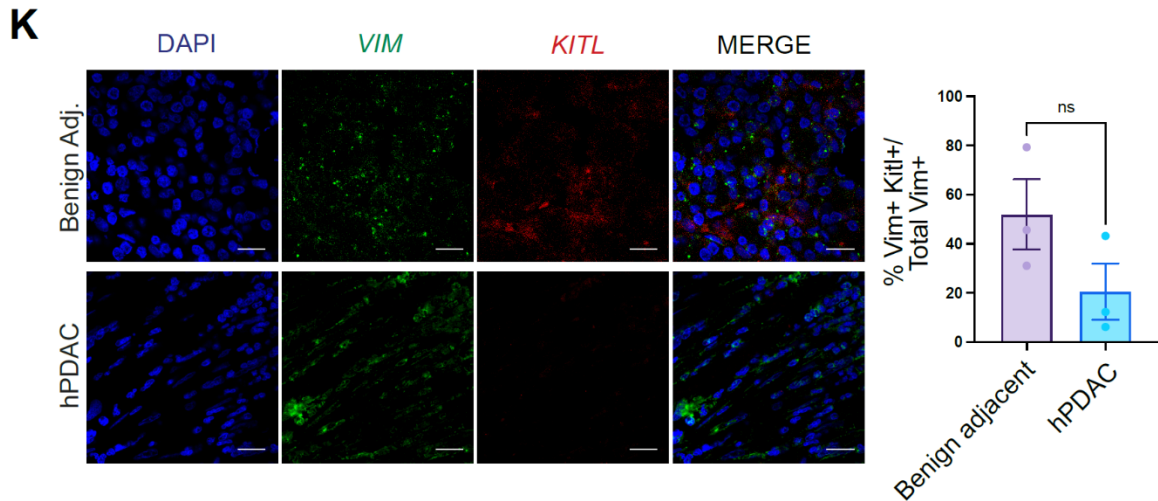
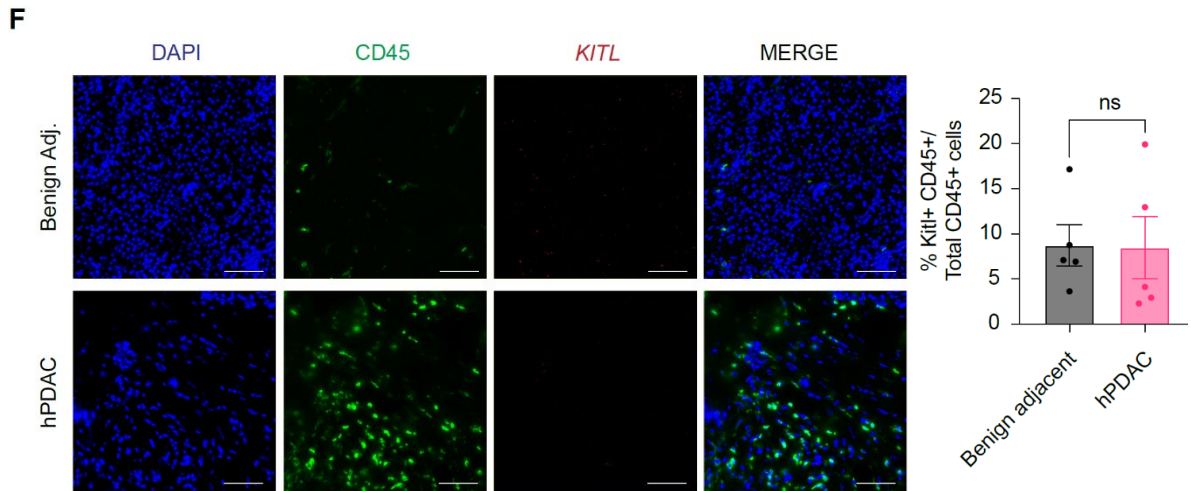


Figure 2.2. Mesenchymal KITL loss within PSCs accompanies pancreatic tumorigenesis. **K**, Representative images and quantification of RNA FISH staining for *VIM* (green) and *KITL* (red) in human PDAC tissues between benign adjacent and PDAC regions ($n = 3$). Scale bar, 20 μm . Unpaired t-test was performed for comparisons between two groups. Data are represented as mean \pm SEM; ns = not significant, * $P < 0.05$, ** $P \leq 0.01$, *** $P \leq 0.001$, **** $P \leq 0.0001$.



Supplementary Figure 2.S2. *Kitl* is expressed by healthy pancreatic mesenchyme and reduced upon activation to a CAF phenotype. **F**, Representative images of RNA FISH staining for *KITL* and IHC for CD45 on human benign pancreas tissue or PDAC ($n = 5$), quantified below. Scale bar, 50 μm . Unpaired t-test was performed for comparisons between two groups. Data are represented as mean \pm SEM; ns = not significant, * $P < 0.05$, ** $P \leq 0.01$, *** $P \leq 0.001$, **** $P \leq 0.0001$.

As perivascular mesenchyme is a critical source of KITL in other tissues (Ding et al., 2012; Lee et al., 2020), we assessed the spatial distribution of mesenchymal *Kitl* expression by combining *Kitl* RNA ISH with IHC for CD31 and GFP on pancreas tissues from *Rosa26^{mTmG/+};Fabp4-Cre* mice. We found that PSCs express *Kitl* in both perivascular regions and when not adjacent to endothelial cells (Figure 2.2L), suggesting that KITL from PSCs is poised to signal to multiple neighboring cell types.

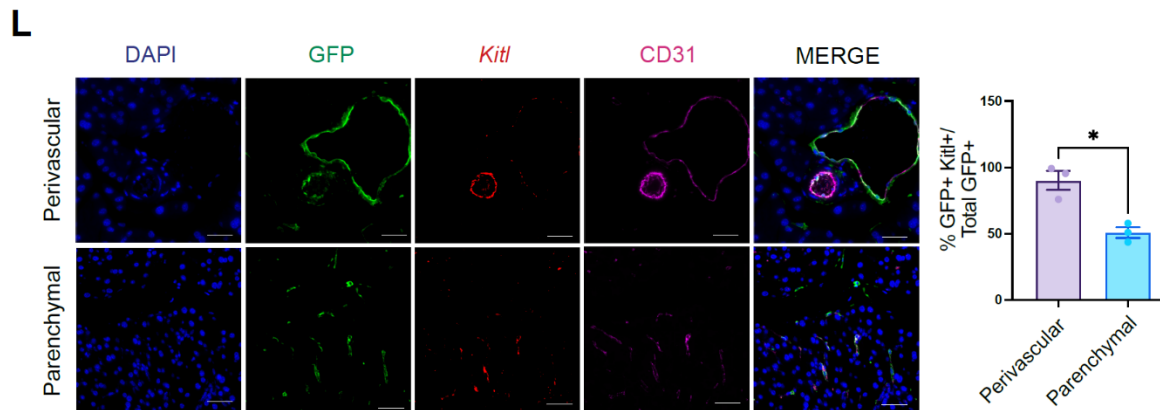


Figure 2.2. Mesenchymal KITL loss within PSCs accompanies pancreatic tumorigenesis.
L, Representative images (left) and quantification (right) of RNAscope staining for *Kitl* (red) mRNA expression, GFP (green) and CD31 (magenta) in murine normal pancreas from *Rosa26^{mTmG/+};Fabp4-Cre* mice (n = 3). Scale bar, 20 μ m. Unpaired t-test was performed for comparisons between two groups. Data are represented as mean \pm SEM; ns = not significant, *P < 0.05, **P \leq 0.01, ***P \leq 0.001, ****P \leq 0.0001.

To assess the stage of pancreatic tumorigenesis at which mesenchymal *Kitl* expression is lost, we combined RNA ISH for *Kitl* and IHC for GFP (to indicate PSCs and PSC-derived CAFs) on tissues from *Kras^{FSF-G12D/+};Trp53^{FRT/+};Pdx1-FlpO;Rosa26^{mTmG/+};Fabp4-Cre* mice and noted retention of *Kitl* expression among GFP-positive stromal cells associated with low-grade PanIN lesions identified by a pathologist (Figure 2.2M), suggesting that loss of stromal *Kitl* accompanies late stages of pancreatic tumorigenesis. Expression of *Kitl* by some GFP-negative cells was noted within these areas of low-grade PanIN as well.

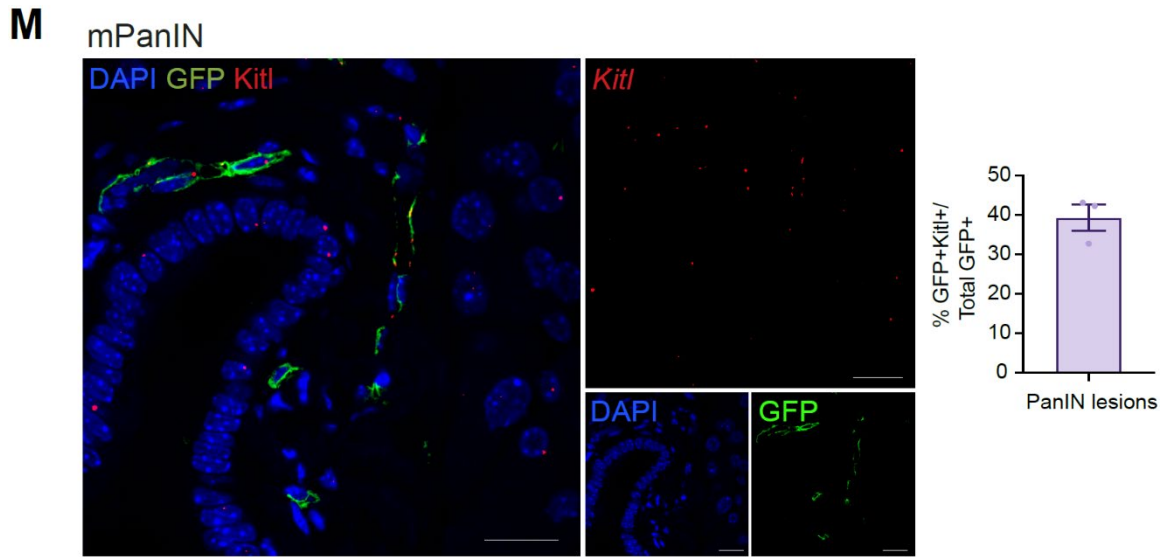


Figure 2.2. Mesenchymal KITL loss within PSCs accompanies pancreatic tumorigenesis. **M**, Representative images and quantification of RNAscope staining for GFP (green) protein and *Kitl* (red) mRNA in GEMM low grade PanIN (n = 3). Scale bar, 20 μ m. Data are represented as mean \pm SEM.

Consistent with production of KITL protein in healthy pancreas, small numbers of phospho-c-KIT-positive cells were identified in murine and human benign pancreas (Figures 2.2N & 2.2O), only detectable on fresh-frozen and not formalin-fixed tissues (see Methods). Together, these analyses revealed expression of *Kitl* by a lineage of healthy pancreatic mesenchyme in mice and humans which is lost upon transition to a CAF phenotype in invasive cancer.

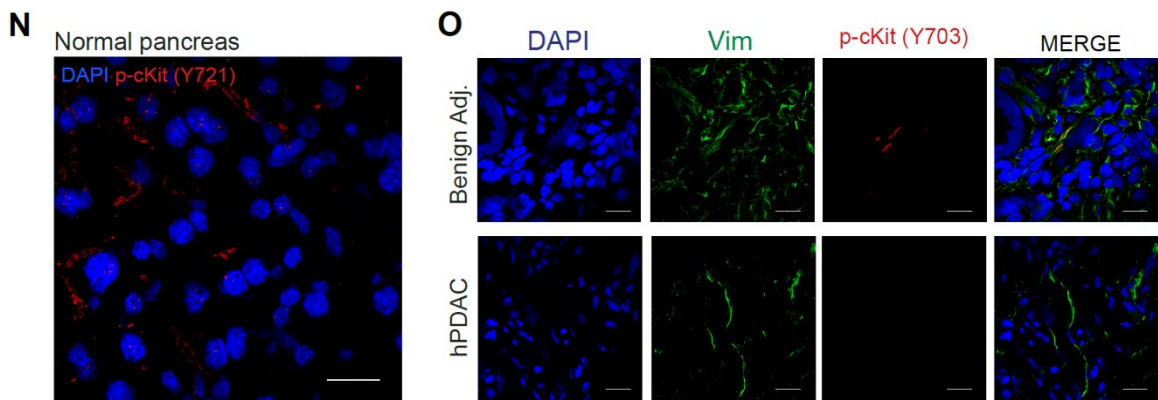
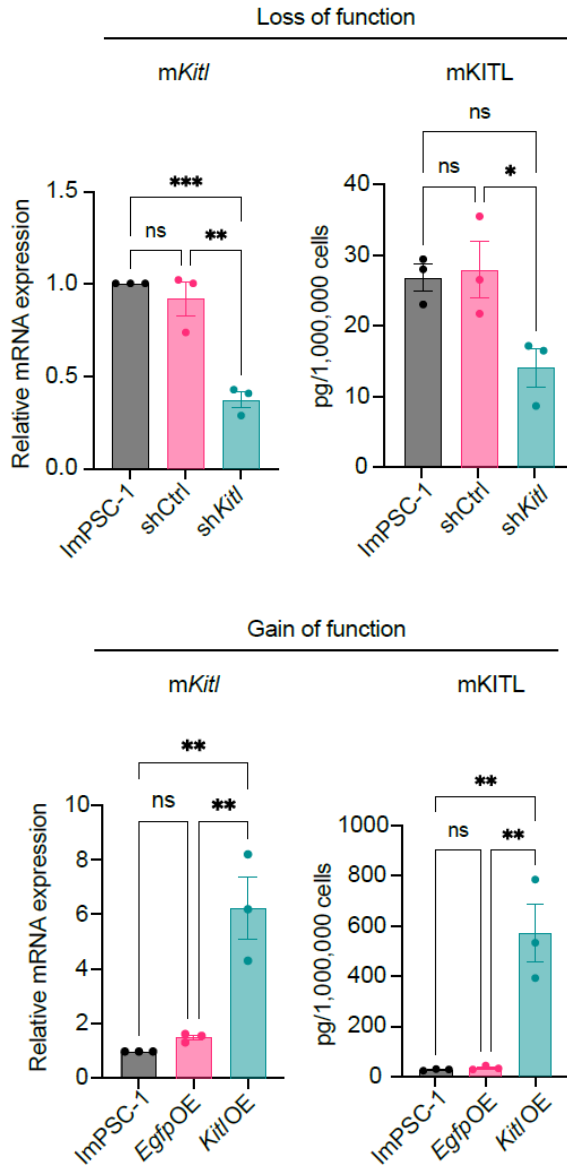


Figure 2.2. Mesenchymal KITL loss within PSCs accompanies pancreatic tumorigenesis. **N**, Representative image of IHC staining for phosphorylated-c-KIT (Y721, red) in normal murine pancreas (n = 3). Scale bar, 10 μ m. **O**, Representative images of IHC staining for Vimentin (VIM, green) and phosphorylated-c-KIT (Y703, red) in benign adjacent and human PDAC tissues (n = 3) Scale bar, 10 μ m.

Supplementary Figure 2.S3. Stromal KITL promotes regulation of pancreas tissue architecture.

A



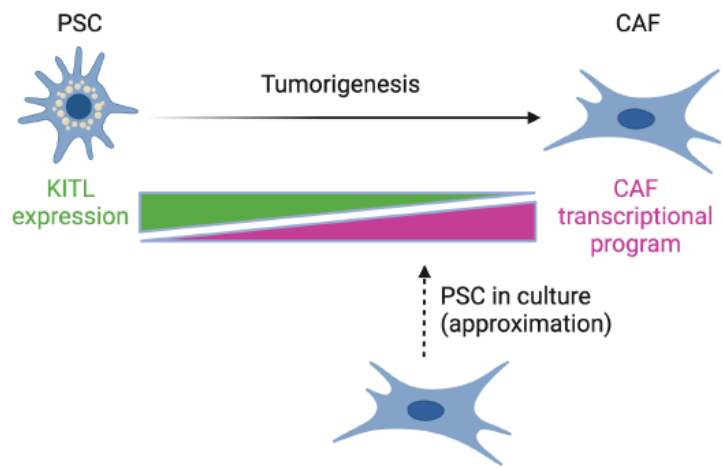
A: Soluble *Kitl* transcript level and protein secretion, quantitated using qRT-PCR and ELISA respectively, of immortalized pancreatic stellate cells (ImpPSC-1) expressing stable *Kitl* knockdown (sh*Kitl*) or overexpression (*Kitl* OE). Parental ImpPSC-1 serves as control for both stable cell lines. Data represents biological triplicates plotted as mean \pm SEM. Significance was determined by ordinary one-way ANOVA; ns = not significant, * $P \leq 0.05$, ** $P \leq 0.01$, *** $P \leq 0.001$.

We next addressed the functional significance of KITL in pancreatic mesenchyme, and assessed the consequence of stromal KITL loss for tissue homeostasis. First, we questioned the cell-intrinsic impact of KITL signaling on pancreatic mesenchymal cells. To address this, we generated loss- and gain-of-function

systems in cell culture by knocking down or overexpressing *Kitl* in immortalized PSCs (Auciello et al., 2019) using shRNA or introduction of the *Kitl* ORF, respectively (Supplementary Figure 2.S3A).

Supplementary Figure 2.S3. Stromal KITL promotes regulation of pancreas tissue architecture. A, continued:

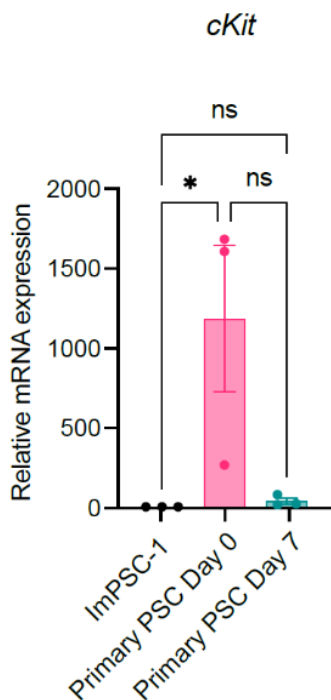
Schema depicting KITL expression of immortalized murine PSCs cultured *in vitro*.



PSCs in culture express low but detectable levels of *Kitl* (Figure 2.2.E), so we reasoned that gene expression changes observed with *Kitl*

overexpression would reflect downstream transcriptional programs in healthy mesenchyme while *Kitl* knockdown would reflect consequences of gene expression changes upon transition to a CAF state.

Supplementary Figure 2.S3. Stromal KITL promotes regulation of pancreas tissue architecture. B



B, qRT-PCR of c-KIT in quiescent (Day 0) and activated (Day 7) primary pancreatic stellate cells (PSCs) with immortalized ImpPSC-1 included as reference point. Data represents biological triplicate plotted as mean \pm SEM. Significance was determined by ordinary one-way ANOVA; ns = not significant, * $P \leq 0.05$.

In culture, PSCs express low but detectable levels of *Kit* (encoding c-KIT) (Supplementary Figure 2.S3B), the paracrine signaling partner for KITL, such that PSC monoculture seemed a reasonable *in vitro* model to begin assessing how KITL signaling impacts pancreatic mesenchyme. To this end, we analyzed the transcriptional profiles of *Kitl*-knockdown and *Kitl*-overexpressing PSCs,

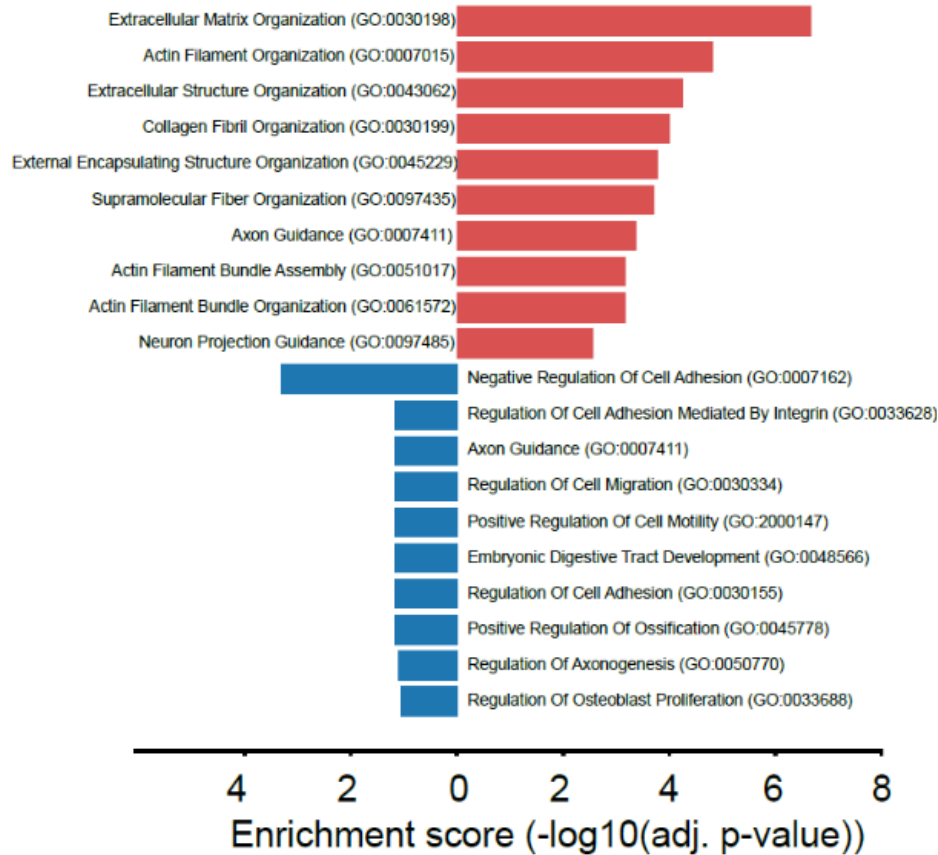
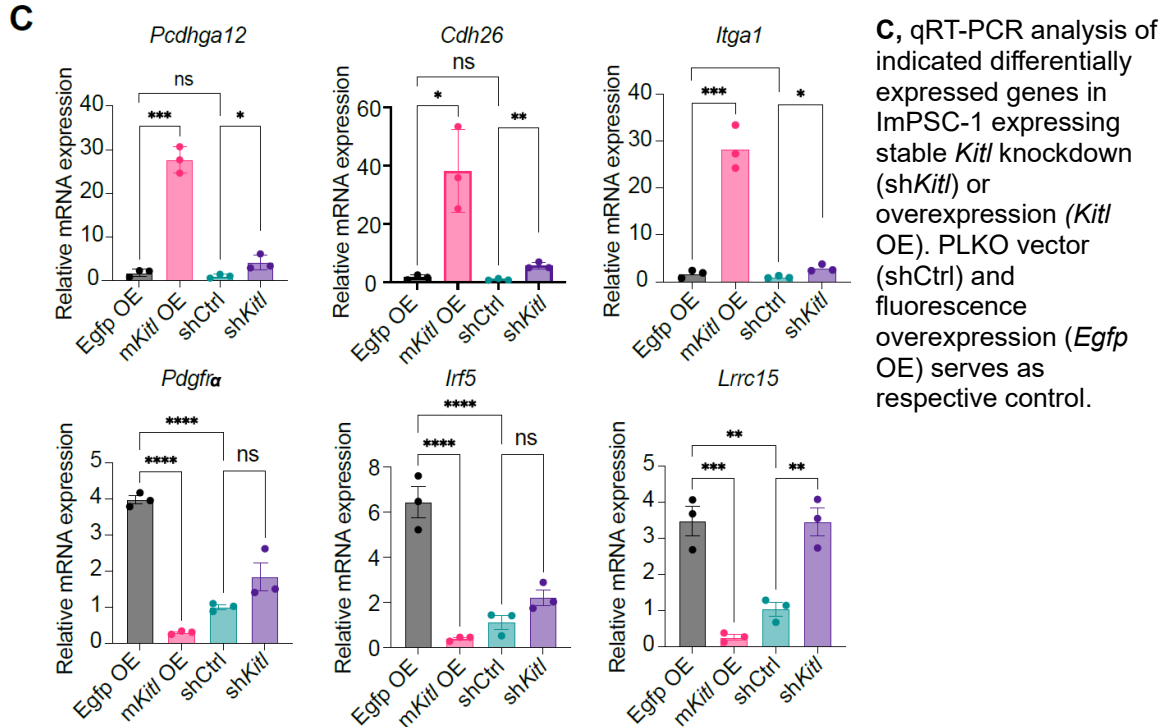
B**Egfp vs *Kitl* OE**

Figure 2.3. KITL regulates PSC state and pancreas tissue homeostasis. B, Gene ontology (GO) analysis of upregulated and downregulated genes in immortalized pancreatic stellate cells (ImpSC-1) overexpressing *Kitl*. Top 10 enrichment categories ranked by adjusted p-values plotted in each direction.

Specific inflammatory and architectural genes modulated by KITL restoration were regulated in the opposite direction by *Kitl* knockdown, supporting a specific role for KITL (Figure 2.3C). We note, though, that a substantial group of genes positively regulated by *Kitl* signaling were expressed at a very low level in control cells and were not significantly downregulated further upon *Kitl* knockdown (Supplementary Figure 2.S3C). These results

suggest that mesenchymal KITL may maintain pancreas tissue homeostasis, prompting us to move into in vivo modeling of KITL function.

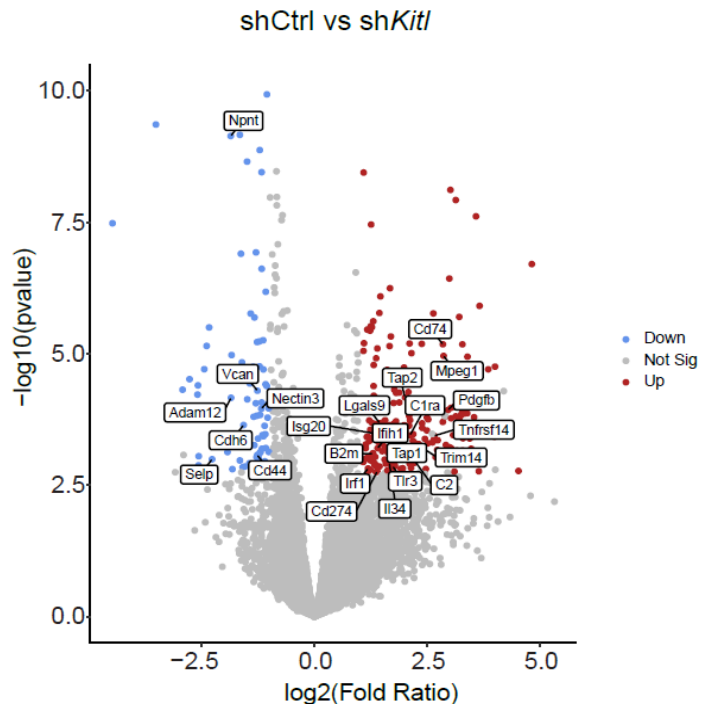
Figure 2.3. KITL regulates PSC state and pancreas tissue homeostasis.



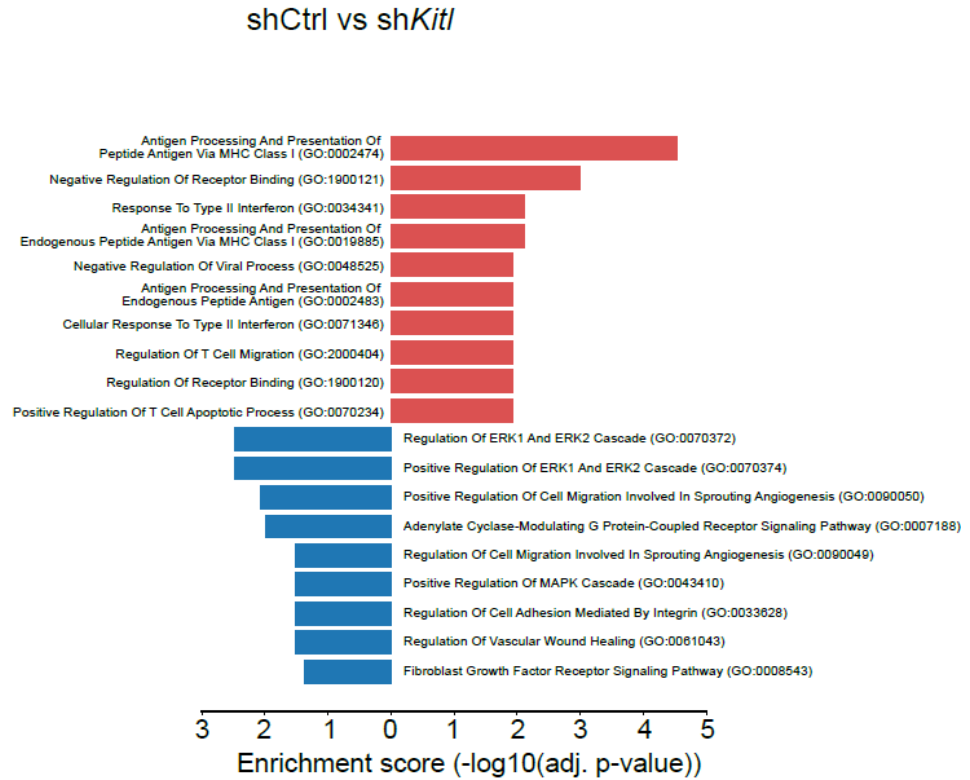
Supplementary Figure 2.S3. Stromal KITL promotes regulation of pancreas tissue architecture.

C: Volcano plot of all upregulated, non-significant, and downregulated differentially expressed genes as defined by the Wald test ($p_{adj} < 0.05$ and $\log_2FC > 1$) from *Kitl* knock down (*shKitl*) ImpSC-1 bulk-RNA seq dataset with representative gene labels included.

Data is representative of 3 biological repeats



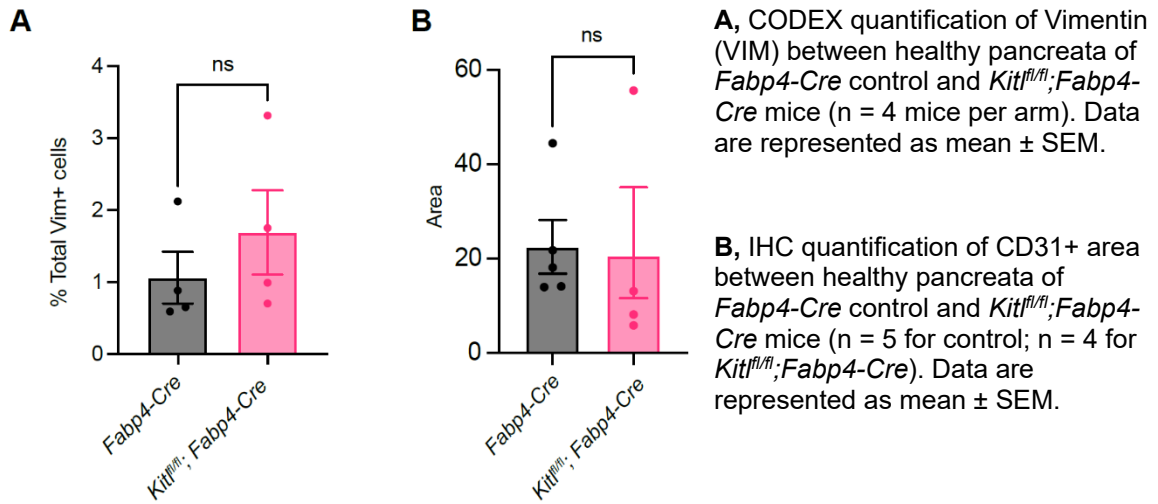
Supplementary Figure 2.S3. Stromal KITL promotes regulation of pancreas tissue architecture.



C, continued: Gene ontology (GO) analysis of upregulated and downregulated differentially expressed genes (DEGs) in immortalized pancreatic stellate cells (ImPSC-1) with *Kitl* stable knockdown. Top 10 enrichment categories ranked by adjusted p-values plotted in each direction.

To assess the relevance of mesenchymal KITL signaling for pancreas tissue architecture, we analyzed the consequences of conditional *Kitl* loss using *Kitl^{fl/fl};Fabp4-Cre* mice compared to *Fabp4-Cre* controls in the settings of homeostasis and tissue injury. First, we analyzed these tissues under normal, homeostatic conditions, and crossed in a *Rosa26^{mTmG/+}* allele to enable visualization of PSCs based on GFP expression in these tissues. Based on our transcriptional profiling results, we compared tissue microenvironments in *Rosa26^{mTmG/+};Kitl^{fl/fl};Fabp4-Cre* mice compared to *Rosa26^{mTmG/+};Fabp4-Cre* controls and using co-detection by indexing (CODEX), a barcode-based, multiplexed imaging approach (Goltsev et al., 2018).

Supplementary Figure 2.S4. Stromal KITL promotes pancreas tissue homeostasis.



While total VIM-positive and CD31-positive cell abundance was not different between genotypes (Supplementary Figures 2.S4A & 2.S4B), we observed clear changes to the perivascular niche with loss of mesenchymal *Kitl* including an increase in GFP-positive mesenchyme adjacent to endothelial cells (Figure 2.3D).

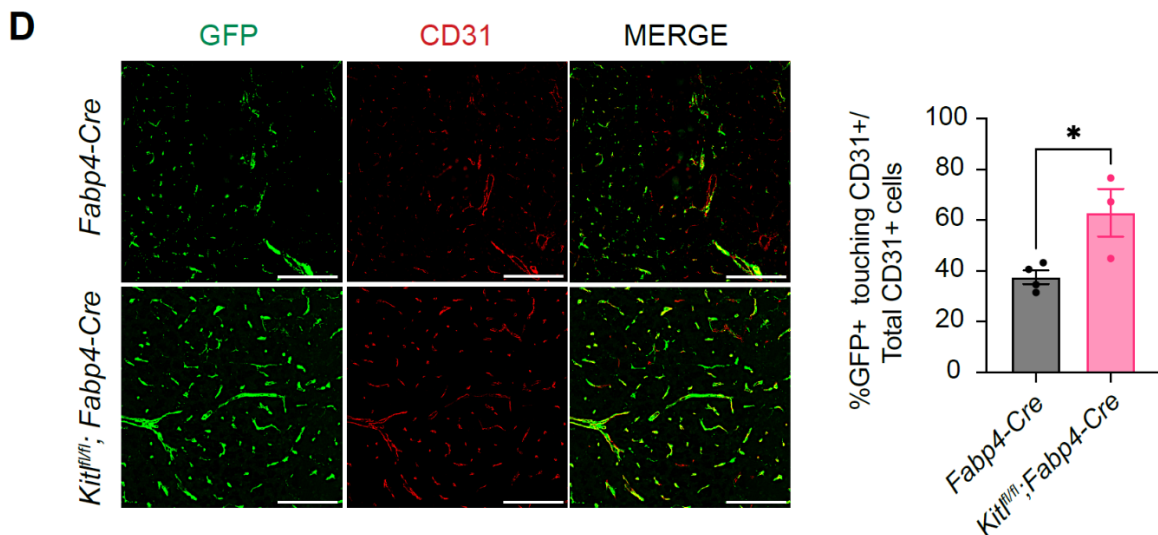
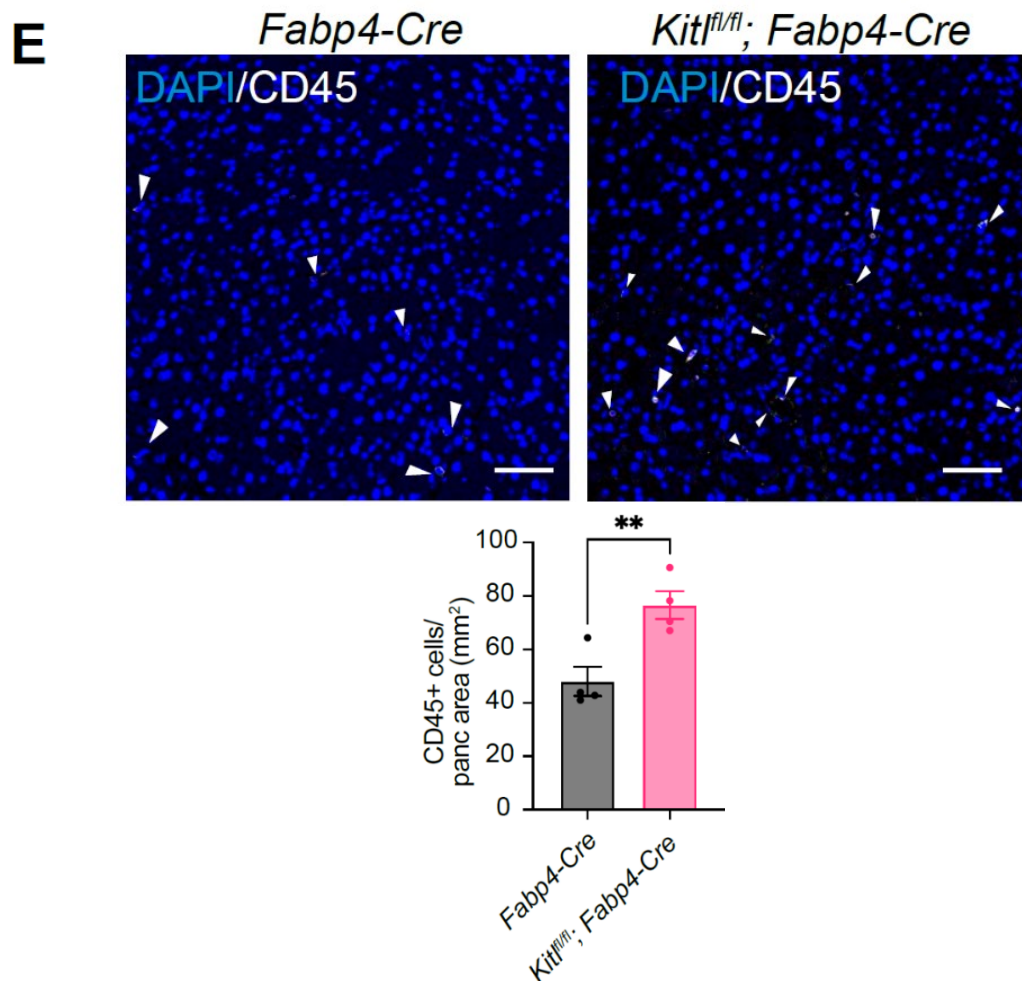
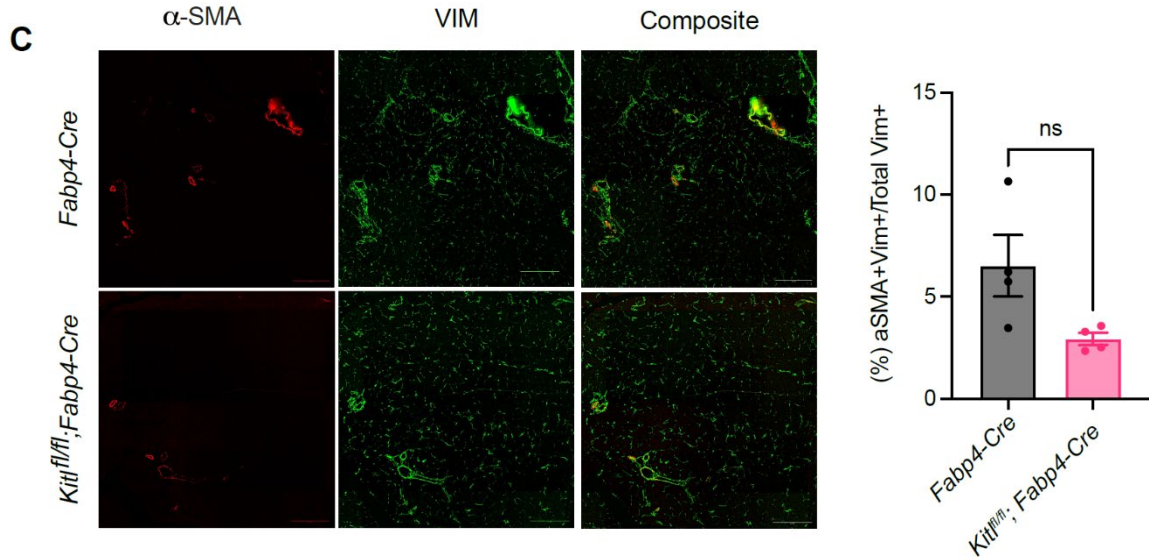


Figure 2.3. KITL regulates PSC state and pancreas tissue homeostasis. **D**, Representative images of CODEX staining (left) and quantification (right) for GFP (green) and CD31 (red) in normal pancreas from *Fabp4-Cre* or *Kitl^{fl/fl};Fabp4-Cre* mouse model (n = 3-4 mice per arm). Scale Bar, 100 μ m. Unpaired t-test was used. Data are represented as mean ± SEM; ns = not significant, *P ≤ 0.05, **P ≤ 0.01, ***P ≤ 0.001, ****P ≤ 0.0001.

We also observed an increase in CD45-positive leukocytes within normal pancreas tissue when stromal *Kitl* was perturbed (Figure 2.3E). We also noted a trend towards decreased α SMA-positive, VIM-positive cells with *Kitl* perturbation (Supplementary Figure 2.S4C)—as fibroblasts are α SMA negative in normal pancreas tissue, this likely reflects a reduction in contractility of vascular smooth muscle cells. To assess potential cellular receivers of mesenchymal KITL which participate in paracrine signaling, we stained pancreas tissues from *Rosa26^{mTmG/+};Fabp4-Cre* mice for GFP, VIM, and KITL receptor c-KIT (shortened as KIT).

Figure 2.3. KITL regulates PSC state and pancreas tissue homeostasis. **E**, Representative images of CODEX composite staining (top) and quantification (bottom) for CD45 (white) in normal pancreas from *Fabp4-Cre* or *Kitl^{fl/fl};Fabp4-Cre* mouse model (n= 4 mice per arm). Scale Bar, 50 μ m. Unpaired t-test was used. Data are represented as mean \pm SEM; ns = not significant, *P \leq 0.05, **P \leq 0.01, ***P \leq 0.001, ****P \leq 0.0001.





Supplementary Figure 2.S4. Stromal KITL promotes pancreas tissue homeostasis. **C**, Representative images of CODEX staining (left) and quantification (right) of 1295 α -SMA and Vimentin (VIM) between healthy pancreata of *Fbp4-Cre* control and *Kitl^{fl/fl}; Fbp4-Cre* mice (n = 4 mice per arm).

KIT-positive cells were found adjacent to GFP-positive mesenchyme, consistent with the potential for cell-cell communication (Figure 2.3F). As PSCs are localized in perivascular regions as well as next to pancreatic epithelium, but KIT-positive cells were few in number in pancreas tissue, we reasoned that acinar cells were unlikely to be the cellular source of KIT but that CD31-positive endothelial cells and cytokeratin-high ductal epithelial cells may be relevant KIT-positive cell populations.

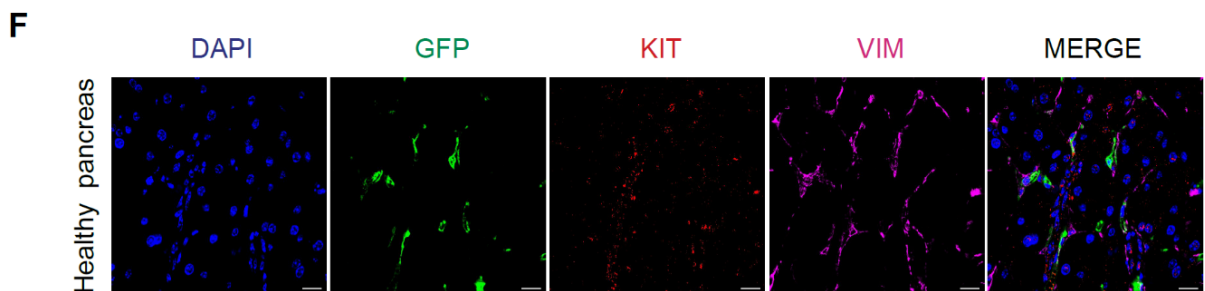


Figure 2.3. KITL regulates PSC state and pancreas tissue homeostasis. **F**, Representative images of IHC staining for GFP (green), c-KIT receptor (KIT, red), and VIM (magenta) in healthy murine pancreas from *Rosa26mTmG/+; Fbp4-Cre* mice. Scale bar, 10 μ m.

Consistent with this notion, IHC demonstrated KIT expression by sub-populations of ductal epithelial cells and few endothelial cells (Figures 2.3G & 2.3H). To confirm these results, we analyzed KIT expression by flow cytometry with co-stains for CD45 (immune cells), CD31 (endothelial cells), or EpCAM (epithelial cells), reasoning that KIT-positive cells negative for these three additional markers represent KIT-positive mesenchyme.

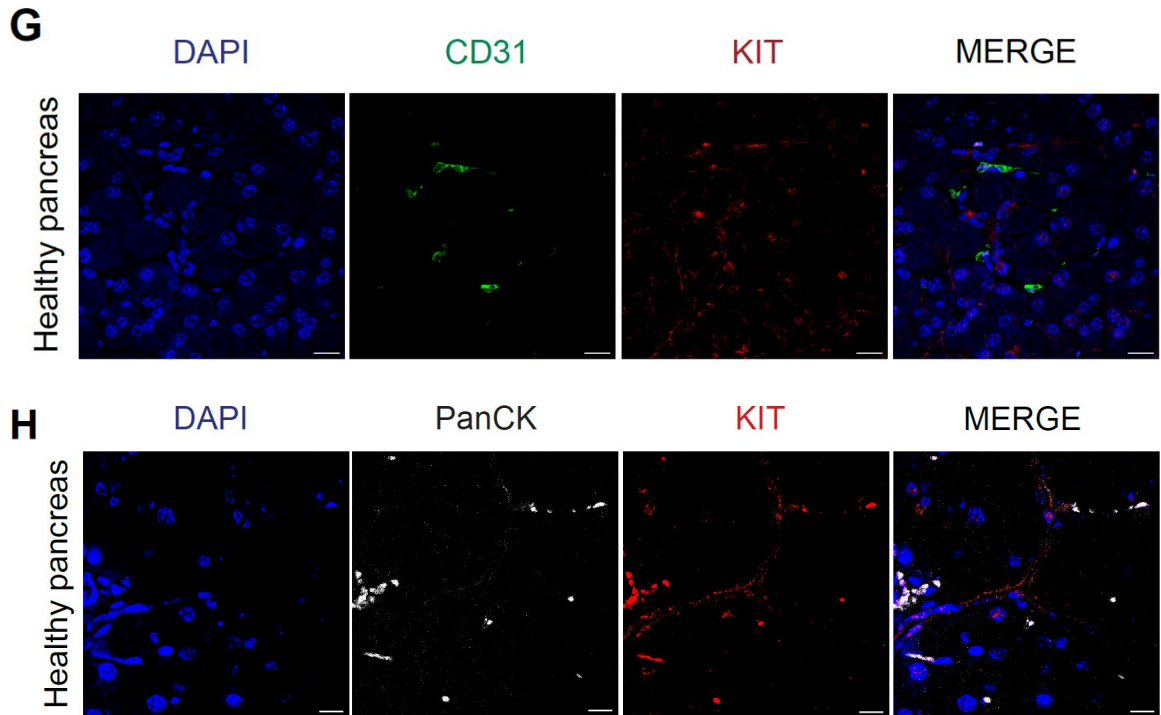
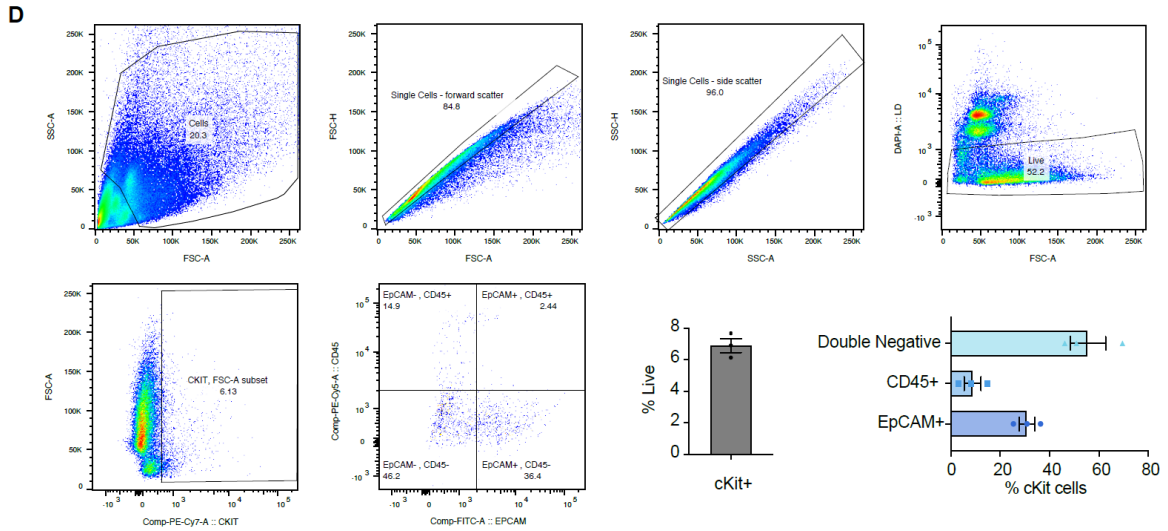


Figure 2.3. KITL regulates PSC state and pancreas tissue homeostasis. **G**, Representative images of IHC staining for CD31 (green) and c-KIT receptor (KIT, red) in healthy murine pancreas. Scale bar, 10 μ m. **H**, Representative images of IHC staining for panCK (white) and c-KIT receptor (KIT, red) in healthy murine pancreas. Scale bar, 10 μ m.

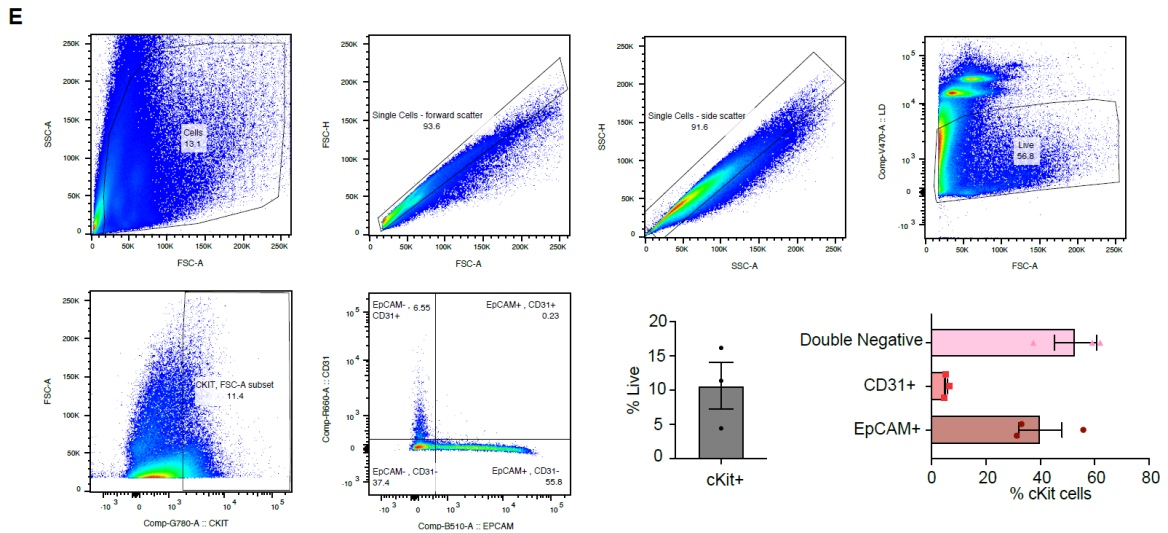
KIT-positive cells were found in the EpCAM-324 positive fraction, consistent with a ductal epithelial identity, and were rarely but measurably positive for CD31 or CD45 (Supplementary Figures 2.S4D & 2.S4E), consistent with our IHC. We also noted a KIT-expressing population negative for these markers, which may be a population of mesenchymal cells expressing KIT. We also note that the fairly high proportion of KIT-positive cells among live cells in our flow cytometry experiments likely reflects substantial

acinar cell death during preparation of single cell suspensions, as acinar cells appear to be negative for KIT and we have likely therefore enriched for KIT-positive cells.

Supplementary Figure 2.S4. Stromal KITL promotes pancreas tissue homeostasis.



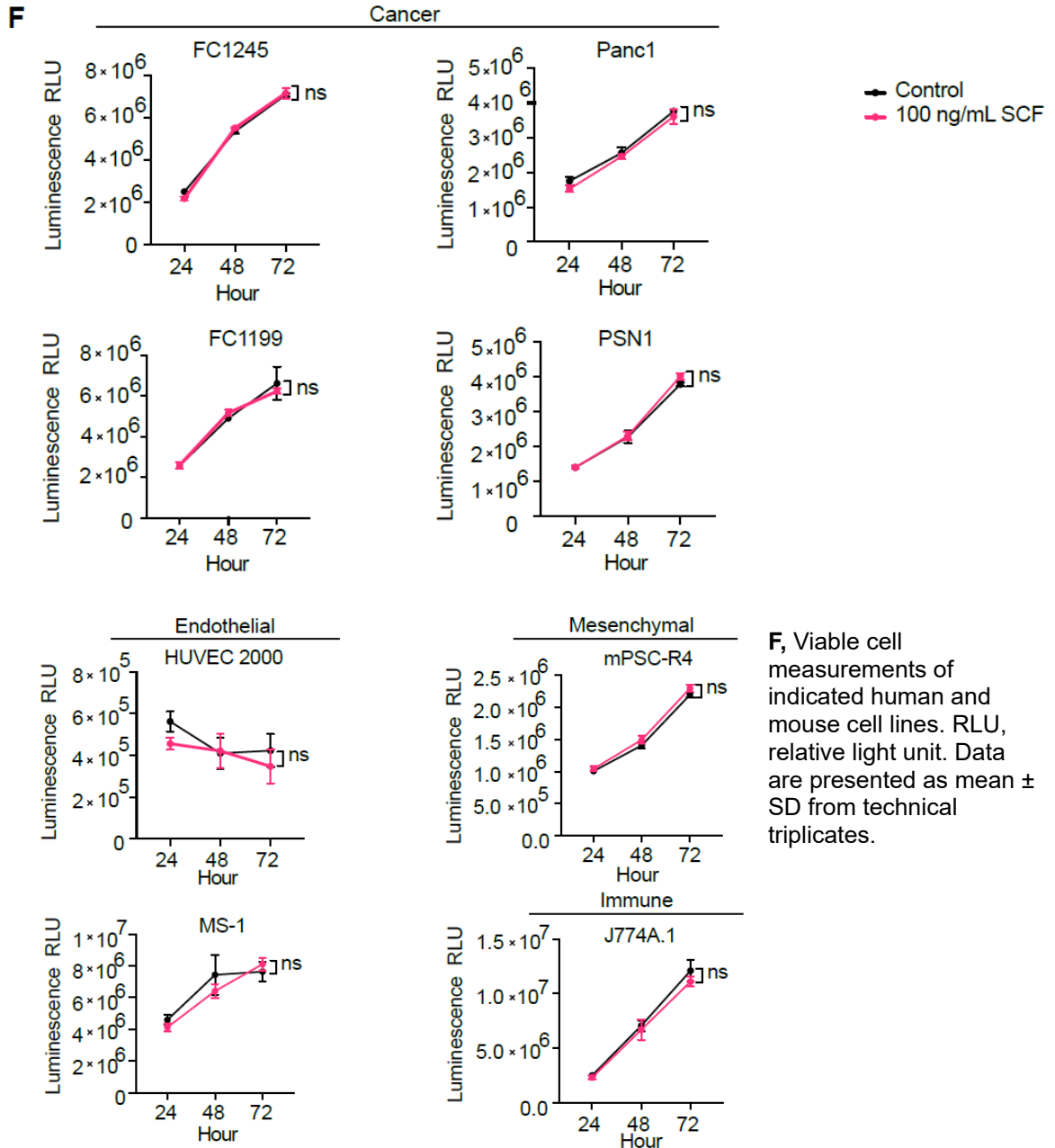
D, Flow cytometry analysis and quantification of c-KIT receptor, EpCAM, and CD45 in healthy pancreata of C57BL/6J age-matched male mice (n = 3 replicates from a total of n = 5 mice divided among samples).



E, Flow cytometry analysis and quantification of c-KIT receptor, EpCAM, and CD31 in healthy pancreata of C57BL/6J age-matched male mice (n = 3 replicates from a total of n = 5 mice divided among samples).

In light of the observed patterns of c-KIT expression, we treated several cell types including PDAC cells and endothelial cells with recombinant KITL in culture, but did not observe changes in cell viability over time (Supplementary Figure 2.S4F). Together, these results suggest that paracrine signaling via KITL influences neighboring cell types and acellular features in an intact tissue context.

Supplementary Figure 2.S4. Stromal KITL promotes pancreas tissue homeostasis.



In light of measurable albeit modest differences to tissue structure upon loss of mesenchymal *Kitl*, we assessed the consequences of this KITL pool in the setting of tissue damage. For this, we subjected *Kitl^{fl/fl};Fabp4-Cre* mice and *Fabp4-Cre* controls to acute pancreatitis by administering repeated injections of the cholecystokinin analog caerulein, or saline as a vehicle control, once every hour for 8 hours, for two days. As expected, in control mice, caerulein induced a mild inflammation characterized by edema and leukocyte accumulation evident by hematoxylin and eosin staining (Figure 2.3I).

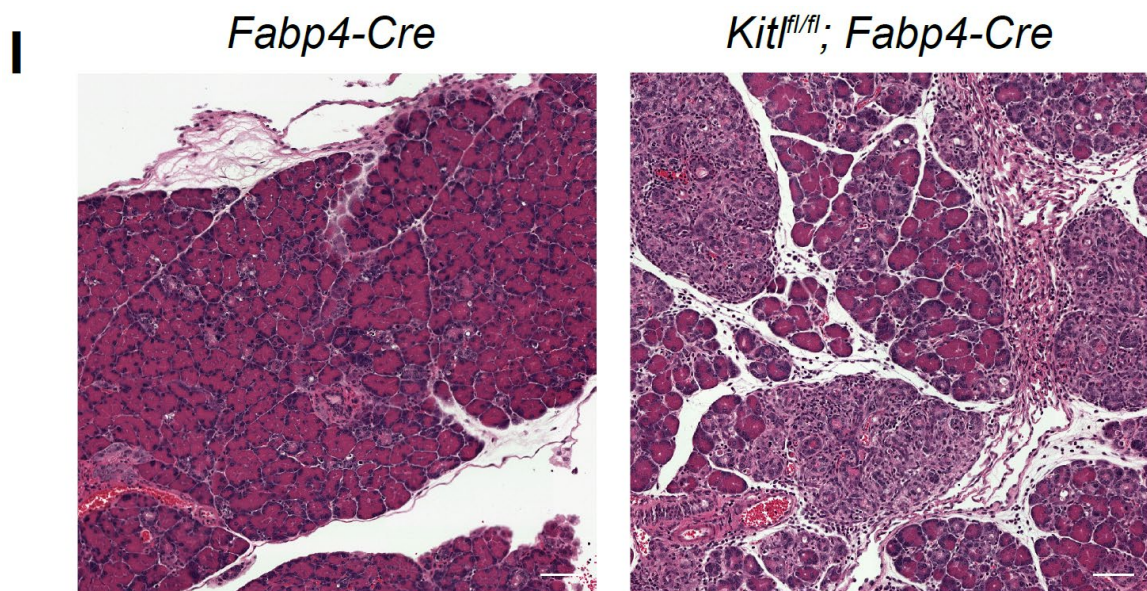


Figure 2.3. KITL regulates PSC state and pancreas tissue homeostasis. I, Representative H&E images between caerulein-treated *Fabp4-Cre* and *Kitl^{fl/fl};Fabp4-Cre* mice. Mice were treated hourly for 8 hours for two days; pancreata were harvested on Day 4. Scale bar, 100 μ m.

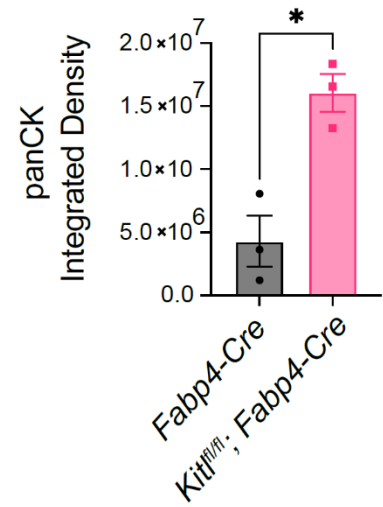
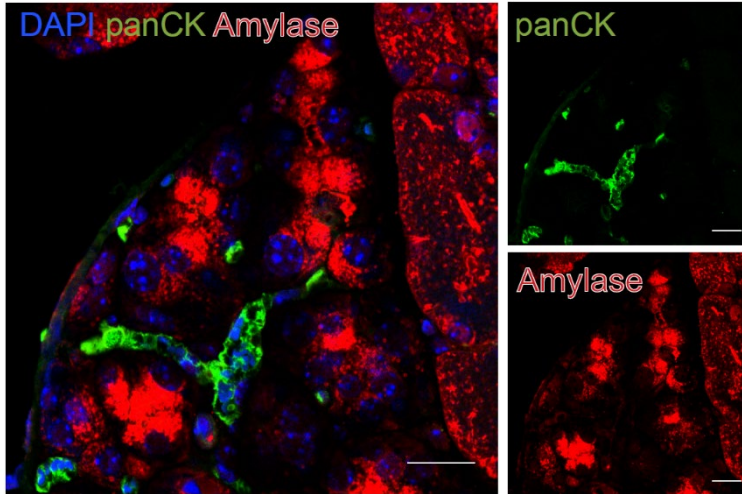
However, in *Kitl* conditional knockout mice, caerulein led to far more pronounced tissue inflammation, as well as greater alterations to the epithelial compartment which we speculated may represent metaplasia or altered epithelial plasticity. To assess this, we co-stained tissues from caerulein-treated mice with amylase (acinar cell marker) and pan-cytokeratin (ductal cell marker), which indicated an increase in ductal marker expression

in the inflamed *Kitl* conditional knockout mice (Figure 2.3J) along with evidence of amylase/pan-cytokeratin co-staining of individual cells.

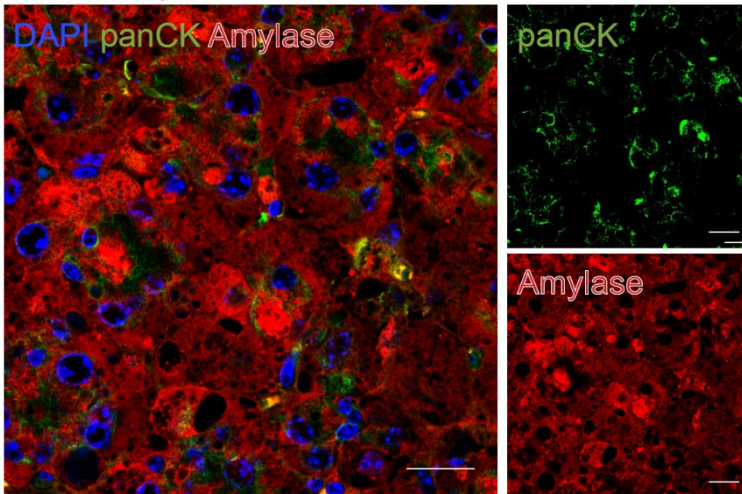
Figure 2.3. KITL regulates PSC state and pancreas tissue homeostasis

J

Fabp4-Cre



Kitl^{fl/fl}; Fabp4-Cre



J, Representative images of IHC staining for panCK (green) and Amylase (red) between caerulein-treated *Fabp4-Cre* and *Kitl^{fl/fl}; Fabp4-Cre* mice. Scale bar, 10 μ m. PanCK quantification ($n = 3$ mice per arm). For comparisons of two groups, unpaired t-test was used. Data are represented as mean \pm SEM; ns = not significant, * $P \leq 0.05$, ** $P \leq 0.01$, *** $P \leq 0.001$, **** $P \leq 0.0001$.

Inflammation was more pronounced in the *Kitl* conditional knockout mice, evidenced by increased abundance of CD45+ leukocytes and CD68+ macrophages in the pancreas compared to control mice (Figures 2.3K & 2.3L). Together, these results implicate

mesenchymal KITL in regulation of pancreas tissue homeostasis such that KITL downregulation promotes inflammation and perturbation of normal tissue architecture.

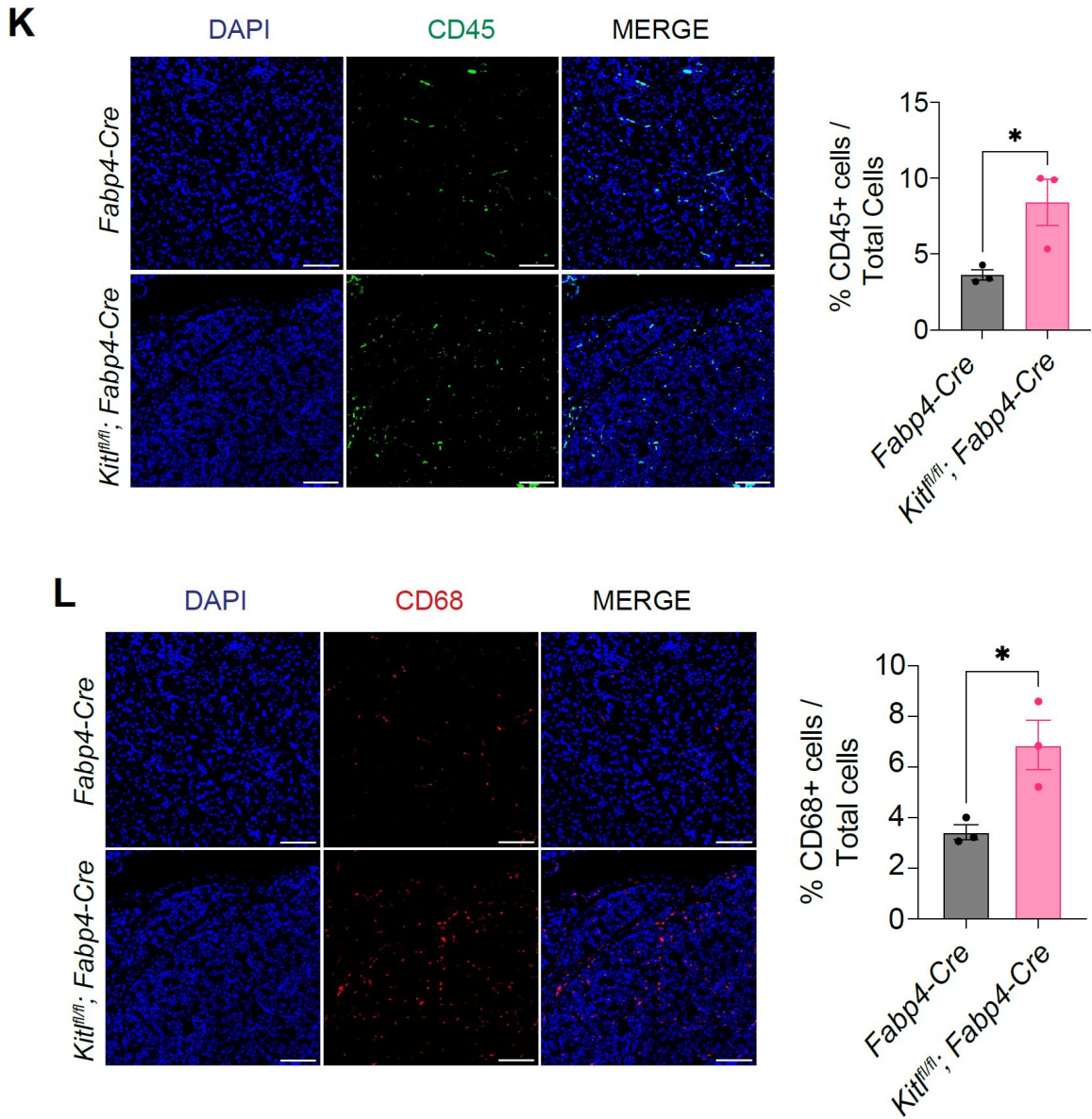


Figure 2.3. KITL regulates PSC state and pancreas tissue homeostasis. **K**, Representative IHC images (left) and quantification (right) for CD45 staining between caerulein-treated *Fabp4-Cre* and *Kitl^{fl/fl};Fabp4-Cre* mice. Scale bar, 100 μ m. **L**, Representative images (left) and quantification (right) for CD68 staining in caerulein- treated *Fabp4-Cre* and *Kitl^{fl/fl};Fabp4-Cre* mouse pancreas. Scale bar, 100 μ m. Unpaired t-test was used. Data are represented as mean \pm SEM; ns = not significant, * $P \leq 0.05$, ** $P \leq 0.01$, *** $P \leq 0.001$, **** $P \leq 0.0001$.

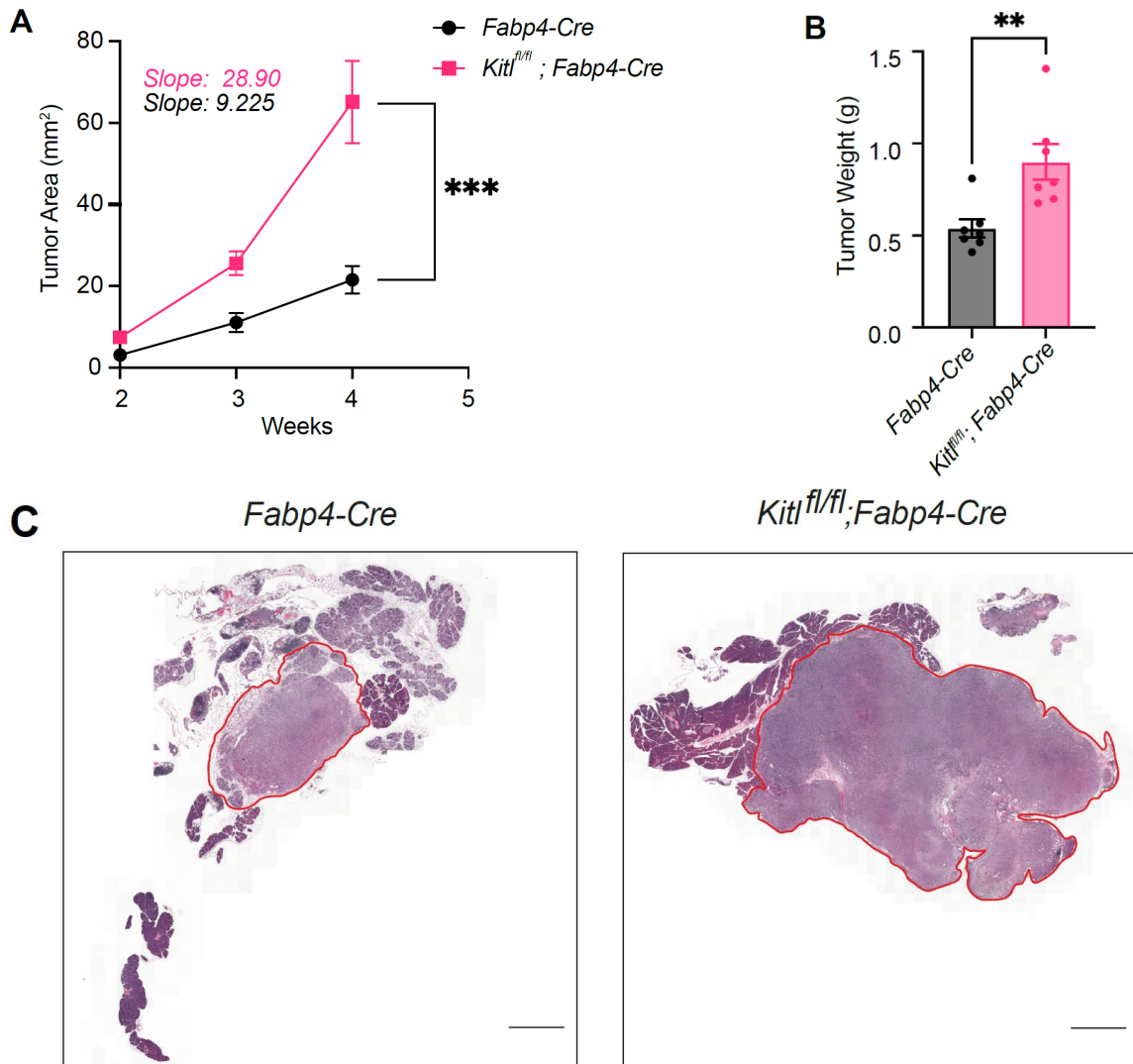


Figure 2.4. Mesenchymal KITL restrains pancreatic tumor growth. **A**, Average tumor area (mm²) between *Fabp4-Cre* control and *Kitl^{fl/fl}; Fabp4-Cre* mice, injected with KPC-derived murine PDAC cells 6419c5 (n = 7 mice per arm). Slopes tabulated via simple linear regression analysis. **B**, Tumor weights (g) at experimental endpoint between *Fabp4-Cre* control and *Kitl^{fl/fl}; Fabp4-Cre* mice, injected with KPC-derived murine PDAC cells 6419c5 (n = 7 mice per arm). **C**, Representative H&E images of *Fabp4-Cre* control and *Kitl^{fl/fl}; Fabp4-Cre* mice injected with KPC-derived murine PDAC cells 6419c5, at the same experimental endpoint. Scale bar, 1mm. Data are represented as mean ± SEM.

We next addressed the potential of stromal KITL to regulate pancreatic tumor growth. We performed orthotopic implantation of KPC-derived PDAC cells from a pure C57BL/6J background into syngeneic *Kitl^{fl/fl}; Fabp4-Cre* mice or *Fabp4-Cre* controls. Despite the aggressive nature of this mouse model, we found that loss of mesenchymal *Kitl*

significantly accelerated tumor growth (Figure 2.4A) and increased tumor weights and tumor burden at experimental endpoint (Figures 2.4B & 2.4C). We then repeated these experiments using moribundity as an experimental endpoint instead of a fixed timepoint. Consistent with the tumor growth measurements, survival studies revealed that loss of mesenchymal *Kitl* significantly shortened survival compared to mice in KITL expressing hosts (Figure 2.4D).

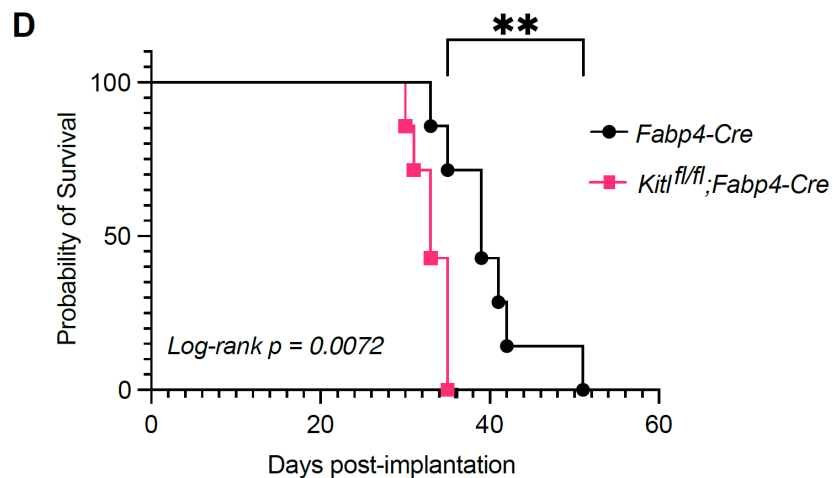


Figure 2.4. Mesenchymal KITL restrains pancreatic tumor growth. D, Kaplan–Meier plot depicting percent probability of survival between *Fabp4-Cre* control and *Kitl^{fl/fl}; Fabp4-Cre* mice, injected with KPC-derived murine PDAC cells 6419c5 (n = 7 mice per arm). Log-rank P value = 0.0072.

We characterized the mesenchymal compartment of these tumors by staining for PDPN (pan-CAF marker) and α SMA (myofibroblast-like CAF marker) and found similar CAF abundance in tumors across genotypes (Figure 2.4E), which is compatible to the notion that mesenchymal KITL regulates tissue homeostasis but is lost in an established tumor microenvironment. Proliferation and apoptosis were also similar across tumor genotypes at experimental endpoint (Figures 2.4F & 2.4G), further supporting a role for KITL in early tumor progression. A tumor-restraining role for stromal KITL was also observed in an independent PDAC model (Figures 2.4H–J), except that tumor weights at humane

endpoint were not different in this model. As implantable models involve introduction of cells which have already undergone malignant transformation into pancreas tissue, these results suggest that mesenchymal KITL expression represents a tissue barrier to PDAC progression at least in part independent of epithelial cell-intrinsic tumor suppression mechanisms.

Figure 2.4. Mesenchymal KITL restrains pancreatic tumor growth. E, Representative images of IHC staining and quantification of α SMA and podoplanin on tumors from *Fabp4-Cre* control mice and *Kit^{fl/fl};Fabp4-Cre* mice, injected with KPC-derived murine PDAC cells 6419c5 (n = 3 mice per arm). Zoomed-out image scale bar, 200 μ m. Zoomed-in image scale bar, 50 μ m.

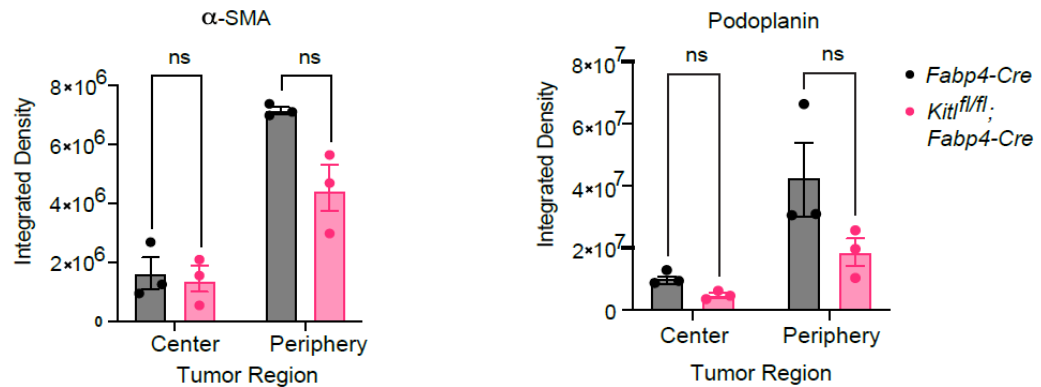
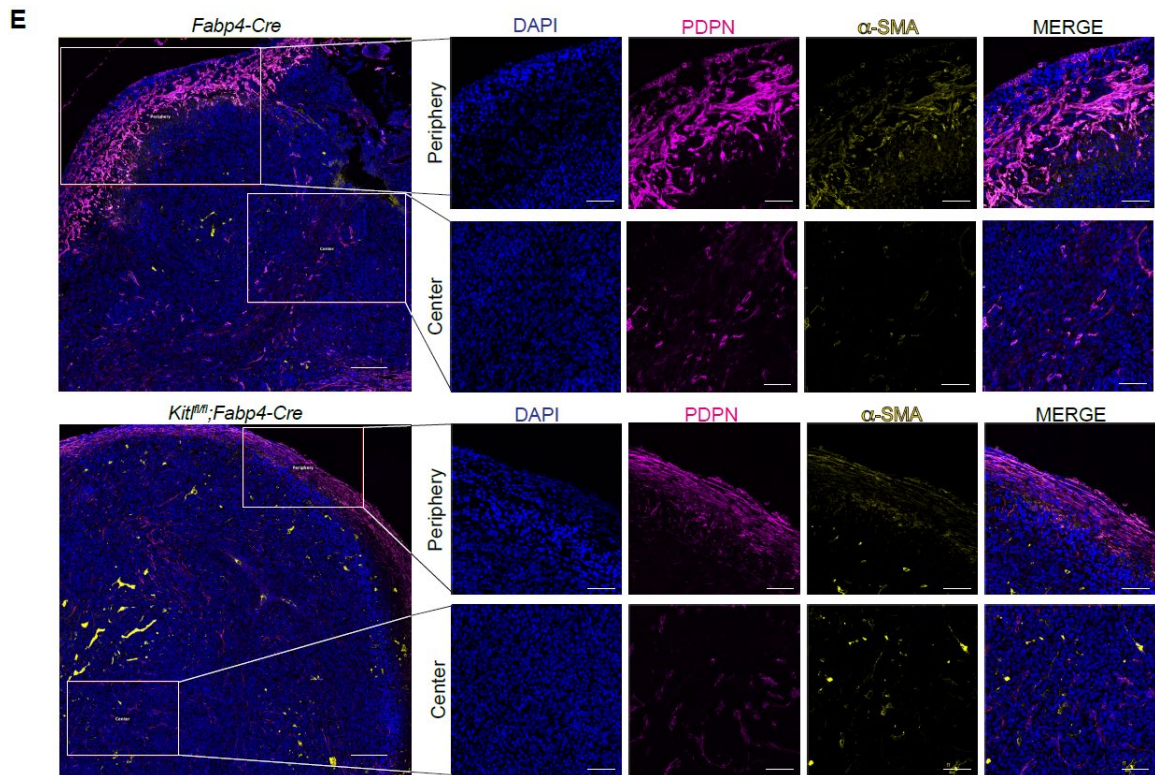
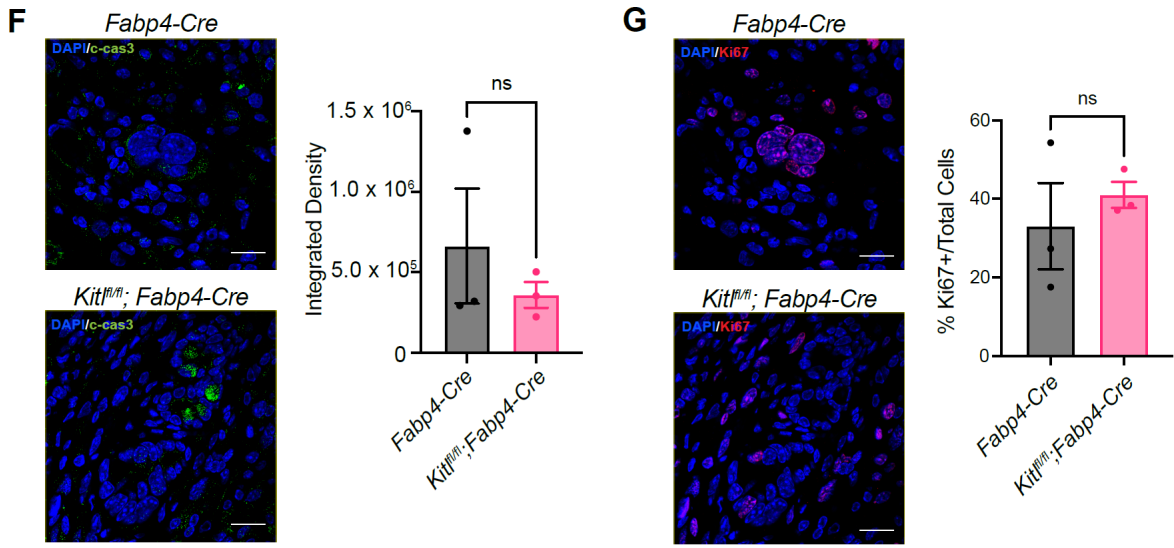
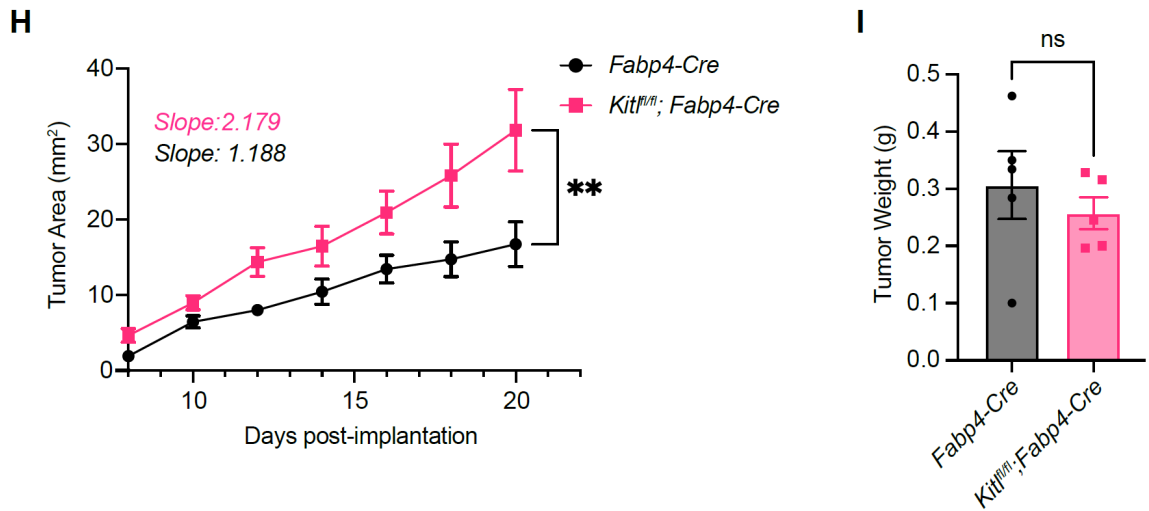


Figure 2.4. Mesenchymal KITL restrains pancreatic tumor growth.

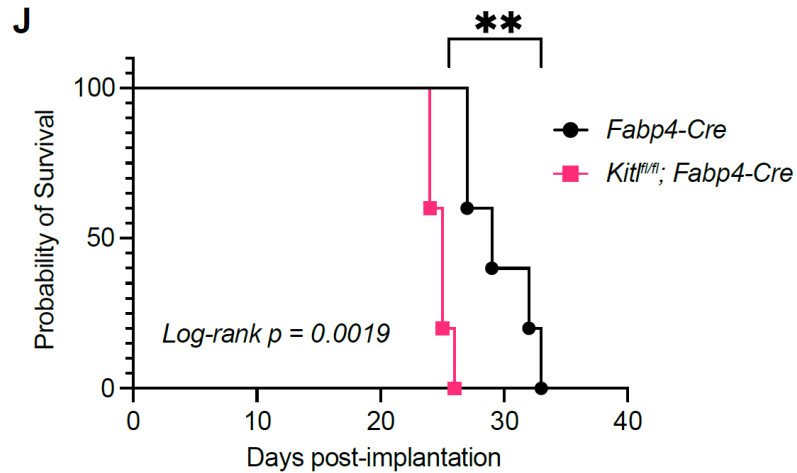


F, Representative image of IHC staining and quantification of cleaved caspase-3 (ccas3) on *Fabp4-Cre* control mice and *Kit^{fl/fl}; Fabp4-Cre* mice, injected with KPC-derived murine PDAC cells 6419c5 (n = 3 mice per arm). Scale bar, 10 μ m. **G**, Representative images of IHC staining and quantification of Ki67 on *Fabp4-Cre* control mice and *Kit^{fl/fl}; Fabp4-Cre* mice, injected with KPC-derived murine PDAC cells 6419c5 (n = 3 mice per arm). Scale bar, 10 μ m. All data are represented as mean \pm SEM. For comparisons of two groups, unpaired Mann-Whitney test was used. *P \leq 0.05, **P \leq 0.01, ***P \leq 0.001, ****P \leq 0.0001; ns, not significant.



H, Average tumor area (mm^2) between *Fabp4-Cre* control mice and *Kit^{fl/fl}; Fabp4-Cre* mice, injected with KPC-derived murine PDAC cells FC1199 (n = 5 mice per arm). Best-fit slopes tabulated via simple linear regression analysis. **I**, Tumor weights (g) at humane endpoint from *Fabp4-Cre* control mice and *Kit^{fl/fl}; Fabp4-Cre* mice, injected with KPC-derived murine PDAC cells FC1199 (n = 5 mice per arm). All data are represented as mean \pm SEM. For comparisons of two groups, unpaired Mann-Whitney test was used. *P \leq 0.05, **P \leq 0.01, ***P \leq 0.001, ****P \leq 0.0001; ns, not significant.

Figure 2.4. Mesenchymal KITL restrains pancreatic tumor growth.



J, Kaplan–Meier plot depicting percent probability of survival between *Fabp4-Cre* control mice and *Kitl^{fl/fl}; Fabp4-Cre* mice, injected with KPC-derived murine PDAC cells FC1199 (n = 5 mice per arm). Log-rank P-value = 0.0019. For comparisons of two groups, unpaired Mann-Whitney test was used. *P ≤ 0.05, **P ≤ 0.01, ***P ≤ 0.001, ****P ≤ 0.0001; ns, not significant.

F. Discussion

In this study, we provide evidence that a cell population in normal pancreatic mesenchyme expresses KITL/SCF; that stromal downregulation of KITL is an accompanying feature of pancreatic tumorigenesis, as CAFs derived from these KITL-positive cells retain a lineage label but do not retain KITL expression; and that, functionally, stromal KITL is a barrier to tumor progression in pancreas tissue. The recent reports of abundant, KRAS-mutant, pre-invasive lesions throughout examined cohorts of PDAC-free human pancreas tissues (Braxton et al., 2024; Carpenter et al., 2023) compared to the relatively low frequency of PDAC across the general population indicates the pervasive relevance of tumor suppression mechanisms in the adult pancreas. These mechanisms likely include epithelial cell-intrinsic mechanisms promoting genome stability and susceptibility to immune surveillance; functions of the immune system, potentially including clearance of highly mutated epithelial cells with tumorigenic potential; and functions of the non-immune stroma. Within the non-immune stroma, mesenchymal components—fibroblasts in

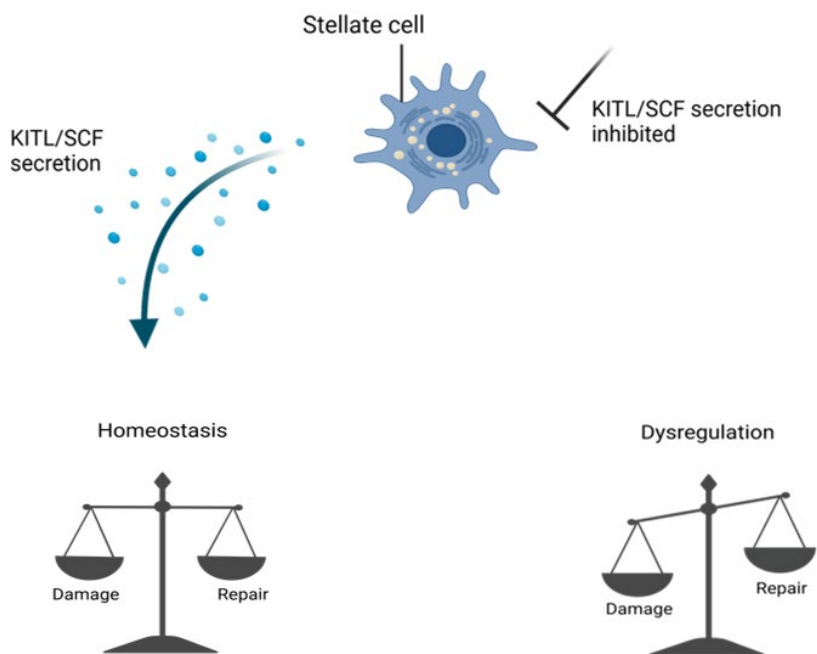
particular—are broadly implicated in maintenance of normal tissue structure or architecture as well as support of healthy tissue homeostasis via production of soluble factors, basement membrane, and ECM components. Perturbation of fibroblast phenotypes to an activated state is an anatomically conserved feature of many solid cancers and some inflammatory conditions (Buechler et al., 2021). While activated fibroblasts in disease states generally express ECM components and immune-modulatory factors, granular features of fibroblast activation programs are tissue- and disease-specific. Though activated fibroblasts in cancer carry out diverse functions to promote tumor progression, normal fibroblasts serve to restrain tumor formation in promoting the ordered tissue structure that must be overcome to enable cancer formation or progression. We propose KITL as a tumor-restraining stromal mechanism in the pancreas, raising the possibility that specific effectors downstream of KITL signaling may hold utility for cancer progression. Though this study suggests that inhibition of effectors downstream of stromal KITL have potential relevance for cancer prevention, we speculate that a therapeutic window prevents use of receptor tyrosine kinase inhibitors such as imatinib—which inhibits c-KIT—from having a meaningful negative impact on normal pancreas tissue homeostasis, consistent with the excellent safety profile of imatinib (Druker et al., 2001). Future efforts will aim to investigate the significance of KITL signaling in the specific context of low-grade PanIN lesions, as these are the lesions found in adult human pancreas (Braxton et al., 2024; Carpenter et al., 2023).

While our study was restricted to the pancreas, these findings fit within a broader context of prior studies implicating mesenchymal KITL and/or LEPR-positive mesenchyme as critical regulators of healthy tissue homeostasis and normal tissue function in diverse organ sites. As briefly discussed above, LEPR-positive mesenchymal cells in the bone

marrow associate tightly with endothelial cells and form a niche critical for hematopoietic stem cells (Ding et al., 2012). Interestingly, upon tissue damage such as irradiation or chemotherapy requiring regeneration of hematopoietic stem cells, LEPR-positive mesenchymal cells differentiate into adipocytes which in turn produce KITL to enable a functional niche and support hematopoietic regeneration (B. O. Zhou et al., 2017). Complementary mesenchymal and signaling components were recently shown to support normal tissue homeostasis and suppress inflammation in brown adipose tissue (BAT): LEPR-positive mesenchyme supports adaptive thermogenesis and restrains inflammation in BAT (Haberman et al., 2024), while endothelial cell-derived KITL/SCF signals to KIT on brown adipocytes to promote homeostatic lipid accumulation when thermogenesis is inhibited (AlZaim et al., 2023). As the stellate cells under investigation in our study are also lipid-storing cells, these studies raise the possibility that lipid-storing stromal cells engage KITL signaling to promote tissue homeostasis and limit inflammation more broadly across organs.

**Figure 2.5.
Mesenchymal KITL
regulates healthy
tissue homeostasis
and normal tissue
function.**

Genetic inhibition of mesenchymal KITL in the mouse pancreas, derived from pancreatic stellate cells, leads to increased immune infiltration in healthy pancreas, greater inflammation in pancreatitis, accelerated tumor growth, and reduced overall survival in PDAC, suggesting a role in regulating healthy tissue homeostasis. Created with Biorender.



Chapter III. Conclusions, Limitations, and Future Directions

Since cancer-associated fibroblasts are not as tumor-permissive as once thought, we look to normal mesenchyme functions attributed to healthy tissue homeostasis and tissue organization as a basis for its tumor-restraining capacity. Previous study established that pancreatic stellate cells, initially thought to be the origin of all CAFs in pancreatic ductal adenocarcinoma, are a small sub-population in this disease, and revealed that fibroblast lineage results in different CAF contributions to the tumor milieu. Thus, it is reasonable to suspect that different fibroblast lineages also have non-redundant applications in the maintenance of healthy tissue homeostasis. In this dissertation, by comparing pancreatic stellate cells in healthy and in cancer-associated mesenchyme, we identify ligand KITL/SCF expressed in the healthy pancreas and is lost in a cancer setting. We validate this loss in both mouse models and human tissues. Further, we interrogate the role of pancreatic stellate cell-derived KITL through *in vivo* studies, which include gene manipulation of murine models of health, inflammation, and cancer, and *in vitro* exploration of primary, immortalized, and activated PSCs.

A. Temporal and Spatial Organization of Pancreatic Stellate Cells

Our first results explore the temporal and spatial organization of pancreatic stellate cells in healthy tissue, low-grade neoplastic lesions, and PDAC lesions of mouse pancreas. Using PDPN and α SMA, our findings validate that PSCs, quiescent or activated as CAFs, are numerically minor in healthy tissue and PDAC lesions (Figures 2.1B & 2.1C). Furthermore, PSC-derived CAFs appeared relatively infrequent in low-grade PanIN lesions, prompting whether there is a sequential order of fibroblast activation with respect to mesenchymal lineage that is pertinent to tumorigenesis (referred to later). Perhaps our results suggest that PSC-derived CAF functions are more significant for later stages of

tumorigenesis. We also report that PSCs reside in both the perivascular and parenchymal regions, as delineated by endothelial marker CD31 (Figures 2.1D & 2.1F). While this dissertation focused on mesenchymal KITL roles in the pancreas irrespective of its spatial context, we show that nearly all perivascular PSCs express *Kitl*, whereas around half of parenchymal PSCs express *Kitl* in *Rosa26^{mTmG/+};Fabp4-Cre* mice (Figure 2.2L). This data prompted questions on the relationship between mesenchymal cells and endothelial cells through the KITL-cKIT axis, as we also observed differences in the perivascular niche between *Rosa26^{mTmG/+};Fabp4-Cre* control and *Rosa26^{mTmG/+};Kitl^{fl/fl};Fabp4-Cre* experimental mice (Figure 2.3D). One possibility to explain the increase of PSCs adjacent to endothelial cells in the *Kitl^{fl/fl}* model is a contact-dependent compensation mechanism activated by a weakened structure of the perivascular region due to reduced tissue scaffolding, since perivascular stromal cells can provide structural support through ECM components (Avolio et al., 2017; Sbierski-Kind et al., 2021). Ultimately, these results propose that spatial residence of PSCs, specifically the specialized perivascular niche, may be affecting its KITL expression, and in turn, its function.

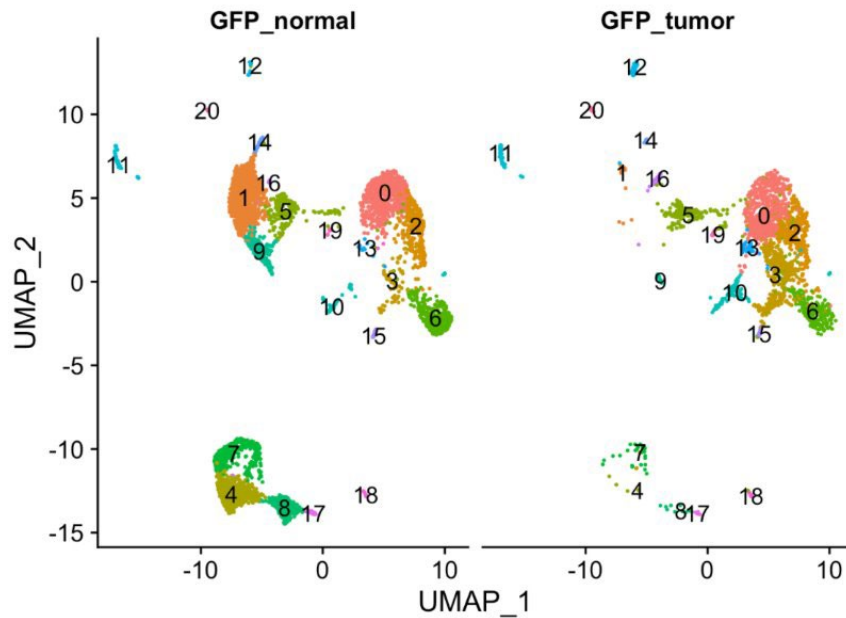
B. Strengths and Limitations of Single cell Technologies

Single cell technologies allowed us to interrogate the differences between pancreatic stellate cells in healthy pancreata and PSC-derived CAFs from orthotopic transplantation models, providing candidate autocrine, juxtacrine, or paracrine factors with the potential for tumor suppression or restraint. From this, we produced the first scRNA-seq dataset focused on PSCs. Single cell sequencing data is limited by technical, biological, and computational challenges (Kiselev et al., 2019): individual cells are treated as biological replicates, not technical, reducing its reproducibility; miniscule amounts of RNA from each

individual cell causes low signal-to-noise ratio; and, parameters within each clustering method heavily impact analysis and clustering resolution.

Figure 3. Secondary clustering analysis of scRNA-seq reveals distinct populations of pancreatic stellate cells from healthy and PDAC murine pancreata.

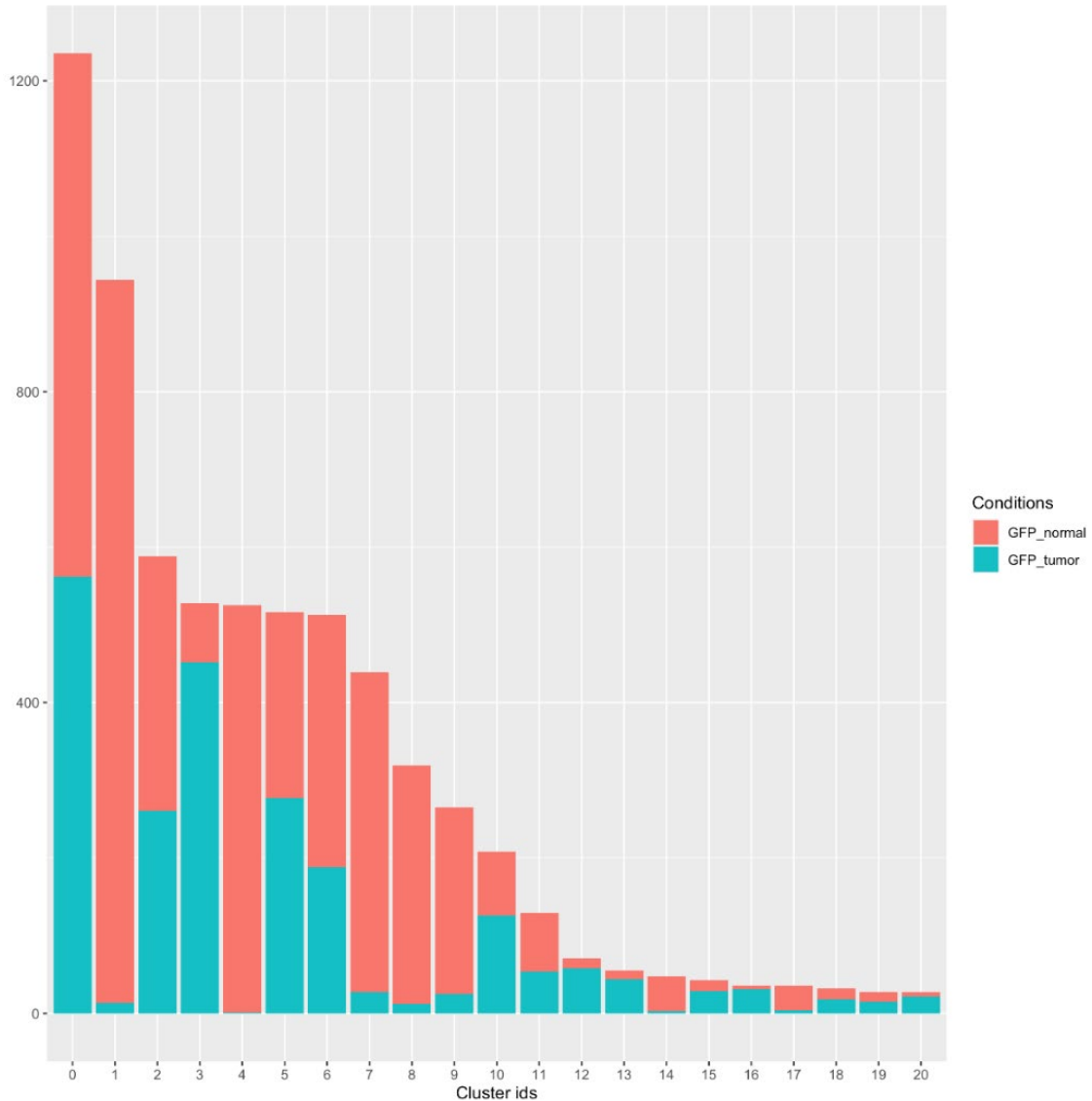
A



A, Secondary clustering analysis of scRNA-seq identifies a total of 20 functionally distinct clusters compiled from all pancreatic stellate cells from both healthy murine pancreata and murine PDAC pancreata (GFP_normal = PSCs from healthy pancreata; GFP_tumor = PSC-derived CAFs from tumor pancreata).

However, we reasoned that reviewing potential factors within the largest cluster with the greatest number of cells would mitigate these problems as it would suggest that most stellate cells in the normal mesenchyme expressed these sets of genes (Figures 3A & 3B). This same cluster was nearly non-existent in the cancer-associated context, strengthening our hypothesis that the cluster we selected to delve into indicated healthy mesenchymal functions (Figures 2.3A & 2.3B). We later provide evidence throughout this thesis that KITL is expressed in PSCs and that PSC activation during tumorigenesis coincides with loss of mesenchymal KITL.

Figure 3. Secondary clustering analysis of scRNA-seq reveals distinct populations of pancreatic stellate cells from healthy and PDAC murine pancreata.



B, Pancreatic stellate cell (PSC) secondary clustering analysis groups (defined here as Cluster IDs) are organized by cell count from each condition (GFP_normal = PSCs from healthy pancreata; GFP_tumor = PSC-derived CAFs from tumor pancreata). More than 800 cells from both conditions combined were grouped in Cluster 1.

C. RNA as a measurement of KITL expression

As alluded to earlier, we show evidence in support of the notion that PSCs in healthy pancreas express KITL, which is then lost during tumorigenesis. KITL expression in intact tissues was measured by RNA ISH and RNAscope to capture *Kitl/KITLG* RNA expression

in mouse and human tissues, respectively (Figures 2.2J, 2.2K, & 2.2M). The power of this strategy enables spatial visualization of KITL RNA expression *in vivo*, implicating PSCs in KITL-mediated paracrine interactions with epithelial, endothelial, and immune cells. Nevertheless, this strategy is also limited by its ability to accurately assess mesenchymal KITL protein expression, as mRNA expression does not always correlate with protein expression. In our work, we indirectly assess KITL protein expression in both mouse healthy pancreas and human PDAC tissues through expression of phosphorylated c-KIT (Figures 2.2N & 2.2O). However, to address if our PSCs express KITL protein, isolation of GFP+ mesenchymal cells in healthy pancreas between *Rosa26^{mTmG/+};Fabp4-Cre* control and *Rosa26^{mTmG/+};Kitl^{fl/fl};Fabp4-Cre* experimental mice followed by western blot analysis (or other means of protein expression analysis or updated versions of ELISA assays) for KITL and FABP4 can sufficiently address if our stellate cells express KITL, and also validate the success of our *Kitl* knock out genetic model. Unfortunately, collecting sufficient protein from primary pancreatic stellate cells for a standard western blot is limited by the low numbers of viable PSCs that are collected from the pancreas. However, neither of these experimental designs would ascertain if there were a difference in KITL expression between perivascular and parenchymal PSCs. This question may be addressed by flow cytometry, observing for GFP, KITL, and CD31, but this approach is limited by antibody availability. And while this method may succeed, it captures only membrane-bound KITL on PSCs, which allows speculation on only KITL-mediated interactions at close contact, not of its farther influences as a soluble ligand.

Combinatory spatial platforms, such as GeoMx Digital Spatial Profiler (DSP) (NanoString Technologies), which allows for both transcriptomic and proteomic analyses in either FFPE or fresh frozen tissue section by combining ISH/IF techniques with high-plex gene

expression analysis, may support in this endeavor. The advantages to these platforms allow flexible, biology-driven profiling, and providing more protein and gene expression data in one slide than a standard RNAscope. For example, one can first use immunofluorescence data to select regions-of-interest—in our context, we can select for markers that target PSCs—then collect all gene expression data from that region. By distinguishing PSCs as our region-of-interest in our mouse models, we can observe for any KITL-mediated downstream transcriptomic or proteomic changes (such as phosphorylated c-KIT activity) in epithelial, endothelial, or immune cellular compartments that surround the mesenchyme. Using these spatial platforms, we can then observe for phosphorylated c-KIT expression and KITL expression (RNA or protein, dependent upon availability GeoMx oligo-labeled antibodies), then assess the extent of spatial colocalization within a niche poised for crosstalk. From this, we can analyze cellular composition of the selected niche. These orthogonal approaches will provide a more comprehensive understanding of mesenchymal KITL expression, activity, and niche in the pancreas.

D. Complementary *in vitro* methods assessing murine KITL expression

Our complementary *in vitro* experiments may be perceived as an overtly reductionist approach in detecting *Kitl* mRNA, wherein newly isolated primary PSCs from mouse pancreas are artificially activated into a CAF-like state, either by exposure to plastic (Figure 2.2E) or by treatment of recombinant TGF- β (Supplementary Figures 2.2B-D). Additionally, our interrogation of cell-intrinsic consequences of KITL signaling on PSCs may not be ideal, as we created loss- and gain-of-function systems on immortalized PSCs, not primary PSCs (Figures 2.3A-C; Supplementary Figures 2.S3A-D). While we ensured appropriate controls to account for the physiological difference, we are cognizant that

neither of these methods do not accurately reflect an *in vivo* setting, therefore interpretation of these results could be challenging. Isolation and bulk RNA-seq of GFP+ mesenchymal cells in *Rosa26^{mTmG/+};Fabp4-Cre* control and *Rosa26^{mTmG/+};Kitl^{fl/fl};Fabp4-Cre* experimental mice, in healthy and PDAC settings, would be an infallible method of assessing *Kitl* expression and cell-intrinsic consequences of KITL signaling, allowing for cleaner analysis and interpretation.

E. Alternative Sources of pancreatic KITL

It is possible that there are other sources of KITL in the pancreas. We also show that a subset of CD45+ cells in the human pancreas tissues express *KITL* mRNA (Supplementary Figure 2.S2F), however we observed more *KITL*+ mesenchymal cells than *KITL*+ leukocytes. We do note that data from RNAscope assay may also suggest that endothelial cells in the murine pancreas express *Kitl* mRNA (Figure 2.2L). Since reports have described endothelial-derived KITL expression and function (Ding et al., 2012), it is plausible that pancreatic endothelial cells in our system also express our ligand-of-interest. It would be meaningful to address if endothelial cells in the pancreas express KITL, considering that the KITL-c-KIT signaling axis can support angiogenesis (Fang et al., 2012; Matsui et al., 2004; Shan et al., 2023), highlighting the importance of the KITL/c-KIT transduction pathway in the maintenance of healthy vasculature. If this were the case, it is consequential in our work to address whether endothelial or mesenchymal cells are the major contributors of KITL in the pancreas, and if KITL source matters in paracrine interactions, in order to parse the mechanisms of multiple functions that were disrupted by PSC-derived KITL loss. Using the same *Kitl^{gfp}* knock-in model from Ding and colleagues, we can observe if pancreatic endothelial cells (and other cells such as PSCs) express GFP in healthy pancreata of mice via flow cytometry. If pancreatic endothelial

cells do express KITL, genetic perturbation of KITL in pancreatic endothelial cells in mouse models can be an avenue worth exploration. While there are currently no established models that enable fate tracing specifically of pancreatic endothelial cells, endothelial cells can be fate traced, thus KITL excision is viable with a dual recombinase GEMM. One such example could be a *Pdx1-FlpO;Pecam-1^{FSF-CRE/+};Kitl^{fl/fl}* model, which targets CD31. Other potential endothelial cell markers include *Tek2* (gene for Tie2) and *Cdh5* (gene for vascular endothelial cadherin), as these Cre mouse models already exist, although without the FRT-stop-FRT (FSF) cassette.

F. Implications of gradual loss of mesenchymal KITL in PDAC

Our data also suggests that complete mesenchymal KITL loss occurs at later stages of pancreatic tumorigenesis (Figure 2.2K & 2.2M, Supplementary Figure 2.S2F). Although our experimental conditions include human benign adjacent tissue sections, its microenvironment is merely a substitute for understanding the microenvironment in early pancreatic neoplasms in humans. To address this, we can investigate datasets wherein human pancreas tissues are derived from donors with no known pancreas diseases. One such example is from Carpenter and colleagues (Carpenter et al., 2023); this seminal work shows that the adult healthy pancreas, regardless of age, harbor early PanINs, which vastly outnumber PDAC cases in frequency, implicating the necessity of fibro-inflammatory reactions to exacerbate precancerous lesions into cancer. Datasets like this provide an excellent opportunity to compare mesenchymal KITL expression between adult healthy pancreas in contrast to PDAC tissues. This will provide a more accurate picture on the temporal loss of mesenchymal KITL, along with the potential for novel candidate biomarkers associated with reduced mesenchymal KITL that indicate a more tumor-permissive environment.

G. Genetic, Epigenetic, and Proteomic Factors controlling mesenchymal KITL expression

If loss of mesenchymal KITL in PDAC tumorigenesis is found to be a gradual process through validation experiments with human benign tissues (as specified in the above paragraph), it is important to study the mechanisms of mesenchymal KITL expression. What about the differences between mesenchymal cells (e.g. pancreatic stellate cells) in low-grade neoplastic lesions versus cancer-associated fibroblasts in PDAC that lead to KITL loss? Are there any differences between PSCs in PanINs versus CAFs in PDAC? Are these mesenchymal cells in early PanIN lesions more akin to activated fibroblasts in a wound healing response as opposed to CAFs? Epigenetic profiling of pancreatic stellate cells or fibroblasts—including DNA methylation and chromatin accessibility assays—in normal, wound-activated, and early- versus late- cancer-activated states can illuminate the nuances among these varied microenvironments. Isolation of pancreatic mesenchymal cells from control, acute pancreatitis, early- and late-PDAC mouse models for epigenetic profiling, with great attention to the *Kitl* locus, may answer these questions. We can also look to genetic profiling of murine *Kitl* and human *KITL* in PSCs by searching for *Kitl/KITL* promoter, enhancer, and silencer regions, reviewing known and candidate transcription factors and other regulatory proteins, then assessing regulatory protein activity in the *Kitl/KITL* locus. Previously it has been shown that growth differentiation factor 9 (GDF9), a member of the TGF- β superfamily, reduces *KITL* expression in human granulosa cells (Tuck et al., 2015). While PSCs and granulosa cells may have varying receptor and transcription factor expression due to their cellular differences, this report proposes that the TGF- β signaling pathway may contribute in the reduction of PSC-derived KITL, corresponding to the gradual loss of mesenchymal KITL in PDAC tumorigenesis.

Post-translational modifications to KITL can also be a factor of mesenchymal KITL loss in PDAC. It is possible that mesenchymal KITL may still be transcribed and translated but degraded before its formation as either a membrane-bound or a soluble isoform. Mass spectrometry can allow us to observe changes in KITL protein between primary murine PSCs versus PSC-derived murine CAFs by identifying protein fragments and degradation products, such as ubiquitinated KITL and KITL fragments in lysosomes.

H. Fibroblast lineage contribution and function in the presence of early mesenchymal KITL loss

Since both our previous work (Helms et al., 2022) and work from di Magliano's group (Garcia et al., 2020) elucidated that fibroblast lineages have different numerical and functional properties in healthy and cancer environments, it would be interesting to address whether disrupted pancreatic stellate cell-derived KITL changes the pancreatic mesenchyme landscape, which may impact downstream changes in the tumor microenvironment. For example, it is currently unknown if there is a sequential order of fibroblast activation with respect to fibroblast lineage—and if this impacts tumorigenesis. Perhaps a reason as to why pancreatic stellate cell KITL loss significantly accelerates tumor growth and reduces survival in mouse models is because of PSC-derived CAF activation (associated with PSC loss of KITL) appears to occur at later stages of tumorigenesis. PSC KITL loss in the normal tissue potentially propels the environment to mimic a more aggressive stage of the disease. Elaborate mouse models that combine lineage tracing of KITL loss in Fabp4+ cells with Gli1+ cells will allow us to explore these questions. Studies should include exploration on fibroblast composition in healthy pancreas and tumor pancreas. Tumor pancreas models could include orthotopic models (using slow- and fast-growing PDAC cancer cells) and tumors of different genotypes (e.g.

p53 R172H vs p53 hemizygous loss vs p53 null mutation), as we've previously shown that different tumor genotypes can impact CAF functions.

I. Mesenchymal KITL and the Immune Compartment

It is pertinent for human PDAC therapies to shift its immunosuppressive microenvironment towards an anti-tumor immune microenvironment, but this Herculean task has proved challenging. Our results further highlight this issue as we parse mesenchymal functions in PDAC. Both *in vitro* and *in vivo* models of mesenchymal KITL loss indicated changes in fibro-inflammatory processes. *Kitl* knock down in immortalized PSCs compared to control result in an increase of gene expressions related to inflammatory processes (Supplementary Figures 2.S3C & 2.S3D). In healthy pancreas, our experimental *Kitl^{fl/fl};Fabp4-Cre* model shows an increase in CD45+ leukocytes compared to *Fabp4-Cre* control mice (Figures 2.3E & 2.3K). We also observe an increase in CD68+ macrophages in our experimental model in contrast to our control model (Figure 2.3L). But our data show with orthotopic models that stellate cell loss of KITL expression resulted in accelerated tumor growth and lower survival (Figures 2.4A-D & 2.4H-J).

This reemphasizes two lessons: 1) increased leukocyte infiltration does not equate to improved pancreatic cancer outcomes; and, 2) the type of immune cells involved matter. Assessment of immune cell types in our *Kitl^{fl/fl};Fabp4-Cre* model compared to controls in healthy and tumor pancreata are necessary to anticipate developments in the inflammatory niche as cancer progresses. Flow cytometry and multiplex IHC can elucidate immune cell types involved in this process, particularly markers associated with regulatory T cells (T_{reg}) and tumor-associated macrophages (TAMs), due to increased expression of both CD45+ and CD68+ markers in our experimental models as well as their

activity in weakening anti-tumor immunity (Beatty et al., 2015; Clark et al., 2007). PDAC is also characterized by the accumulation of immunosuppressive myeloid-derived suppressor cells (MDSCs) (Bayne et al., 2012; Siret et al., 2020), which can differentiate into TAMs (Kumar et al., 2016). However, perturbation of mesenchymal KITL is not equivalent to true tumor conditions, therefore we must include other immune markers involved in immune dysregulation when investigating healthy pancreata. Such markers include CD11b+, Gr-1+, CD25+, FOXP3+ (Glaubitz et al., 2022; Kataru et al., 2009) and other immune cells (i.e. neutrophils, eosinophils) seen in chronic pancreatitis are eligible immune types to investigate (Leppkes et al., 2016; Manohar et al., 2018), as pancreas of *Kitl^{fl/fl};Fabp4-Cre* experimental models expressed a more aggressive inflammatory response after caerulein treatment, reflecting chronic pancreatitis. Furthermore, it is important to investigate innate immune cells such as mast cells, NK cells, and dendritic cells, as they are known to express and are regulated by c-KIT signaling (Tsai et al., 2022). Mesenchymal loss of KITL may severely impact functions of these innate immune cells, dysregulating normal tissue immune homeostasis. For example, the KITL/c-KIT axis has been implicated dendritic cell regulation and equilibrium (Barroeta Seijas et al., 2022; Simonetti et al., 2019). These results should then be validated by analysis of human benign adjacent pancreatic tissues, and adult healthy pancreas, which have recently been shown to harbor PanINs (Carpenter et al., 2023)

J. Mesenchymal KITL maintains tissue architecture

Additionally, in the context of inflammation, mesenchymal KITL appears to restrain epithelial plasticity, as *Kitl^{fl/fl};Fabp4-Cre* experimental mice upon caerulein treatment expressed more of the ductal marker panCK in the pancreas, compared to *Fabp4-Cre* control mice (Figure 2.3J). This overlap of both ductal marker panCK and epithelial marker

amylase found throughout pancreata of experimental mice is indicative of acinar-to-ductal metaplasia (ADM), considered to be an early step in pancreatic tumorigenesis. This suggests that one of the purposes of epithelial-mesenchymal interactions through the KITL/c-KIT signaling axis is to maintain normal tissue architecture. Pancreatic organoids may be a useful model for this hypothesis. To replicate acute pancreatitis in an *in vitro* setting, treatment of cytokines—such as IL-1 β , IL-6, IL-8, TNF- α —to pancreatic organoids may mimic acute pancreatitis in an *in vitro* setting, as these cytokines have increased expression in acute pancreatitis that leads to a hyperinflammatory response reflective of this disease (Malheiro et al., 2024). Cytokine-induced organoids are either treated with or without exogenous KITL, then quantified for differences in ductal and epithelial markers, whether by immunofluorescence or flow cytometry.

K. “All Models are Wrong...”: Mouse Models

Scientific inquiry requires control of all conditions, which, as a human being first and a scientist second, sounds comically absurd to say the least. British statistician George E. P. Box described it best when he said, “all models are wrong”. Models, such as the genetically modified mouse models used in this dissertation, are not an accurate reflection of human biology. The anatomy between the two species is quite distinct: whereas the human pancreas is described as “compact,” comprising of discrete regions (e.g. head, uncinata process, neck, body, tail), the mouse pancreas is “mesenteric”—stretched and dispersed between other gastrointestinal organs due to mesenteric fat and connective tissue (Liggitt & Dintzis, 2018). This could suggest that stromal components and adipose tissue may have a greater impact on homeostasis and disease development in murine pancreas than in human pancreas, a perspective that cannot be taken lightly in the context of this dissertation. Interestingly, human acinar and islet cells tend to accumulate lipid

droplets, whereas rodent acinar and islet cells (whether from mouse or rat) do not appear to accumulate lipid droplets, regardless of age or dietary changes (Tong et al., 2020). This distinctive feature of human acinar and islet cells may provide a partial explanation regarding the challenge of producing murine PDAC models that are reliably metastatic, as it has been shown that lipid droplets are a key energetic source for invasive migration (Rozeveld et al., 2020). However, the other half of Box's aphorism, "... but some [models] are useful," reminds us that models provide important knowledge and insight to the mechanisms we endeavor to illuminate, so long as we are conscientious in the applications of one's findings onto other systems.

L. Potential KITL/c-KIT tumor-promoting capacity in PDAC

Much of scientific literature paints the c-KIT signaling pathway as a mechanism for tumorigenesis (Heinrich et al., 2000; Mazzoldi et al., 2019). In PDAC, evidence has shown that patients that expressed both KITL and c-KIT had significantly lower survival than other patients (Yasuda et al., 2006), associating c-KIT activation with overall lower PDAC survival. However, the authors explored the potential mechanisms underlying this association through reductionist *in vitro* methods, wherein immortalized pancreatic cancer cells were treated with recombinant KITL. On the other hand, our use of sophisticated mouse models and improved imaging technologies to interrogate human PDAC tissues distinguishes that KITL source matters; we also note that temporal events are important since it appears that mesenchymal KITL loss is gradual. Furthermore, Yasuda and colleagues used both c-KIT high (PANC-1, SW1990) and c-KIT low (BxPC-3, Canpan-2, MIA PaCa-2) expressing PDAC cells, and only c-KIT high expressing cells showed an increase in invasiveness, while invasiveness in c-KIT low expressing cells did not change relative to controls. In fact, there was a reduction in invasiveness for MIA PaCa-2; however, the reduction did not appear to be statistically significant. One could only

surmise from this result that PDAC with high expression of c-KIT would be impacted by KITL treatment. But the fact remains that we are uncertain if the *in vitro* concentrations of KITL are reflective of *in vivo* settings. It is also unanswered whether the same invasive patterns would be seen in a heterogeneous cancer cell population, which may have a mixture of c-KIT high and c-KIT low expressing cancer cells. Data from the Human Protein Atlas Network (collected from TCGA) show that there is relatively little expression of c-KIT protein in pancreatic adenocarcinoma. Thus, it appears that c-KIT signaling in PDAC cancer cells is unnecessary for tumorigenesis. What our results show, rather, is that mesenchymal KITL expression and the c-KIT signaling pathway is poised towards regulation of healthy tissue homeostasis and normal tissue function.

M. Dysfunctional Mechanisms from mesenchymal KITL loss as Evidence for Liver Metastasis and Disease

It is reasonable to suggest that HSCs in the adult liver express KITL/SCF, considering that the findings from this dissertation were directed by the fact that hepatic stellate cells in the developing liver express KITL. Thus, it is critical to assess for 1) hepatic stellate cell-derived KITL in the adult liver; 2) loss of hepatic stellate cell-derived KITL in PDAC liver metastasis; and 3) compensatory mechanisms in the liver due to HSC-derived KITL loss. If point 1 were confirmed, and point 2 were consistently observed, it is plausible to consider loss of KITL as a candidate biomarker for PDAC liver metastasis. If KITL in blood serum is undetectable even in healthy adults, it may still be possible to evaluate homeostatic mechanisms, such as inflammation and immune cell function. For example, clinicians may be able to elucidate functions of immune cells from patient blood serum. In particular, the c-KIT signaling pathway is critical for mast cell function, as it is one of the few immune cells (including natural killer cells and dendritic cells) to express c-KIT receptor post-differentiation (Matos et al., 1993; Ray et al., 2010; Simonetti et al., 2019; Tsai et al., 2022).

Additionally, mast cells are known to reside within the hepatic vasculature in human and rodent liver (Jarido et al., 2017; Johnson et al., 2016), and that the liver filters blood, suggesting that other mast cells circulating the body will enter the liver. Observing for functional changes in mast cells (or other immune cells) as another barometer included in liver functional tests may provide researchers and clinicians nuanced insight on a patient's liver health.

That said, this conclusion would be dependent upon point 3. For example, if other cells within the liver express KITL to compensate for loss of HSC-derived KITL (perhaps hepatic endothelial cells), determining early or non-invasive indications of liver metastasis through KITL protein expression may be moot. However, as previously mentioned in Chapter III, Section E, the cellular source of KITL may matter. Thus, homeostatic functions associated with the c-KIT pathway in the liver may still be disrupted, requiring further investigation on the role of KITL in PDAC liver metastasis. Lastly, it would be important to address if liver metastasis developed from other primary cancers, such as breast and lung, also resulted in hepatic stellate cell-derived KITL loss. Mesenchymal KITL loss in the liver could be used as a candidate marker for pan-cancer liver metastasis.

N. Anti-stromal/fibrotic Cancer Treatments as Treatments for other Fibroinflammatory Diseases

While malignant solid tumors are the most lethal form of disease associated with a fibro-inflammatory response, other non-cancerous diseases (categorized as fibroinflammatory diseases) including idiopathic pulmonary fibrosis, cirrhosis, rheumatoid arthritis, Crohn's disease, etc. are either caused by or result in an overactive fibro-inflammatory reaction. Fibrosis and persistent inflammation may not be the original causes of these diseases. However, tissue architecture is often disrupted from scarring, which can result in chronic

conditions that can ultimately lead to organ failure and death. Thus, it is reasonable to suggest that anti-stromal/fibrotic cancer treatments may also be used for other fibroinflammatory diseases, as these treatments may resolve aberrant and chronic tissue scarring, therefore allowing other treatments to target the underlying mechanisms for each specific disease and improving tissue architecture of the organ(s) affected. It may also be possible to use anti-fibrotic treatments initially intended for non-cancerous fibroinflammatory diseases, such as nintedanib and pirfenidone (for idiopathic pulmonary fibrosis), to malignant solid tumors such as lung adenocarcinoma, colorectal cancer, and PDAC. Lastly, exploration into mesenchymal KITL functions in pancreatic cancer are still at its nascent stage; nonetheless, based on evidence from this dissertation, one can anticipate that mesenchymal KITL functional roles in maintaining healthy tissue architecture could also be applied to non-cancer fibroinflammatory diseases.

O. Concluding Remarks

This dissertation elucidates the impacts of pancreatic stellate cell loss of KITL in normal murine pancreas and in pancreatic tumorigenesis, implicating that mesenchymal KITL expression and the c-KIT signaling pathway is poised towards regulation of healthy tissue homeostasis and normal tissue function. Pursuit toward KITL was due to previous findings from Sean Morrison and Lei Ding, wherein mesenchymal KITL/SCF regulate hematopoietic stem cell expansion and maturity. In another context, LEPR+ mesenchymal cells have been shown to promote bone marrow innervation and regeneration (X. Gao et al., 2023). There may be underlying biological factors as to why it appears that mesenchymal cells, especially those that reside within the perivascular space, maintain normal tissue homeostasis and activate tissue (re)organization through juxtacrine and paracrine interactions via growth factors such as KITL/SCF. This dissertation also reminds us that normal tissue homeostasis is a form of tumor-restraint, which the field should

explore as another avenue for both cancer treatment and prevention. Lastly, we have reason to suspect that mesenchymal KITL, specifically from pancreatic stellate cells, may partially explain the more aggressive fibro-inflammatory responses found in later stages of PDAC that is lacking in adult healthy pancreas with precancerous lesions, since genetic inhibition of KITL expression in our murine PSCs showed an increase of CD45+ immune cells in healthy pancreas (Figure 2.3E), and altered epithelial plasticity in the context of acute pancreatitis, in comparison to control mice (Figures 2.3 J-L). This harkens back to the importance of understanding how fibroblast lineage can resolve discrepancies of tumor-promoting and tumor-suppressive features seen in cancer-associated fibroblasts. The dissertation, and continuation of this work, contributes to deciphering the non-immune stromal functions of the tumor microenvironment, with the hope this will advance PDAC early detection, therapies, and the new frontier of cancer prevention.

References

- AlZaim, I., de Rooij, L. P. M. H., Sheikh, B. N., Börgeson, E., & Kalucka, J. (2023). The evolving functions of the vasculature in regulating adipose tissue biology in health and obesity. *Nature Reviews Endocrinology*, *19*(12), 691–707. <https://doi.org/10.1038/s41574-023-00893-6>
- Andes, L. J., Cheng, Y. J., Rolka, D. B., Gregg, E. W., & Imperatore, G. (2020). Prevalence of Prediabetes Among Adolescents and Young Adults in the United States, 2005-2016. *JAMA Pediatrics*, *174*(2), e194498–e194498. <https://doi.org/10.1001/jamapediatrics.2019.4498>
- Apte, M. V., Haber, P. S., Applegate, T. L., Norton, I. D., McCaughan, G. W., Korsten, M. A., Pirola, R. C., & Wilson, J. S. (1998). Periacinar stellate shaped cells in rat pancreas: Identification, isolation, and culture. *Gut*, *43*(1), 128–133. <https://doi.org/10.1136/gut.43.1.128>
- Apte, M. V., Haber, P. S., Darby, S. J., Rodgers, S. C., McCaughan, G. W., Korsten, M. A., Pirola, R. C., & Wilson, J. S. (1999). Pancreatic stellate cells are activated by proinflammatory cytokines: Implications for pancreatic fibrogenesis. *Gut*, *44*(4), 534–541. <https://doi.org/10.1136/gut.44.4.534>
- Atkinson, M. A., Campbell-Thompson, M., Kusmartseva, I., & Kaestner, K. H. (2020). Organisation of the human pancreas in health and in diabetes. *Diabetologia*, *63*(10), 1966–1973. <https://doi.org/10.1007/s00125-020-05203-7>
- Attali, M., Stetsyuk, V., Basmaciogullari, A., Aiello, V., Zanta-Boussif, M. A., Duvillie, B., & Scharfmann, R. (2007). Control of β -Cell Differentiation by the Pancreatic Mesenchyme. *Diabetes*, *56*(5), 1248–1258. <https://doi.org/10.2337/db06-1307>
- Auciello, F. R., Bulusu, V., Oon, C., Tait-Mulder, J., Berry, M., Bhattacharyya, S., Tumanov, S., Allen-Petersen, B. L., Link, J., Kendsersky, N. D., Vringer, E., Schug, M., Novo, D., Hwang, R. F., Evans, R. M., Nixon, C., Dorrell, C., Morton, J. P., Norman, J. C., ... Sherman, M. H. (2019). A Stromal Lysolipid–Autotaxin Signaling Axis Promotes Pancreatic Tumor Progression. *Cancer Discovery*, *9*(5), 617–627. <https://doi.org/10.1158/2159-8290.CD-18-1212>
- Avolio, E., Alvino, V. V., Ghorbel, M. T., & Campagnolo, P. (2017). Perivascular cells and tissue engineering: Current applications and untapped potential. *Pharmacology & Therapeutics*, *171*, 83–92. <https://doi.org/10.1016/j.pharmthera.2016.11.002>
- Bailey, J. M., Swanson, B. J., Hamada, T., Eggers, J. P., Singh, P. K., Caffery, T., Ouellette, M. M., & Hollingsworth, M. A. (2008). Sonic Hedgehog Promotes

- Desmoplasia in Pancreatic Cancer. *Clinical Cancer Research*, 14(19), 5995–6004. <https://doi.org/10.1158/1078-0432.CCR-08-0291>
- Barriga, F. M., Tsanov, K. M., Ho, Y.-J., Sohail, N., Zhang, A., Baslan, T., Wuest, A. N., Del Priore, I., Meškauskaitė, B., Livshits, G., Alonso-Curbelo, D., Simon, J., Chaves-Perez, A., Bar-Sagi, D., Iacobuzio-Donahue, C. A., Notta, F., Chaligne, R., Sharma, R., Pe'er, D., & Lowe, S. W. (2022). MACHETE identifies interferon-encompassing chromosome 9p21.3 deletions as mediators of immune evasion and metastasis. *Nature Cancer*, 3(11), 1367–1385. <https://doi.org/10.1038/s43018-022-00443-5>
- Barroeta Seijas, A. B., Simonetti, S., Filippi, I., Naldini, A., Favaretto, G., Colombo, T., Natalini, A., Antonangeli, F., Laffranchi, M., Sozzani, S., Santoni, A., & Di Rosa, F. (2022). Mouse dendritic cells in the steady state: Hypoxia, autophagy, and stem cell factor. *Cell Biochemistry and Function*, 40(7), 718–728. <https://doi.org/10.1002/cbf.3737>
- Bayne, L. J., Beatty, G. L., Jhala, N., Clark, C. E., Rhim, A. D., Stanger, B. Z., & Vonderheide, R. H. (2012). Tumor-Derived Granulocyte-Macrophage Colony-Stimulating Factor Regulates Myeloid Inflammation and T Cell Immunity in Pancreatic Cancer. *Cancer Cell*, 21(6), 822–835. <https://doi.org/10.1016/j.ccr.2012.04.025>
- Beatty, G. L., Winograd, R., Evans, R. A., Long, K. B., Luque, S. L., Lee, J. W., Clendenin, C., Gladney, W. L., Knoblock, D. M., Guirnalda, P. D., & Vonderheide, R. H. (2015). Exclusion of T Cells From Pancreatic Carcinomas in Mice Is Regulated by Ly6Clow F4/80+ Extratumoral Macrophages. *Gastroenterology*, 149(1), 201–210. <https://doi.org/10.1053/j.gastro.2015.04.010>
- Besmer, P., Murphy, J. E., George, P. C., Qiu, F., Bergold, P. J., Lederman, L., Snyder, H. W., Brodeur, D., Zuckerman, E. E., & Hardy, W. D. (1986). A new acute transforming feline retrovirus and relationship of its oncogene v-kit with the protein kinase gene family. *Nature*, 320(6061), 415–421. <https://doi.org/10.1038/320415a0>
- Blaisdell, A., Crequer, A., Columbus, D., Daikoku, T., Mittal, K., Dey, S. K., & Erlebacher, A. (2015). Neutrophils Oppose Uterine Epithelial Carcinogenesis via Debridement of Hypoxic Tumor Cells. *Cancer Cell*, 28(6), 785–799. <https://doi.org/10.1016/j.ccell.2015.11.005>

- Blomhoff, R., Rasmussen, M., Nilsson, A., Norum, K. R., Berg, T., Blaner, W. S., Kato, M., Mertz, J. R., Goodman, D. S., & Eriksson, U. (1985). Hepatic retinol metabolism. Distribution of retinoids, enzymes, and binding proteins in isolated rat liver cells. *Journal of Biological Chemistry*, *260*(25), 13560–13565.
[https://doi.org/10.1016/S0021-9258\(17\)38759-8](https://doi.org/10.1016/S0021-9258(17)38759-8)
- Braxton, A. M., Kiemen, A. L., Grahn, M. P., Forjaz, A., Parksong, J., Mahesh Babu, J., Lai, J., Zheng, L., Niknafs, N., Jiang, L., Cheng, H., Song, Q., Reichel, R., Graham, S., Damanakis, A. I., Fischer, C. G., Mou, S., Metz, C., Granger, J., ... Wood, L. D. (2024). 3D genomic mapping reveals multifocality of human pancreatic precancers. *Nature*, *629*(8012), 679–687.
<https://doi.org/10.1038/s41586-024-07359-3>
- BRCA Gene Changes: Cancer Risk and Genetic Testing Fact Sheet - NCI* (nciglobal,ncienterprise). (2024, August 3). [cgvArticle].
<https://www.cancer.gov/about-cancer/causes-prevention/genetics/brca-fact-sheet>
- Brown, S., Pineda, C. M., Xin, T., Boucher, J., Suozzi, K. C., Park, S., Matte-Martone, C., Gonzalez, D. G., Rytlewski, J., Beronja, S., & Greco, V. (2017). Correction of aberrant growth preserves tissue homeostasis. *Nature*, *548*(7667), 334–337.
<https://doi.org/10.1038/nature23304>
- Brügger, M. D., Valenta, T., Fazilaty, H., Hausmann, G., & Basler, K. (2020). Distinct populations of crypt-associated fibroblasts act as signaling hubs to control colon homeostasis. *PLOS Biology*, *18*(12), e3001032.
<https://doi.org/10.1371/journal.pbio.3001032>
- Buchholz, M., Kestler, H. A., Holzmann, K., Ellenrieder, V., Schneiderhan, W., Siech, M., Adler, G., Bachem, M. G., & Gress, T. M. (2005). Transcriptome analysis of human hepatic and pancreatic stellate cells: Organ-specific variations of a common transcriptional phenotype. *Journal of Molecular Medicine*, *83*(10), 795–805. <https://doi.org/10.1007/s00109-005-0680-2>
- Buechler, M. B., Pradhan, R. N., Krishnamurty, A. T., Cox, C., Calviello, A. K., Wang, A. W., Yang, Y. A., Tam, L., Caothien, R., Roose-Girma, M., Modrusan, Z., Arron, J. R., Bourgon, R., Müller, S., & Turley, S. J. (2021). Cross-tissue organization of the fibroblast lineage. *Nature*, *593*(7860), 575–579.
<https://doi.org/10.1038/s41586-021-03549-5>

- Campbell, J. E., & Newgard, C. B. (2021). Mechanisms controlling pancreatic islet cell function in insulin secretion. *Nature Reviews. Molecular Cell Biology*, 22(2), 142–158. <https://doi.org/10.1038/s41580-020-00317-7>
- Cancer of the Pancreas—Cancer Stat Facts*. (n.d.). SEER. Retrieved January 9, 2025, from <https://seer.cancer.gov/statfacts/html/pancreas.html>
- Cao, J., Spielmann, M., Qiu, X., Huang, X., Ibrahim, D. M., Hill, A. J., Zhang, F., Mundlos, S., Christiansen, L., Steemers, F. J., Trapnell, C., & Shendure, J. (2019). The single-cell transcriptional landscape of mammalian organogenesis. *Nature*, 566(7745), 496–502. <https://doi.org/10.1038/s41586-019-0969-x>
- Carpenter, E. S., Elhossiny, A. M., Kadiyala, P., Li, J., McGue, J., Griffith, B. D., Zhang, Y., Edwards, J., Nelson, S., Lima, F., Donahue, K. L., Du, W., Bischoff, A. C., Alomari, D., Watkoske, H. R., Mattea, M., The, S., Espinoza, C. E., Barrett, M., ... Pasca di Magliano, M. (2023). Analysis of Donor Pancreata Defines the Transcriptomic Signature and Microenvironment of Early Neoplastic Lesions. *Cancer Discovery*, 13(6), 1324–1345. <https://doi.org/10.1158/2159-8290.CD-23-0013>
- Catenacci, D. V. T., Bahary, N., Edelman, M. J., Nattam, S. R., Marsh, R. de W., Kaubisch, A., Wallace, J. A., Cohen, D. J., Stiff, P. J., Sleckman, B. G., Thomas, S. P., Lenz, H.-J., Henderson, L., Zagaya, C., Vannier, M., Karrison, T., Stadler, W. M., & Kindler, H. L. (2012). A phase IB/randomized phase II study of gemcitabine (G) plus placebo (P) or vismodegib (V), a hedgehog (Hh) pathway inhibitor, in patients (pts) with metastatic pancreatic cancer (PC): Interim analysis of a University of Chicago phase II consortium study. *Journal of Clinical Oncology*, 30(15_suppl), 4022–4022. https://doi.org/10.1200/jco.2012.30.15_suppl.4022
- Chen, W., Gendrault, J.-L., Steffan, A.-M., Jeandidier, E., & Kirn, A. (1989). Isolation, culture and main characteristics of mouse fat-storing cells: Interaction with viruses. *Hepatology*, 9(3), 352–362. <https://doi.org/10.1002/hep.1840090303>
- Cheng, H.-W., Onder, L., Novkovic, M., Sonesson, C., Lütge, M., Pikor, N., Scandella, E., Robinson, M. D., Miyazaki, J., Tersteegen, A., Sorg, U., Pfeiffer, K., Rülcke, T., Hehlhans, T., & Ludewig, B. (2019). Origin and differentiation trajectories of fibroblastic reticular cells in the splenic white pulp. *Nature Communications*, 10(1), 1739. <https://doi.org/10.1038/s41467-019-09728-3>

- Clark, C. E., Hingorani, S. R., Mick, R., Combs, C., Tuveson, D. A., & Vonderheide, R. H. (2007). Dynamics of the Immune Reaction to Pancreatic Cancer from Inception to Invasion. *Cancer Research*, *67*(19), 9518–9527. <https://doi.org/10.1158/0008-5472.CAN-07-0175>
- Collet, L., Ghurburrun, E., Meyers, N., Assi, M., Pirlot, B., Leclercq, I. A., Couvelard, A., Komuta, M., Cros, J., Demetter, P., Lemaigre, F. P., Borbath, I., & Jacquemin, P. (2020). Kras and Lkb1 mutations synergistically induce intraductal papillary mucinous neoplasm derived from pancreatic duct cells. *Gut*, *69*(4), 704–714. <https://doi.org/10.1136/gutjnl-2018-318059>
- Collins, M. A., Bednar, F., Zhang, Y., Brisset, J.-C., Galbán, S., Galbán, C. J., Rakshit, S., Flannagan, K. S., Adsay, N. V., & Magliano, M. P. di. (2012). Oncogenic Kras is required for both the initiation and maintenance of pancreatic cancer in mice. *The Journal of Clinical Investigation*, *122*(2), 639–653. <https://doi.org/10.1172/JCI59227>
- Comazzetto, S., Murphy, M. M., Berto, S., Jeffery, E., Zhao, Z., & Morrison, S. J. (2019). Restricted Hematopoietic Progenitors and Erythropoiesis Require SCF from Leptin Receptor+ Niche Cells in the Bone Marrow. *Cell Stem Cell*, *24*(3), 477–486.e6. <https://doi.org/10.1016/j.stem.2018.11.022>
- Common Cancer Sites—Cancer Stat Facts*. (n.d.). SEER. Retrieved January 9, 2025, from <https://seer.cancer.gov/statfacts/html/common.html>
- Conroy, T., Desseigne, F., Ychou, M., Bouché, O., Guimbaud, R., Bécouarn, Y., Adenis, A., Raoul, J.-L., Gourgou-Bourgade, S., Fouchardière, C. de la, Bennouna, J., Bachet, J.-B., Khemissa-Akouz, F., Péré-Vergé, D., Delbaldo, C., Assenat, E., Chauffert, B., Michel, P., Montoto-Grillot, C., & Ducreux, M. (2011). FOLFIRINOX versus Gemcitabine for Metastatic Pancreatic Cancer. *New England Journal of Medicine*, *364*(19), 1817–1825. <https://doi.org/10.1056/NEJMoa1011923>
- Copeland, N. G., Gilbert, D. J., Cho, B. C., Donovan, P. J., Jenkins, N. A., Cosman, D., Anderson, D., Lyman, S. D., & Williams, D. E. (1990). Mast cell growth factor maps near the steel locus on mouse chromosome 10 and is deleted in a number of steel alleles. *Cell*, *63*(1), 175–183. [https://doi.org/10.1016/0092-8674\(90\)90298-S](https://doi.org/10.1016/0092-8674(90)90298-S)
- Cui Zhou, D., Jayasinghe, R. G., Chen, S., Herndon, J. M., Iglesia, M. D., Navale, P., Wendl, M. C., Caravan, W., Sato, K., Storrs, E., Mo, C.-K., Liu, J., Southard-Smith, A. N., Wu, Y., Naser Al Deen, N., Baer, J. M., Fulton, R. S., Wyczalkowski,

- M. A., Liu, R., ... Ding, L. (2022). Spatially restricted drivers and transitional cell populations cooperate with the microenvironment in untreated and chemo-resistant pancreatic cancer. *Nature Genetics*, 54(9), Article 9. <https://doi.org/10.1038/s41588-022-01157-1>
- Cukierman, E. (2021). A Reflection on How Carcinoma-Associated Fibroblasts Were Recognized as Active Participants of Epithelial Tumorigenesis. *Cancer Research*, 81(18), 4668–4670. <https://doi.org/10.1158/0008-5472.CAN-21-2553>
- De Jesus-Acosta, A., Sugar, E. A., O'Dwyer, P. J., Ramanathan, R. K., Von Hoff, D. D., Rasheed, Z., Zheng, L., Begum, A., Anders, R., Maitra, A., McAllister, F., Rajeshkumar, N. V., Yabuuchi, S., de Wilde, R. F., Batukbhai, B., Sahin, I., & Laheru, D. A. (2020). Phase 2 study of vismodegib, a hedgehog inhibitor, combined with gemcitabine and nab-paclitaxel in patients with untreated metastatic pancreatic adenocarcinoma. *British Journal of Cancer*, 122(4), 498–505. <https://doi.org/10.1038/s41416-019-0683-3>
- DelGiorno, K. E., Naeem, R. F., Fang, L., Chung, C.-Y., Ramos, C., Luhtala, N., O'Connor, C., Hunter, T., Manor, U., & Wahl, G. M. (2020). Tuft Cell Formation Reflects Epithelial Plasticity in Pancreatic Injury: Implications for Modeling Human Pancreatitis. *Frontiers in Physiology*, 11. <https://www.frontiersin.org/articles/10.3389/fphys.2020.00088>
- Demetri, G. D., Mehren, M. von, Blanke, C. D., Abbeele, A. D. V. den, Eisenberg, B., Roberts, P. J., Heinrich, M. C., Tuveson, D. A., Singer, S., Janicek, M., Fletcher, J. A., Silverman, S. G., Silberman, S. L., Capdeville, R., Kiese, B., Peng, B., Dimitrijevic, S., Druker, B. J., Corless, C., ... Joensuu, H. (2002). Efficacy and Safety of Imatinib Mesylate in Advanced Gastrointestinal Stromal Tumors. *New England Journal of Medicine*, 347(7), 472–480. <https://doi.org/10.1056/NEJMoa020461>
- Dimanche-Boitrel, M. T., Vakaet Jr, L., Pujuguet, P., Chauffert, B., Martin, M. S., Hammann, A., Van Roy, F., Mareel, M., & Martin, F. (1994). In vivo and in vitro invasiveness of a rat colon-cancer cell line maintaining E-cadherin expression: An enhancing role of tumor-associated myofibroblasts. *International Journal of Cancer*, 56(4), 512–521. <https://doi.org/10.1002/ijc.2910560410>
- Ding, L., & Morrison, S. J. (2013). Haematopoietic stem cells and early lymphoid progenitors occupy distinct bone marrow niches. *Nature*, 495(7440), 231–235. <https://doi.org/10.1038/nature11885>

- Ding, L., Saunders, T. L., Enikolopov, G., & Morrison, S. J. (2012). Endothelial and perivascular cells maintain haematopoietic stem cells. *Nature*, *481*(7382), Article 7382. <https://doi.org/10.1038/nature10783>
- Donahue, K. L., Watkoske, H. R., Kadiyala, P., Du, W., Brown, K., Scales, M. K., Elhossiny, A. M., Espinoza, C. E., Lasse Opsahl, E. L., Griffith, B. D., Wen, Y., Sun, L., Velez-Delgado, A., Renollet, N. M., Morales, J., Nedzesky, N. M., Baliira, R. K., Menjivar, R. E., Medina-Cabrera, P. I., ... Pasca di Magliano, M. (2024). Oncogenic KRAS-Dependent Stromal Interleukin-33 Directs the Pancreatic Microenvironment to Promote Tumor Growth. *Cancer Discovery*, OF1–OF26. <https://doi.org/10.1158/2159-8290.CD-24-0100>
- Druker, B. J., Talpaz, M., Resta, D. J., Peng, B., Buchdunger, E., Ford, J. M., Lydon, N. B., Kantarjian, H., Capdeville, R., Ohno-Jones, S., & Sawyers, C. L. (2001). Efficacy and Safety of a Specific Inhibitor of the BCR-ABL Tyrosine Kinase in Chronic Myeloid Leukemia. *New England Journal of Medicine*, *344*(14), 1031–1037. <https://doi.org/10.1056/NEJM200104053441401>
- DuFort, C. C., DelGiorno, K. E., & Hingorani, S. R. (2016). Mounting Pressure in the Microenvironment: Fluids, Solids, and Cells in Pancreatic Ductal Adenocarcinoma. *Gastroenterology*, *150*(7), 1545-1557.e2. <https://doi.org/10.1053/j.gastro.2016.03.040>
- Dumont, N., Liu, B., DeFilippis, R. A., Chang, H., Rabban, J. T., Karnezis, A. N., Tjoe, J. A., Marx, J., Parvin, B., & Tlsty, T. D. (2013). Breast Fibroblasts Modulate Early Dissemination, Tumorigenesis, and Metastasis through Alteration of Extracellular Matrix Characteristics. *Neoplasia (New York, N.Y.)*, *15*(3), 249–262.
- DuPage, M., Cheung, A. F., Mazumdar, C., Winslow, M. M., Bronson, R., Schmidt, L. M., Crowley, D., Chen, J., & Jacks, T. (2011). Endogenous T Cell Responses to Antigens Expressed in Lung Adenocarcinomas Delay Malignant Tumor Progression. *Cancer Cell*, *19*(1), 72–85. <https://doi.org/10.1016/j.ccr.2010.11.011>
- Earl, J., Galindo-Pumariño, C., Encinas, J., Barreto, E., Castillo, M. E., Pachón, V., Ferreira, R., Rodríguez-Garrote, M., González-Martínez, S., Cajal, T. R. y, Diaz, L. R., Chirivella-Gonzalez, I., Rodriguez, M., Castro, E. M. de, García-Seisdedos, D., Muñoz, G., Rosa, J. M. R., Marquez, M., Malats, N., & Carrato, A. (2020). A comprehensive analysis of candidate genes in familial pancreatic cancer families reveals a high frequency of potentially pathogenic germline variants. *eBioMedicine*, *53*. <https://doi.org/10.1016/j.ebiom.2020.102675>

- Ebia, M. I., Hitchins, M. P., & Hendifar, A. E. (2023). Immunotherapy for deficient mismatch repair (dMMR) pancreatic ductal adenocarcinoma. *Journal of Gastrointestinal Oncology*, *14*(2). <https://doi.org/10.21037/jgo-23-12>
- Fang, S., Wei, J., Pentimikko, N., Leinonen, H., & Salven, P. (2012). Generation of Functional Blood Vessels from a Single c-kit⁺ Adult Vascular Endothelial Stem Cell. *PLOS Biology*, *10*(10), e1001407. <https://doi.org/10.1371/journal.pbio.1001407>
- Feng, Z.-C., Riopel, M., Popell, A., & Wang, R. (2015). A survival Kit for pancreatic beta cells: Stem cell factor and c-Kit receptor tyrosine kinase. *Diabetologia*, *58*(4), 654–665. <https://doi.org/10.1007/s00125-015-3504-0>
- Fletcher, A. L., Malhotra, D., & Turley, S. J. (2011). Lymph node stroma broaden the peripheral tolerance paradigm. *Trends in Immunology*, *32*(1), 12–18. <https://doi.org/10.1016/j.it.2010.11.002>
- Forsthuber, A., Aschenbrenner, B., Korosec, A., Jacob, T., Annusver, K., Krajic, N., Kholodniuk, D., Frech, S., Zhu, S., Purkhauser, K., Lipp, K., Werner, F., Nguyen, V., Griss, J., Bauer, W., Soler Cardona, A., Weber, B., Weninger, W., Gesslbauer, B., ... Lichtenberger, B. M. (2024). Cancer-associated fibroblast subtypes modulate the tumor-immune microenvironment and are associated with skin cancer malignancy. *Nature Communications*, *15*(1), 9678. <https://doi.org/10.1038/s41467-024-53908-9>
- Friedman, S. L., Rockey, D. C., McGuire, R. F., Maher, J. J., Boyles, J. K., & Yamasaki, G. (1992). Isolated hepatic lipocytes and kupffer cells from normal human liver: Morphological and functional characteristics in primary culture. *Hepatology*, *15*(2), 234–243. <https://doi.org/10.1002/hep.1840150211>
- Frost, M. J., Ferrao, P. T., Hughes, T. P., & Ashman, L. K. (2002). Juxtamembrane mutant V560GKit is more sensitive to Imatinib (STI571) compared with wild-type c-kit whereas the kinase domain mutant D816VKit is resistant. *Molecular Cancer Therapeutics*, *1*(12), 1115–1124.
- Gallini, S., Annusver, K., Rahman, N.-T., Gonzalez, D. G., Yun, S., Matte-Martone, C., Xin, T., Lathrop, E., Suozzi, K. C., Kasper, M., & Greco, V. (2023). Injury prevents Ras mutant cell expansion in mosaic skin. *Nature*, *619*(7968), 167–175. <https://doi.org/10.1038/s41586-023-06198-y>
- Gao, L., Lei, X.-F., Miyauchi, A., Noguchi, M., Omoto, T., Haraguchi, S., Miyazaki, T., Miyazaki, A., & Kim-Kaneyama, J. (2020). Hic-5 is required for activation of

- pancreatic stellate cells and development of pancreatic fibrosis in chronic pancreatitis. *Scientific Reports*, 10(1), 19105. <https://doi.org/10.1038/s41598-020-76095-1>
- Gao, X., Murphy, M. M., Peyer, J. G., Ni, Y., Yang, M., Zhang, Y., Guo, J., Kara, N., Embree, C., Tasdogan, A., Ubellacker, J. M., Crane, G. M., Fang, S., Zhao, Z., Shen, B., & Morrison, S. J. (2023). Leptin receptor+ cells promote bone marrow innervation and regeneration by synthesizing nerve growth factor. *Nature Cell Biology*, 1–12. <https://doi.org/10.1038/s41556-023-01284-9>
- Garcia, P. E., Adoumie, M., Kim, E. C., Zhang, Y., Scales, M. K., El-Tawil, Y. S., Shaikh, A. Z., Wen, H.-J., Bednar, F., Allen, B. L., Wellik, D. M., Crawford, H. C., & Pasca di Magliano, M. (2020). Differential Contribution of Pancreatic Fibroblast Subsets to the Pancreatic Cancer Stroma. *Cellular and Molecular Gastroenterology and Hepatology*, 10(3), 581–599. <https://doi.org/10.1016/j.jcmgh.2020.05.004>
- Gaskill, C. E., Maxwell, J., Ikoma, N., Kim, M. P., Tzeng, C.-W., Lee, J. E., & Katz, M. H. G. (2021). History of preoperative therapy for pancreatic cancer and the MD Anderson experience. *Journal of Surgical Oncology*, 123(6), 1414–1422. <https://doi.org/10.1002/jso.26394>
- Geerts, A. (2001). History, Heterogeneity, Developmental Biology, and Functions of Quiescent Hepatic Stellate Cells. *Seminars in Liver Disease*, 21(3), 311–336. <https://doi.org/10.1055/s-2001-17550>
- Geerts, A., Vrijsen, R., Rauterberg, J., Burt, A., Schellinck, P., & Wisse, E. (1989). In vitro differentiation of fat-storing cells parallels marked increase of collagen synthesis and secretion. *Journal of Hepatology*, 9(1), 59–68. [https://doi.org/10.1016/0168-8278\(89\)90076-7](https://doi.org/10.1016/0168-8278(89)90076-7)
- Geissler, E. N., Ryan, M. A., & Housman, D. E. (1988). The dominant-white spotting (W) locus of the mouse encodes the c-kit proto-oncogene. *Cell*, 55(1), 185–192. [https://doi.org/10.1016/0092-8674\(88\)90020-7](https://doi.org/10.1016/0092-8674(88)90020-7)
- Gharbia, F. Z., Abouhashem, A. S., Moqidem, Y. A., Elbaz, A. A., Abdellatif, A., Singh, K., Sen, C. K., & Azzazy, H. M. E. (2023). Adult skin fibroblast state change in murine wound healing. *Scientific Reports*, 13(1), 886. <https://doi.org/10.1038/s41598-022-27152-4>
- Gilmour, J., Assi, S. A., Jaegle, U., Kulu, D., van de Werken, H., Clarke, D., Westhead, D. R., Philipsen, S., & Bonifer, C. (2014). A crucial role for the ubiquitously expressed transcription factor Sp1 at early stages of hematopoietic specification.

Development (Cambridge, England), 141(12), 2391–2401.

<https://doi.org/10.1242/dev.106054>

- Glaubitz, J., Wilden, A., Golchert, J., Homuth, G., Völker, U., Bröker, B. M., Thiele, T., Lerch, M. M., Mayerle, J., Aghdassi, A. A., Weiss, F. U., & Sendler, M. (2022). In mouse chronic pancreatitis CD25+FOXP3+ regulatory T cells control pancreatic fibrosis by suppression of the type 2 immune response. *Nature Communications*, 13(1), 4502. <https://doi.org/10.1038/s41467-022-32195-2>
- Goltsev, Y., Samusik, N., Kennedy-Darling, J., Bhate, S., Hale, M., Vazquez, G., Black, S., & Nolan, G. P. (2018). Deep Profiling of Mouse Splenic Architecture with CODEX Multiplexed Imaging. *Cell*, 174(4), 968-981.e15. <https://doi.org/10.1016/j.cell.2018.07.010>
- Gong, J., Zhang, G., Tian, F., & Wang, Y. (2012). Islet-derived stem cells from adult rats participate in the repair of islet damage. *Journal of Molecular Histology*, 43(6), 745–750. <https://doi.org/10.1007/s10735-012-9447-6>
- Goto, N., Westcott, P. M. K., Goto, S., Imada, S., Taylor, M. S., Eng, G., Braverman, J., Deshpande, V., Jacks, T., Agudo, J., & Yilmaz, Ö. H. (2024). SOX17 enables immune evasion of early colorectal adenomas and cancers. *Nature*, 627(8004), 636–645. <https://doi.org/10.1038/s41586-024-07135-3>
- Grant, R. C., Selander, I., Connor, A. A., Selvarajah, S., Borgida, A., Briollais, L., Petersen, G. M., Lerner-Ellis, J., Holter, S., & Gallinger, S. (2015). Prevalence of Germline Mutations in Cancer Predisposition Genes in Patients With Pancreatic Cancer. *Gastroenterology*, 148(3), 556–564. <https://doi.org/10.1053/j.gastro.2014.11.042>
- Greenbaum, A., Hsu, Y.-M. S., Day, R. B., Schuettpeiz, L. G., Christopher, M. J., Borgerding, J. N., Nagasawa, T., & Link, D. C. (2013). CXCL12 in early mesenchymal progenitors is required for haematopoietic stem-cell maintenance. *Nature*, 495(7440), 227–230. <https://doi.org/10.1038/nature11926>
- Greten, F. R., Wagner, M., Weber, C. K., Zechner, U., Adler, G., & Schmid, R. M. (2001). TGF α transgenic mice: A model of pancreatic cancer development. *Pancreatology*, 1(4), 363–368. <https://doi.org/10.1159/000055835>
- Guedj, M., Marisa, L., de Reynies, A., Orsetti, B., Schiappa, R., Bibeau, F., MacGrogan, G., Lerebours, F., Finetti, P., Longy, M., Bertheau, P., Bertrand, F., Bonnet, F., Martin, A. L., Feugeas, J. P., Bièche, I., Lehmann-Che, J., Lidereau, R.,

- Birnbaum, D., ... Theillet, C. (2012). A refined molecular taxonomy of breast cancer. *Oncogene*, *31*(9), 1196–1206. <https://doi.org/10.1038/onc.2011.301>
- Gupta, P. B., Pastushenko, I., Skibinski, A., Blanpain, C., & Kuperwasser, C. (2019). Phenotypic Plasticity: Driver of Cancer Initiation, Progression, and Therapy Resistance. *Cell Stem Cell*, *24*(1), 65–78. <https://doi.org/10.1016/j.stem.2018.11.011>
- Haber, P. S., Keogh, G. W., Apte, M. V., Moran, C. S., Stewart, N. L., Crawford, D. H. G., Pirola, R. C., McCaughan, G. W., Ramm, G. A., & Wilson, J. S. (1999). Activation of Pancreatic Stellate Cells in Human and Experimental Pancreatic Fibrosis. *The American Journal of Pathology*, *155*(4), 1087–1095.
- Haberman, E. R., Sarker, G., Arús, B. A., Ziegler, K. A., Meunier, S., Martínez-Sánchez, N., Freiberggerová, E., Yilmaz-Özcan, S., Fernández-González, I., Zentai, C., O'Brien, C. J. O., Grainger, D. E., Sidarta-Oliveira, D., Chakarov, S., Raimondi, A., Iannaccone, M., Engelhardt, S., López, M., Ginhoux, F., & Domingos, A. I. (2024). Immunomodulatory leptin receptor+ sympathetic perineurial barrier cells protect against obesity by facilitating brown adipose tissue thermogenesis. *Immunity*, *57*(1), 141-152.e5. <https://doi.org/10.1016/j.immuni.2023.11.006>
- Han, C., Liu, T., & Yin, R. (2020). Biomarkers for cancer-associated fibroblasts. *Biomarker Research*, *8*(1), 64. <https://doi.org/10.1186/s40364-020-00245-w>
- Han, Z.-B., Ren, H., Zhao, H., Chi, Y., Chen, K., Zhou, B., Liu, Y., Zhang, L., Xu, B., Liu, B., Yang, R., & Han, Z.-C. (2008). Hypoxia-inducible factor (HIF)-1 α directly enhances the transcriptional activity of stem cell factor (SCF) in response to hypoxia and epidermal growth factor (EGF). *Carcinogenesis*, *29*(10), 1853–1861. <https://doi.org/10.1093/carcin/bgn066>
- Hao, Y., Hao, S., Andersen-Nissen, E., Mauck, W. M., Zheng, S., Butler, A., Lee, M. J., Wilk, A. J., Darby, C., Zager, M., Hoffman, P., Stoeckius, M., Papalexi, E., Mimitou, E. P., Jain, J., Srivastava, A., Stuart, T., Fleming, L. M., Yeung, B., ... Satija, R. (2021). Integrated analysis of multimodal single-cell data. *Cell*, *184*(13), 3573-3587.e29. <https://doi.org/10.1016/j.cell.2021.04.048>
- Heinrich, M. C., Griffith, D. J., Druker, B. J., Wait, C. L., Ott, K. A., & Zigler, A. J. (2000). Inhibition of c-kit receptor tyrosine kinase activity by STI 571, a selective tyrosine kinase inhibitor. *Blood*, *96*(3), 925–932.
- Helms, E. J., Berry, M. W., Chaw, R. C., DuFort, C. C., Sun, D., Onate, M. K., Oon, C., Bhattacharyya, S., Sanford-Crane, H., Horton, W., Finan, J. M., Sattler, A.,

- Makar, R., Dawson, D. W., Xia, Z., Hingorani, S. R., & Sherman, M. H. (2022). Mesenchymal Lineage Heterogeneity Underlies Nonredundant Functions of Pancreatic Cancer–Associated Fibroblasts. *Cancer Discovery*, *12*(2), 484–501. <https://doi.org/10.1158/2159-8290.CD-21-0601>
- Hill, W., Lim, E. L., Weeden, C. E., Lee, C., Augustine, M., Chen, K., Kuan, F.-C., Marongiu, F., Evans, E. J., Moore, D. A., Rodrigues, F. S., Pich, O., Bakker, B., Cha, H., Myers, R., van Maldegem, F., Boumelha, J., Veeriah, S., Rowan, A., ... Swanton, C. (2023). Lung adenocarcinoma promotion by air pollutants. *Nature*, *616*(7955), 159–167. <https://doi.org/10.1038/s41586-023-05874-3>
- Hoff, D. D. V., Ervin, T., Arena, F. P., Chiorean, E. G., Infante, J., Moore, M., Seay, T., Tjulandin, S. A., Ma, W. W., Saleh, M. N., Harris, M., Reni, M., Dowden, S., Laheru, D., Bahary, N., Ramanathan, R. K., Tabernero, J., Hidalgo, M., Goldstein, D., ... Renschler, M. F. (2013). Increased Survival in Pancreatic Cancer with nab-Paclitaxel plus Gemcitabine. *New England Journal of Medicine*, *369*(18), 1691–1703. <https://doi.org/10.1056/NEJMoa1304369>
- Hu, C.-J., Wang, L.-Y., Chodosh, L. A., Keith, B., & Simon, M. C. (2003). Differential Roles of Hypoxia-Inducible Factor 1 α (HIF-1 α) and HIF-2 α in Hypoxic Gene Regulation. *Molecular and Cellular Biology*, *23*(24), 9361–9374. <https://doi.org/10.1128/MCB.23.24.9361-9374.2003>
- Hu, M., Yao, J., Carroll, D. K., Weremowicz, S., Chen, H., Carrasco, D., Richardson, A., Violette, S., Nikolskaya, T., Nikolsky, Y., Bauerlein, E. L., Hahn, W. C., Gelman, R. S., Allred, C., Bissell, M. J., Schnitt, S., & Polyak, K. (2008). Regulation of In Situ to Invasive Breast Carcinoma Transition. *Cancer Cell*, *13*(5), 394–406. <https://doi.org/10.1016/j.ccr.2008.03.007>
- Hu, Z. I., Shia, J., Stadler, Z. K., Varghese, A. M., Capanu, M., Salo-Mullen, E., Lowery, M. A., Diaz, L. A., Mandelker, D., Yu, K. H., Zervoudakis, A., Kelsen, D. P., Iacobuzio-Donahue, C. A., Klimstra, D. S., Saltz, L. B., Sahin, I. H., & O'Reilly, E. M. (2018). Evaluating Mismatch Repair Deficiency in Pancreatic Adenocarcinoma: Challenges and Recommendations. *Clinical Cancer Research : An Official Journal of the American Association for Cancer Research*, *24*(6), 1326–1336. <https://doi.org/10.1158/1078-0432.CCR-17-3099>
- Iacobuzio-Donahue, C. A., Velculescu, V. E., Wolfgang, C. L., & Hruban, R. H. (2012). The Genetic Basis of Pancreas Cancer Development and Progression: Insights From Whole-Exome and Whole-Genome Sequencing. *Clinical Cancer Research :*

- An Official Journal of the American Association for Cancer Research*, 18(16), 4257–4265. <https://doi.org/10.1158/1078-0432.CCR-12-0315>
- Jakobsen, S. T., Jensen, R. A. M., Madsen, M. S., Ravnsborg, T., Vaagenso, C. S., Siersbæk, M. S., Einarsson, H., Andersson, R., Jensen, O. N., & Siersbæk, R. (2024). MYC activity at enhancers drives prognostic transcriptional programs through an epigenetic switch. *Nature Genetics*, 56(4), 663–674. <https://doi.org/10.1038/s41588-024-01676-z>
- Jamieson, J. D. (1975). Prospectives for cell and organ culture systems in the study of pancreatic carcinoma. *Journal of Surgical Oncology*, 7(2), 139–141. <https://doi.org/10.1002/jso.2930070209>
- Jarido, V., Kennedy, L., Hargrove, L., Demieville, J., Thomson, J., Stephenson, K., & Francis, H. (2017). The emerging role of mast cells in liver disease. *American Journal of Physiology-Gastrointestinal and Liver Physiology*, 313(2), G89–G101. <https://doi.org/10.1152/ajpgi.00333.2016>
- Jaster, R. (2004). Molecular regulation of pancreatic stellate cell function. *Molecular Cancer*, 3(1), 26. <https://doi.org/10.1186/1476-4598-3-26>
- Johnson, C., Huynh, V., Hargrove, L., Kennedy, L., Graf-Eaton, A., Owens, J., Trzeciakowski, J. P., Hodges, K., DeMorrow, S., Han, Y., Wong, L., Alpini, G., & Francis, H. (2016). Inhibition of Mast Cell-Derived Histamine Decreases Human Cholangiocarcinoma Growth and Differentiation via c-Kit/Stem Cell Factor–Dependent Signaling. *The American Journal of Pathology*, 186(1), 123–133. <https://doi.org/10.1016/j.ajpath.2015.09.016>
- Kambayashi, T., & Laufer, T. M. (2014). Atypical MHC class II-expressing antigen-presenting cells: Can anything replace a dendritic cell? *Nature Reviews Immunology*, 14(11), 719–730. <https://doi.org/10.1038/nri3754>
- Kanda, M., Matthaei, H., Wu, J., Hong, S., Yu, J., Borges, M., Hruban, R. H., Maitra, A., Kinzler, K., Vogelstein, B., & Goggins, M. (2012). Presence of Somatic Mutations in Most Early-Stage Pancreatic Intraepithelial Neoplasia. *Gastroenterology*, 142(4), 730–733.e9. <https://doi.org/10.1053/j.gastro.2011.12.042>
- Kataru, R. P., Jung, K., Jang, C., Yang, H., Schwendener, R. A., Baik, J. E., Han, S. H., Alitalo, K., & Koh, G. Y. (2009). Critical role of CD11b+ macrophages and VEGF in inflammatory lymphangiogenesis, antigen clearance, and inflammation resolution. *Blood*, 113(22), 5650–5659. <https://doi.org/10.1182/blood-2008-09-176776>

- Kaukonen, R., Mai, A., Georgiadou, M., Saari, M., De Franceschi, N., Betz, T., Sihto, H., Ventelä, S., Elo, L., Jokitalo, E., Westermarck, J., Kellokumpu-Lehtinen, P.-L., Joensuu, H., Grenman, R., & Ivaska, J. (2016). Normal stroma suppresses cancer cell proliferation via mechanosensitive regulation of JMJD1a-mediated transcription. *Nature Communications*, *7*(1), 12237.
<https://doi.org/10.1038/ncomms12237>
- Khorana, A. A., McKernin, S. E., Berlin, J., Hong, T. S., Maitra, A., Moravek, C., Mumber, M., Schulick, R., Zeh, H. J., & Katz, M. H. G. (2019). Potentially Curable Pancreatic Adenocarcinoma: ASCO Clinical Practice Guideline Update. *Journal of Clinical Oncology*. <https://doi.org/10.1200/JCO.19.00946>
- Kinnersley, B., Sud, A., Everall, A., Cornish, A. J., Chubb, D., Culliford, R., Gruber, A. J., Lärkeryd, A., Mitsopoulos, C., Wedge, D., & Houlston, R. (2024). Analysis of 10,478 cancer genomes identifies candidate driver genes and opportunities for precision oncology. *Nature Genetics*, *56*(9), 1868–1877.
<https://doi.org/10.1038/s41588-024-01785-9>
- Kiselev, V. Y., Andrews, T. S., & Hemberg, M. (2019). Challenges in unsupervised clustering of single-cell RNA-seq data. *Nature Reviews Genetics*, *20*(5), 273–282. <https://doi.org/10.1038/s41576-018-0088-9>
- Klatte, D. C. F., Boekestijn, B., Onnekink, A. M., Dekker, F. W., Geest, L. G. van der, Wasser, M. N. J. M., Feshtali, S., Mieog, J. S. D., Luelmo, S. A. C., Morreau, H., Potjer, T. P., Inderson, A., Boonstra, J. J., Vasen, H. F. A., Hooft, J. E. van, Bonsing, B. A., & Leerdam, M. E. van. (2023). Surveillance for Pancreatic Cancer in High-Risk Individuals Leads to Improved Outcomes: A Propensity Score-Matched Analysis. *Gastroenterology*, *164*(7), 1223-1231.e4.
<https://doi.org/10.1053/j.gastro.2023.02.032>
- Ko, A. H., LoConte, N., Tempero, M. A., Walker, E. J., Kate Kelley, R., Lewis, S., Chang, W.-C., Kantoff, E., Vannier, M. W., Catenacci, D. V., Venook, A. P., & Kindler, H. L. (2016). A Phase I Study of FOLFIRINOX Plus IPI-926, a Hedgehog Pathway Inhibitor, for Advanced Pancreatic Adenocarcinoma. *Pancreas*, *45*(3), 370.
<https://doi.org/10.1097/MPA.0000000000000458>
- Kobi, D., Steunou, A.-L., Dembélé, D., Legras, S., Larue, L., Nieto, L., & Davidson, I. (2010). Genome-wide analysis of POU3F2/BRN2 promoter occupancy in human melanoma cells reveals Kitl as a novel regulated target gene. *Pigment Cell &*

- Melanoma Research*, 23(3), 404–418. <https://doi.org/10.1111/j.1755-148X.2010.00697.x>
- Korc, M. (1998). Role of Growth Factors in Pancreatic Cancer. *Surgical Oncology Clinics*, 7(1), 25–41. [https://doi.org/10.1016/S1055-3207\(18\)30283-7](https://doi.org/10.1016/S1055-3207(18)30283-7)
- Korman, A. J., Garrett-Thomson, S. C., & Lonberg, N. (2022). The foundations of immune checkpoint blockade and the ipilimumab approval decennial. *Nature Reviews Drug Discovery*, 21(7), 509–528. <https://doi.org/10.1038/s41573-021-00345-8>
- Korsunsky, I., Millard, N., Fan, J., Slowikowski, K., Zhang, F., Wei, K., Baglaenko, Y., Brenner, M., Loh, P., & Raychaudhuri, S. (2019). Fast, sensitive and accurate integration of single-cell data with Harmony. *Nature Methods*, 16(12), 1289–1296. <https://doi.org/10.1038/s41592-019-0619-0>
- Kumar, V., Cheng, P., Condamine, T., Mony, S., Languino, L., McCaffrey, J., Hockstein, N., Guarino, M., Masters, G., Penman, E., Denstman, F., Xu, G., Altieri, D., Du, H., Yan, C., & Gabilovich, D. I. (2016). CD45 phosphatase regulates the fate of myeloid cells in tumor microenvironment by inhibiting STAT3 activity. *The Journal of Immunology*, 196(1_Supplement), 211.4. <https://doi.org/10.4049/jimmunol.196.Supp.211.4>
- Kuperwasser, C., Chavarria, T., Wu, M., Magrane, G., Gray, J. W., Carey, L., Richardson, A., & Weinberg, R. A. (2004). Reconstruction of functionally normal and malignant human breast tissues in mice. *Proceedings of the National Academy of Sciences*, 101(14), 4966–4971. <https://doi.org/10.1073/pnas.0401064101>
- Kupffer, C. (1876). Ueber Sternzellen der Leber. *Archiv für mikroskopische Anatomie*, 12(1), 353–358. <https://doi.org/10.1007/BF02933897>
- Larsen, B. M., Hrycaj, S. M., Newman, M., Li, Y., & Wellik, D. M. (2015). Mesenchymal Hox6 function is required for mouse pancreatic endocrine cell differentiation. *Development*, 142(22), 3859–3868. <https://doi.org/10.1242/dev.126888>
- Lee, Y., Leslie, J., Yang, Y., & Ding, L. (2020). Hepatic stellate and endothelial cells maintain hematopoietic stem cells in the developing liver. *Journal of Experimental Medicine*, 218(3), e20200882. <https://doi.org/10.1084/jem.20200882>
- Lennartsson, J., & Rönstrand, L. (2012). Stem Cell Factor Receptor/c-Kit: From Basic Science to Clinical Implications. *Physiological Reviews*, 92(4), 1619–1649. <https://doi.org/10.1152/physrev.00046.2011>

- Leppkes, M., Maueröder, C., Hirth, S., Nowecki, S., Günther, C., Billmeier, U., Paulus, S., Biermann, M., Munoz, L. E., Hoffmann, M., Wildner, D., Croxford, A. L., Waisman, A., Mowen, K., Jenne, D. E., Krenn, V., Mayerle, J., Lerch, M. M., Schett, G., ... Becker, C. (2016). Externalized decondensed neutrophil chromatin occludes pancreatic ducts and drives pancreatitis. *Nature Communications*, 7(1), 10973. <https://doi.org/10.1038/ncomms10973>
- Li, J., Goodyer, C. G., Fellows, F., & Wang, R. (2006). Stem cell factor/c-Kit interactions regulate human islet-epithelial cluster proliferation and differentiation. *The International Journal of Biochemistry & Cell Biology*, 38(5), 961–972. <https://doi.org/10.1016/j.biocel.2005.08.014>
- Liggitt, D., & Dintzis, S. M. (2018). 14—Pancreas. In P. M. Treuting, S. M. Dintzis, & K. S. Montine (Eds.), *Comparative Anatomy and Histology (Second Edition)* (pp. 241–250). Academic Press. <https://doi.org/10.1016/B978-0-12-802900-8.00014-2>
- Linder, S., Castañeros-Velez, E., von Rosen, A., & Biberfeld, P. (2001). Immunohistochemical expression of extracellular matrix proteins and adhesion molecules in pancreatic carcinoma. *Hepato-Gastroenterology*, 48(41), 1321–1327.
- Liu, Y., Guerrero-Juarez, C. F., Xiao, F., Shettigar, N. U., Ramos, R., Kuan, C.-H., Lin, Y.-C., de Jesus Martinez Lomeli, L., Park, J. M., Oh, J. W., Liu, R., Lin, S.-J., Tartaglia, M., Yang, R.-B., Yu, Z., Nie, Q., Li, J., & Plikus, M. V. (2022). Hedgehog signaling reprograms hair follicle niche fibroblasts to a hyper-activated state. *Developmental Cell*, 57(14), 1758-1775.e7. <https://doi.org/10.1016/j.devcel.2022.06.005>
- Mahadevan, K. K., LeBleu, V. S., Ramirez, E. V., Chen, Y., Li, B., Sockwell, A. M., Gagea, M., Sugimoto, H., Sthanam, L. K., Tampe, D., Zeisberg, M., Ying, H., Jain, A. K., DePinho, R. A., Maitra, A., McAndrews, K. M., & Kalluri, R. (2023). Elimination of oncogenic KRAS in genetic mouse models eradicates pancreatic cancer by inducing FAS-dependent apoptosis by CD8+ T cells. *Developmental Cell*, 58(17), 1562-1577.e8. <https://doi.org/10.1016/j.devcel.2023.07.025>
- Mahadevan, K. K., McAndrews, K. M., LeBleu, V. S., Yang, S., Lyu, H., Li, B., Sockwell, A. M., Kirtley, M. L., Morse, S. J., Diaz, B. A. M., Kim, M. P., Feng, N., Lopez, A. M., Guerrero, P. A., Paradiso, F., Sugimoto, H., Arian, K. A., Ying, H., Barekattain, Y., ... Kalluri, R. (2023). KRASG12D inhibition reprograms the microenvironment of early and advanced pancreatic cancer to promote FAS-mediated killing by

- CD8+ T cells. *Cancer Cell*, 41(9), 1606-1620.e8.
<https://doi.org/10.1016/j.ccell.2023.07.002>
- Malheiro, F., Ângelo-Dias, M., Lopes, T., Martins, C. G., & Borrego, L. M. (2024). Cytokine Dynamics in Acute Pancreatitis: The Quest for Biomarkers from Acute Disease to Disease Resolution. *Journal of Clinical Medicine*, 13(8), Article 8.
<https://doi.org/10.3390/jcm13082287>
- Manohar, M., Verma, A. K., Venkateshaiah, S. U., & Mishra, A. (2018). Role of eosinophils in the initiation and progression of pancreatitis pathogenesis. *American Journal of Physiology-Gastrointestinal and Liver Physiology*, 314(2), G211–G222. <https://doi.org/10.1152/ajpgi.00210.2017>
- Margreet Leeuw, A. D., Mccarthy, S. P., Geerts, A., & Knook, D. L. (1984). Purified Rat Liver Fat-Storing Cells in Culture Divide and Contain Collagen. *Hepatology*, 4(3), 392–403. <https://doi.org/10.1002/hep.1840040307>
- Martin, F. H., Suggs, S. V., Langley, K. E., Lu, H. S., Ting, J., Okino, K. H., Morris, C. F., McNiece, I. K., Jacobsen, F. W., & Mendiaz, E. A. (1990). Primary structure and functional expression of rat and human stem cell factor DNAs. *Cell*, 63(1), 203–211. [https://doi.org/10.1016/0092-8674\(90\)90301-t](https://doi.org/10.1016/0092-8674(90)90301-t)
- Masamune, A., & Shimosegawa, T. (2009). Signal transduction in pancreatic stellate cells. *Journal of Gastroenterology*, 44(4), 249–260.
<https://doi.org/10.1007/s00535-009-0013-2>
- Masson, K., Heiss, E., Band, H., & Rönstrand, L. (2006). Direct binding of Cbl to Tyr568 and Tyr936 of the stem cell factor receptor/c-Kit is required for ligand-induced ubiquitination, internalization and degradation. *Biochemical Journal*, 399(1), 59–67. <https://doi.org/10.1042/BJ20060464>
- Mathew, E., Collins, M. A., Fernandez-Barrena, M. G., Holtz, A. M., Yan, W., Hogan, J. O., Tata, Z., Allen, B. L., Fernandez-Zapico, M. E., & Magliano, M. P. di. (2014). The Transcription Factor GLI1 Modulates the Inflammatory Response during Pancreatic Tissue Remodeling *. *Journal of Biological Chemistry*, 289(40), 27727–27743. <https://doi.org/10.1074/jbc.M114.556563>
- Matos, M. E., Schnier, G. S., Beecher, M. S., Ashman, L. K., William, D. E., & Caligiuri, M. A. (1993). Expression of a functional c-kit receptor on a subset of natural killer cells. *Journal of Experimental Medicine*, 178(3), 1079–1084.
<https://doi.org/10.1084/jem.178.3.1079>

- Matsui, J., Wakabayashi, T., Asada, M., Yoshimatsu, K., & Okada, M. (2004). Stem Cell Factor/c-kit Signaling Promotes the Survival, Migration, and Capillary Tube Formation of Human Umbilical Vein Endothelial Cells*. *Journal of Biological Chemistry*, 279(18), 18600–18607. <https://doi.org/10.1074/jbc.M311643200>
- Matsusaka, S., Tsujimura, T., Toyosaka, A., Nakasho, K., Sugihara, A., Okamoto, E., Uematsu, K., & Terada, N. (1999). Role of C-Kit Receptor Tyrosine Kinase in Development of Oval Cells in the Rat 2-Acetylaminofluorene/Partial Hepatectomy Model. *Hepatology*, 29(3), 670. <https://doi.org/10.1002/hep.510290304>
- Mazzoldi, E. L., Pavan, S., Pilotto, G., Leone, K., Pagotto, A., Frezzini, S., Nicoletto, M. O., Amadori, A., & Pastò, A. (2019). A juxtacrine/paracrine loop between C-Kit and stem cell factor promotes cancer stem cell survival in epithelial ovarian cancer. *Cell Death & Disease*, 10(6), Article 6. <https://doi.org/10.1038/s41419-019-1656-4>
- Mederacke, I., Hsu, C. C., Troeger, J. S., Huebener, P., Mu, X., Dapito, D. H., Pradere, J.-P., & Schwabe, R. F. (2013). Fate tracing reveals hepatic stellate cells as dominant contributors to liver fibrosis independent of its aetiology. *Nature Communications*, 4(1), 2823. <https://doi.org/10.1038/ncomms3823>
- Mews, P., Phillips, P., Fahmy, R., Korsten, M., Pirola, R., Wilson, J., & Apte, M. (2002). Pancreatic stellate cells respond to inflammatory cytokines: Potential role in chronic pancreatitis. *Gut*, 50(4), 535–541.
- Micke, P., & Tman, A. (2004). Tumour-stroma interaction: Cancer-associated fibroblasts as novel targets in anti-cancer therapy? *Lung Cancer*, 45, S163–S175. <https://doi.org/10.1016/j.lungcan.2004.07.977>
- Mikkola, H. K. A., & Orkin, S. H. (2006). The journey of developing hematopoietic stem cells. *Development*, 133(19), 3733–3744. <https://doi.org/10.1242/dev.02568>
- Moore, R., Carlson, S., & Madara, J. L. (1989). Villus contraction aids repair of intestinal epithelium after injury. *American Journal of Physiology-Gastrointestinal and Liver Physiology*, 257(2), G274–G283. <https://doi.org/10.1152/ajpgi.1989.257.2.G274>
- Morris, J. P., Wang, S. C., & Hebrok, M. (2010). KRAS, Hedgehog, Wnt and the twisted developmental biology of pancreatic ductal adenocarcinoma. *Nature Reviews Cancer*, 10(10), 683–695. <https://doi.org/10.1038/nrc2899>

- Mueller, M. M., & Fusenig, N. E. (2004). Friends or foes—Bipolar effects of the tumour stroma in cancer. *Nature Reviews Cancer*, *4*(11), 839–849.
<https://doi.org/10.1038/nrc1477>
- O'Connor, C. A., Harrold, E., Lin, Y.-T., Walch, H. S., Gazzo, A., Kane, S. R., Keane, F., Schoenfeld, J. D., Moss, D., Suehnholz, S. P., Chakravarty, D., Balogun, F., Varghese, A. M., Yu, K. H., Kelsen, D. P., Latham, A., Weigelt, B., Park, W., Stadler, Z. K., & O'Reilly, E. M. (2024). Somatic mismatch repair deficiency in pancreas cancer (PC): Immune checkpoint blockade (ICB) outcomes and exploratory genomic analyses. *Journal of Clinical Oncology*, *42*(16_suppl), 4144–4144. https://doi.org/10.1200/JCO.2024.42.16_suppl.4144
- Ogawa, M., LaRue, A. C., & Drake, C. J. (2006). Hematopoietic origin of fibroblasts/myofibroblasts: Its pathophysiologic implications. *Blood*, *108*(9), 2893–2896. <https://doi.org/10.1182/blood-2006-04-016600>
- Öhlund, D., Franklin, O., Lundberg, E., Lundin, C., & Sund, M. (2013). Type IV collagen stimulates pancreatic cancer cell proliferation, migration, and inhibits apoptosis through an autocrine loop. *BMC Cancer*, *13*(1), 154.
<https://doi.org/10.1186/1471-2407-13-154>
- Öhlund, D., Handly-Santana, A., Biffi, G., Elyada, E., Almeida, A. S., Ponz-Sarvisé, M., Corbo, V., Oni, T. E., Hearn, S. A., Lee, E. J., Chio, I. I. C., Hwang, C.-I., Tiriác, H., Baker, L. A., Engle, D. D., Feig, C., Kultti, A., Egeblad, M., Fearon, D. T., ... Tuveson, D. A. (2017). Distinct populations of inflammatory fibroblasts and myofibroblasts in pancreatic cancer. *Journal of Experimental Medicine*, *214*(3), 579–596. <https://doi.org/10.1084/jem.20162024>
- Olivares, O., Mayers, J. R., Gouirand, V., Torrence, M. E., Gicquel, T., Borge, L., Lac, S., Roques, J., Lavaut, M.-N., Berthezène, P., Rubis, M., Secq, V., Garcia, S., Moutardier, V., Lombardo, D., Iovanna, J. L., Tomasini, R., Guillaumond, F., Vander Heiden, M. G., & Vasseur, S. (2017). Collagen-derived proline promotes pancreatic ductal adenocarcinoma cell survival under nutrient limited conditions. *Nature Communications*, *8*(1), 16031. <https://doi.org/10.1038/ncomms16031>
- Ooi, L. P. J., Crawford, D. H. G., Gotley, D. C., Clouston, A. D., Strong, R. W., Gobé, G. C., Halliday, J. W., Bridle, K. R., & Ramm, G. A. (1997). Evidence that “myofibroblast-like” cells are the cellular source of capsular collagen in hepatocellular carcinoma. *Journal of Hepatology*, *26*(4), 798–807.
[https://doi.org/10.1016/S0168-8278\(97\)80245-0](https://doi.org/10.1016/S0168-8278(97)80245-0)

- Özdemir, B. C., Pentcheva-Hoang, T., Carstens, J. L., Zheng, X., Wu, C.-C., Simpson, T. R., Laklai, H., Sugimoto, H., Kahlert, C., Novitskiy, S. V., De Jesus-Acosta, A., Sharma, P., Heidari, P., Mahmood, U., Chin, L., Moses, H. L., Weaver, V. M., Maitra, A., Allison, J. P., ... Kalluri, R. (2014). Depletion of Carcinoma-Associated Fibroblasts and Fibrosis Induces Immunosuppression and Accelerates Pancreas Cancer with Reduced Survival. *Cancer Cell*, 25(6), 719–734.
<https://doi.org/10.1016/j.ccr.2014.04.005>
- Pannala, R., Basu, A., Petersen, G. M., & Chari, S. T. (2009). New-onset diabetes: A potential clue to the early diagnosis of pancreatic cancer. *The Lancet Oncology*, 10(1), 88–95. [https://doi.org/10.1016/S1470-2045\(08\)70337-1](https://doi.org/10.1016/S1470-2045(08)70337-1)
- Pedersen, M., Löfstedt, T., Sun, J., Holmquist-Mengelbier, L., Pålman, S., & Rönstrand, L. (2008). Stem cell factor induces HIF-1alpha at normoxia in hematopoietic cells. *Biochemical and Biophysical Research Communications*, 377(1), 98–103. <https://doi.org/10.1016/j.bbrc.2008.09.102>
- Philo, J. S., Wen, J., Wypych, J., Schwartz, M. G., Mendiaz, E. A., & Langley, K. E. (1996). Human Stem Cell Factor Dimer Forms a Complex with Two Molecules of the Extracellular Domain of Its Receptor, Kit (*). *Journal of Biological Chemistry*, 271(12), 6895–6902. <https://doi.org/10.1074/jbc.271.12.6895>
- Pineda, C. M., Gonzalez, D. G., Matte-Martone, C., Boucher, J., Lathrop, E., Gallini, S., Fons, N. R., Xin, T., Tai, K., Marsh, E., Nguyen, D. X., Suozzi, K. C., Beronja, S., & Greco, V. (2019). Hair follicle regeneration suppresses Ras-driven oncogenic growth. *Journal of Cell Biology*, 218(10), 3212–3222.
<https://doi.org/10.1083/jcb.201907178>
- Pitot, H. C. (1993). The molecular biology of carcinogenesis. *Cancer*, 72(S3), 962–970.
[https://doi.org/10.1002/1097-0142\(19930801\)72:3+<962::AID-CNCR2820721303>3.0.CO;2-H](https://doi.org/10.1002/1097-0142(19930801)72:3+<962::AID-CNCR2820721303>3.0.CO;2-H)
- Plikus, M. V., Wang, X., Sinha, S., Forte, E., Thompson, S. M., Herzog, E. L., Driskell, R. R., Rosenthal, N., Biernaskie, J., & Horsley, V. (2021). Fibroblasts: Origins, definitions, and functions in health and disease. *Cell*, 184(15), 3852–3872.
<https://doi.org/10.1016/j.cell.2021.06.024>
- Pour, P., Althoff, J., & Takahashi, M. (1977). Early lesions of pancreatic ductal carcinoma in the hamster model. *The American Journal of Pathology*, 88(2), 291–308.
- Prados, A., Onder, L., Cheng, H.-W., Mörbe, U., Lütge, M., Gil-Cruz, C., Perez-Shibayama, C., Koliaraki, V., Ludewig, B., & Kollias, G. (2021). Fibroblastic

- reticular cell lineage convergence in Peyer's patches governs intestinal immunity. *Nature Immunology*, 22(4), 510–519. <https://doi.org/10.1038/s41590-021-00894-5>
- Provenzano, P. P., Cuevas, C., Chang, A. E., Goel, V. K., Von Hoff, D. D., & Hingorani, S. R. (2012). Enzymatic Targeting of the Stroma Ablates Physical Barriers to Treatment of Pancreatic Ductal Adenocarcinoma. *Cancer Cell*, 21(3), 418–429. <https://doi.org/10.1016/j.ccr.2012.01.007>
- Pylayeva-Gupta, Y., Lee, K. E., Hajdu, C. H., Miller, G., & Bar-Sagi, D. (2012). Oncogenic Kras-Induced GM-CSF Production Promotes the Development of Pancreatic Neoplasia. *Cancer Cell*, 21(6), 836–847. <https://doi.org/10.1016/j.ccr.2012.04.024>
- Quail, D. F., & Joyce, J. A. (2013). Microenvironmental regulation of tumor progression and metastasis. *Nature Medicine*, 19(11), 1423–1437. <https://doi.org/10.1038/nm.3394>
- Rachdi, L., El Ghazi, L., Bernex, F., Panthier, J.-J., Czernichow, P., & Scharfmann, R. (2001). Expression of the Receptor Tyrosine Kinase KIT in Mature β -Cells and in the Pancreas in Development. *Diabetes*, 50(9), 2021–2028. <https://doi.org/10.2337/diabetes.50.9.2021>
- Racine-Samson, L., Rockey, D. C., & Bissell, D. M. (1997). The Role of $\alpha 1\beta 1$ Integrin in Wound Contraction: A QUANTITATIVE ANALYSIS OF LIVER MYOFIBROBLASTS IN VIVO AND IN PRIMARY CULTURE *. *Journal of Biological Chemistry*, 272(49), 30911–30917. <https://doi.org/10.1074/jbc.272.49.30911>
- Ray, P., Krishnamoorthy, N., Oriss, T. B., & Ray, A. (2010). Signaling of c-kit in dendritic cells influences adaptive immunity. *Annals of the New York Academy of Sciences*, 1183, 104–122. <https://doi.org/10.1111/j.1749-6632.2009.05122.x>
- Reber, L., Da Silva, C. A., & Frossard, N. (2006). Stem cell factor and its receptor c-Kit as targets for inflammatory diseases. *European Journal of Pharmacology*, 533(1), 327–340. <https://doi.org/10.1016/j.ejphar.2005.12.067>
- Rhim, A. D., Oberstein, P. E., Thomas, D. H., Mirek, E. T., Palermo, C. F., Sastra, S. A., Dekleva, E. N., Saunders, T., Becerra, C. P., Tattersall, I. W., Westphalen, C. B., Kitajewski, J., Fernandez-Barrena, M. G., Fernandez-Zapico, M. E., Iacobuzio-Donahue, C., Olive, K. P., & Stanger, B. Z. (2014). Stromal Elements Act to

- Restrain, Rather Than Support, Pancreatic Ductal Adenocarcinoma. *Cancer Cell*, 25(6), 735–747. <https://doi.org/10.1016/j.ccr.2014.04.021>
- Rosenthal, E., McCrory, A., Talbert, M., Young, G., Murphy-Ullrich, J., & Gladson, C. (2004). Elevated expression of TGF- β 1 in head and neck cancer-associated fibroblasts. *Molecular Carcinogenesis*, 40(2), 116–121. <https://doi.org/10.1002/mc.20024>
- Rozeveld, C. N., Johnson, K. M., Zhang, L., & Razidlo, G. L. (2020). KRAS Controls Pancreatic Cancer Cell Lipid Metabolism and Invasive Potential through the Lipase HSL. *Cancer Research*, 80(22), 4932–4945. <https://doi.org/10.1158/0008-5472.CAN-20-1255>
- Saisho, Y., Butler, A. e., Meier, J. j., Monchamp, T., Allen-Auerbach, M., Rizza, R. a., & Butler, P. c. (2007). Pancreas volumes in humans from birth to age one hundred taking into account sex, obesity, and presence of type-2 diabetes. *Clinical Anatomy*, 20(8), 933–942. <https://doi.org/10.1002/ca.20543>
- Salas-Escabillas, D. J., Hoffman, M. T., Brender, S. M., Moore, J. S., Wen, H.-J., Benitz, S., Davis, E. T., Long, D., Wombwell, A. M., Chianis, E. R. D., Allen-Petersen, B. L., Steele, N. G., Sears, R. C., Matsumoto, I., DelGiorno, K. E., & Crawford, H. C. (2024). Tuft cells transdifferentiate to neural-like progenitor cells in the progression of pancreatic cancer. *Developmental Cell*. <https://doi.org/10.1016/j.devcel.2024.12.003>
- Sarkar, R., Xu, Z., Perera, C. J., & Apte, M. V. (2023). Emerging role of pancreatic stellate cell-derived extracellular vesicles in pancreatic cancer. *Seminars in Cancer Biology*, 93, 114–122. <https://doi.org/10.1016/j.semcancer.2023.05.007>
- Sbierski-Kind, J., Mroz, N., & Molofsky, A. B. (2021). Perivascular stromal cells: Directors of tissue immune niches. *Immunological Reviews*, 302(1), 10–31. <https://doi.org/10.1111/imr.12984>
- Scarpa, A., Capelli, P., Mukai, K., Zamboni, G., Oda, T., Iacono, C., & Hirohashi, S. (1993). Pancreatic adenocarcinomas frequently show p53 gene mutations. *The American Journal of Pathology*, 142(5), 1534–1543.
- Schmitt-Gräff, A., Krüger, S., Bochard, F., Gabbiani, G., & Denk, H. (1991). Modulation of alpha smooth muscle actin and desmin expression in perisinusoidal cells of normal and diseased human livers. *The American Journal of Pathology*, 138(5), 1233–1242.

- Schneider, E., Schmid-Kotsas, A., Zhao, J., Weidenbach, H., Schmid, R. M., Menke, A., Adler, G., Waltenberger, J., Grünert, A., & Bachem, M. G. (2001). Identification of mediators stimulating proliferation and matrix synthesis of rat pancreatic stellate cells. *American Journal of Physiology-Cell Physiology*, *281*(2), C532–C543. <https://doi.org/10.1152/ajpcell.2001.281.2.C532>
- Schultz, G. S., Chin, G. A., Moldawer, L., & Diegelmann, R. F. (2011). Principles of Wound Healing. In R. Fitridge & M. Thompson (Eds.), *Mechanisms of Vascular Disease: A Reference Book for Vascular Specialists*. University of Adelaide Press. <http://www.ncbi.nlm.nih.gov/books/NBK534261/>
- Schwitalla, S., Fingerle, A. A., Cammareri, P., Nebelsiek, T., Göktuna, S. I., Ziegler, P. K., Canli, O., Heijmans, J., Huels, D. J., Moreaux, G., Rupec, R. A., Gerhard, M., Schmid, R., Barker, N., Clevers, H., Lang, R., Neumann, J., Kirchner, T., Taketo, M. M., ... Greten, F. R. (2013). Intestinal Tumorigenesis Initiated by Dedifferentiation and Acquisition of Stem-Cell-like Properties. *Cell*, *152*(1), 25–38. <https://doi.org/10.1016/j.cell.2012.12.012>
- Shan, H., Jiang, K., Zhao, M., Deng, W., Cao, W., Li, J., Li, K., She, C., Luo, W., Yao, J., Zhou, X., Zhang, D., & Cao, C. (2023). SCF/c-Kit-activated signaling and angiogenesis require Gai1 and Gai3. *International Journal of Biological Sciences*, *19*(6), 1910–1924. <https://doi.org/10.7150/ijbs.82855>
- Sherman, M. H. (2018). Stellate Cells in Tissue Repair, Inflammation, and Cancer. *Annual Review of Cell and Developmental Biology*, *34*(1), 333–355. <https://doi.org/10.1146/annurev-cellbio-100617-062855>
- Sherman, M. H., Yu, R. T., Engle, D. D., Ding, N., Atkins, A. R., Tiriach, H., Collisson, E. A., Connor, F., Van Dyke, T., Kozlov, S., Martin, P., Tseng, T. W., Dawson, D. W., Donahue, T. R., Masamune, A., Shimosegawa, T., Apte, M. V., Wilson, J. S., Ng, B., ... Evans, R. M. (2014). Vitamin D Receptor-Mediated Stromal Reprogramming Suppresses Pancreatitis and Enhances Pancreatic Cancer Therapy. *Cell*, *159*(1), 80–93. <https://doi.org/10.1016/j.cell.2014.08.007>
- Shiozawa, Y., Pedersen, E. A., Havens, A. M., Jung, Y., Mishra, A., Joseph, J., Kim, J. K., Patel, L. R., Ying, C., Ziegler, A. M., Pienta, M. J., Song, J., Wang, J., Loberg, R. D., Krebsbach, P. H., Pienta, K. J., & Taichman, R. S. (2011). Human prostate cancer metastases target the hematopoietic stem cell niche to establish footholds in mouse bone marrow. *The Journal of Clinical Investigation*, *121*(4), 1298–1312. <https://doi.org/10.1172/JCI43414>

- Simon-Assmann, P., Bouziges, F., Arnold, C., Haffen, K., & Kedinger, M. (1988). Epithelial-mesenchymal interactions in the production of basement membrane components in the gut. *Development*, *102*(2), 339–347. <https://doi.org/10.1242/dev.102.2.339>
- Simonetti, S., Seijas, A. B. B., Natalini, A., Vitale, S., Runci, D., Soriani, A., Di Virgilio, A., Aricò, E., Gabriele, L., Santoni, A., & Di Rosa, F. (2019). Dendritic cells modulate c-kit expression on the edge between activation and death. *European Journal of Immunology*, *49*(4), 534–545. <https://doi.org/10.1002/eji.201847683>
- Siret, C., Collignon, A., Silvy, F., Robert, S., Cheyrol, T., André, P., Rigot, V., Iovanna, J., van de Pavert, S., Lombardo, D., Mas, E., & Martirosyan, A. (2020). Deciphering the Crosstalk Between Myeloid-Derived Suppressor Cells and Regulatory T Cells in Pancreatic Ductal Adenocarcinoma. *Frontiers in Immunology*, *10*. <https://doi.org/10.3389/fimmu.2019.03070>
- Smit, V. T., Boot, A. J., Smits, A. M., Fleuren, G. J., Cornelisse, C. J., & Bos, J. L. (1988). KRAS codon 12 mutations occur very frequently in pancreatic adenocarcinomas. *Nucleic Acids Research*, *16*(16), 7773–7782.
- Sousa, C. M., Biancur, D. E., Wang, X., Halbrook, C. J., Sherman, M. H., Zhang, L., Kremer, D., Hwang, R. F., Witkiewicz, A. K., Ying, H., Asara, J. M., Evans, R. M., Cantley, L. C., Lyssiotis, C. A., & Kimmelman, A. C. (2016). Pancreatic stellate cells support tumour metabolism through autophagic alanine secretion. *Nature*, *536*(7617), 479–483. <https://doi.org/10.1038/nature19084>
- Springfeld, C., Ferrone, C. R., Katz, M. H. G., Philip, P. A., Hong, T. S., Hackert, T., Büchler, M. W., & Neoptolemos, J. (2023). Neoadjuvant therapy for pancreatic cancer. *Nature Reviews Clinical Oncology*, *20*(5), 318–337. <https://doi.org/10.1038/s41571-023-00746-1>
- Steele, N. G., Biffi, G., Kemp, S. B., Zhang, Y., Drouillard, D., Syu, L., Hao, Y., Oni, T. E., Brosnan, E., Elyada, E., Doshi, A., Hansma, C., Espinoza, C., Abbas, A., The, S., Irizarry-Negron, V., Halbrook, C. J., Franks, N. E., Hoffman, M. T., ... Pasca di Magliano, M. (2021). Inhibition of Hedgehog Signaling Alters Fibroblast Composition in Pancreatic Cancer. *Clinical Cancer Research*, *27*(7), 2023–2037. <https://doi.org/10.1158/1078-0432.CCR-20-3715>
- Strickler, J. H., Satake, H., George, T. J., Yaeger, R., Hollebecque, A., Garrido-Laguna, I., Schuler, M., Burns, T. F., Coveler, A. L., Falchook, G. S., Vincent, M., Sunakawa, Y., Dahan, L., Bajor, D., Rha, S.-Y., Lemech, C., Juric, D., Rehn, M.,

- Ngarmchamnanrith, G., ... Hong, D. S. (2023). Sotorasib in KRAS p.G12C–Mutated Advanced Pancreatic Cancer. *New England Journal of Medicine*, 388(1), 33–43. <https://doi.org/10.1056/NEJMoa2208470>
- Stuart, T., Butler, A., Hoffman, P., Hafemeister, C., Papalexi, E., Mauck, W. M., Hao, Y., Stoeckius, M., Smibert, P., & Satija, R. (2019). Comprehensive Integration of Single-Cell Data. *Cell*, 177(7), 1888-1902.e21. <https://doi.org/10.1016/j.cell.2019.05.031>
- Syed Nabeel Zafar, M. D. (2024). *Exploring the Nuances of Postoperative Considerations in Pancreatic Cancer*. 25. <https://www.onclive.com/view/exploring-the-nuances-of-postoperative-considerations-in-pancreatic-cancer>
- Tang, D., Wu, Q., Zhang, J., Zhang, H., Yuan, Z., Xu, J., Chong, Y., Huang, Y., Xiong, Q., Wang, S., Tian, Y., Lu, Y., Ge, X., Shen, W., & Wang, D. (2018). Galectin-1 expression in activated pancreatic satellite cells promotes fibrosis in chronic pancreatitis/pancreatic cancer via the TGF- β 1/Smad pathway. *Oncology Reports*, 39(3), 1347–1355. <https://doi.org/10.3892/or.2018.6202>
- Thayer, S. P., di Magliano, M. P., Heiser, P. W., Nielsen, C. M., Roberts, D. J., Lauwers, G. Y., Qi, Y. P., Gysin, S., Castillo, C. F., Yajnik, V., Antoniu, B., McMahon, M., Warshaw, A. L., & Hebrok, M. (2003). Hedgehog is an early and late mediator of pancreatic cancer tumorigenesis. *Nature*, 425(6960), 851–856. <https://doi.org/10.1038/nature02009>
- Théou-Anton, N., Tabone, S., Brouty-Boyé, D., Saffroy, R., Ronnstrand, L., Lemoine, A., & Emile, J.-F. (2006). Co expression of SCF and KIT in gastrointestinal stromal tumours (GISTs) suggests an autocrine/paracrine mechanism. *British Journal of Cancer*, 94(8), 1180–1185. <https://doi.org/10.1038/sj.bjc.6603063>
- Tian, C., Clauser, K. R., Öhlund, D., Rickelt, S., Huang, Y., Gupta, M., Mani, D. R., Carr, S. A., Tuveson, D. A., & Hynes, R. O. (2019). Proteomic analyses of ECM during pancreatic ductal adenocarcinoma progression reveal different contributions by tumor and stromal cells. *Proceedings of the National Academy of Sciences*, 116(39), 19609–19618. <https://doi.org/10.1073/pnas.1908626116>
- Ting, S. B., Caddy, J., Hislop, N., Wilanowski, T., Auden, A., Zhao, L., Ellis, S., Kaur, P., Uchida, Y., Holleran, W. M., Elias, P. M., Cunningham, J. M., & Jane, S. M. (2005). A Homolog of *Drosophila* grainy head Is Essential for Epidermal Integrity in Mice. *Science*, 308(5720), 411–413. <https://doi.org/10.1126/science.1107511>

- Tlsty, T. D., & Coussens, L. M. (2006). TUMOR STROMA AND REGULATION OF CANCER DEVELOPMENT. *Annual Review of Pathology: Mechanisms of Disease*, 1(Volume 1, 2006), 119–150.
<https://doi.org/10.1146/annurev.pathol.1.110304.100224>
- Toksoz, D., Zsebo, K. M., Smith, K. A., Hu, S., Brankow, D., Suggs, S. V., Martin, F. H., & Williams, D. A. (1992). Support of human hematopoiesis in long-term bone marrow cultures by murine stromal cells selectively expressing the membrane-bound and secreted forms of the human homolog of the steel gene product, stem cell factor. *Proceedings of the National Academy of Sciences*, 89(16), 7350–7354. <https://doi.org/10.1073/pnas.89.16.7350>
- Tong, X., Dai, C., Walker, J. T., Nair, G. G., Kennedy, A., Carr, R. M., Hebrok, M., Powers, A. C., & Stein, R. (2020). Lipid Droplet Accumulation in Human Pancreatic Islets Is Dependent On Both Donor Age and Health. *Diabetes*, 69(3), 342–354. <https://doi.org/10.2337/db19-0281>
- Tsai, M., Valent, P., & Galli, S. J. (2022). KIT as a master regulator of the mast cell lineage. *The Journal of Allergy and Clinical Immunology*, 149(6), 1845–1854. <https://doi.org/10.1016/j.jaci.2022.04.012>
- Tuck, A. R., Mottershead, D. G., Fernandes, H. A., Norman, R. J., Tilley, W. D., Robker, R. L., & Hickey, T. E. (2015). Mouse GDF9 decreases KITL gene expression in human granulosa cells. *Endocrine*, 48(2), 686–695. <https://doi.org/10.1007/s12020-014-0335-6>
- Vandenbark, G. R., Chen, Y., Friday, E., Pavlik, K., Anthony, B., deCastro, C., & Kaufman, R. E. (1996). Complex regulation of human c-kit transcription by promoter repressors, activators, and specific myb elements. *Cell Growth & Differentiation: The Molecular Biology Journal of the American Association for Cancer Research*, 7(10), 1383–1392.
- Velez-Delgado, Donahue, Brown, Du, Irizarry-Negron, Menjivar, Lasse Opsahl, Steele, The, Lazarus, Sirihorachai, Yan, Kemp, Kerk, Bollampally, Yang, Scales, Avritt, Lima, ... di Magliano. (2022). Extrinsic KRAS Signaling Shapes the Pancreatic Microenvironment Through Fibroblast Reprogramming. *Cellular and Molecular Gastroenterology and Hepatology*, 13(6), 1673–1699. <https://doi.org/10.1016/j.jcmgh.2022.02.016>
- Vennin, C., Méléneç, P., Rouet, R., Nobis, M., Cazet, A. S., Murphy, K. J., Herrmann, D., Reed, D. A., Lucas, M. C., Warren, S. C., Elgundi, Z., Pinese, M., Kalna, G.,

- Roden, D., Samuel, M., Zaratzian, A., Grey, S. T., Da Silva, A., Leung, W., ... Timpson, P. (2019). CAF hierarchy driven by pancreatic cancer cell p53-status creates a pro-metastatic and chemoresistant environment via perlecan. *Nature Communications*, *10*(1), 3637. <https://doi.org/10.1038/s41467-019-10968-6>
- Vonlaufena, A., Phillipsa, P. A., Yanga, L., Xua, Z., Fiala-Beera, E., Zhanga, X., Pirola, R. C., Wilson, J. S., & Apte, M. V. (2010). Isolation of Quiescent Human Pancreatic Stellate Cells: A Promising in vitro Tool for Studies of Human Pancreatic Stellate Cell Biology. *Pancreatology*, *10*(4), 434–443. <https://doi.org/10.1159/000260900>
- Wake, K. (1971). “Sternzellen” in the liver: Perisinusoidal cells with special reference to storage of vitamin A. *American Journal of Anatomy*, *132*(4), 429–461. <https://doi.org/10.1002/aja.1001320404>
- Wang, N., Yang, S., Li, Y., Gou, F., Lv, Y., Zhao, X., Wang, Y., Xu, C., Zhou, B., Dong, F., Ju, Z., Cheng, T., & Cheng, H. (2024). P21/Zbtb18 repress the expression of cKit to regulate the self-renewal of hematopoietic stem cells. *Protein & Cell*, *15*(11), 840–857. <https://doi.org/10.1093/procel/pwae022>
- Wang, P., Wan, W., Xiong, S.-L., Feng, H., & Wu, N. (2017). Cancer stem-like cells can be induced through dedifferentiation under hypoxic conditions in glioma, hepatoma and lung cancer. *Cell Death Discovery*, *3*(1), 1–10. <https://doi.org/10.1038/cddiscovery.2016.105>
- Wang, X. M., Yu, D. M. T., McCaughan, G. W., & Gorrell, M. D. (2005). Fibroblast Activation Protein Increases Apoptosis, Cell Adhesion, and Migration by the LX-2 Human Stellate Cell Line*. *Hepatology*, *42*(4), 935. <https://doi.org/10.1002/hep.20853>
- Whatcott, C. J., Diep, C. H., Jiang, P., Watanabe, A., LoBello, J., Sima, C., Hostetter, G., Shepard, H. M., Von Hoff, D. D., & Han, H. (2015). Desmoplasia in Primary Tumors and Metastatic Lesions of Pancreatic Cancer. *Clinical Cancer Research: An Official Journal of the American Association for Cancer Research*, *21*(15), 3561–3568. <https://doi.org/10.1158/1078-0432.CCR-14-1051>
- Williams, D. E., Eisenman, J., Baird, A., Rauch, C., Ness, K. V., March, C. J., Park, L. S., Martin, U., Mochizuki, D. Y., Boswell, H. S., Burgess, G. S., Cosman, D., & Lyman, S. D. (1990). Identification of a ligand for the c-kit proto-oncogene. *Cell*, *63*(1), 167–174. [https://doi.org/10.1016/0092-8674\(90\)90297-R](https://doi.org/10.1016/0092-8674(90)90297-R)
- Wollberg, P., Lennartsson, J., Gottfridsson, E., Yoshimura, A., & Rönstrand, L. (2003). The adapter protein APS associates with the multifunctional docking sites Tyr-

- 568 and Tyr-936 in c-Kit. *Biochemical Journal*, 370(Pt 3), 1033–1038.
<https://doi.org/10.1042/BJ20020716>
- Wu, H., Ou, S., Zhang, H., Huang, R., Yu, S., Zhao, M., & Tai, S. (2022). Advances in biomarkers and techniques for pancreatic cancer diagnosis. *Cancer Cell International*, 22(1), 220. <https://doi.org/10.1186/s12935-022-02640-9>
- Yang, D., Liu, J., Qian, H., & Zhuang, Q. (2023). Cancer-associated fibroblasts: From basic science to anticancer therapy. *Experimental & Molecular Medicine*, 55(7), 1322–1332. <https://doi.org/10.1038/s12276-023-01013-0>
- Yarden, Y., Kuang, W. J., Yang-Feng, T., Coussens, L., Munemitsu, S., Dull, T. J., Chen, E., Schlessinger, J., Francke, U., & Ullrich, A. (1987). Human proto-oncogene c-kit: A new cell surface receptor tyrosine kinase for an unidentified ligand. *The EMBO Journal*, 6(11), 3341–3351. <https://doi.org/10.1002/j.1460-2075.1987.tb02655.x>
- Yasuda, A., Sawai, H., Takahashi, H., Ochi, N., Matsuo, Y., Funahashi, H., Sato, M., Okada, Y., Takeyama, H., & Manabe, T. (2006). The stem cell factor/c-kit receptor pathway enhances proliferation and invasion of pancreatic cancer cells. *Molecular Cancer*, 5(1), 46. <https://doi.org/10.1186/1476-4598-5-46>
- Yen, T. W. F., Aardal, N. P., Bronner, M. P., Thorning, D. R., Savard, C. E., Lee, S. P., & Bell, R. H. (2002). Myofibroblasts are responsible for the desmoplastic reaction surrounding human pancreatic carcinomas. *Surgery*, 131(2), 129–134.
<https://doi.org/10.1067/msy.2002.119192>
- Yushkov, B. G., Danilova, I. G., Ponezheva, Zh. B., Brykina, I. A., Abidov, M. T., & Kalyuzhin, O. V. (2011). Modulation of Reparative Regeneration and CD117 Expression by Liver Cells after Partial Hepatectomy in Mice. *Bulletin of Experimental Biology and Medicine*, 150(3), 352–354.
<https://doi.org/10.1007/s10517-011-1140-3>
- Zeissig, M. N., Ashwood, L. M., Kondrashova, O., & Sutherland, K. D. (2023). Next batter up! Targeting cancers with KRAS-G12D mutations. *Trends in Cancer*, 9(11), 955–967. <https://doi.org/10.1016/j.trecan.2023.07.010>
- Zhang, J., Zhang, J., Liu, Q., Fan, X.-X., Leung, E. L.-H., Yao, X.-J., & Liu, L. (2022). Resistance looms for KRAS G12C inhibitors and rational tackling strategies. *Pharmacology & Therapeutics*, 229, 108050.
<https://doi.org/10.1016/j.pharmthera.2021.108050>

- Zhao, L., Cai, B., Lu, Z., Tian, L., Guo, S., Wu, P., Qian, D., Xu, Q., Jiang, K., & Miao, Y. (2016). Modified methods for isolation of pancreatic stellate cells from human and rodent pancreas. *Journal of Biomedical Research*, *30*(6), 510–516. <https://doi.org/10.7555/JBR.30.20160033>
- Zhong, Y., Macgregor-Das, A., Saunders, T., Whittle, M. C., Makohon-Moore, A., Kohutek, Z. A., Poling, J., Herbst, B. T., Javier, B. M., Cope, L., Leach, S. D., Hingorani, S. R., & Iacobuzio-Donahue, C. A. (2017). Mutant p53 Together with TGF β Signaling Influence Organ-Specific Hematogenous Colonization Patterns of Pancreatic Cancer. *Clinical Cancer Research: An Official Journal of the American Association for Cancer Research*, *23*(6), 1607–1620. <https://doi.org/10.1158/1078-0432.CCR-15-1615>
- Zhou, B. O., Yu, H., Yue, R., Zhao, Z., Rios, J. J., Naveiras, O., & Morrison, S. J. (2017). Bone marrow adipocytes promote the regeneration of stem cells and haematopoiesis by secreting SCF. *Nature Cell Biology*, *19*(8), 891–903. <https://doi.org/10.1038/ncb3570>
- Zhou, X., Guo, X., Chen, M., Xie, C., & Jiang, J. (2018). HIF-3 α Promotes Metastatic Phenotypes in Pancreatic Cancer by Transcriptional Regulation of the RhoC–ROCK1 Signaling Pathway. *Molecular Cancer Research*, *16*(1), 124–134. <https://doi.org/10.1158/1541-7786.MCR-17-0256>
- Zimmermann, A., Gloor, B., Kappeler, A., Uhl, W., Friess, H., & Büchler, M. W. (2002). Pancreatic stellate cells contribute to regeneration early after acute necrotising pancreatitis in humans. *Gut*, *51*(4), 574–578. <https://doi.org/10.1136/gut.51.4.574>
- Zsebo, K. M., Williams, D. A., Geissler, E. N., Broudy, V. C., Martin, F. H., Atkins, H. L., Hsu, R.-Y., Birkett, N. C., Okino, K. H., Murdock, D. C., Jacobsen, F. W., Langley, K. E., Smith, K. A., Takeish, T., Cattanach, B. M., Galli, S. J., & Suggs, S. V. (1990). Stem cell factor is encoded at the Sl locus of the mouse and is the ligand for the c-kit tyrosine kinase receptor. *Cell*, *63*(1), 213–224. [https://doi.org/10.1016/0092-8674\(90\)90302-U](https://doi.org/10.1016/0092-8674(90)90302-U)